

Sulfur-functional polymers for biomedical applications

Dissertation zur Erlangung des
naturwissenschaftlichen Doktorgrades
der Julius-Maximilians-Universität Würzburg

vorgelegt von
Matthias Kuhlmann
aus Essen

Würzburg 2015

Eingereicht am: _____

Bei der Fakultät für Chemie und Pharmazie

Gutachter der schriftlichen Arbeit:

1. Gutachter: Prof. Dr. Jürgen Groll
2. Gutachter: Prof. Dr. Robert Luxenhofer

Prüfer des öffentlichen Promotionskolloquium:

1. Prüfer: _____
2. Prüfer: _____
3. Prüfer: _____

Datum des öffentlichen Promotionskolloquiums:

Doktorurkunde ausgehändigt am:

This work was conducted from August 2010 till May 2015 at the Department for Functional Materials in Medicine and Dentistry, University of Würzburg, Würzburg, Germany under supervision of Prof. Dr. Jürgen Groll.

„Insanity laughs under pressure we're breaking [...]"
Queen – Under Pressure

Acknowledgements

I want to thank Prof. Dr. Jürgen Groll for all basic things useful for the thesis, an interesting topic, money and a now fully equipped workplace. Even more thankful am I for his confidence in me, doing my work (most of the time) independently but guiding me when I started to get mentally unorganized. I was and am very happy finding a supervisor that supports and focuses my ideas and let me work non-project related, although I am still not convinced of the term “free agent”. Furthermore I am very happy that I changed with him the University from Aachen to Würzburg. This taught me a lot about white wine, lots of franconian words and offered me a beautiful city to live for 5 years. Working in the exclave for 2 years, in the workgroup of Prof. Frank Würthner, was demanding regarding seminar participation, birthday cakes, group integration etc., but in the retrospective I met people from all kinds of workgroups, found friends and now know how to start from the scratch.

Chronologically continuing, I thank Prof. Dr. Frank Würthner for the lab space within the first 2 years and especially Dr. Matthias Stolte for his support from the very beginning to the end of Hubland-times and also thereafter (for Käsekuchen, but also for the pain during Lacrosse excercises). Dr. Marcel Gsänger, Jana Gershberg, Dr. Sabin Lucian-Suraru, Dr. Martin Berberich, Dr. Charlotte Grzeszkiewicz, Dr. Volker Dehm, Dr. Angel Jimenez, Ana-Maria Krause, Benjamin Fimmel, Andreas Kraft, Andreas Liess, Dr. Florian Beuerle, Dr. Gustavo Fernandez, Dr. Vladimir Stepanenko, Daniel Görl, Eva Kirchner, Stefanie Klotzbach, Christina Rest, Jenny Begall, Annike Weißenstein, Peter Spent, Dr. Maria Mayoral Munoz, Dr. Thomas & Stefanie Rehm, Dr. Peter Frischmann and from other groups Dr. Steffi Gloza, Benjamin Fröhlich, Johannes Becker, Thomas Schmidt, Christof Walter, Prof. Dr. Bernd Engels, Uschi Rüppel, Lisa Mailänder and many more thanks to all of you (and the ones that I forgot) for technical and organization support, jokes, coffee, more coffee and the time outside of the lab.

The whole continuously growing group of the FMZ and the ones related to it, more or less chronologically, Prof. Uwe Gbureck, Dr. Andrea Ewald, Isabell Biermann, Dr. Claus Mosecke, Dr. Elke Vorndran, Maria Aniolek, Dr. Karl-Heinz “Kalle” Heffels, Dr. Meike Beer, Tobias Schmitz, Kai Stuckensen, Tomasz Jüngst, Michael + Julia Schmitz, Theresa Christel, Markus Meininger, Susi Christ, Ilona “Zille-Bazille-Ziehkowski” Zilkowski, Kathrin Hahn, Verena Schill,

Simone Stichler, Susanne JUTTA Feineis, Dr. Ana Sancho, Laura Wistlich, Gernot Hochleitner, Steffi Jäger + Andre Hauck + Lotta Hauck, Martina Keßler, Eva Esser, Dr. Jörg Teßmar, Angela Rossi, Martha Geffers + Hannes Schamel, Michaela Rödel, Julia Blöhbaum + Achim Liebscher and Willi Smolan thanks for sharing the time with me, helping me, answering questions, support, playing Tekken, parties, Weinfeste and much more. Thanks to the students Sabrina Ullmann, Hannah Heil, Stefanie Jäger, Matthias Weis and Christina Endres that I (co)supervised. You taught me questions that I never asked before, do corrections and read a lot ;).

Especially I'd like to thank the permanent staff namely Toni Hofmann, Harald Hümpfer for constructing, filing, sawing, glueing, computer fixing..., and Simone Werner for biologic experiments.

Thanks to my family Ingrid, Jörg, Sabine, Nora, Julia, Jan, Lena, Irene and Friedrich, that always supported me with jokes, discussions, hugs, coffee and infectious smiles. Your motivation was and is still awesome!

Thank you, Sarah, for your love, support and humor in the last 1.5 years and especially in the final stage of my thesis.

Thanks to my friends Wiebke, Sebastian, kleine Wiebke, Inga, Anna, Maren, Andi, Ela, Melanie, Franko, Kerstin, Björn that reloaded my battery during my study and my thesis, switched off my brain but also partially "joined" the path of doctoral studies.

I'd like to thank also Petra and Gurki for offering the "Grillhaus", a silent garden, hospitality, (lots of) Jack Daniels and support for the motorbike.

Thanks to all members of AV Agricola Aachen for lots of beer(-Stiefel), cigarettes, non-sense- and scientific support and discussions regarding almost everything and the irregular supply with Döbler Reichstadtbeer from Bad Windsheim.

PUBLICATIONS

1. Kuhlmann, M., & Groll, J. (2015). *Dispersity control of linear poly(glycidyl ether)s by slow monomer addition*. **submitted**
2. Schmitz, M.*, Kuhlmann, M.*, Reimann, O., Hackenberger, C. P. R., & Groll, J. (2015). *Side-Chain Cysteine Functionalized Poly(2-oxazoline)s for Multiple Peptide Conjugation by Native Chemical Ligation*. *Biomacromolecules*, 16(4), 1088-1094.
<http://dx.doi.org/10.1021/bm501697t>
3. Kuhlmann, M., Reimann, O., Hackenberger, C. P. R., & Groll, J. (2015). *Cysteine-Functional Polymers via Thiol-ene Conjugation*. *Macromolecular Rapid Communications*, 36(5), 472-476.
dx.doi.org/10.1002/marc.201400703
4. Christel, T., Kuhlmann, M., Vorndran, E., Groll, J., & Gbureck, U. (2013). *Dual setting α -tricalcium phosphate cements*. *Journal of Materials Science: Materials in Medicine*, 24(3), 573-581.
dx.doi.org/10.1007/s10856-012-4828-7
5. Kuhlmann, M., Singh, S., & Groll, J. (2012). *Controlled Ring-Opening Polymerization of Substituted Episulfides for Side-Chain Functional Polysulfide-Based Amphiphiles*. *Macromolecular Rapid Communications*, 33(17), 1482-1486.
dx.doi.org/10.1002/marc.201200297
6. Kuhlmann, M., Baumgartner, T., & Parvez, M. (2008). *A new polymorph of dimesitylborinic acid*. *Acta Crystallographica Section E*, 64(7), o1185.
dx.doi.org/10.1107/S1600536808015638

*shared first authorship

Table of Contents

1. Introduction	1
2. Background	5
2.1. The role of sulfur in biology.....	7
2.1.1. Cysteine and methionine	7
2.1.2. Pathologic aspects.....	11
2.2. Mechanistic insight into sulfur redox-chemistry.....	13
2.2.1. Oxidation of thiol and thioethers.....	13
2.2.2. Detection and quantification of thiols	16
2.3. Anionic ring-opening polymerization	19
2.4. Polyglycidols	22
2.4.1. Polymerization.....	22
2.4.2. Functionalization	27
2.4.3. Cytocompatibility	31
2.5. Polythioethers	31
2.6. Sulfur-functional polymers for biomedical applications	37
2.6.1. Applications for reductive environments.....	37
2.6.2. Applications for oxidative environments.....	40
2.6.3. Conjugation applications.....	44
3. Results and discussion	53
3.1. Synthesis of polyglycidols	55
3.1.1. Polymerization in Eppendorf caps.	56
3.1.2. Polymerization with KO t Bu in THF	58
3.1.3. Polymerization with Cs ⁺ as counter ion in THF	77
3.1.4. Polymerization with Cs ⁺ /TEGME-alkoxide in THF	90
3.1.5. Polymerization with KO t Bu in bulk	93
3.1.6. Polymerization with Cs ⁺ /TEGME-alkoxide in bulk.....	101
3.1.7. Discussion of the rate constants	112
3.1.8. Discussion of the dispersities	115
3.1.9. Control of side-reaction by slow monomer addition.....	117
3.2. Synthesis of polythioglycidols.....	129
3.2.1. Synthesis of the monomer	130
3.2.2. Homo- and copolymerization of ATGE and EETGE with thiolates	131
3.2.3. Deprotection of the acetal-group	155

3.2.4.	Particle formation	159
3.3.	Synthesis of cysteine-functional poly(glycidol)s.....	161
3.3.1.	Thiazolidine formation	162
3.3.2.	Polymer-analog functionalization via isocyanates.....	170
3.3.3.	Polymer-analog functionalization via thiol-ene chemistry	173
3.4.	Native Chemical Ligation with cystein-functional poly(glycidol) [#]	191
4.	Summary/Zusammenfassung	197
5.	Experimental Section	207
5.1.	Materials and Methods	209
5.2.	Syntheses.....	213
5.2.1.	Ethoxy ethyl glycidyl ether	213
5.2.2.	Cesium initiator preparation for IROP of glycidyl ethers	214
5.2.3.	Kinetics of glycidyl ether polymerizations.....	214
5.2.4.	Synthesis of the polymers via slow monomer addition.....	219
5.2.5.	Ethoxy ethyl thioglycidyl ether.....	219
5.2.6.	Allyl thioglycidyl ether	220
5.2.7.	Homopolymerization of ATGE with thiophenol/DBU.	220
5.2.8.	Homopolymerization of EETGE with mercaptoethanol/DBU	222
5.2.9.	Homopolymerization of ATGE with mercaptoethanol/DBU.....	223
5.2.10.	Poly(EETGE) terminated with methyl acrylate.	224
5.2.11.	Blockcopolymerization of EETGE and ATGE with butanethiol/DBU.	225
5.2.12.	Blockcopolymerization of ATGE and EETGE with mercaptoethanol/DBU ...	226
5.2.13.	Homopolymerization of ATGE with phenol/DBU as initiator.....	227
5.2.14.	Homopolymerization of EETGE with DTT/DBU as initiator.	228
5.2.15.	Synthesis of PEETGE- <i>block</i> -mPEG480.....	229
5.2.16.	Acetal-cleavage for the synthesis of PTG.	230
5.2.17.	Acetal-cleavage for the synthesis of PTG- <i>block</i> -mPEG.	232
5.2.18.	Synthesis of 2,2-dimethyl-4-carboxyl-thiazolidine	233
5.2.19.	Formylation of 2,2-dimethyl-4-thiazolidine	234
5.2.20.	Synthesis of mercaptothiazolidine	235
5.2.21.	Synthesis of 3-formyl-2,2-dimethylthiazolidine-4-carbonyl azide	236
5.2.22.	Polymer-analog functionalization with isocyanates.....	237
5.2.23.	Polymer-analog functionalization with thiols with AIBN	238
5.2.24.	Polymer-analog functionalization with FTz4Cys via UV irradiation	240
5.2.25.	Hydrolysis of thiazolidine-functional poly(glycidol)s.....	243

5.2.26.	Polymer-analog functionalization with thioacetic acid via UV irradiation...	244
5.2.27.	Synthesis of ester-free thiol-functional poly(glycidol)	246
5.2.28.	Synthesis of amine-functional poly(glycidol)	247
5.2.29.	Synthesis of carboxyl-functional poly(glycidol)	247
5.2.30.	Thiol-quantification (Ellman assay)	248
5.2.31.	Cysteine-quantification (Oxidative TNBSA assay)	250
5.2.32.	Native Chemical Ligation [#]	251
5.2.33.	Tricin SDS-PAGE	252
6.	Literature.....	255

List of abbreviations and symbols

Abbreviation/Symbol	Meaning
3D	Three-dimensional
Å	Angstrom
a.u.	Arbitrary units
ABD-F	4-(Aminosulfonyl)-7-fluoro-2,1,3-benzoxadiazole
Ac	Acrylate
AGE	Allyl glycidyl ether
AIBN	2,2'-Azobis(2-methylpropionitrile)
APS	Ammonium persulfate
aROP	Anionic ring-opening polymerization
ATGE	Allyl thioglycidyl ether
ATRP	Atom transfer radical polymerization
β-Gal	β-galactosidase
br	Broad
BSA	Bovine Serum Albumin
BzCl	Benzyl chloride
c	Concentration
°C	Degree Celsius
ca	Circa
CCD	Charge-coupled device
cm	Centimeter
Cys	Cysteine
CySS	Cysteine-dimer
<i>d</i>	Diameter
d	Day(s)
d	Doublet (for NMR assignment)
Đ	Dispersity
DBAG	Dibenzylamino glycidol
DBTDL	Dibutyl tin dilaurate
DBU	1,8-diazabicyclo[5.4.0]undec-7-ene
DCC	Dicyclohexyl carbodiimide
DF	Degree of functionalization
DLS	Dynamic light scattering
DMAP	4-Dimethylaminopyridine
DMF	Dimethylformamide
DMPA	2,2-dimethoxy-2-phenylacetophenon
DMSO	Dimethylsulfoxide
DMSO- <i>d</i> 6	Deuterated DMSO
DNA	Deoxyribonucleic acid

DP	Degree of polymerization
DPPA	Diphenylphosphoryl azide
DTNB	5,5'-dithiobis(2-nitrobenzoic acid)
DTT	Dithiotreitol
e.g.	Exempli gratia (for example)
EDC	1-Ethyl-3-(3-dimethylaminopropyl)carbodiimide
EDTA	Ethylenediaminetetraacetic acid
EEGE	Ethoxy ethyl glycidyl ether
EETGE	Ethoxy ethyl thioglycidyl ether
EG	Ethylene glycol
E_{hc}	Electrode potential (half-cell)
EO	Ethylene oxide
eq	Equilibrium (as index)
Eq.	Equivalents
ESI	Electrospray ionization
Et	Ethyl
et al.	Et alii (and others)
Et ₂ O	Diethylether
Et ₃ N	Triethylamine
EtOAc	Ethyl acetate
EtOH	Ethanol
FDA	Food and Drug Administration
FITC	Fluorescein-isothiocyanate
Fmoc	Fluorenylmethyloxycarbonyl
g	Gram
GFP	Green-fluorescent protein
GG	Glyceryl glycerol
g-ion	Grams of ions
GSH	Glutathion
GSSG	Glutathion-disulfide
<i>H</i>	Enthalpy
h	Hour(s)
HA	Hyaluronic acid
HCl	Hydrochloric acid
HMPA	N-hydroxypropyl methacrylamide
hMSC	Human mesenchymal stem cells
HOBt	Hydroxybenzotriazole
HOEtSH	Mercaptoethanol
HPLC	High-performance liquid chromatography
HRMS	High-resolution mass spectrometry
HRP	Horseradish peroxidase

HSAB	Hard and soft acids and bases
HSQC	Heteronuclear Single Quantum Coherence
Hz	Hertz
/	Integral
[I]	Initiator concentration
i.e.	Id est (that is)
IFN	Interferon
IGG	Isopropylidene glyceryl glycidyl ether
IL	Interleukin
IME	Inverse-mini-emulsion
IR	Infrared
IUPAC	International Union of Pure and Applied Chemistry
K_{app}	Apparent rate constant
k	Rate constant of polymerization
kDa	Kilodalton
kg	Kilogramm
kJ	Kilojoule
KOtBu	Potassium tert-butoxide
K_{ss}	Equilibrium constant for thiol-disulfide exchange
kV	Kilovolt
L	Liter
LCST	Lower-critical solution temperature
LED	Light-emitting diode
ln	Natural logarithm
IROP	Living ring-opening polymerization
M	Molar
[M]	Monomer concentration
m	Multiplet (for NMR assignment)
M(ATGE)	Molar mass of ATGE
M(EETGE)	Molar mass of EETGE
M_0	Monomer concentration at the beginning of the polymerization
MALDI	Matrix-assisted laser desorption/ionization
mbar	Millibar
MeCN	Acetonitril
Met	Methionine
MetO	Methionine sulfoxide
mg	Milligram
MHz	Megahertz
min	Minute
mL	Milliliter
mM	Millimolar

mm	Millimeter
mm ²	square-millimeter
μL	Microliter
μm	Micrometer
μMol	Micromolar
M _n	Number-averaged molar mass
MPAA	4-mercaptophenylacetic acid
MPAL	Mercaptopropionic acid-leucin
mPEG	Methoxy-terminated PEG
MS	Mass spectrometry
MSR	Methionine sulfoxide reductase
M _t	Monomer concentration at time point t
MTT	3-(4,5-dimethylthiazol-2-yl)-2,5-diphenyltetrazolium bromide
mV	Millivolt
M _w	Weight-averaged molar mass
mW	Milli-Watt
MWCO	Molecular-weight cut off
n.d.	Not determined
NADPH	Nicotinamide adenine dinucleotide phosphate
Nbz	<i>N</i> -acyl-benzimidazolinone
NCL	Native Chemical Ligation
NCO	Isocyanate
NHS	N-Hydroxysuccinimide
nm	Nanometer
NMR	Nuclear magnetic resonance
obs	Observed
OMe	Methoxide-
PBS	Phosphate buffered saline
PEG	Poly(ethylene glycol)
PEI	Poly(ethylene imine)
pep	Peptide
PG	Poly(glycidol)
PGMA	Poly(glycerylmethacrylate)
pH	Negative logarithm of the H ⁺ concentration
pKa	Logarithmic constant of the acid dissociation constant
PMMA	Poly(methyl methacrylate)
PNIPAAm	Poly(<i>N</i> -isopropylacrylamide)
pol	polymer
ppm	parts per million
PPS	Poly(propylene sulfide)
PR	Photoreactor

PS	Propylene sulfide
PSH	Thiol-bearing proteine
PSSP	Dimerized thiol-bearing proteine
PTFE	Poly(tetrafluoroethylene)
pTsOH	<i>para</i> -Toluene sulfonic acid
q	quartet
quin	quintett
R	Organic residue
R _f	Retardation factor
rhGCSF	Recombinant human granulocyte colony stimulating factor
RNA	Ribonucleic acid
ROS	Reactive oxygen species
RP	Reversed-phase
RT	Room temperature
s	Second(s)
s	Singlet (for NMR assignment)
SDS-PAGE	Sodium dodecyl sulfate - Polyacrylamide gel electrophoresis
SEC	Size-exclusion chromatography
SEM	Scanning electron microscopy
sex	Sextet (for NMR assignment)
siRNA	Small interfering RNA
SN2	Substitution nucleophilic bimolecular
SPPS	Solid phase peptide synthesis
sulfo-NHS	N-hydroxysulfosuccinimide
T	Temperature
t	Time
t	Triplet (for NMR assignment)
TBAB	Tetrabutyl ammonium bromide
tBGE	<i>tert</i> -butyl glycidyl ether
TCEP	Tris(2-carboxyethyl)phosphine
TEGME	Triethyleneglycol monomethyl ether
TFA	Trifluoroacetic acid
THF	Tetrahydrofuran
Thz	Thiazolidine
tlc	Thin-layer chromatography
TMS	Trimethyl silyl-
TMSG	Trimethylsilyl glycidyl ether
TNBSA	Trinitrobenzosulfonic acid
ToF	Time-of-Flight
Trx	Thioredoxin
TrxR	Thioredoxin reductase

US	United States of America
US-\$	US-Dollar
UV	Ultraviolet
UV-Vis	Ultraviolet-Visible (Spectroscopy)
\dot{V}	Volume flux
W	Watt
w/o	Water-in-oil
w/v	Mass/Volume
wt	Weight
x	Conversion
z	Charge
δ	Chemical shift (NMR spectroscopy)
Δ	Difference
λ	Wavelength
ν	Wavenumber

1. Introduction

Sulfur belongs to the group of chalcogenes and sulfur-containing compounds are almost omnipresent. Both, inorganic materials (e.g. FeS, HgS and ZnS) and living organisms (e.g. plants and humans) can have a high fraction of sulfur. Approximately 2.5 g sulfur/kg is present in the human tissue, bound as amino acids, vitamins and (co)enzymes. Here the sulfur-moieties are available in various oxidation states and are used for different purposes, such as metal-complexation.[1] In the human body a balanced oxidation-reduction reaction is crucial (homeostasis) that relies on the redox-chemistry of sulfur compounds. Depending on the site in the human body, this equilibrium is altered, leading for example to a reductive potential in the intracellular environment, the cytosol. In extracellular environments, the redox-potential is more oxidative than in the cytosol, and the equilibrium between reduced and oxidized species is shifted towards the latter. Here, the oxidation of thiol-groups leads to disulfides that are significantly stable under extracellular conditions and aids to maintain e.g. the structural integrity of folded proteins. The 3D-conformation of proteins is a crucial factor for their activity. Therefore, the effectiveness of proteins, for example of the immune system, depends on the redox-chemical properties of sulfur-moieties.[2] An abnormal equilibration shift of oxidants and antioxidants can refer to pathological conditions that could indicate cancer, cardiovascular diseases, diabetes and many others.[3] Furthermore, fundamental research in recent years indicated that sulfur-functional sites in proteins can act as scavengers for reactive oxidizing species, protecting the active sites of proteins towards both endogenous and exogenous oxidants.[4]

The functionalization of materials with biologically-relevant sulfur groups hence gained interest for biomedical applications. As an example, thiol-functionalized hyaluronic acid (Glycosil®) and thiol-functionalized collagen (Gelin-S®) are commercially available materials. These are crosslinked via thiols and used for mimicking the extracellular matrix to cultivate cells.[5, 6] Besides this, the direct interactions of the sulfur-residues of the materials with biochemical processes were investigated. Polymers, bearing the same functionalities as present in biological systems, can interact with the naturally occurring structures and exhibit a desired function. For example, redox-sensitive polymers functionalized with thiols-, disulfides or thioethers, are able to respond to e.g. the reductive cytosol or oxidative inflammation sites and were used for drug delivery applications.[7, 8] Thiol- and disulfide-containing polymers can also interact with biologic structures that lead to the adhesion of

the material at specific sites, such as the eye or the intestine. These adhesions were used for a local administration of drugs.[9] Not only sulfur-*modified* polymers, but also their reactivity *towards* sulfur-functionalities were exploited for biomaterial applications. Here the conjugation of thiol- and disulfide containing proteins with reactive synthetic polymers were performed that allowed the beneficial combination of therapeutic effects with reduced immunogenicity and prolonged circulation times.[10]

Polymers for biomedical applications require numerous properties such as biocompatibility, accurate synthesis in significant quantities and a defined structure. Biological polymers, such as peptides and proteins, are highly defined structures with respect to their conformation and their molar mass, but can lack in their biocompatibility due to immunogenic responses. Other naturally derived biopolymers, such as hyaluronic acid and alginates, can exhibit biocompatibility, but exhibit both a source dependent batch-to-batch variation and a broad molar mass *distribution*. This means that the polymer has not a definite molar mass, but fractions of polymers with different chain lengths and different molar masses. Synthetic polymers can exhibit a compromise. Different polymers were already tested in the past to be biocompatible, but still exhibit a molar-mass distribution. Minimizing this drawback was accomplished by using polymers with a narrow molar-mass distribution. As the most prominent material, poly(ethylene glycol) established as a hydrophilic biocompatible polymer that is already used for various applications. Commercial availability and highly defined structure of this polymer makes it useful for various applications. Unfortunately, only the termini of PEG are prone to synthetic modifications and this polymer is hence restricted in the quantity of functional groups.

To further expand the sulfur-based chemistry to hydrophilic synthetic polymeric biomaterials, a multifunctional PEG analog would be promising. The alternative polymer has to exhibit more reactive sites for modifications, but also the benefits of PEG. In recent years, poly(glycidol)s gained interest as PEG-analog, bearing additional hydroxymethylene and other side-chains at each repeating unit. Poly(glycidol)s established as a multifunctional PEG alternative having similar cyto- and hemocompatible properties. Combining biologically based sulfur-chemistries with structurally more versatile synthetic poly(glycidol)s would

allow expanding the scope of established sulfur-functional polymers for further biomedical application purposes.

Aim of this thesis was therefore to explore poly(glycidol)s as sulfur-containing polymers as tool for biomedical applications. Here, the focus was the control over synthesis, i.e. molar-mass distribution, of poly(glycidol)s, of the thioether-analog poly(thioglycidol)s for oxidative-responsive applications and the cysteine-functionalization of poly(glycidol)s for chemical orthogonal coupling of peptides for multivalent interaction studies.

For this, first in **chapter 3.1** the controlled polymerization of glycidol-derivatives with respect to a statistical copolymerization of acetal-protected glycidol and allyl-functional glycidyl ether is attempted. Control over molar mass and molar-mass distribution are two key aspects determining the scope of this material for further functionalization and applications. A controlled copolymerization allows the determination of the polymer composition, and orthogonal reactivities of the side-chains determine the quantity of subsequent functionalization.

Furthermore in **chapter 3.2** it is aimed to synthesize thioether-derivatives of poly(glycidol), i.e. poly(thioglycidol)s, that would reveal oxidation-sensitive multi-hydroxy functional polymers. It is assumed that the multi-hydroxy functionalization allows post-polymerization modification, concurrently rendering the polymers sensitive towards oxidation due to the thioether-functional backbone.

In **chapter 3.3** cysteine-functionalization of poly(glycidol)s was aimed via a newly synthesized low molar-mass building block. With this, thiol-ene click chemistry was attempted, as this opens an easy and fast route for derivatization. Together with allyl-functional poly(glycidol)s, a controlled degree of functionalization of the polymer can be obtained. This newly developed cysteine-modification of polymers allows for both combination of redox-sensitivity with electrostatic interaction and for orthogonal coupling via Native Chemical Ligation.

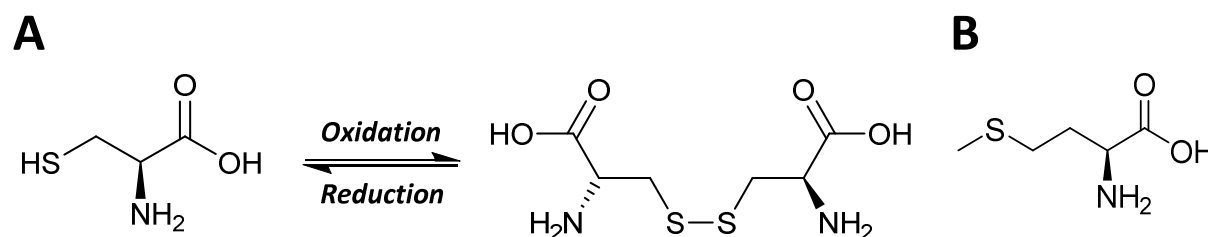
Before entering the experimental part, the following chapter introduces relevant background information and the literature overview.

2. Background

2.1. The role of sulfur in biology

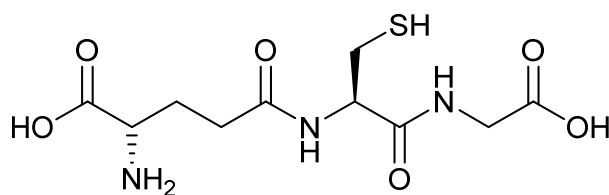
2.1.1. Cysteine and methionine

Among the 20 proteinogenic amino acids exactly two bear sulfur functionalities, i.e. cysteine and methionine. Here cysteine bears a thiol group, whereas methionine has a thioether group (Scheme 1).



Scheme 1: (A) Cysteine with the cysteine-dimer cystine and (B) methionine.

For cysteine, the most prominent function of the thiols is the formation of disulfide-bonds in peptides and proteins. For this, in protein biosynthesis, thiols of the cysteine-residues are oxidized to the corresponding disulfides, folding the peptide chain into its 3D-structure. One path is the oxidation mediated via glutathione-disulfide, with glutathione being a tripeptide consisting of glutamic acid, cysteine and glycine (Scheme 2). Besides glutathione/glutathione-disulfide the cysteine/cystine (Scheme 1) system itself is common as low molar-mass redox-couple. Although macromolecular redox systems, such as e.g. thioredoxin, are also present, their content is low compared to the GSH/GSSG couple. Literature states that depending on the cells the ratio is ca. GSH/GSSG:thioredoxin = 100-1000:1.[11]



Scheme 2: Glutathione, an active agent participating in many intracellular redox-processes.

Thiols can be oxidized forming disulfides, by other disulfides, changing the oxidation state from -II to -I, or -I to 0. Here literature is partially inconsistent, as the electronegativity differences between C and S is only marginal (C: 2.50-2.52; S: 2.44-2.58)[12] and the bond

hence non-polar. For the oxidation of the example thiol-containing peptide-chain PSH and glutathione GSH the equilibrium

$$K_{SS} = \frac{[PSSP][GSH]^2}{[PSH][GSSG]}$$

is given, as for the reduction of oxidized protein PSSP two molecules of glutathione are consumed. As the two thiols of the protein-to-fold are intramolecular, both concentrations are to the power of one. Literature values for intracellular GSH concentrations are given by 1 – 10 mM and only 1 % accounts for the oxidized form GSSG.[11] With these values only a small portion of the protein is oxidized intracellularly and only cysteines in close proximity, in the primary structure, are converted to the corresponding disulfides. Depending on the micro-environment, the potentials vary e.g. in mitochondria with GSH/GSSG: -300 mV; cytoplasm: -260 – -230 mV and endoplasmic reticulum: -150 mV (Figure 1). In contrast to the reductive intracellular environment, extracellular plasma was determined to have a potential of -140 mV for the GSH/GSSG equilibrium.[13] These potential values already indicate that extracellularly the most probable species from the thiol/disulfide-couple is the disulfide. As mentioned before this is crucial for the protein folding and hence their stability in the extracellular environment.

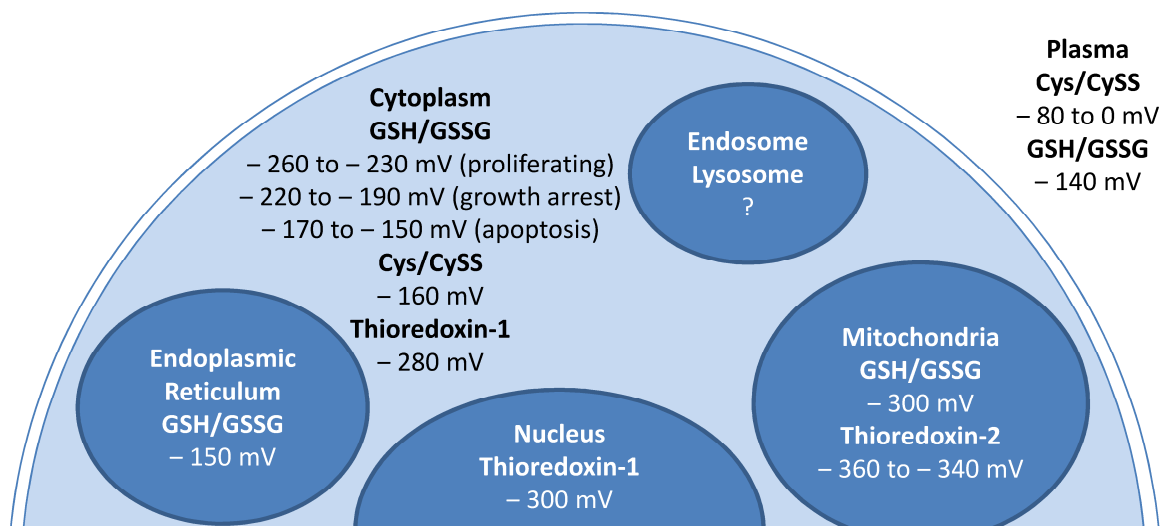


Figure 1: Intra- and extracellular redox potentials obtained from various literature sources, summarized by Brülisauer et al. Modified from [13], with permission from Elsevier.

Extracellularly, parts with a very high content of disulfide-bridged (glyco)proteins are mucus layers. Mucous membranes are omnipresent and cover the inner surface of hollow organs such as the gastrointestinal tract or the respiratory system, but also on outer surfaces such as the conjunctiva of the eyelids.[14-16] Structurally, first the connective tissue than the upper lying epithelial layer und finally the mucus layer build the basic form of these mucous membranes. Single epithelial layers are found in the stomach and the intestine, whereas the multilayered epithelial layers can be found e.g. in the vagina and the esophagus. Epithelial layers contain numerous goblet cells, for example the healthy conjunctiva contains approximately 1.5 million cells with a cell density of up to 10 cells per mm². These cells are responsible for the secretion of the mucus. This is a viscous gel-like substrate containing mainly water and glycoproteins but also salts and lipids. It helps to e.g. protect the underlying tissue, but are also able to adsorb and secrete substances.[14] The glycoproteins itself (mucine) are highly O-linked glycosylated proteins with e.g. 984 amino acids (human intestinal MUC2) in its primary sequence and are present in the mucus with 0.5-5%. Regarding glycosylation, it is assumed that in the case of human intestinal MUC2 78 % of the threonines are glycosylated, with 11 % of overall amino acids content to be threonine. Studies indicated a high content of disulfide-bridges, having 34 disulfides per molecule of mucin, derived from the goblet cells of rats,[16] and 9 % of the amino acids are cysteins for the above mentioned human MUC2.[17]

Beside thiols and disulfides, the thioether-functional proteinogenic amino acid methionine plays an important role in redox-activities. This thioether residue gained more and more interest both in biologic basic research but also biomedical applications. Whereas nowadays the essential roles of cysteine in proteins is for structural stabilization or antioxidant defense, methionine was generally known for its hydrophobic character in proteins and initiation of protein biosynthesis.[18] In the last decades, numerous redox-activities of the thioether-moiety of methionine were evaluated. Results show that this amino-acid plays also a crucial role for protein protection as antioxidant and for the structural integrity. For the oxidation of the thioether moieties stronger oxidative agents are necessary than for thiols. Mechanistically, for methionine, the reversible oxidation and reduction can be obtained with reactive oxygen species and methionine sulfoxide reductase (MSR), respectively. The

detailed discussion of ROS would exceed this introduction and only a short summary is shown to indicate the importance of these species in conjunction with sulfur-moieties.

ROS draw attention over the last decades and the term itself covers numerous short-living species as e.g. superoxide or hydroxyl radicals.[19] Together with nitric oxide, numerous functions are related to these highly active species including signaling pathways, ROS-mediated response of oxidative stress, caused by the ROS itself, activation of transcription factors but also aging. ROS are produced e.g. in mitochondria as a side-product of oxidative energy metabolism.[20] A balanced formation and scavenging of ROS is essential as numerous processes, such as defence mechanisms by phagocytic cells, proliferation regulation and general signaling, rely on it. Once formed and exhibited their function, ROS has to be scavenged, as e.g. intracellularly over produced ROS can cause numerous drawbacks such as the denaturation of proteins. These denaturations and other ROS-caused drawbacks are often discussed in the context of aging and diseases (see chapter 2.1.2).[4]

In the last decades, more publications arise giving the thioether-functionality of methionine a protective role in protein activity maintenance as “molecular bodyguards”.[4] The formed oxidative stress, caused by ROS, oxidizes the thioether and leads to methionine sulfoxide (Figure 2). After the oxidation a cascade of reduction processes follows and oxidized methionine (MetO) is reduced by MSR, regaining the unoxidized methionine. Reduction of (MetO) is caused by the thiol-oxidation of methionine sulfoxide reductase (MSR), followed by the reduction of the oxidized MSR by the thiol-oxidation of thioredoxin that is finally reduced by NADPH.[21] An oxidation of the sulfur to the corresponding sulfoxide increases the dipole moment that can cause the deformation of proteins.[4] With this mechanism the thioether of methionine scavenges the ROS, leading to a potential structural conformation change but concurrently protecting active sites of the protein from being irreversibly denaturated by ROS.

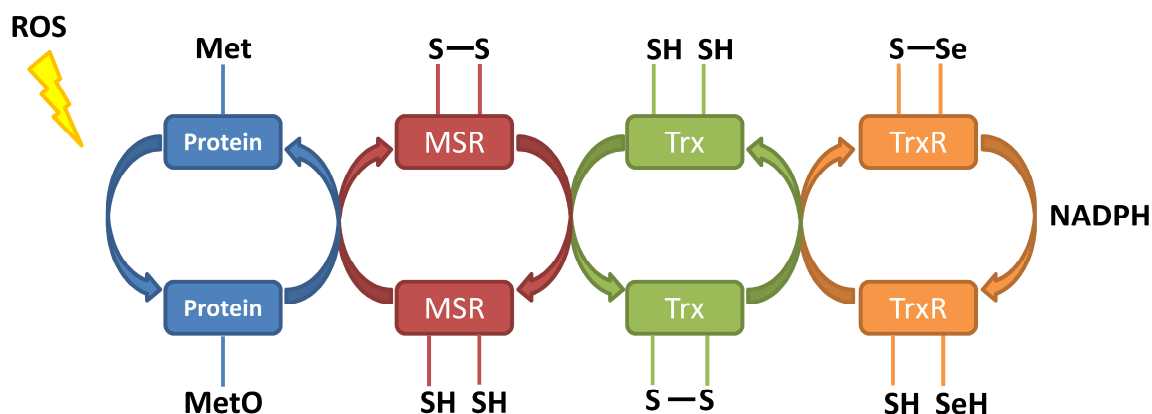


Figure 2: Redox-couples involved in the reduction of methionine sulfoxide-containing proteins. A cascade involving methionine sulfoxide reductase (MSR), thioredoxin (Trx) and thioredoxin reductase (TrxR) leads finally to the use of NADPH for compensating ROS initiated oxidation of a protein. Adapted from [21].

2.1.2. Pathologic aspects

Intra- and extracellular redox-chemistries involve thiols, disulfides, thioethers and sulfoxides and are a complex interplay between all species, covering a tremendous amount of biochemical processes. These systems control numerous pathways that are interconnected with each other. Disturbance of these redox-processes is therefore in many discussion regarding pathologic effects.

As mentioned in chapter 2.1 ROS species play an important role in signaling for breathing, red blood cell production, cell adhesion, apoptosis and cell proliferation and can e.g. induce digestion of proteins by oxidation.[20] Besides this, many other functions are regulated, induced and hindered by ROS. This omnipresence of ROS demands well controlled production and scavenging of the ROS, as the high reactivity and overproduction can lead to severe effects such as denaturation of proteins, inflammations and others. A crucial mechanism for this scavenging is based on the GSH/GSSG redox couple. Regarding different cell states the most negative reductive potential of cells is during proliferation (Figure 3 A). Here it is a rather qualitative description of the cell cycle as the determination of specific values is demanding and depends on cell types and pH-values that can alter in different compartments. Collecting data from literature, Schafer and Buettner state that the whole

cycles happens roughly in an interval of $E_{hc} = -250 \text{ mV} - 190 \text{ mV}$ (half-cell potential E_{hc}). [22] Upon reaching a specific value of the potential (indicated as E_{hc} in Figure 3), differentiation is induced (Figure 3 C) that is switched off (Figure 3 D) reaching redox-potential values that induce apoptosis (Figure 3 E). Too oxidative potentials lead to necrosis (Figure 3 F), as the apoptotic pathways cannot be exhibited anymore.

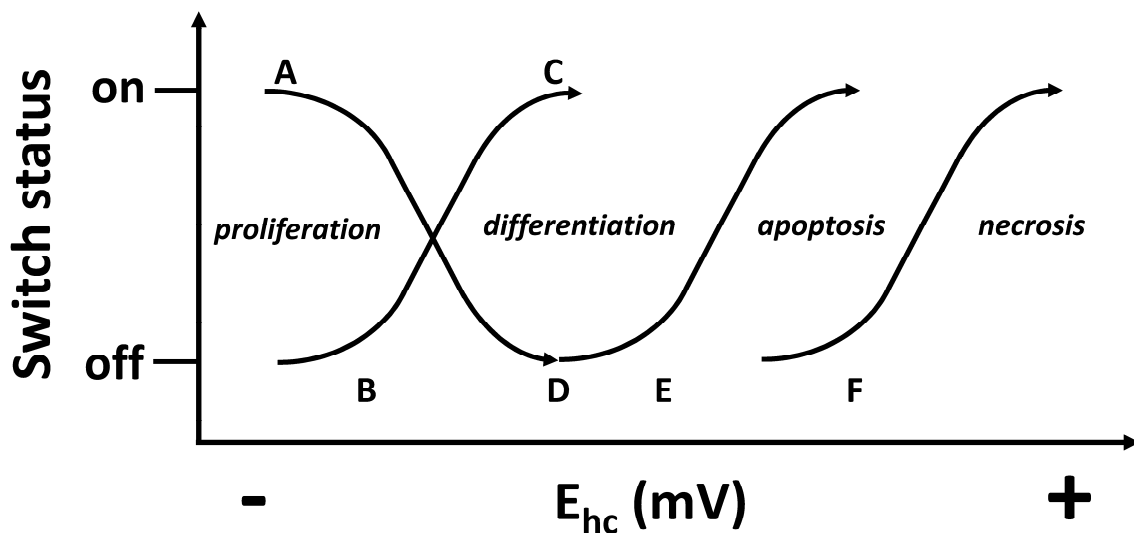


Figure 3: GSH/GSSG potential of cells during the different states. Modified from [22], 2001, with permission from Elsevier.

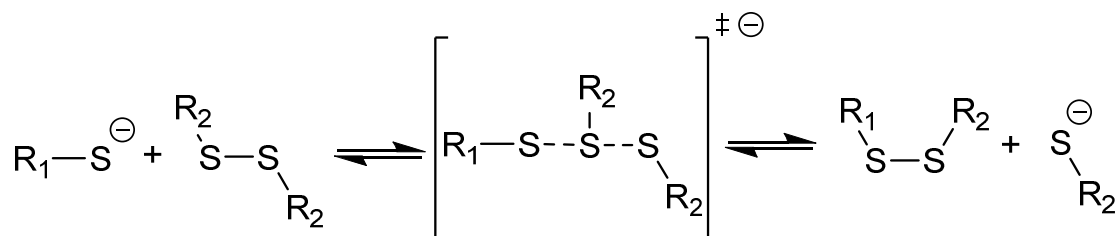
It is noteworthy that oxidative stimuli do not necessarily change the states of the cell and the cause-and-effect relation is not always obvious. As one factor, oxidative stimuli (ROS) are *responsible* for the induction of proliferation, although the cells are here in the most reductive phase of the whole cell cycle. [20, 22] This has led to the observation that many ROS triggered processes were induced, leading to an uncontrolled proliferation of cells and a pro-oxidative shift of the plasma. This led to an enhanced redox-couple production of the cell that finally results in a more reductive extracellular microenvironment in tumor tissues. Investigation of the redox-state of tissues showed that tumor tissue can contain a 4-fold higher concentration of GSH compared to healthy tissue. The increased reductive environment was observed for both intra- and extracellular regions. These data suggest that an oxidative trigger is responsible for an imbalanced cellular response giving somehow contradictory results. [13, 20, 22, 23] This further shows that the complex interplay of oxidants and reductants is very sensitive towards stimuli and an imbalance can cause severe

effects. In contrast to reductive malignant tissues, inflammation sites were shown to be oxidative caused by an oxidative stress involving ROS. [24-27]

2.2. Mechanistic insight into sulfur redox-chemistry

2.2.1. Oxidation of thiol and thioethers

Mechanistically, thiol-disulfide exchange, i.e. oxidation of thiols with disulfides, is assumed to happen via a S_N2 reaction mechanism with the thiolate as active species and the charge delocalized during the transition state (Scheme 3).[28] Calculations further indicate that the charge is transferred without any accumulation at the substitution center.[29]



Scheme 3: Thiol-disulfide exchange is assumed proceeding via a S_N2 mechanism with the thiolate being the active species initiating the exchange.

Experimentally, the determination of the thiol-disulfide exchange rates is rather complicated to investigate as the content of thiolate-species depends on the pH and quenching methods potentially falsify the results. Rothwarf and Scheraga published a detailed study of the rates of the reduction of GSH with DTT examined at different pH values and different temperature. These results further indicated the rather complex determination of rate constants, but eventually the pH-independent rate constants for the glutathione-dithiothreitol equilibrium were shown to be $3.1 - 8.0 \cdot 10^3 \text{ min}^{-1} \text{ M}^{-1}$ (25-37 °C, pH 7.0 – 8.7).[30] This rather fast reaction leads to an equilibration of the system, assuming to have homo- and mixed disulfides. The quantity of the species is based on the stability of the single disulfides and thiols and hence also depends on the reaction partner. DTT forms a six-membered ring upon oxidation, leading to a high thermodynamic stability. DTT is hence a useful agent for the reduction of other disulfides to the corresponding thiol under thermodynamic aspects. In general, upon oxidation of monothiols, dimerization occurs resulting in a loss of entropy. Hence the reduction of disulfides with DTT is preferential for

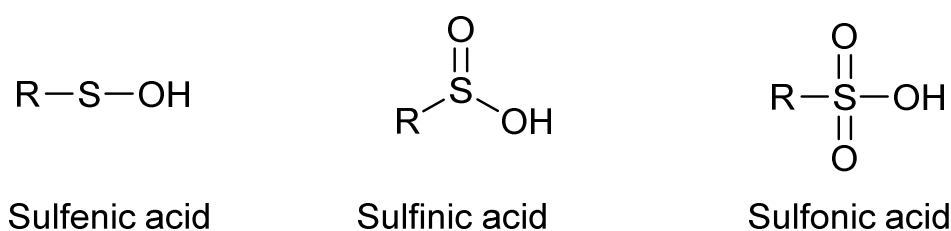
disulfides being cleaved to single molecules as enthalpic and entropic energies do not compete. Reduction potential of DTT is therefore also influenced by the reaction partner. Intramolecular reduction of disulfides by DTT, e.g. by polymers and proteins, has a hypothetically less pronounced entropic driving force as the cleavage of dimers. For equilibration constants, published prior to the studies of Rothwarf and Scheraga, data were between 200 M – 13,000 M (pH 7-8.7, 25 °C-30 °C) for the given equilibrium (in analogy to above mentioned equilibration)

$$K_{eq}^{obs} = \frac{[DTT^{ox}][GSH]^2}{[DTT^{red}][GSSG]}$$

Using different concentrations of GSH and DTT and altered starting conditions for the reaction, Rothwarf and Scheraga ruled out experimental errors and obtained values of $K_{eq}^{obs} = 194 - 237$ M for their studies of the equilibrium at pH 8.0 and 25 °C. DTT is indicated to be a good reduction agent for glutathione. Deviation of their results with other literature was assigned to the investigated systems itself, but also on the method used by altered methods e.g. quenching and analysis.[30] Whereas the direct determination of the species can be accomplished e.g. by HPLC, a derivatization and quantification of the thiols is restricted to alkaline media making the thiolate active for quenching reactions. For the reduction of disulfides and the scrambling of disulfides with thiolate anion, it is generally assumed that the exchange is commonly fast and reduction potential of DTT is heavily determined by the counterpart of exchange due to entropic reasons and pKa values of the thiols.

Additionally being oxidized by disulfides, thiols are also prone to oxidation by oxygen. Thiols are commonly stored under inert atmosphere to prevent their oxidation by O₂, probably catalyzed by impurities. Oxidation of pure thiols in the absence of impurities is also possible but with lower rates. O₂ was described in the beginning of investigation in the 1950 for biologic motifs to readily oxidize thiols (“self-oxidation”), but hints are given that this was caused by metal ions and oxidation is under neutral metal ion-free conditions a rather slow process.[31] Bagiyani et al. studied the self-oxidation in presence of Cu, Mn, Fe, Ni and Co ions at different oxidation states and compared these results to the oxidation in the absence of the ions. They showed that although oxidation of thiols occurs with oxygen under alkaline

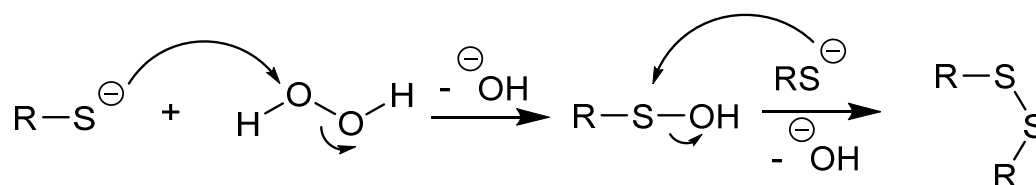
conditions without addition of metal ions, a remarkable increase in oxidation rates can be observed by simply changing the purity of the reaction media. Metal impurities in the borate buffer were responsible for the oxidation, commonly neglected as they were in the range of $5 \cdot 10^{-7} - 3 \cdot 10^{-6}$ g-ion L^{-1} . For acidic (pH 4-5) and alkaline media (pH 9) the self-oxidation was observable. Artificially adding the above mentioned metal ions showed different rates for the oxidation depending on the metal ion. Chelating substrates such as EDTA and cyanide-ions suppressed the oxidation in neutral or basic media, whereas in acidic media the presence of metal ions does not show a significant influence on the oxidation with oxygen. Additionally to the influence of catalytically active metal ions, the oxidation of thiols to the corresponding disulfides can be accompanied by an overoxidation leading to sulfonic acids (Scheme 4) e.g. by O_2 in polar solvents under basic conditions. At 23.5 °C after 24 h 97 % of butanethiol were oxidized to the corresponding sulfonic acid by using hexamethylphosphoramide and KOH.[32] Unfortunately, in this case an analysis of the metal ion content was not performed and hence a possible inconvenient combination of polar media and metal ions must be taken into account.



Scheme 4: Different oxo-acids of sulfur with increasing oxidation from sulfenic acid to sulfonic acid.

As the self-oxidation of thiols by O_2 is a rather uncontrolled process, the storage of thiols under inert atmosphere is essential. For an artificially induced oxidation, and hence dimerization, commonly H_2O_2 , or H_2O_2 producing agents (e.g horseradish peroxidase and alloxan) are used.[33-35] Under basic conditions the thiolate-anion nucleophilically attacks one of the oxygen atoms in hydrogen peroxide. An additional complexation of the leaving group (OH^-) of hydrogen peroxide concurrently leads to an enhanced rate of oxidation as the leaving group is more likely removed.[36] Substitution of the OH^- group forms sulfenic acid that is readily attacked by a second thiolate anion. This formed acid readily reacts with a

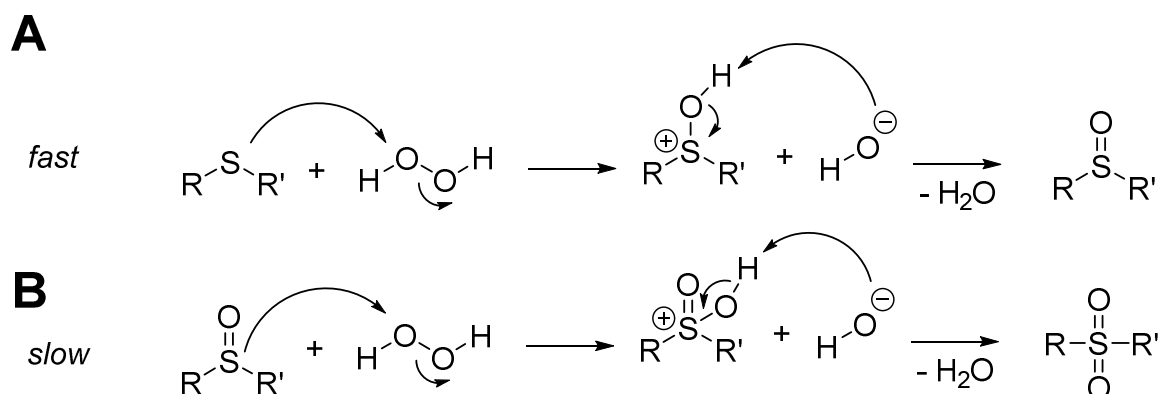
thiolate anion and builds the corresponding disulfide (Scheme 5), whereas with an excess of hydrogen peroxide an overoxidation to sulfonic acid and other sulfoxides might occur.[37]



Scheme 5: Oxidation of thiols by hydrogen peroxide.

A corresponding reduction of the obtained disulfides is commonly accomplished using other thiols (DTT), phosphines (TCEP) or reductive agents such as NaBH_4 .

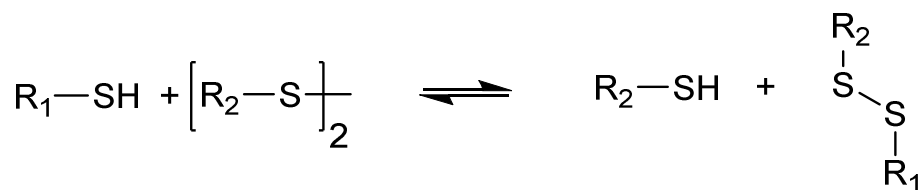
The mechanism for thioether oxidation is based on the nucleophilic attack of the free electron pairs of sulfur to e.g. hydrogen peroxide (Scheme 6).[38] In contrast to the oxidation of thiols to disulfides, the oxidation of thioethers also proceeds in neutral and acidic media. Here the first oxidation is faster than the subsequent oxidation making the isolation of sulfoxides easy.[38]



Scheme 6: (A) Oxidation of thioethers with hydrogen peroxide to the corresponding sulfoxide and (B) to the corresponding sulfones afterwards. The oxidation to sulfones is generally slower than the first oxidation to sulfoxides.

2.2.2. Detection and quantification of thiols

Detection and quantification of thiols is mainly based on the same thiol-disulfide exchange. Here, aromatic disulfides are used having a high driving force to oxidize thiols to the corresponding disulfide. For the equilibrium shown in Scheme 7 a low pKa of the disulfide (assuming to be the quantification reagent) facilitates the exchange and a release of $\text{R}_2\text{-SH}$.[39]

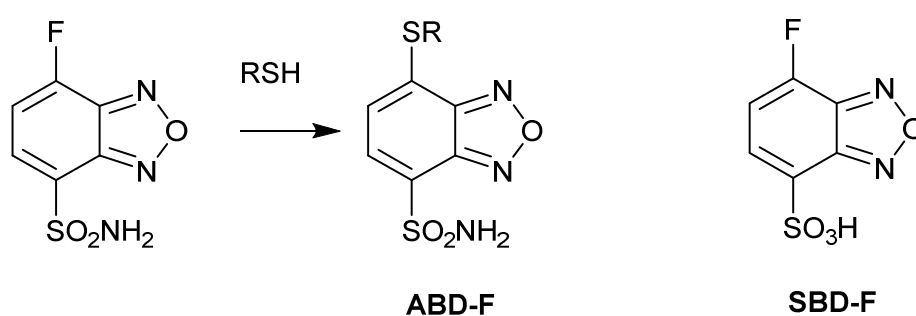


Scheme 7: Thiol-disulfide equilibrium with the disulfide species being the substrate for the quantification of the thiol species R_1-SH .

Ellman showed in the 1960s the use of a disulfide readily exchanging with thiols due to electron withdrawing substituents. 5,5'-dithiobis-(2-nitrobenzoic acid) reacting with the thiols to be quantified is still a versatile method nowadays for UV-Vis spectroscopy based determination of thiols by derivatization. Here the nitro- and carboxyl-substituted dimerized thiophenol is used, having a reduced electron density at the sulfur-atom due to an aromatic conjugation and the electron withdrawing effects. The disulfide-bond of Ellmans reagent is hence readily attacked by thiolate anions forming the mixed disulfide (Scheme 7 $R_2-S-S-R_1$ with $R_2 = 2\text{-nitro-5-thiobenzoic acid}$). An aromatic compound detectable by UV-Vis spectroscopy is released and its absorbance measured at $\lambda = 412 \text{ nm}$ yielding the content of thiols in the solution, after calibration with a known thiol-compound. As the exchange is caused by the thiolate species, pH values lower than 7, depending on the thiol, are required for the quantification. Drawbacks, such as limited sensitivity, are approached by alternatives also detectable by UV-Vis spectroscopy with higher extinction coefficients.[40-42]

Although also restricted to higher pH-values, alternatives to the thiol-disulfide exchange based quantification are applied. Thiols being deprotonated under neutral to alkaline conditions are strong (soft, with respect to the HSAB concept) nucleophiles and addition to fluorophores can be used for the quantification. It has to be noted that Ellmans reagent releases a UV-Vis detectable moiety, whereas the direct attachment of fluorophores stains the thiol itself. Unfortunately, fluorophore attachment usually lacks in selectivity as electrophilic groups, e.g. isothiocyanates, at the fluorophore are also prone to the attack of nucleophiles such as amines. More selective Michael-acceptors, such as maleimides in conjunction with a fluorophore, react fast with the thiolate-anion and are applied for a quantification of thiol-compounds. Here, depending on the conditions, a reverse Michael-addition and thiol exchanges were reported for maleimides or α,β -unsaturated ketones (e.g.

observed at the open form of furazolidone).[43, 44] A permanent selective dye changing the fluorescent properties specifically by the reaction with thiols was described in 1984.[45] 4-(Aminosulfonyl)-7-fluoro-2,1,3-benzoxadiazole (ABD-F) was synthesized and showed enhanced reactivities towards thiols, compared to its alternative that also detected amines (SBD-F) (Scheme 8). The reaction with thiol model compounds was completed to 90 % after 5 min at 50 °C at a pH of 8 and showed no reaction with amines under these conditions making it selective for thiol quantification.[45, 46] Furthermore, in contrast to SBD-F, the reaction conditions were quite mild allowing this method being applicable for biologic motifs.



Scheme 8: Fluorescent benzoxadiazole dyes used for the quantification of thiols.

Quantification of thiols are widely applied and performed extrinsically by fluorophores using UV-Vis spectroscopy. Although methods such as NMR, IR and Raman spectroscopy are able to detect the thiols as intrinsic moieties, these methods are commonly not applied for quantification purposes. In IR-spectroscopy the stretching vibration of R-S-H is observed at $\nu = 2551 \text{ cm}^{-1}$ for cysteine in H₂O and the presence of thiols can be investigated. The large mass of the sulfur atom leads to a shift of the stretching band to a region commonly less crowded with other IR signals, beneficial for the detection of thiols.[47] Unfortunately, the signal strength is weak in IR spectroscopy, making low contents of thiols hard to detect. Changes in the dipole moment during vibration are the basic principle of IR spectroscopy and a more pronounced change in the dipole moment during vibration yields a higher absorption coefficient and hence a higher signal intensity. As environmental changes such as coordination or solvent effects alter the intensity, an alteration in the band intensity is not solely concentration but also environment-dependent. For Raman spectroscopy the change in polarizability is significant and for thiols higher signal intensities can be observed. Although this method is beneficial for the detection of thiols, this method is not quantitative.

A same trend can be observed for disulfides, being detected only as a weak signal in IR-spectroscopy but yield stronger signals in Raman spectroscopy.

^1H -Nuclear magnetic resonance spectroscopy allows the detection and quantification of thiols yielding a signal at high fields with $\delta \approx 1.3\text{-}2.5$ ppm depending on the substituents and neighboring groups. Protic deuterated solvent, such as D_2O , can cause a deuteration of the thiol by a fast H-D exchange. The deuterated thiol-group cannot be detected by ^1H -NMR spectroscopy. With this, only non-protic solvents such as CDCl_3 are useful for the thiol quantification via ^1H -NMR. Here, quantification is possible, however applications are quite restricted and commonly not useful for biologic systems with thiols as they either require aqueous environments or demand polar-protic solvents for dissolving the substrates. ^{33}S -NMR spectroscopy is possible due to the 3/2 spin nucleus, but the natural abundance is low (0.75 %) and signals are commonly broad. Although quantification is possible, the relative abundance might cause large errors that make this method inappropriate for a standard quantification of thiols.

2.3. Anionic ring-opening polymerization

The application of polymers in biological systems requires the control of molar masses to gain e.g. reproducibility and tailoring the system. Depending on the polymer, different techniques are used to control the DP and molar-mass distributions. For synthetic polymers, in contrast to biologic polymers such as proteins, usually a molar mass distribution is obtained that can be characterized by the dispersity \mathcal{D} . This is defined as the ratio between mass-average molar mass M_w and number-average molar mass M_n . [48]

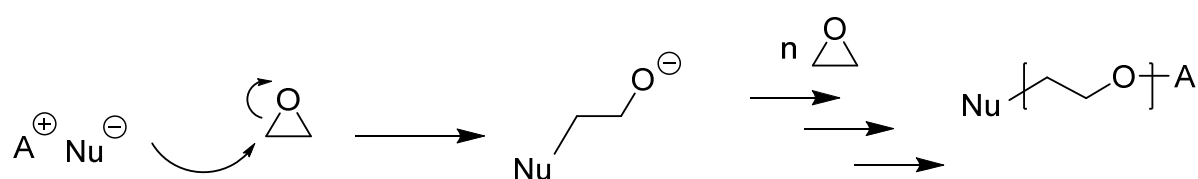
$$\text{Number-average molar mass} \quad M_n = \frac{\sum_i n_i M_i}{\sum_i n_i}$$

$$\text{Weight-average molar mass} \quad M_w = \frac{\sum_i n_i M_i^2}{\sum_i n_i M_i}$$

$$\text{Dispersity} \quad \mathcal{D} = \frac{M_w}{M_n}$$

Here n polymer molecules with mass M are summed up and divided by all polymer molecules. Therefore M_n is the arithmetic mean. For the weight-averaged molar mass the contribution of high molar-mass molecules is larger than of low molar-mass molecules. In the case of a specific molar mass, such as for proteins, $M_w = M_n$ and hence $\mathcal{D} = 1$. For polymers, synthesized by a polymerization without transfer or termination reactions, usually values close to 1 can be obtained. Techniques for the controlled polymerization of polymers depend on the nature of the monomer. Polymerizations of unsaturated monomers, e.g. (meth)acrylates via radicals mechanisms, can be controlled with transition metals (Atom-Transfer-Radical Polymerization ATRP) or organic agents (Reversible Addition-Fragmentation chain Transfer (RAFT), Nitroxide-Mediated Polymerization (NMP)). This control is a focus of polymer synthesis research to expand the polymer variety with respect to monomers, architecture and functionalities.

Another technique for synthesizing polymers with a narrow molar-mass distribution relies on the ring-opening polymerization of strained rings. Ring-strain of three- and four-membered heterocycles, such as epoxides and episulfides, allows an easy opening of the ring via nucleophiles. Monomers bearing strained heterocycles are therefore prone to be polymerized, initiated with nucleophiles, e.g. alkoxides. For instance, ring-strain enthalpy of epoxides of $H = 114 \text{ kJ mol}^{-1}$ [49] allows the thermodynamically favored opening, forming an alkoxide that can open further epoxides resulting in a sequential opening and addition of epoxide-containing monomers (Scheme 9).



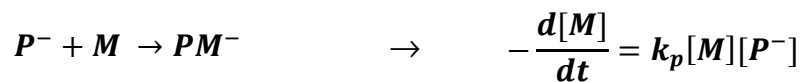
Scheme 9: Ring-opening polymerization of ethylene oxide with a nucleophile and its corresponding counter-ion A^+ .

This ionic polymerization is a chain growth polymerization having an active chain end and, in case of no termination or transfer reaction, this terminal alkoxide will add more and more monomers until no monomer is left. This *living* anionic ring-opening polymerization leads to narrow molar-mass distributions in the case that all chains are started at the same time. As all active ends are equally reactive, and no termination occurs, the ratio of monomer-to-

initiator determines how many monomers can be added to each initiator and hence the ratio $[M]:[I]$ determines the DP.

Initiation starts with the first nucleophilic attack of the initiator at the monomer that is assumed to be fast, relative to the polymerization itself. With this, and the assumption that no termination and transfer reactions occurs, the concentration of the initiator $[I^-]$ equals the concentration of the active chain ends $[P^-]$.

Time-dependent decrease of the monomer concentration $[M]$ is therefore determined by the concentration of the monomer itself $[M]$ and the active chain end $[P^-]$ with the rate constant k_p .



Assuming that the concentration of the active end, equaling the initial concentration of the initiator, is constant it can be combined with the polymerization rate yielding the observable, apparent, rate constant k_{app} .

$$k_p[P^-] = k_{app} = \text{const} \quad \rightarrow \quad -\frac{d[M]}{dt} = k_{app}[M]$$

With this, the time-dependent change of $[M]$ can be written and integrated.

$$\frac{d[M]}{[M]} = -k_{app}dt \quad \rightarrow \quad -\int_{[M_0]}^{[M_t]} \frac{1}{[M]} d[M] = k_{app} \int_{t=0}^t dt$$

Solving the integral gives, with $\int 1/x = \ln(x)$ and $\ln(x) - \ln(y) = \ln(x/y)$,

$$-(\ln([M_t]) - \ln([M_0])) = -\ln\left(\frac{[M_t]}{[M_0]}\right) = k_{app}t$$

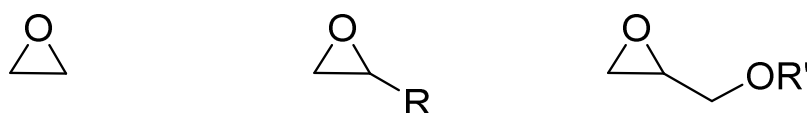
With this equation, plotting $-\ln\left(\frac{[M_t]}{[M_0]}\right)$ against t leads with the slope to the apparent rate constant k_{app} . Furthermore does this data processing indicate side-reactions and deviations from the living polymerization, as a non-linear relation would be observable.

The structurally most simple epoxide monomer available for this anionic ROP is ethylene oxide (EO) forming poly(ethylene glycol)/poly(ethylene oxide) after polymerization. Although structurally equal, for molar masses $M > 20000 \text{ g mol}^{-1}$ the term poly(ethylene oxide) is used, whereas the term poly(ethylene glycol) is used for molar masses $M < 20000 \text{ g mol}^{-1}$. The resulting oligomers or polymers have \bar{D} close to 1, and are used in a variety of fields, e.g. biomedical formulations, calibration standards or as solvent. A chemical modification of PEG/PEO happens controlled at the termini as no other functionalities are available, making this modification highly selective, but restricted. Several publications are available purely dealing with the chemistry of peptide and protein PEGylation.[50]

2.4. Polyglycidols

2.4.1. Polymerization

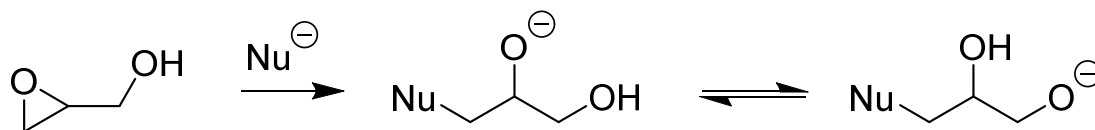
Structural variations of ethylene oxide using mono-substituted epoxide rings were investigated over the last decades and give a more detailed view on possibilities, problems and varying kinetics. Recently published reviews of Carlotti et al.[51] and Frey et al.[52] summarize the synthetic efforts done and mechanistic issues overcome over the last decades to control polymerization of epoxide- and glycidol-derivatives (Scheme 10). In general, for both epoxide- and glycidol-derived polymers, the structural varieties and influencing factors on polymerizations show that there is no standard protocol that can be used for the ring-opening polymerizations. The interplay of complexation, nature of the active species, side-reactions and polymerizability of the monomer have to be balanced for each newly synthesized or commercially available monomer.



Scheme 10: Ethylene oxide (left), epoxide (middle) and glycidyl-ether (right) units used for anionic ring-opening polymerizations.

Glycidol allows the tailor-made modification of glycidol-based polymers already at the monomer-stage through hydroxy-chemistry. The focus will therefore be given on the literature overview of glycidol-derivatives containing and -derived polymers.

Attempts to directly polymerize glycidol lead to branched polyglycidol as the hydroxy-group of glycidol undergoes an acid–base reaction with the active chain ends (Scheme 11).



Scheme 11: Acid-base reaction of the active chain end and the hydroxy group of glycidol during polymerization.

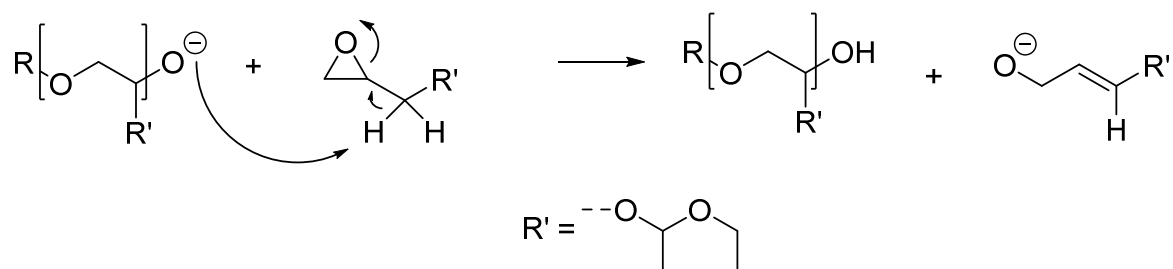
A detailed investigation of the glycidol-polymerization with various bases at room temperature was given by Sandler and Berg[53] in 1966. Amine bases, hydroxides and alkoxides and calcium chloride were stirred at room temperature for 1-3 d with conversion determined to be 38-88 %. The authors assumed to have synthesized linear poly(glycidol) that was corrected later on by Vandenberg et al.[54] Decades later the group of Frey published the synthesis of hyperbranched polyglycidols being able to control the molecular weight, branching and dispersity. Using a triol as initiator activated to only 10 % and slowly adding glycidols allows the synthesis of hyperbranched poly(glycerol)s with DP = 15-83 and dispersities below $\bar{D} = 1.5$. Additionally, a control of the reaction parameters allows to diminish and avoid cyclization reactions known for glycidol polymerization.[55, 56]

In parallel to the branched poly(glycidol)s the synthesis of linear poly(glycidol)s was also investigated since the discovery of polymerizing glycidol. The first synthesis of linear poly(glycidol)s was described in 1968 by Tsuruta et al. by polymerizing trimethylsilyl glycidyl ether (TMSGE) with organometallic compound as dibutyl-magnesium, partially hydrolyzed triethyl aluminium or partially hydrolyzed diethyl zinc.[57] The obtained poly(trimethyl silyl glycidyl ether) was hydrolyzed either with hydrochloric acid in water or methanol yielding the first described “pure” linear poly(glycidol). As the stability of the TMS group under basic conditions was insufficient a more base-stable protective group for the hydroxy-group of glycidol was developed. Acetal-derivatization of the hydroxy-group of glycidol was described by Fitton et al. giving a highly stable protective group under basic condition.[58] Using a *p*-toluene sulfonic acid catalyzed hydroxylation of ethyl vinyl ether with glycidol yielded ethoxy ethyl glycidyl ether (EEGE), still a common monomer nowadays for poly(glycidol) synthesis.[59-65] The first attempt to polymerize EEGE and obtain linear poly(EEGE) was

performed in 1994 in the group of Spassky with CsOH, an aluminium-salcn complex or potassium intercalated into a graphite structure, as initiator.[66] Only CsOH gave polymeric products with $DP \approx 200$ and $M_n = 32,000 - 34,000 \text{ g mol}^{-1}$. Unfortunately, dispersities were not satisfying ranging from $\mathcal{D} = 1.38-1.89$ depending on the conditions. After the successful synthesis of poly(EEGE) the acidic hydrolysis was performed either with formic or hydrochloric acid. The disadvantage of formic acid was the formic ester formation of the obtained OH-side chains. A saponification step had to be performed afterwards to obtain pure poly(glycidol). Using HCl in THF for acetal-hydrolysis directly gave the desired poly(glycidol) although a chain degradation of $DP = 234$ to $DP = 174$ was describe with a concurrent broadening of the dispersity from $\mathcal{D} = 1.4$ to $\mathcal{D} = 1.6$. According to Dworak et al. the broad dispersity of poly(EEGE) was a result of the synthesis in a heterogeneous system due to the insolubility of CsOH under such conditions. Hence, polymerizing EEGE with potassium *tert*-butoxide (KO*t*Bu), soluble in dry THF, as oxyanionic initiator at 60 °C yielded poly(EEGE) with molar masses $M_n = 2550-13390 \text{ g mol}^{-1}$ and $\mathcal{D} = 1.18-1.20$. Quenching the oxyanionic species was achieved using *p*-chloromethyl styrene. Acetal-protected styrene-terminated poly(EEGE) and OH-functional styrene-terminated poly(glycidol) were subsequently radically copolymerized with styrene yielding poly(EEGE)- or poly(glycidol)-grafted poly(styrene).[67] Lack of dispersity- and molar mass-control caused by a heterogeneous polymerization by Taton et al.[66] with Cs^+ as counter ion was circumvented by Dworak et al. later on. PEG with molar masses $M_n > 1000 \text{ g mol}^{-1}$ was converted with CsOH to the corresponding Cs-alkoxide as a benzene-soluble initiator.[65] For this, CsOH was dissolved in water and reacted with PEG having $DP = 45-227$. Refluxing with benzene and subsequently azeotropically removing water and benzene yielded the bifunctional Cs-alkoxide that initiated the polymerization of EEGE with 27-68 repeating units at each terminus at 60 °C. Resulted triblock-copolymers were crosslinked via the poly(glycidol) side-chains with glutaraldehyde and it was demonstrated that swelling occurs mainly due to sorption of the water or methanol at the PEG sites. Swelling studies of glutaraldehyde crosslinked poly(glycidol) and glutaraldehyde crosslinked poly(vinyl alcohol) indicates a higher hydrophilicity of poly(glycidol) ascribed to the hydrophilic backbone. After controlled polymerization protocols were published, a detailed investigation of further glycidyl-monomers was published in 2007 by the group of Möller.[62] Here EEGE, allyl glycidyl ether

(AGE) and *tert*-butyl glycidyl ether (*t*BGE) monomers were (co)polymerized at 120 °C in diglyme with potassium 3-phenylpropanoate and the kinetics of the polymerization investigated. Molar masses of $M_n = 2400\text{-}3800 \text{ g mol}^{-1}$ were obtained with 21-40 repeating units, depending on the monomer. First-order kinetic plots and a linear $\ln(M_0/M_t)$ -conversion relationship indicate the living character of all monomer polymerizations. Dispersities are given to be $\mathcal{D} = 1.09\text{-}1.27$. Subsequent deprotection leads to the selective removal of different protective groups yielding e.g. poly(allyl glycidyl ether-*co*-glycidol). Although narrow molar-mass distributions could be obtained with M_n up to 3800 g mol^{-1} , side-reactions might occur with AGE[68] and especially at higher temperatures and higher molar masses also with EEGE.[61] It was shown that with polymerizing EEGE, AGE and *t*BGE at the mentioned conditions the polymerization rates decrease in the order EEGE > AGE > *t*BGE. Interestingly, with a polymerization at 40 °C in bulk with Cs/triethyleneglycol monomethylether as initiator the copolymerization rate of EEGE and AGE indicate a slightly higher rate for AGE than EEGE as was published recently.[69]

Besides the limited control of molar mass and dispersity occurring in heterogeneous polymerizations,[66] known side-reactions also occur in homogeneous media. Side-reactions are also well known in anionic ring-opening polymerizations for propylene oxide and rely on H-abstraction by the active chain end. Deprotonation of the CH₃-group at propylene oxide produces allyl-alkoxides able to initiate the polymerization as was already investigated decades ago.[70] This kind of side-reaction was also observed within EEGE polymerization (Scheme 12). Studies were performed with potassium 3-phenylpropanoate in THF at 60 °C and in diglyme at 120 °C as well as with Li/phosphazene base at 20 °C.[61]

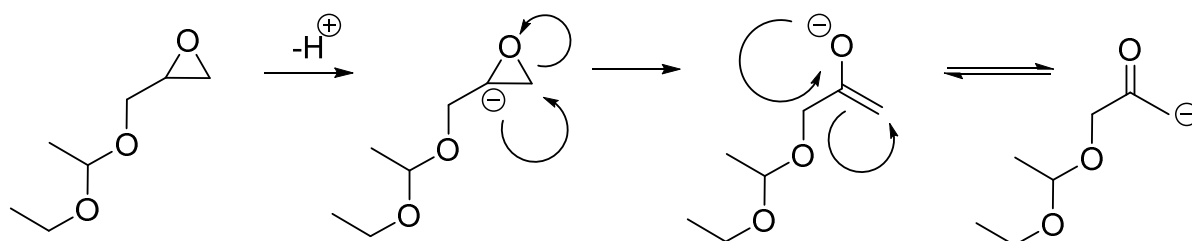


Scheme 12: H-abstraction at EEGE initiated by the active chain end of poly(EEGE).

Low-molecular weight fractions are obtained if the formed allyl-alkoxide is able to initiate a new polymer chain. This terminal allyl alcohol starts to polymerize EEGE upon formation and

can be observed in SEC as a tailing in the elugramm. The side-reaction of H^+ -abstraction due to the basicity of the active species is said to reduce the overall molar-mass and increase dispersity \mathcal{D} . Hans et al.[61] state that polymerization performed at 60 °C (with K^+ as counter ion) is the highest temperature that should be used to minimize this side-reaction. Here, the formed allyl-functional monomer is able to initiate the EEGE polymerization and, depending on the reaction conditions, up to 44 % of the end groups were determined to be initiated by this unsaturated monomer. It was concluded that upon aiming higher degrees of polymerization a reduction of the basicity of the active chain end and keeping the nucleophilicity of the alkoxide constant is necessary. This theory can be confirmed by the investigation of EEGE polymerization with Li^+ /phosphazene base. The reaction was shown to already happen at room temperature, simultaneously increasing the content of allylic end groups. With this method only $DP \approx 200$ can be obtained as the upper limit giving $M_n \approx 30.000 \text{ g mol}^{-1}$.

Beside the deprotonation reaction in vicinity to the epoxide ring, this H-abstraction can also occur at the epoxide-ring itself. This type of side-reaction is determined by the H^+ -abstraction of the monomer by the active species. [52, 61] The formation of a carbanion results in a ring-opening of the epoxide and the obtained enolate equilibrates with the corresponding carbanionic carbonyl compound (Scheme 13).



Scheme 13: Mechanism assumed for the formation of the enolate species by former H^+ -abstraction.

This carbanion is also able to initiate a new polymerization. In contrast to the former side-reaction the carbonyl- group is also prone to nucleophilic attacks by oxyanions already existent in the reaction mixture. Upon addition of an active chain to the carbonyl-terminated polymer, a coupling of two polymer chains occurs, leading to a doubling of the molar mass, observable as an additional high-molecular weight fraction in SEC.

Limitations by these side-reactions were recently overcome by activating the monomer and increasing its electrophilicity. With this monomer activation, the basicity of the active species stays constant. This was possible changing the initiator system from alkali-alkoxide initiated anionic ring-opening polymerization to a monomer-activated anionic polymerization with triisobutylaluminium and tetraoctylammonium bromide as initiator.[71] Another approach of reducing the side-reactions was performed directly using the alcohol as initiator and a phosphazene base (without the use of Li^+ as in the paper of Hans et al[61]) giving degrees of polymerizations for poly(EEGE) and poly(AGE) up to $\text{DP}=80$ with dispersities of 1.08-1.15.[72]

A way to reduce the side-reaction with alkali-alkoxide mediated polymerization in the lower molar-mass region is the simple reduction of the temperature as was stated above. Regarding this, inconsistent approaches to polymerize EEGE, EO and AGE are published. Polymerization temperature ranges are from RT to 120 °C and solvents such as diglyme, THF, DMSO and dioxane or bulk conditions are used. Additionally, although dispersities of published polymers are shown to be narrow, work-up is only sometimes performed. Depending on the publication, washing[62] or precipitation[68] is performed and no values are given for the crude polymer. As the solubility properties might depend on the polymer length[73], work-up might alter the results for high- or low molar mass fractions, falsifying the values obtained by analytics. Information on the raw-polymer is not always given, making the choice of good reaction conditions hard to find. Recently, a statistical and block-copolymerization of EEGE and AGE was published at 40 °C with cesium as counterion[69] in analogy to the statistical and block-copolymerization of EO with AGE.[68] The degrees of polymerization of poly(EEGE-co-AGE) were up to 25 repeating units and no hint was given on the side-reactions for with longer polymer chains under these conditions.

2.4.2. Functionalization

Nowadays, the polyether polyol poly(glycidol) is found in a variety of research disciplines, whereas the focus varies a lot. A more polymer-chemical focus relies on the introduction of functional groups by polymer-analog modification strategies or the synthesis and polymerization of new monomers. Wurm et al. described the synthesis of a monomer with vicinal hydroxy-groups protected with an acetal-group. Polymerization of ethylene oxide was

performed first with Cs⁺ as counterion and subsequently the synthesized isopropylidene glyceryl glycidyl ether (IGG) was polymerized with the Cs-initiator at 80-90 °C yielding poly(EO-*block*-IGG) block-copolymers. Homopolymeric poly(glyceryl glycerol) (poly(GG)) or copolymeric poly(EO-*block*-GG) with molar masses of $M_n = 1100-7800 \text{ g mol}^{-1}$ and $\bar{D} = 1.05-1.18$ were obtained after acidic hydrolysis with HCl. The introduction of amine-functionalities into poly(ethylene oxide)/poly(glycidol) was presented in the group of Frey. The synthesis of two new monomers, i.e. dibenzylamino glycidol (DBAG)[74] and *N,N*-diallylglycidyl amine[75], was described allowing an incorporation of 2-24 % amino-functionalities into the polymer. Although the functionality is introduced by a functional monomer, a polymer-analog deprotection has to be performed. Synthesizing dibenzylamino glycidol requires the reaction of dibenzylamine with epichlorhydrin with a subsequent ring-closure of the obtained *N,N*-dibenzyl-3-chloro-2-hydroxypropylamine under basic conditions. Copolymerization of EO and DBAG was monitored using a modified ¹H-NMR protocol with a delay of 30 s between the measurements. Although the polymerization of EO is slightly faster, a random copolymer is obtained as both monomers are available until the very end of polymerization. This effect was temperature-independent as was investigated between 25 and 70 °C. Removal of the protective group was obtained under Pd-catalyzed hydrogenolysis. In 2012 the group of Frey claimed to have improved the efficacy of the amine-functionalization using *N,N*-diallyl glycidyl amine as comonomer. Here, the monomer is obtained via a one-step procedure in contrast to aforementioned two steps. After copolymerization, isomerization of the *N,N*-diallyl-groups leads to enamines that are cleaved under acidic conditions via hydroxylation of the double bond and final cleavage of the obtained hemiaminal, yielding the amine-functional poly(ethylene oxide). Generally the yields are higher and shorter reaction times required. The copolymerization was showing the same trend as was found before for the *N,N*-dibenzylglycidyl amine yielding random-copolymers with a slightly higher polymerization of EO observed by online ¹H-NMR monitoring.[75]

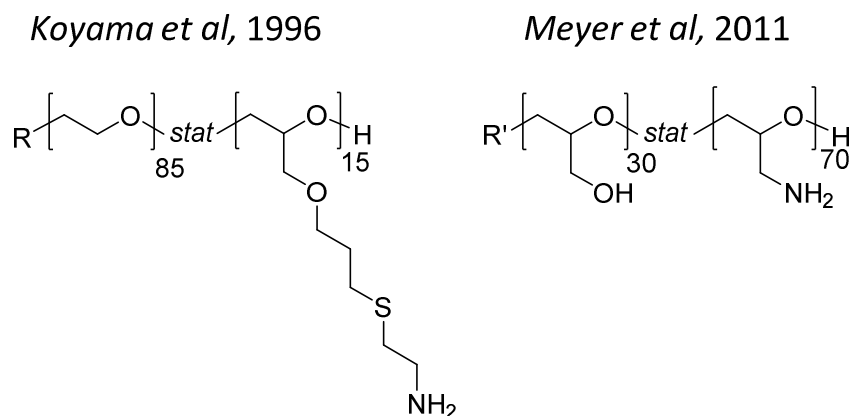
Another approach of functionalization of homopolymeric poly(glycidol)s is performed by polymer-analog reactions. A nice library of polymer-analog derivatized poly(glycidol)s was given in 2009 mainly using Williamson ether synthesis and esterification reactions to obtain multiple functional groups at the poly(glycidol)s side-chain.[76] Deprotonation of the

hydroxy-groups with sodium hydride gives alkoxides being readily reactive towards alkyl halides in THF. Solely with this ether synthesis carboxy-, alkynyl-, epoxide- and allyl-functional poly(glycidol)s were available with yields usually higher than 80 % and efficiencies higher than 60 % indicating an enormous versatility of poly(glycidol)s regarding their functionalization.[76]

Copolymerizations of different monomers were performed to introduce functionalities that allow a more precise polymer-analog functionalization. Monomers used for the synthesis of linear poly(glycidol)s comprise e.g. trimethyl silyl glycidyl ether, *tert*-butyl glycidyl ether, allyl glycidyl ether and ethoxy ethyl glycidyl ether. Although all are commercially available the latter is commonly described to be self-synthesized due to the high price of approximately 1000 US-\$/100 g (Synthonix).[52, 65, 77-79] Allyl glycidyl ether was copolymerized with ethylene oxide yielding allyl-functional poly(ethylene oxide) derivatives. Cysteamine-addition via thiol-ene chemistry was already described in 1996 by the group of Koyama. These amine-functional poly(ethylene oxide) derivatives form complexes with fatty acids.[80] Later, the compaction of DNA was shown by the same group.[81] Polymer-analog amine-functionalization of poly(ethylene oxide) described by Koyama was reinvestigated by Obermeier et al. in 2011.[68] Copolymerization of EO and allyl glycidyl ether was investigated in more detail than done before by Koyama. Random poly(ethylene oxide-*stat*-allyl glycidyl ether) copolymers were obtained that showed monomodal and narrowly distributed molar-mass distributions. Additionally, both monomers were equally introduced into the polymer. A thermal initiated thiol-ene reaction was performed with various thiols, e.g. cysteamine, thioglycolic acid and glutathione. With this copolymer a large variety of functionalized copolymers are accessible, if a thiol-derivative is used as a substrate.

Orthogonal polymer-analog introduction of amine-functionalities was also shown by Meyer et al..[82] Here, epichlorhydrin was copolymerized with EEGE using triisobutylaluminium and tetraoctylammonium bromide as initiator. After acidic hydrolysis of the acetal-protective group a chlorine substituted poly(glycidol) was obtained. This polymer was modified with an azide and subsequently reduced with triphenylphosphine to yield poly(glycidol-*stat*-glycidyl amine). The amine-functionalities introduced by Koyama and Meyer differ, as the distance of the amine-functionality to the backbone is altered that might hinder reactions with steric

demanding substrates (Scheme 14). Hydrophilic PEO and PG backbone are functionalized with amines being protonated in aqueous environment and therefore further increase hydrophilicity. Whereas the side-chains of Koyamas polymer insert hydrophobic parts, it is assumed that the polymers with the direct attachment of the amine do not show significant hydrophobic parts.



Scheme 14: Amine-functional polyethers synthesized by Koyama et al. and Meyer et al.[80, 82]

Direct thiol functionalization of poly(glycidol)s, via the thiol-ene route of Koyama, is not possible as thiols are consumed during the thiol-ene reaction. Direct polymerization of thiol-functional glycidol is also not possible as thiols are approximately 7 orders of magnitude more acidic than alcohols, leading to the protonation of the active species. For this, esterification reaction of the hydroxy-group of poly(glycidol) was published by Li et al.[76] as well as Groll et al.[83] leading to thiol-functional poly(glycidol)s. Here either thiol-functional 3-thiopropionic acid or the disulfide-linked 3,3'-dithiopropionic acid were used and esterified with $\text{HfCl}_4 \cdot 2\text{THF}$ or DCC/DMAP, respectively. Subsequent cleavage of the disulfides with DTT or TCEP as reducing agent gave thiol-functional poly(glycidol). Hydrolytic instability of the ester-containing redox-sensitive poly(glycidol) was circumvented by the group of Tovar, synthesizing ester-free thiol-functional poly(glycidol).[77] For this, poly(ethylene oxide-*stat*-ethoxy ethyl glycidyl ether) was synthesized having molar-masses of $M_n = 2760 \text{ g mol}^{-1} - 4700 \text{ g mol}^{-1}$ and dispersities of $\mathcal{D} = 1.42 - 1.88$. A $\text{KO}t\text{Bu}$ initiated polymerization was performed in a mixture of dry DMSO and THF (resulting from the initiator solution) at 60°C . The authors assigned the broad dispersity to the use of DMSO as solvent, causing chain-transfer reactions. Acidic cleavage of the acetal protective group gave hydroxymethylene

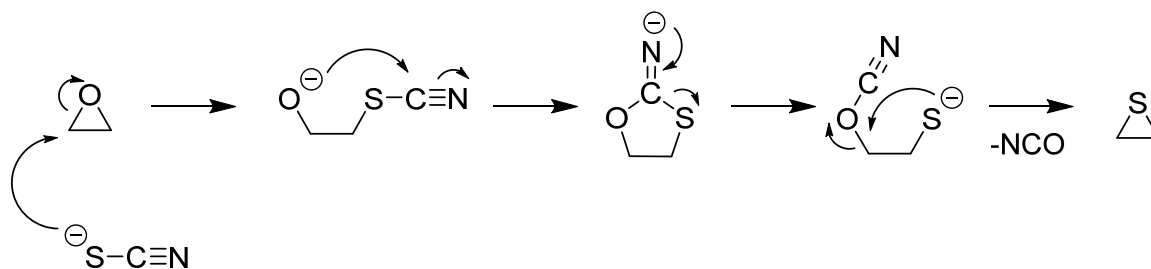
substituted poly(ethylene oxide). The tosylation of the hydroxy-groups was performed with 1.5 eq. of tosyl chloride with respect to the hydroxy-groups yielding a quantitative conversion to the corresponding tosylates. Only at higher degrees of approximately 60 % hydroxy-groups the conversion drops to about 87 % caused by steric hindrance. Under basic condition the polymer-tosylates were converted to the corresponding polymer-trityl thioethers that could be deprotected using TFA yielding poly(ethylene oxide-*stat*-glycidyl thiol). Hydrogels with these polymers and PEG-diacrylates showed no toxic effect towards human fibroblasts.[77]

2.4.3. Cytocompatibility

In 2006 a detailed study of the cytocompatibility of linear and branched poly(glycidol)s was published.[71] The authors performed coagulation-, red cell aggregation-, complement- and platelet activation, and cytotoxicity test with linear and branched poly(glycidol) and animal studies with branched poly(glycidol). No negative effect on coagulation and red cell aggregation could be observed and no effect of polymers towards platelets was visible. For complement activation only after prolonged incubation (2 h) an effect was visible but was in the same extent as the phosphate buffered saline control. MTT assays performed with L929 mouse fibroblasts and human umbilical vein endothelial cells showed results for hyperbranched- and linear poly(glycidol) comparable to PEG. The authors stated that there is a good biocompatibility of the polymer and the compatibility is comparable to PEG. Studies by Kainthan et al. confirm the compatibility.[84] The beneficial combination of polymerization, modification and cytocompatibility makes poly(glycidol)s an interesting polymer system for biomedical applications. Published studies make use of poly(glycidol)s in heterogeneous- and homogeneous system, as branched or linear homopolymers, copolymers or 3D-networks forming hydrogels.

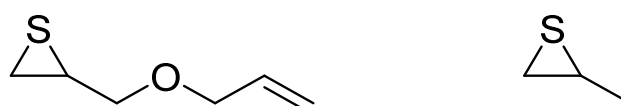
2.5. Polythioethers

The thioanionic polymerizations require the prior synthesis of the corresponding episulfides. As early as in the 1950s a simple transformation of ethylene oxides to the corresponding episulfides was described by using thiocyanates.[85, 86] Here the proposed mechanism relies on the opening of the epoxide by thiocyanates (Scheme 15).



Scheme 15: Mechanism of the ring-transformation of epoxides to episulfides with thiocyanate.

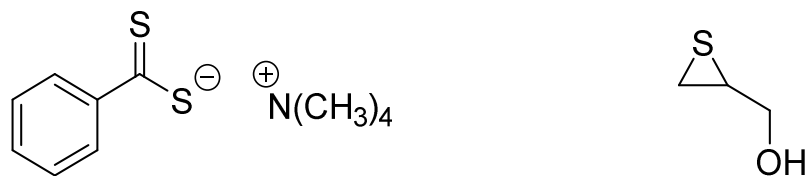
The ambident thiocyanate attacks the epoxide preferably at the lowest steric hindered site, if no electronic effects alter the electrophilic properties of the epoxide ring-atoms. As the sulfur-group of the thiocyanate is more nucleophilic than the nitrogen-atom, a vicinal thiocyanate-alkoxide is obtained. Electron deficiency at the thiocyanate-C leads to the nucleophilic attack of the alkoxide to the thiocyanate forming the five-membered oxathiolanimine-ring. Ring-opening by thiolate release forms an isocyanate-thiolate that eliminates the isocyanate under episulfide-formation. According to Sander, the final opening of the oxathiolanimine and release of the episulfides is slow compared to the initial epoxide-opening and oxathiolanimine formation.[87] Although formed episulfides have a lower ring-strain enthalpy ($H_{\text{episulfide}} = 83 \text{ kJ mol}^{-1}$ [49]) in contrast to epoxides ($H_{\text{epoxide}} = 114 \text{ kJ mol}^{-1}$ [49]) they are less stable and the first syntheses of ethylene sulfide were often accompanied by a spontaneous polymerization even at low temperatures, controllable by additives.[86] Poly(ethylene sulfide) was finally used as a commercial polymer (Thiolon by Thiokol Chemical Co.) due to its inherent insolubility and high crystallinity.[88] The simple synthesis of the episulfide-monomers allowed the simple variation of episulfide-monomers. As an example allyl-functional thioglycidol and propylene sulfide were used as comonomers and polymerized with partially hydrolyzed Et_2Zn as initiator, giving unsaturated poly(thioethers) that were finally vulcanized (Scheme 16).[89]



Scheme 16: Allyl thioglycidyl ether and propylene sulfide.

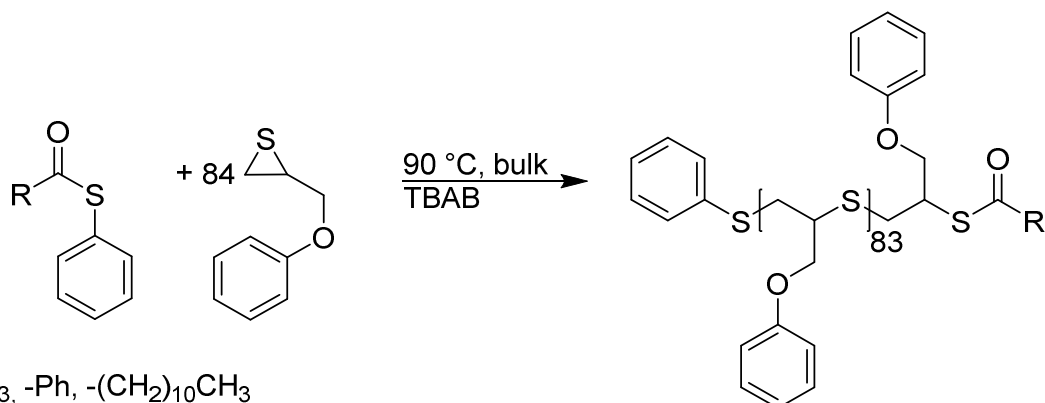
It should be noted that the focus of this introduction is based on the ethylene-sulfide backbone polymers, as e.g. aromatic backbone polysulfides (e.g. Ryton as high performance plastic) are out of the scope.

In general, at the beginning of the investigation of episulfide polymerizations (1950s onwards), academics were deeply focusing on the investigation and understanding of initiation, propagation and the resulting physical aspects using different initiating systems. In 1972 Lautenschlaeger published a review about the polymerizations already investigated including stereoregulatory aspects. Already at this time anionic (with e.g. alkyllithium and -sodium, Na^+ , K^+ , Ca^{2+} , Ba^{2+} , Cd^{2+} -thiolates...), cationic (diisobutyl aluminium, $\text{BF}_3/\text{Et}_2\text{O}$, $\text{Et}_2\text{Zn}/\text{H}_2\text{O}$, ...) initiators and amines (primary, secondary, tertiary and poly(ethylene imine)) were used to polymerize various episulfides, but commonly using propylene sulfide **6**.^[90] Comparisons with earlier polymerizations showed that by simply changing from epoxides to episulfides physical aspects, kinetics, stabilities and even stereochemical aspects alter, caused by the polymerization itself. Vandenberg investigated the polymerization of epoxides and episulfides i.e. (*E*)-2,3-dimethylthiirane (*trans*-2-butene episulfide) and (*Z*)-2,3-dimethylthiirane (*cis*-2-butene episulfide) with coordinative and cationic catalysts. Upon polymerization of (*Z*)-2,3-dimethyl**thiirane** both, the coordinative ($\text{Et}_2\text{Mg-NH}_3$, $\text{Et}_3\text{Al-H}_2\text{O-acetylacetonate}$) and cationic catalysts (BF_3 , $i\text{Bu}_3\text{Al-H}_2\text{O}$) gave crystalline racemic isotactic polymers. On the other hand, for the polymerization of (*Z*)-2,3-dimethyl**epoxide** the coordination catalysts gave also crystalline isotactic polymers, whereas the cationic catalyst gave amorphous syndiotactic poly((*Z*)-2,3-dimethyl**epoxide**). For the corresponding polymerization of (*E*)-2,3-dimethylthiirane with cationic catalysts, elevated temperatures, compared to (*E*)-2,3-dimethyl**epoxide**, were necessary. Here the resulting poly(thioether)-based polymer was mainly amorphous, whereas the polyether-based polymer was highly crystalline. This effect was explained by enabling a longer distance bond with the sulfur-atom than with oxygen for the attacking monomer on the active cationic end. The new formed thioether-bond tolerates a larger distance and the steric demand between the active cationic end and the monomer is decreased.^[91]



Scheme 17: Tetramethyl ammonium dithiobenzoate (left) used by Bonnans-Plaisance for the polymerization of functional episulfides, e.g. thioglycidol (right).

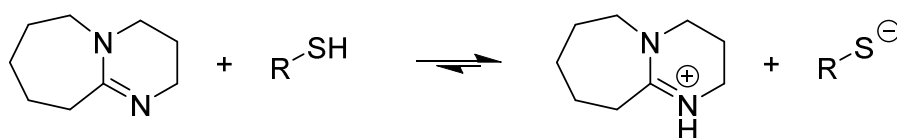
Although the initiators changed sparsely over the first decades of episulfide polymerization research, several new classes of initiators were established. Ammonium salts of dithiocarboxylates (Scheme 17) were described by Bonnans-Plaisance offering a new anionic initiator capable for the anionic ring-opening polymerization.[92] In one of the first descriptions of these initiators, the direct polymerization of 2-(hydroxymethyl)thiirane (thioglycidol, Scheme 17) was described without using a protective group that is in contrast necessary for the polymerization of thiol-functional episulfide as a transfer reaction occurs.[93] Although a good control over the molar-mass was obtained having values of $M_n = 7100 - 44200 \text{ g mol}^{-1}$, the dispersities were quite high having values of $\mathcal{D} = 1.24 - 1.77$. [92] The group of Bonnans-Plaisance was able to synthesize various polysulfides finally bearing homofunctional alkyl[92]-, hydroxy[94]-, ester[95]-, carboxy[95] and heterofunctional CH₃-/OH-[96] side-chains. The robustness of the thioanionic polymerization against functionalities and especially protic substrates was later confirmed using a monomer-in-water emulsion polymerization to successfully synthesize Pluronic adsorbed poly(propylene sulfide) particles.[97] Another approach for episulfide polymerization was given by the group of Inoue, showing that the sequential polymerization of episulfides and epoxides was possible using an external stimulus. The group used a Zn-porphyrin initiator that reversibly binds the active thiolate, polymerizes episulfides and is inert against alcohols. Propylene oxide can be block-copolymerized with poly(propylene sulfide) as macroinitiator, still attached to the Zn-porphyrin complex, starting the oxyanionic polymerization upon irradiation of the porphyrin-Zn/propylene oxide solution with $\lambda > 420 \text{ nm}$. With this polymerization it was possible to synthesize poly(propylene sulfide)-*block*-poly(propylene oxide) polymers with e.g. $M_n = 3400 \text{ g mol}^{-1}$ and $\mathcal{D} = 1.06$. [98, 99] The group of Nishikubo used the high reactivity of thioesters to establish an acyl-group transfer polymerization of episulfides (Scheme 18).



Scheme 18: Polymerization of 3-phenoxypropylene sulfide with thioesters in the presence of tetrabutyl ammonium bromide (TBAB).

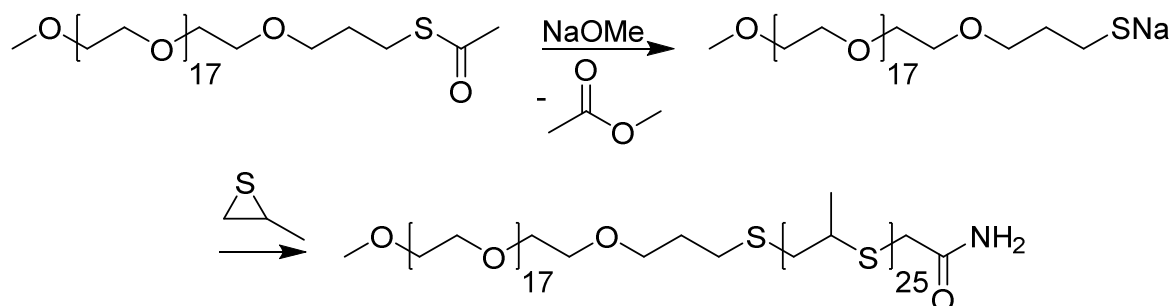
For this e.g. phenyl-thioesters are used as initiator and tetrabutylammonium bromide as catalyst. 3-phenoxypropylene sulfide (phenyl thioglycidyl ether) was polymerized yielding a polymer with $M_n = 11.800 \text{ g mol}^{-1}$ and $D = 1.22$. Furthermore they proved the polymerization to proceed in a living manner showing a straight linear relationship between molar-mass and conversion.[100]

Although several techniques are available the most “simple” polymerization uses thiols and 1,8-diazabicyclo[5.4.0]undec-7-ene (DBU), as a non-nucleophilic base, rendering the nucleophilic thiolate. In contrast to aforementioned alkaline-metal thiolates, here the acid-base reaction equilibrates, although the basicity of DBU is very high and the acidity of thiol is also more pronounced compared to alcohols (Scheme 19).



R = -(CH₂)₅-CH₃, -CH₂-COOMe,
cyclohexane, -(CH₂)₆-SH, -CH₂-C(OH)CH₂OH

Scheme 19: DBU/thiol initiator with various thiols used by Nicol et al.[101]



Scheme 20: PEG-thiols are generated by PEG-thioacetates in situ using sodium methylate. This approach is used by Napoli et al. for the subsequent polymerization of propylene sulfide yielding amphiphilic block-copolymers.[102]

First attempts to synthesize poly(propylene sulfide) in THF with the thiol/DBU system showed that the reaction proceeds very well, but is slow compared to the polymerization in DMF. The group of Bonnans-Plaisance investigated the versatility of the polymerization protocol for functional thiol-initiators, such as mono- and difunctional, hydroxy-bearing and ester-bearing thiols.[101] The same technique was used to synthesize star-shaped poly(propylene sulfide)s with a heterocyclic core.[103]

An alternative route to generate thiolates *in situ* was shown by Napoli et al. using thioacetate macroinitiators that were treated with sodium methylate (Scheme 20).[102] Cleavage of the thioacetate results in the thiolate-macroinitiator and methyl acetate as side-product. As esters are inert towards episulfide polymerization, as was already shown by Bonnans-Plaisance, this side-product did not disturb the polymerization.[104] The formed PEG-thiolate initiates the polymerization of propylene sulfide and, depending on the protocol, amphiphilic Pluronic-analogs were synthesized with poly(propylene sulfide) as hydrophobic block. As these amphiphilic block-copolymers showed lyotropic behavior a follow-up study was performed, published in 2002. Lamellar phases were observed depending on the concentration and symmetry of the PEG-PPS-PEG polymers and a temperature dependent sol-gel transition was observed by polarized optical microscopy and quantified by rheology. At 20 wt % of EG₁₆-PS₂₅-EG₈ in water lamellar structure were observed using freeze-fracture TEM that changes its structure to vesicles at 1 % suspension of the same polymer.[105]

2.6. *Sulfur-functional polymers for biomedical applications*

2.6.1. Applications for reductive environments

The reductive potential of the cytosol prompted researchers to develop particles protecting a payload in an oxidative environment (extracellular) that is released upon reduction (intracellular). This reduction sensitivity is mainly obtained by the incorporation of disulfide-links that can stabilize the particles and get destabilized by reductive cleavage of the disulfides. Depending on the drug itself it is worth evaluating the hydrophilicity of the drug and use different approaches for loading and delivery. With increasing interest in the delivery of hydrophilic drugs, such as proteins and DNA, a hydrophilic environment is required to prevent denaturation. Well established micelles offer good opportunities for the delivery of hydrophobic drugs due to their hydrophobic inner core but miss the use as drug delivery vehicles for hydrophilic drugs. Networks made of hydrophilic polymers (hydrogels) swell in water and gained interest as potential drug delivery systems for these hydrophilic drugs. Triggering the controlled release of their payload was accomplished by synthesizing disulfide-crosslinked particles that degrade upon reduction, preferentially intracellularly.

Inverse miniemulsion is a common technique to synthesize nanogels. Two immiscible liquids forming a continuous phase of one liquid bearing droplets of the other liquid, with significant stability of the small droplets inside, are termed emulsions. Reducing the size of the small droplets to the range of $d = 100\text{-}400$ nm, these emulsions are generally termed miniemulsion.[106, 107] Stabilization of these miniemulsions can be obtained using mixtures of agents with one immiscible in the continuous phase but miscible with the dispersed phase and the other one vice versa.[106] Preparation of the dispersed phase by ultrasonication induces high stress that leads to a continuous reduction and homogenization in droplet size upon reaching the equilibration of droplet fusion and droplet fission.[107] Steric hindrance by the agents and reduced material flux in the dispersed phase between the droplets stabilizes the system towards coalescence and Ostwald ripening, respectively.

Water-in-oil (w/o) systems are termed *inverse* miniemulsion and were used to synthesize hydrogels in the nanometer range. Oh et al. used PEG-derivatives for the synthesis of biocompatible nanogels in 2006.[108] ATRP in inverse miniemulsion was performed using

oligo(ethylene glycol) methacrylate with 7 and 23 EO units per monomer together with a water-soluble initiator (PEG5000-Bromide) and a copper(II)bromide made water-soluble by complexation with [(2-pyridyl)methyl]amine. Cyclohexane was used as continuous phase with Span 80 for stabilization of the droplets. As crosslinker 1.5 mol% of a disulfide-functional dimethacrylate with 10 EO units between methacrylate and disulfide-functionality formed nanogels having a diameters of 260 nm, as was determined by DLS and could be reduced by Bu_3P in THF to yield the single polymers that could be characterized by SEC to have $M_n = 74,000 \text{ g mol}^{-1}$ with dispersities of $M_w/M_n = 1.5$. Neither cytocompatibility experiments nor desintegration under cytosolic conditions studies were given.[108]

Branched synthetic poly(glycidol)s were also used for the formation of reduction-sensitive nanogels as was shown by Steinhilber et al.[109] The monomers were glycerol and glycerol trisglycidyl ether whereas bis-3-thioglycerol disulfide or hydroxyethylthio-bis-glycidylether was used as crosslinkers. As surfactant poly(ethylene-co-butylene)-*block*-poly(ethylene oxide) was used with cyclohexane as continuous phase and DMSO as polar phase. Initial studies showed that the choice of the correct composition between hydrophilic (glycerol) and more hydrophobic monomers was crucial for the solubility of the particles after inverse miniemulsion. The parameters of the inverse miniemulsion influenced the diameter of the particles. With increasing DMSO concentrations, diameters up to $340 \pm 41 \text{ nm}$ were obtained, whereas the use of glycerol reduced the particle sizes down to $23 \pm 5 \text{ nm}$ as was determined by DLS. Degradation studies were performed with FITC-labeled particles ($d = 56 \pm 11 \text{ nm}$) subjected to 5 mM DTT solutions in PBS at 37 °C. SEC-analysis showed that after 120 h no residual nanogels could be detected and polymers had molar masses <5 kDa, suitable for renal clearance. Cellular uptake with the smallest synthesized nanogels was investigated using rhodamine B labeled nanogels and A549 lung cancer cells. In contrast to low molar-mass rhodamine B-labeled glycerol, the particles were readily taken up reaching a plateau after 4 h. The authors investigated the cytotoxicity with human hematopoietic U-937 cells but only at high concentrations (5 mg/mL) reduced metabolic activity was observable. Successful endosomal release of the particles by late-endosomal staining was finally obtained with a commercial assay.[109]

Both approaches used the in situ polymerization/crosslinking to synthesize reduction-sensitive nanogels. It has to be noted that after successful degradation and drug delivery the single polymers shall be removed from the cell to be either renally cleared or biochemically processed. It is therefore important to gain control over the degradation products. Promising nanogel approaches with defined degradation products were approached by Groll et al. Here, thiol-functional polymers are synthesized prior to the nanogel process and crosslinked via oxidative during the inverse miniemulsion process. High degrees of functionalization of polyglycidols and its modification strategies, shown by Li and Chau,[76] made linear poly(glycidols) prone to be used for nanogel synthesis by this polymeric precursor-approach. Thiol-functionalization of poly(glycidol) was shown by Singh et al. making the polymers sensitive towards oxidation under formation of disulfide-crosslinked nanogels.[83] All-hydroxy functional poly(glycidol) with DP=60 was functionalized with 3,3'-dithiodipropionic acid via DCC/DMAP mediated esterification. Subsequent reduction of the disulfide-bridges gave poly(glycidol) with 16 % thiol-functionalities as was determined by ¹H-NMR spectroscopy. Oxidation with H₂O₂ during inverse miniemulsion lead to nanogels with diameters $d = 100\text{-}350$ nm in the swollen state determined by cryo-SEM. The cytotoxicity was investigated using L929 mouse fibroblast and almost no cytotoxicity was detected within 72 h. Two follow-up studies from 2013 used the mild oxidation with alloxane[110] and horseradish-peroxidase (HRP) [111] obtaining macroscopic hydrogels and nanogels with a diameter of $d = 200\text{-}350$ nm. With the mild crosslinking procedure with HRP the vitality of L929 cells was not affected during the encapsulation process as was shown by a Live/Dead[®] staining after 18 h. The formation of nanogels crosslinked via HRP-oxidation with the concurrent incorporation of β -galactosidase (β -Gal) was successful. Subsequent reduction of the nanogels with glutathione and activity testing of the β -Gal showed that up to 43 % of the intended β -Gal was incorporated and up to 85 % still active. This study showed that the cytocompatibility of linear poly(glycidol)s and this crosslinking techniques bears a high potential for 3D-cell culture systems and drug delivery applications.

Naturally derived polymers such as hyaluronic acid were also used for the precursor-approach to obtain nanogels as Lee et al. described in 2007.[112] Here, delivering GFP-encoding siRNA into HCT-116 cells was accomplished using thiolated HA and it was shown that the CD44-receptor is responsible for the uptake. Hyaluronic acid was modified with

thiols by activating the carboxylic acid with EDC and HOBt. The activated ester was reacted with cystamine dihydrochloride, yielding thiol-functional HA after reduction with DTT (42 % thiolation). This hyaluronic acid-derivative was subjected to the inverse miniemulsion process using PBS as the aqueous phase and hexane as oil phase. Interestingly, no additional oxidant was necessary to obtain disulfide-crosslinked HA. Span 65, Span 80 and Tween 80 were used as surfactants and HA nanogels with a diameter of 198 ± 28 nm were obtained for a mixture of 1:1 = Span 80:Tween 80 as was determined by DLS. Other mixtures led to nanogels with diameters between 200 and 500 nm. Loading efficiencies were about 50 % for siRNA that encoded the GFP-protein. Concentration-dependent reduction of the loaded particles with GSH showed a steady increase in degradation rate upon GSH increase from 0.1 mM to 10 mM, yielding a full siRNA release within 60 min for 10 mM GSH media. Investigation of rhodamin-loaded nanogels with CD44-overexpressed cell (HCT-116) and CD44-deficient cells (NIH-3T3) showed labeled nanogels only inside of HCT-116 cells. This indicated an endocytotic pathway via the CD44 receptor. As cytotoxicity test revealed no toxic effects of the particles, gene silencing experiments with GFP overexpressed HCT-116 cells were conducted and compared with PEI. Especially in experiments containing 10 % FBS a more efficient gene silencing was observable having a GFP expression reduction for siRNA/PEI of 37.8 ± 2.3 % and for siRNA/HA nanogels of 62.1 ± 6.1 %. It should be noted that the HA-based nanogels itself act as targeting moiety for CD44-receptor mediated uptake.[112]

2.6.2. Applications for oxidative environments

The inherent switch in hydrophilicity of thioethers upon oxidation is a promising feature in drug delivery applications. One of the first attempts to translate the poly(thioether)s into biological applications was described in 2003. Here $EG_{17}-PS_{25}-EG_9$ was coated on a gold surface, chemisorbing due to its thioether backbone. The resistance of the adlayers towards protein adhesion was tested with whole blood serum with up to 55 mg ml^{-1} protein content. Subsequent washing with PBS led to a almost complete removal of the protein from the surface. The same polymer was used for micropatterning of a gold surface. Preseeding of the gold surface with rat fibroblasts showed that the tested cells do not migrate into the coated areas.[113] A photocatalytic lithography was performed using chemisorbed poly(propylene)-*block*-poly(ethylene glycol), coated on a gold surface.

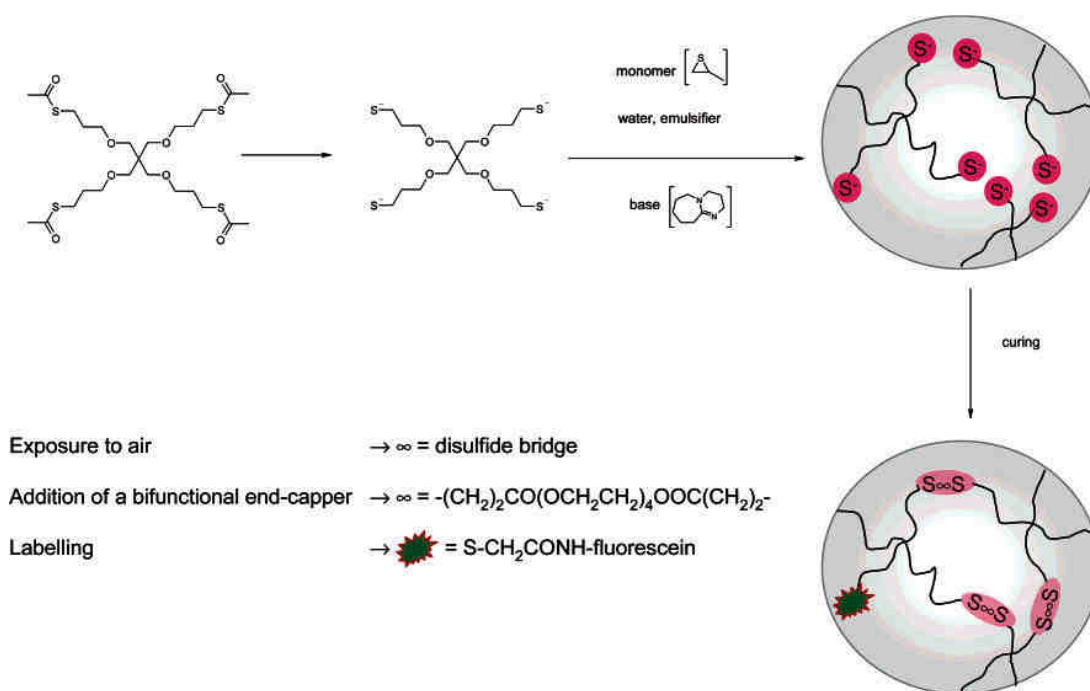


Figure 4: Synthesis of poly(propylene sulfide) nanoparticles with entangled Pluronic (emulsifier) at the surface. Reprinted with permission from literature [8]. Copyright 2005 American Chemical Society.

An appropriate mask with a porphyrin- based photocatalyst was able to oxidize the thioether upon contact. Non-oxidized block-copolymers retained on the surface, whereas the oxidized polymers could be removed by washing.[114] Hubbel et al. described in 2004 the preparation of oxidation-sensitive vesicles in a proof-of-principle study. They showed that $\text{EG}_{16}\text{-PS}_{50}\text{-EG}_{16}$ triblock copolymers can be used to form polymersomes that disintegrate upon oxidation. An initially formed bilayer was stable over months and could be destroyed forming unimolecular micelles upon oxidation of the thioether bridges forming hydrophilic sulfones and sulfoxides without cleavage of the triblock-copolymers.[115]

A four-arm thioacetate-initiator was used to prepare poly(propylene sulfide) nanoparticles with an entangled Pluronic surface (see Figure 4).[8] Investigation of Pluronic leakage was studied over several months, but no indication was given that “anchored” Pluronic of the shell detaches from the poly(propylene sulfide) particles. With the Pluronic:PPS ratio the size of the particles can be determined in a range of $d = 27 - 225$ nm. No cytotoxic effects were observed for human foreskin fibroblasts and a complete oxidation and disintegration could be obtained within hours or days, depending on the H_2O_2 concentration.

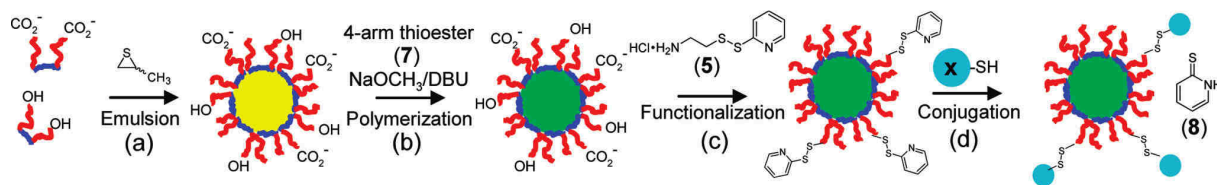


Figure 5: Pluronic-derivative coated poly(propylene sulfide)-nanoparticles can be derivatized with pyridine-disulfides for further surface-functionalization. Reprinted with permission from literature [116]. Copyright 2010 American Chemical Society.

Particle functionalization was either performed inside of the hydrophobic core with thiolate-reactive iodoacetamide fluoresceine, or at the outer shell of the particle via Pluronic that is used as a surfactant. Pluronic derivatization with glucose-oxidase was performed and led to the responsivity of the particles to the environmental glucose-level. Hydrogen peroxide is produced when the glucose-oxidase was exposed to glucose leading ultimately to the oxidation of the particle. Interestingly, the initial particle formation was not significantly influenced by the modified Pluronic, yielding particles with a diameter of $d = 90$ nm that were subsequently oxidized.[117] As it is assumed that the particle formation can be dependent on the functional-groups of Pluronic a more general approach to surface-functionalizations was aimed. An alternative Pluronic-modification was published by van der Vlies using the same emulsion polymerization technique with the four-arm initiator already published. The entangled synthesized carboxy-functional Pluronic parts were modified after particle formation using carbodiimide chemistry for the introduction of a pyridyl-disulfide (Figure 5). Disulfide-bound pyridine is afterwards prone to thiol–disulfide exchange offering an interesting approach to a variety of thiol reactive species and thiols that are attempted to be used to modify the nanoparticles.[116]

Pharmaceutical applications of polymeric biomaterials for the mucous membrane benefit from the thiol-disulfide exchange possibilities that lead to an adherence of the material with the mucous (mucoadhesion). This allows the direct contact leading to a locally restricted delivery, long term persistence of the substrate and an increased drug concentration gradient.[118] At the very beginning hydrophilic polymers exhibiting numerous hydrogen bonds were used as mucoadhesives. Here poly(acrylic acid) (carbomers), chitosans, alginates and cellulose-derivatives were used, as they can form hydrogen bonds but are also able to electrostatically interact with the mucous layer. An interpenetration of the mucus layer with

the substrate is obtained and prevents the removal of the substrate upon mechanical stress such as movements e.g. by the mouth if applied to the oral cavity. Further strengthening of the mucoadhesion was gained by Bernkop-Schnürch in 1999.[119] The authors hypothesized that the high cysteine and therefore high disulfide-content of the mucuslayer will be beneficial for the covalent attachment of thiol-functional polymers. Upon contacting the disulfide-rich mucus the thiomers would readily start thiol/disulfide-exchange reactions formally oxidizing the thiols of the polymer to the corresponding disulfides (Figure 6). The authors used the common mucoadhesive polycarbophil (divinyl glycol crosslinked poly(acrylic acid)) and activated the carboxyl-functionalities with EDC. Cysteine was used and coupled with the activated polycarbophil to form a stable amide bond and obtain thiol-functional polymers. Taking into account the potential oxidation of the thiols, the authors added EDTA to bind transition metals in the first dialysis step. Between 0.5 μmol and 142.2 μmol thiols per gram polymer were determined by Ellmans assay showing a successful modification of the polymers with variable thiol content. Swelling studies indicate a higher swelling behavior of higher cysteine-functionalized polymers that were shown to readily oxidize and increase its viscosity above a pH of 5. Keeping the pH at 5 leads to stable polymers for at least 8 hours without notifiable degree of oxidation.[119] These pH-finding were also influencing the total work of adhesion, showing an improved adhesion of the thiol-modified polymers to porcine intestinal mucosa at lower pH-values. An increased attachment of the thiolated polymers (thiomers) to the mucosa at pH 6.8 compared to the attachment at pH 3 indicate the thiolate as active exchange species for the thiol-disulfide exchange reaction of the construct with the mucus layer.[119] For the thiol-modification itself the total work of adhesion was doubled using a conjugate of polymer:cysteine = 8:1 compared to the pure polymer at pH 6.8.

Comparing the adhesion of thiolated polymers were investigated covering polyanions (e.g. poly(acrylic acid), divinyl glycol crosslinked poly(acrylic acid) and alginate), polycations (e.g. chitosan) and non-ionic polymers (e.g. hydroxyethyl- and hydroxypropylcellulose). All data revealed that thiolated polymers exhibited a higher adhesion to the porcine small intestinal mucosa in comparison to their un-modified references.[120] Here the polymers prepared at lower pH-values showed an improved adhesion towards the mucosa. This was explained by the readily exchanging thiols and disulfides.

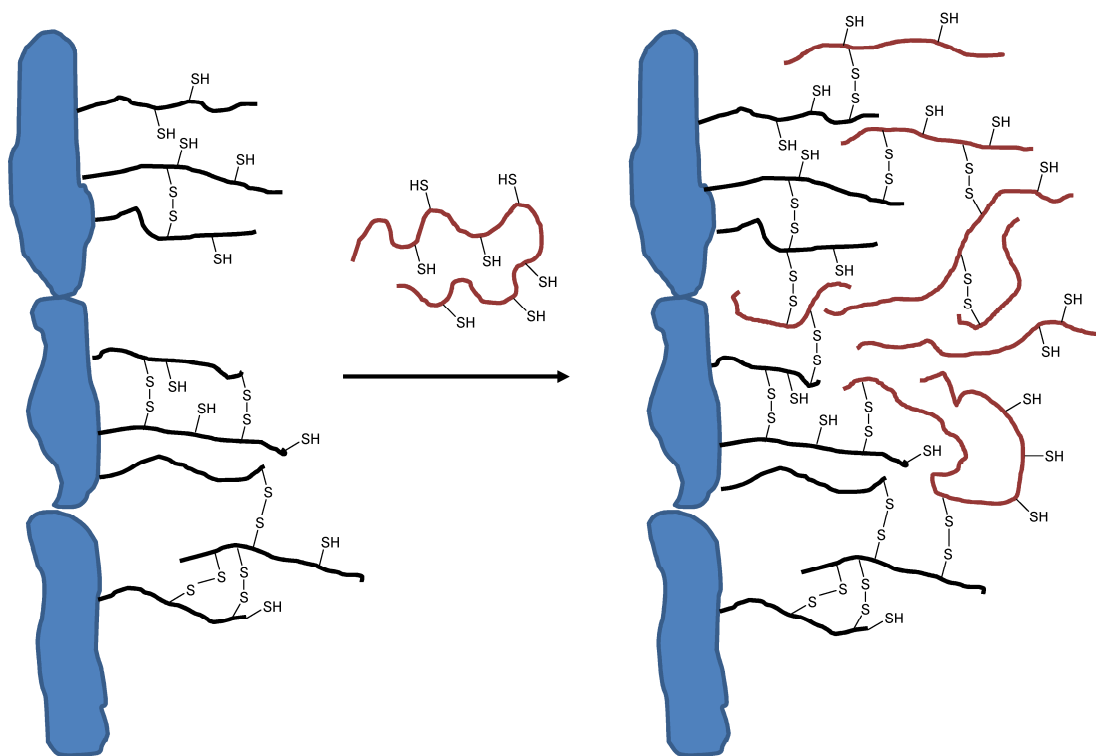


Figure 6: Mucoadhesion of thiol-functional polymers with the mucosa. A thiol-disulfide-exchange/oxidation results in the interpenetrating and fixation of the thiomers in the mucosa.[15]

Although in contrast to above mentioned results, regarding the oxidation at $\text{pH} > 5$, the preparation of polymers in acidic media at $\text{pH} 3$ (dialysis) and its drying leads to polymers with no disulfide-formation or thiol-disulfide exchange. The authors stated that the mucous layer is at a pH of 5-7 and upon interpenetration of the polymer into the mucus, thiol-disulfide exchange starts, adhering the polymers with the mucus.

2.6.3. Conjugation applications

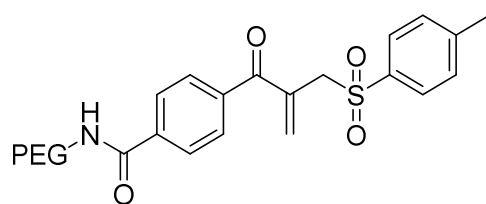
Although the conjugation of peptides with polymers does not necessarily target redox-sites its applications in biomaterial research is also widespread. As sulfur-based chemistries evolved within the last years improving the efficacy and control of these conjugations the concepts are also presented.

PEGylation of proteins denotes the attachment of PEG chains to the proteins and was described in the late 1970s by the group of Frank F. Davis. At that time non-human derived proteins often led to immunogenicity and, with exceptions, could not be administered to

patients. Proof-of-concept studies with the PEGylation of bovine serum albumin and bovine liver catalase led to the first articles dealing with the reduced immunogenicity through synthetic polymer modifications.[121-123] mPEG1900 was reacted with cyanuric chloride rendering the mPEG-chain reactive towards amines. As hydrolysis of the activated PEG-substrate in aqueous solution was an issue a 5-fold excess of activated PEG with respect to available amines was used. Blood circulating time experiments with ¹²⁵I-labeled substrates were used indicating an increased circulating time for mPEG1900-¹²⁵I-BSA compared to ¹²⁵I-BSA in albumin-immunized rabbits.[122] Nowadays, the most abundant polymer used for the conjugation of proteins and peptides is still PEG. Over the last decades the emerging field of PEGylation led to the FDA-approval of numerous conjugates that were reviewed in 2011 by Alconcel et al.[124] Covering the surface of the protein and increasing the size of the conjugate leads to the reduced immunogenicity and the conjugates are not actively removed by the immune system. Furthermore a prolonged circulation time can be obtained as the conjugates are artificially enlarged and renal clearance reduced. For this clearance it is stated that below 5 kDa the substances are completely removed whereas the upper limit for renal clearance is at 50 kDa.[125] Although stated in literature for molar masses, it has to be noted that the hydrodynamic size of artificial and synthetic polymers is substance-dependent and these molar masses are only rough estimations and have to be evaluated for each system. Substances and pharmaceuticals with molar masses, or better hydrodynamic sizes, within the above mentioned range can be artificially modified e.g. with PEG to expand circulation time in the blood.

Synthetic strategies for the PEGylation vary, depending on numerous factors such as resulting activity, available groups, purification procedure etc.. Derivatization of proteins via their lysine amine side-chains can be accomplished using activated PEG-chains such as above mentioned cyanuric chlorides, succinimidyl carbonates, para-nitrophenyl carbonate, succinate N-hydroxysuccinimide and other activated electrophiles.[50] Although the application of amine-coupling is well established and applied in commercial products it lacks in site-selectivity potentially leading to an active-site derivatization and hence reducing the applicability of the derivatization. Therefore different strategies were attempted using other functional groups along the primary structure of the protein to gain higher selectivity for PEGylation and a better control of quantity and site. A sulfur-targeting PEGylation of

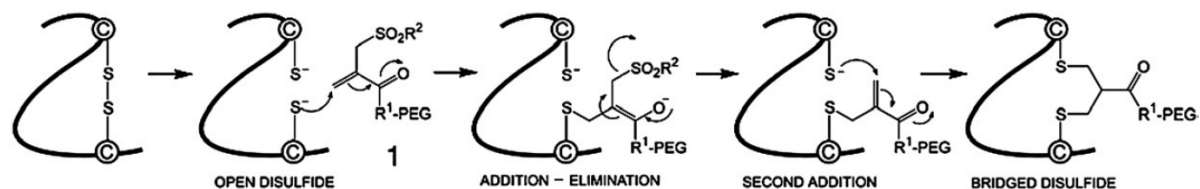
proteins is a promising alternative to amine-targeting approaches as the sites are more specific and groups such as maleimides are highly reactive towards thiols, yielding an improved site- and chemoselectivity. In general, the cysteine sites can either be along the amino acids sequence or at its terminus. Furthermore they can be bridged and “used” as disulfides stabilizing the structure. The number of naturally occurring proteins with free thiols is restricted. Hence artificially introduced cysteines allow the selective incorporation of the cysteine at a desired accessible site, but it has to be ruled out that negative effects, such as activity reduction or denaturation, occur. With both approaches, naturally occurring free-cysteine-functional proteins and recombinantly modified, proteins were PEGylated. It could be shown for e.g α 1proteinase inhibitor (α 1PI) a protein applied for the treatment of hereditary emphysema,[10] recombinantly derived human granulocyte colony stimulating factor (rhGCSF) for treatment of neutropenia, [126, 127], glucagon-like peptide 1 for blood sugar level control, [128] and Interferon IFN- α 2[129]. To gain even more specificity an intriguing approach for PEGylation was published by Brocchini using the insertion of a three-carbon long bridge into the protein disulfides. Disulfide bridges are a regularly appearing structural motif and are an even more specific group for protein conjugation than amines. It was long assumed that the structural integrity of disulfide-bridges rules out the functionalization via this motif. In 2006 Shaunak et al. published the bis-alkylation of the reduced disulfide with an α -, β -unsaturated β' -sulfone-PEG derivative (Scheme 21).



Scheme 21: α -, β -unsaturated β' -sulfone-PEG used for the three-carbon bridged structural fixation of proteins derived from former native disulfide-bridges.

Solvent accessible disulfides were assumed to be cleaved by reductive agent though other non-accessible disulfides are sufficient to maintain the structure of the protein. The disulfides are cleaved by a reductive agent such as TCEP, followed by a nucleophilic attack of the thiolate species at the enone (Michael-acceptor). Upon elimination of the sulfinic acid the Michael –acceptor is regained being accessible for the second attack of another thiolate (Scheme 22). As the authors stated, this system is beneficial as the sequential addition

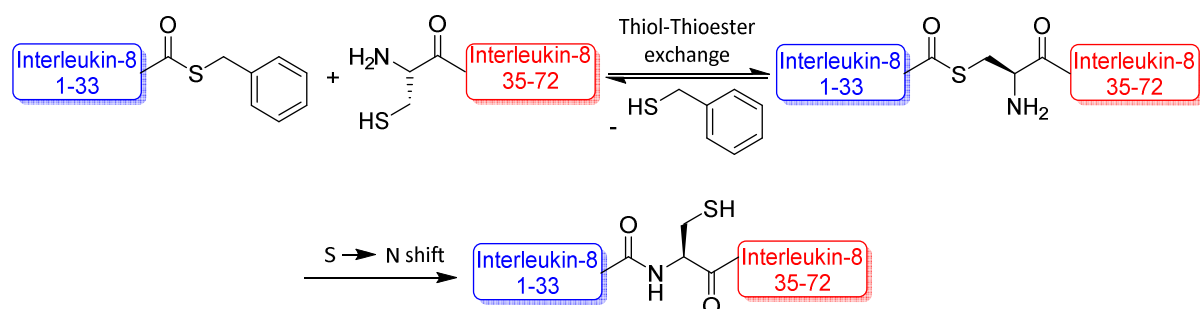
occurs making the reaction dependent on each other. “Common” difunctionalized acceptors, such as bis-vinylsulfones, exhibit a larger space between the reactive Michael-acceptors, react independent on each other and lack in control in crosslinking of the *original* disulfide-participating sulfur-atoms.



Scheme 22: PEGylation of disulfide-bridges using α,β -unsaturated- β' -mono-sulfone functionalized PEG. Reprinted from [130] with permission from Elsevier

With this method Interferon- $\alpha 2$ (INF- $\alpha 2$) was PEGylated yielding mono- and di- PEGylated INF- $\alpha 2$ with similar activities as commercially available PEGylated IFN- $\alpha 2$ underlying the validity of this PEGylation strategy. This method offers a promising alternative based on the sulfur-modification strategies, although it is assumed to lack in large-scale application due to the seven step synthetic strategy starting from 4-acetyl benzoic acid.[130]

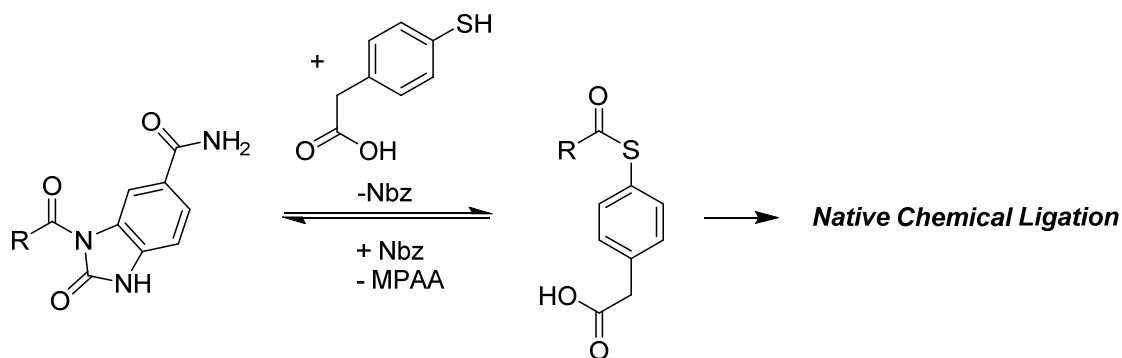
All PEGylation strategies discussed rely on the sulfur-functionalities in the proteins along the primary amino acid sequence. A recent emerging chemoselective terminal functionalization approach was originally attempted to couple different protein parts for the synthesis of whole proteins. The group of Kent published the linking of a C-terminal thioester peptide with an N-terminal cysteine in 1994 and showed that Native Chemical Ligation is a valid method for the synthesis of proteins.[131] Chemoselective reaction between the synthesized thioester (IL-8 (1-33) α COS-benzyl) and a cysteine (IL-8(34-72)) first yields a thioester linked Interleukin-8 (Scheme 23).



Scheme 23: Synthesis of Interleukin-8 using a thioester modified peptide (IL-8(1-33)) and an N-terminal cysteine-peptide.[131]

A stable amide bond is formed upon nucleophilic attacks of the amine adjacent to the thioester (S→N shift)). Both parts contained cysteine-residues that could not be observed to participate in the reaction and only the N-terminal cysteine leads to the conjugation, finally forming IL-8. Successful folding of the formed peptide under disulfide-formation was confirmed by X-ray crystal structure and showed the clean reaction obtaining an active Cys³⁴-side-chain.[131] Here the sulfur-moiety is regained after successful NCL making the thiol group assisting the reaction, yielding a high chemoselectivity, but not being consumed.

In the past years NCL was shown to be a highly selective method for coupling various peptides and synthesize proteins. Limited sequence length of amino acids (e.g. by solid-phase peptide synthesis) can be expanded by coupling synthetic peptide blocks via NCL or synthetically and biologically derived peptides (expressed protein ligation). C-terminal thioester peptides substituted with aromatic or aliphatic thiols as leaving group can be used to perform a kinetically controlled NCL combining various peptide sequences at both termini.[132] Addition of aromatic thiols such as 4-mercaptophenylacetic acid (MPAA) is commonly used to catalyze the NCL starting from a quite stable synthesized aliphatic thioester.[133] These are the preferential synthesized compound as aromatic thiophenol-esters are less stable in aqueous solution. Alternatives to the “standard” thioesters are a focus of research balancing the stability of the active ester and its hydrolysis. Blanco-Canosa introduced the *N*-acyl-benzimidazolinone (Nbz)-peptides for Fmoc-SPPS-based synthesis of proteins. Here the Nbz-peptide rapidly reacts with thiols (MPAA) in aqueous solution yielding the NCL-active thioester (Scheme 24).[134]



Scheme 24: Nbz-activated peptides undergo Nbz-MPAA exchange forming thioesters, able to perform NCL experiments.

Bis(2-sulfanylethyl)amine functionalized C-termini were used to generate the thioester *in situ*. Here the disulfide-containing 1,2,5-dithiazepane amide is reduced with TCEP and two thiols in proximity to the amide are generated (Figure 7). N→S-shift is obtained by the “excess” of thiols, compared to the amine, and a thioester results, able to perform NCL, catalyzed with MPAA.

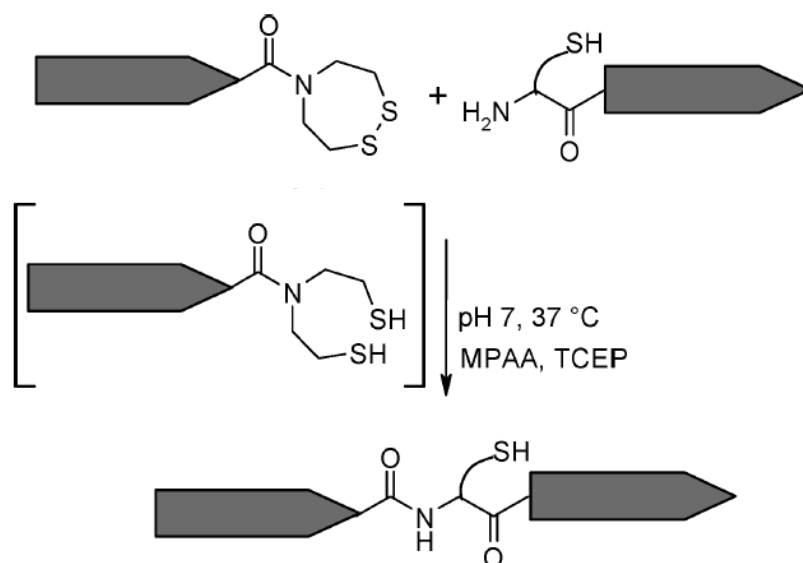


Figure 7: Oxidized bis(2-sulfanylethyl)amine-functional peptide performs NCL upon the presence of a N-terminal cysteine peptide and MPAA as reduction agent. Adapted with permission from [135]. Copyright 2010 American Chemical Society.

Coupling thioester-peptides with cysteine-functional polymers allows the specific conjugation of these components without side-reactions and multiple conjugation as it is generally observed for above mentioned methods via active esters, maleimides or α -, β -unsaturated β '-sulfone-PEGs. Thioester-functional PEG was synthesized by Marsac et al. allowing a terminal-PEGylation of Rab6 without permanently modifying other protein-sites. Activity retention of PEG-Rab6 conjugate was shown in the performed prenylation experiments.[136] Thioester side-chain functional poly(*N*-hydroxypropyl methacrylamide) derivatives were coupled with peptides, as was shown by Ruttekkolk et al in 2008. A commercially obtained *p*-nitrophenyl ester functional polymer (poly-(HMPA-co-methacrylate-GG-*p*-nitrophenyl ester) was activated with benzyl mercaptan and subsequently reacted with the pro-apoptotic *N*-terminal cysteine-modified AVPIAQK-peptide. The AVPIAQK-peptides–functional HMPA polymer promotes the peptide-activity, assigned to a protective behavior of the polymer regarding the peptide-proteolysis.[137] Cysteine-functionalization of synthetic polymers was shown in 2005 using poly(propylene amine) dendrimers. Trityl-protected cysteine was converted to the succinimide-ester, being reactive towards the terminal amine-groups. Poly(propylene amine) dendrimers equipped with cysteine-residues were reactive towards MPAL-thioester (mercaptopropionic acid-leucin)-peptides as was confirmed by ESI-MS.[138] NCL solely with synthetic polymers was shown in 2009 by Hu et al. using thioester-terminal 4-arm PEG and cysteine-terminal 4-arm PEG forming hydrogels upon mixing. After 6 min a hydrogel formed using a 20 % (w/v) polymer solution (in total) at pH = 8.3 and 37 °C. Adhesion of human mesenchymal stem cells was obtained by RGD-modification of the hydrogel. Blank NCL-crosslinked hydrogels did not show adhesion of hMSCs upon absence of the adhesive peptide.[139] Heteropolymeric thermoresponsive hydrogels were synthesized by Boere et al. using HA-, or PEG-thioesters that crosslink with a PEG-PNIPAAm copolymer (Scheme 25). Physical pregelation, caused by the LCST of the NIPAAm, was followed by NCL crosslinking strengthening the gel. Cysteine-terminal CGPRGQOGVMGFO-peptide, that was described being beneficial for differentiation, proliferation and adhesion, was successfully ligated to the polymer as could be confirmed by ¹H-NMR and SEC.[140]

3. Results and discussion

3.1. *Synthesis of polyglycidols*

In this chapter the copolymerization of already established polyglycidols with allyl glycidyl ether (AGE) was performed. The statistical introduction of AGE allows the polymer-analog modification of the polymers via the double bond together with a control over polymerization. Parameters such as solvent effects, the counter ion and the monomer feed rate were investigated for both homo- and copolymers regarding the kinetics, molar mass and dispersity.

Parts of this chapter were already submitted for publication, but are neither yet accepted, nor published.
--

3.1.1. Polymerization in Eppendorf caps.

All polymerizations are necessarily performed under inert atmosphere with the absence of water or other compounds with an acidic proton that can be abstracted by the active oxyanionic species. All hardware used for the polymerization (glass ware, Eppendorf caps) was heated prior being used and flushed with Ar or N₂. Eppendorf caps were equipped with a stirring bar, heated to 85 °C and subsequently inserted into the glovebox chamber, immediately starting an evacuation protocol. This includes evacuation for 5 min, purging with N₂ (2x) and finally evacuation for 30 min and finally purging with N₂. A stock solution of the initiator, the monomer and the solvent was prepared. After preparation, Eppendorf caps were each equipped with 50 µL of the stock solution, enough for ¹H NMR and SEC measurements. For analysis, the reaction in the Eppendorf cap was quenched with 650 µL of 1 % ethanol in deuterated chloroform (1% EtOH/CDCl₃). This solution was directly analyzed by ¹H-NMR spectroscopy to determine the conversion. Afterwards, the volatile components of the NMR tube were removed and the residual polymer dissolved in the SEC-eluent (DMF with 1 g L⁻¹ LiBr).

The kinetic investigation of the polymerization was performed in Eppendorf caps equipped with stirring bars. Commonly, anionic ring-opening polymerizations (aROP) of oxiranes are performed in glassware that was dried under heating und reduced pressure conditions. Both methods have their advantages and disadvantages. The glassware can be dried at higher temperatures as the melting point of glass is much higher than that of poly(propylene) out of which Eppendorf caps are made. As a drawback for the reactions in glassware, a septum is used that is punctured several times with a needle to introduce solvents, monomers or to remove samples of the ongoing reaction. Viscosity of the solution is especially for bulk polymerizations an issue and an aliquot cannot be removed properly by using a syringe. This drawback of aliquotation can be circumvented using Eppendorf caps, as each data point is obtained by quenching one cap. Nonetheless, it should be noted that the volume of the Eppendorf-cap experiments are rather small. With this, no direct information transfer to larger scales can be drawn, as mass and heat transport in the small caps are assumed to be more efficient.

Kinetic experiments were investigated in Eppendorf caps as both polymerizations with solvent and in bulk were attempted. Here, every cap is used as a single reactor. No published

procedure is known that describes the polymerization of EEGE and AGE in Eppendorf caps, and air- and water-tightness of the caps were critical points for the reaction. First, the suitability of this method was tested. According to the literature, at $T < 60\text{ }^{\circ}\text{C}$ with $DP < 100$ no side-reactions were observed that results in allylic end-group formation. This side-reaction occurs at high temperatures and high molar masses, i.e. a high $[M]:[I]$ ratio.[61] Therefore, a temperature of $45\text{ }^{\circ}\text{C}$ and a DP of 50 were chosen for the evaluation of the Eppendorf caps as reaction vessels.

As described in the introduction, the living ring-opening polymerization of EEGE and AGE exhibits first-order kinetics without transfer or termination reactions. For all experiments performed, the suitability was hence checked by monitoring the linear growth of the molar mass with conversion.

THF from the initiator solution (1M KOtBu in THF) was the only solvent present in the experiment. A linear relation between molar-mass and conversion was obtained at $45\text{ }^{\circ}\text{C}$ within one day (Figure 8). Molar-masses were determined by SEC in DMF with 1 g L^{-1} LiBr and a flow rate of 1 mL min^{-1} with PEG as calibration standard. Each data point reflects the quenching of an Eppendorf cap with $\text{CDCl}_3/\text{EtOH}$ solution (EtOH 1%). The conversions were directly analyzed by $^1\text{H-NMR}$ spectroscopy and subsequently M_n and \bar{D} were determined by SEC measurements using a RI detector.

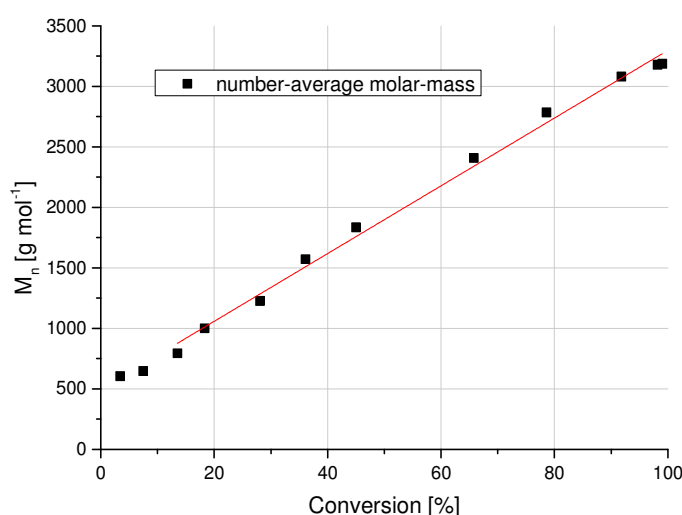


Figure 8: Molar-mass–time plot for the polymerization of EEGE with KOtBu in THF at $45\text{ }^{\circ}\text{C}$ in Eppendorf caps and linear fitting (red line) of the data points (first two data points excluded).

Workup of the reaction solutions were not performed as smaller or higher fractions of the polymer might be removed. Determination of M_n and \bar{D} via a universal calibration was not performed as residual amounts of monomer, solvent and potassium ethoxide, formed upon quenching, are still present. The calibration of the SEC system was performed using PEG with $M > 600 \text{ g mol}^{-1}$ as standard. Molar masses below the lower limit of the calibration hence do not necessarily have to be correct. Additionally, system signals and injection signal at the low molar-mass region merge with the polymer signal leading to an inaccurate determination of the polymer curve and hence the molar mass. The non-linear relation between M_n and conversion, observed at a conversion of less than 10 % (Figure 8), was assigned to these analytical inaccuracies. From 13.5 % till 100 % conversion, a linear increase of the molar mass with the conversion is observed indicating the living character of the reaction. These data show that Eppendorf caps equipped with stirring bars are appropriate reactions vessels for the living-anionic ring opening polymerization studies of glycidols under the chosen conditions.

3.1.2. Polymerization with KOtBu in THF

3.1.2.1. DP influence of EEGE polymerization

The polymerization of EEGE was performed with potassium *tert*-butoxide as initiator with THF as the solvent. At the beginning every 10 min, then every 30 min and finally every 60 min an Eppendorf cap was quenched with $\text{CDCl}_3/\text{EtOH}$ (1 % EtOH). The conversion was determined using $^1\text{H-NMR}$ spectroscopy. At $\delta = 4.70 \text{ ppm}$ the signal of the acetal-H of the monomer was detected that slightly shifts upfield to $\delta = 4.63 \text{ ppm}$ in the polymer (Figure 9). As the overall integral equals all monomer and polymerized units the integral was set to 100. The average integral of the three oxirane-ring protons at $\delta = 3.08, 2.74$ and 2.56 ppm was used to determine the residual content of the monomer and calculate the conversion. For the example $^1\text{H-NMR}$ spectrum after 50 min in Figure 9 the conversion is

$$X = 100 - \frac{(I_{3.08\text{ppm}} + I_{2.74\text{ppm}} + I_{2.56\text{ppm}})}{3} = 44\%.$$

The conversions of all quenched Eppendorf caps were determined and plotted against time (Figure 10). Up to 30 min a non-linear increase of the conversion with time was observed. Afterwards a linear slope between 30 and 100 minutes was detected, followed by a continuous decrease of the slope.

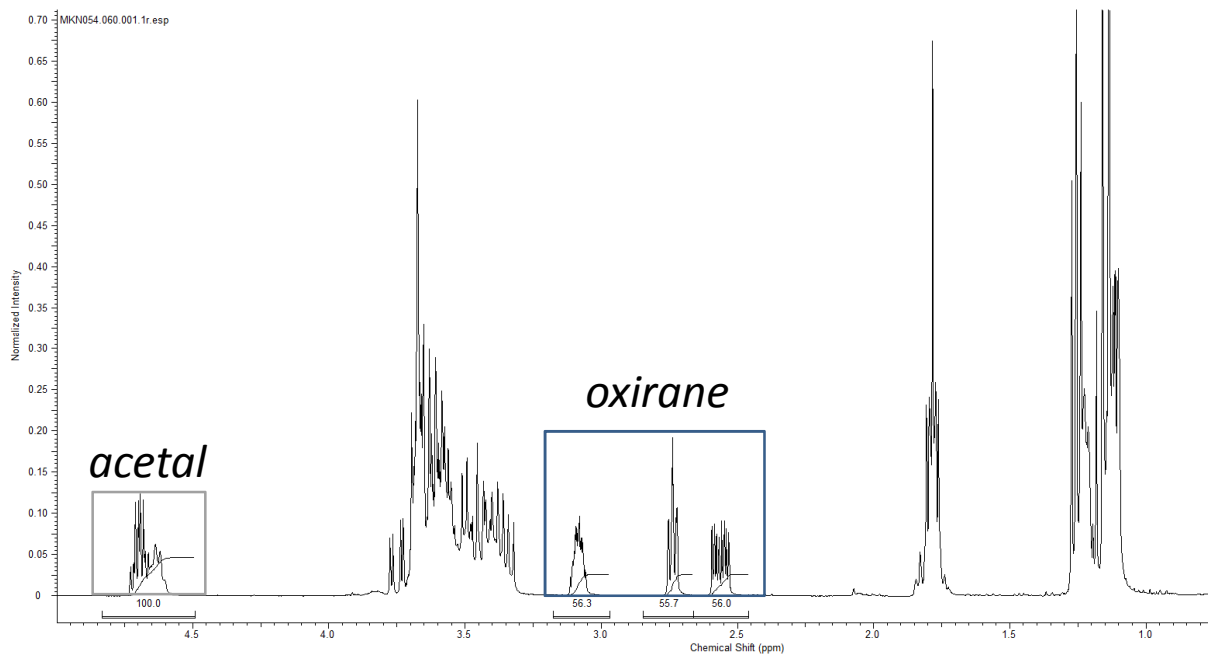


Figure 9: $^1\text{H-NMR}$ spectrum of poly(EEGE) with DP = 20 in CDCl_3 at 44 % conversion.

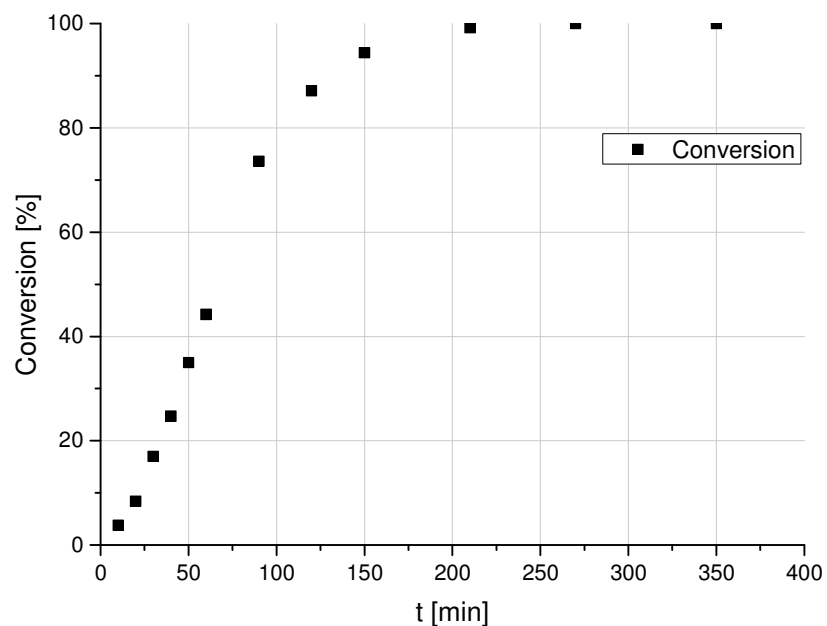


Figure 10: Conversion–time plot of EEGE polymerization with DP = 20 and KOtBu as initiator at 45 °C in THF.

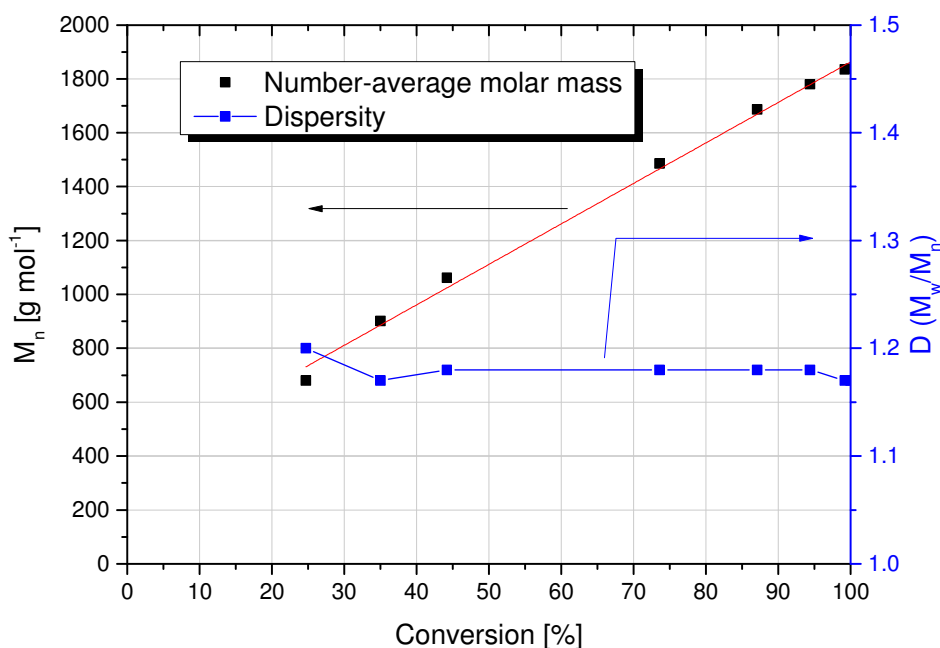


Figure 11: Molar-mass and dispersity–conversion plot of EEGE polymerization initiated with KOtBu in THF at 45 °C. Molar mass (■) increases linearly (linear fit: red line) with conversion typical for a living polymerization. Dispersity (■) slightly decreases with increasing conversion.

Number-average molar masses M_n as well as dispersities \bar{D} were determined by SEC and plotted against the conversion (Figure 11). A linear increase of M_n with conversion was observed for conversions higher 25 %. As the linearity of the reaction would be disturbed by e.g. water or other protic impurities with proceeding conversion, a living character of the polymerization is assumed by the relationship of molar-mass and conversion. Figure 11 also shows the evolution of the dispersity \bar{D} determined for poly(EEGE) with DP = 20. In general, values of $\bar{D} < 1.2$ were arbitrarily chosen to define polymers as narrowly distributed. The dispersities of the synthesized poly(EEGE) with DP = 20 at the various stages of conversion are always below $\bar{D} = 1.2$. Therefore a narrow molar-mass distributed polymer was obtained. Figure 12 shows the SEC-elugram in DMF of the final polymer having a monomodal distribution with $M_n = 1840 \text{ g mol}^{-1}$ and $\bar{D} = 1.17$.

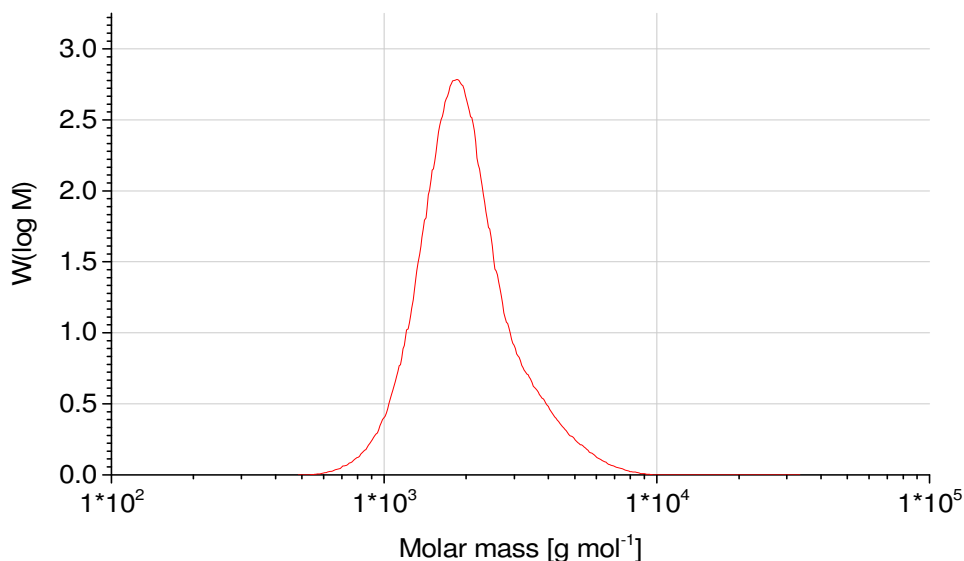


Figure 12: SEC trace of the final poly(EEGE) obtained with KOtBu as initiator at 45 °C and DP=20 in THF. A final $M_n = 1840 \text{ g mol}^{-1}$ and $\bar{D} = 1.17$ was obtained.

The living ring-opening polymerization is a reaction of first-order in the monomer. In chapter 2.3 the following equation was derived.

$$-\ln\left(\frac{M_t}{M_0}\right) = k_{\text{app}}t$$

Regarding this equation, plotting $-\ln(M_t/M_0)$ against t leads to a linear relation with the slope k_{app} that is the apparent rate constant of the reaction. This first-order kinetics plot is shown in Figure 13. At the beginning of the polymerization an induction period with a steady non-linear increase of the apparent rate constant was detected. After 3600 s (60 min, 44 % conversion) a linear increase indicates that the reaction is of first-order in this time slot up to 9000 s (150 min, 94 % conversion). The apparent rate constant k_{app} was also determined and a value of $k_{\text{app}} = 4.23 \cdot 10^{-4} \text{ s}^{-1}$ was obtained for the linear relation.

To determine the rate of propagation k , k_{app} has to be divided by the initial concentration of the initiator $[I]$.

$$k = \frac{k_{\text{app}}}{[I]}$$

With a concentration of $[I] = 0.249 \text{ M}$ and $k_{\text{app}} = 4.23 \cdot 10^{-4} \text{ s}^{-1}$ the rate of propagation is $k = 1.70 \cdot 10^{-3} \text{ L mol}^{-1} \text{ s}^{-1}$ for EEGE with DP = 20 initiated with KOtBu at 45 °C.

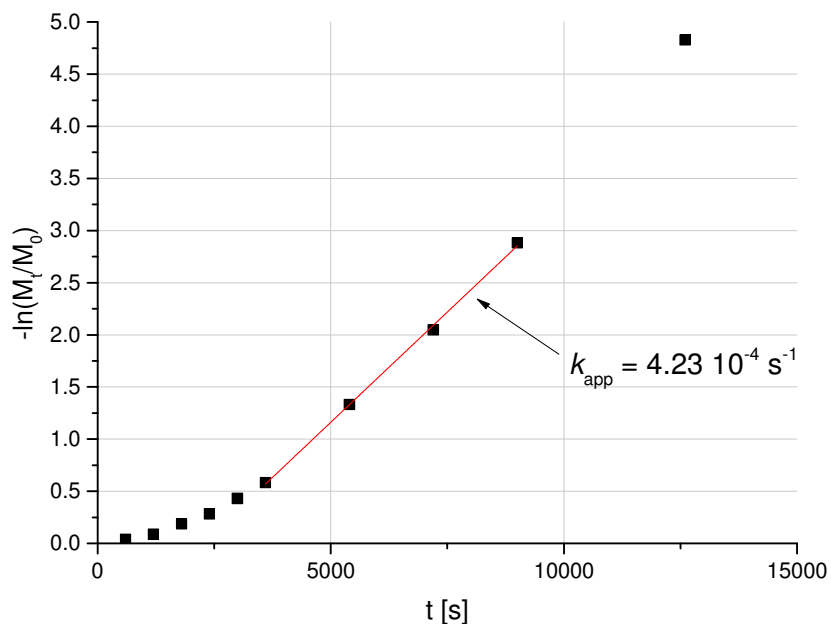


Figure 13: First-order kinetics plot of the polymerization of EEGE with DP = 20 initiated with KOtBu in THF at 45 °C. A linear relation was determined between 3600 and 9000 s (60-150 min). The apparent rate constant was obtained by a linear fit (red line) and the slope is inserted with $k_{app} = 4.23 \cdot 10^{-4} \text{ s}^{-1}$.

The conversion–time plot observed for the same reaction parameters with an aimed DP = 50 can be seen in Figure 14. After 40 min a linear increase of the conversion with time can be observed. After 100 min a continuous decrease in the slope can be observed. In contrast to the reaction with DP = 20 after 300 min, the reaction with DP = 50 was incompleted after 370 min with a conversion of 99 %.

Figure 15 shows a linear increase of M_n with conversion, indicating a chain polymerization of EEGE without transfer or termination reactions also for DP = 50. Of course due to the aimed higher DP in this case, the absolute values of M_n are higher as compared to the values shown in Figure 11. Here a $M_n = 3200 \text{ g mol}^{-1}$ was determined in contrast to $M_n = 1840 \text{ g mol}^{-1}$ for DP = 20. It should be noted that the M_n determined for DP = 50 was at 99 % conversion.

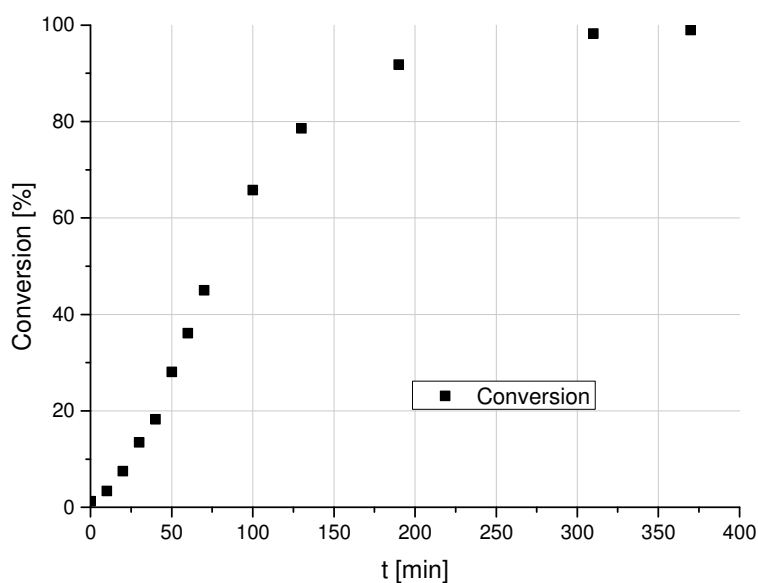


Figure 14: Conversion–time plot of EEGE polymerization with DP=50 and KOtBu as initiator at 45 °C in THF.

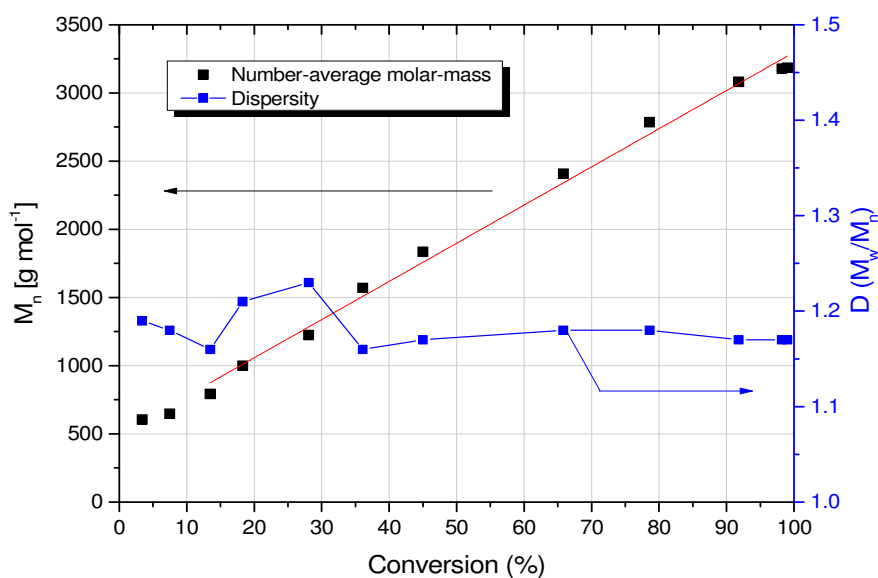


Figure 15: Molar-mass- and dispersity-conversion plot of EEGE polymerization with DP=50 initiated with KOtBu at 45 °C in THF. Linear relationship (linear fit: red line) between number-average molar mass (■) and conversion is indicated which is typical for a living polymerization. Dispersity (■) is decreasing with the conversion. The initial increase is assigned to the inaccuracy of SEC analysis.

The evolution of the molar-mass and \bar{D} with conversion is shown in Figure 15. \bar{D} is finally below 1.2 as it is expected for a living polymerization and reaches a value of $\bar{D} = 1.17$. Initial variation of \bar{D} up to 28 % conversion is assigned to the inaccuracy of SEC measurements as the polymer signal cannot completely be separated from residual monomer or solvent signals. After 28 % conversion \bar{D} decreases to $\bar{D} = 1.17$ and does not significantly change over time. The SEC elugramm in Figure 16 also shows a monomodal molar-mass distribution of poly(EEGE) with $DP = 50$ and $M_n = 3200 \text{ g mol}^{-1}$ at a conversion of 99 %. For this elugram a small high molar-mass fraction is observed. In contrast to described protocols with e.g. $120 \text{ }^\circ\text{C}$ in diglyme and potassium as counterion,[61] this higher molar-mass fraction is less present due to lower polymerization temperatures. As the fraction in literature can be observed as a clear separated signal in the elugramm, here only an almost negligible shoulder is observed. Comparing the results with the $DP = 20$ experiment, $\bar{D} = 1.17$ for both experiments, indicates that there is no obvious change in control over polymerization. In both EEGE polymerizations, with 20 and 50 repeating units, control over molar-mass, dispersity and modality is good. Although $\bar{D} = 1.17$ is at the upper limit of the definition of narrow molar-mass distribution the distribution is still judged as narrow.

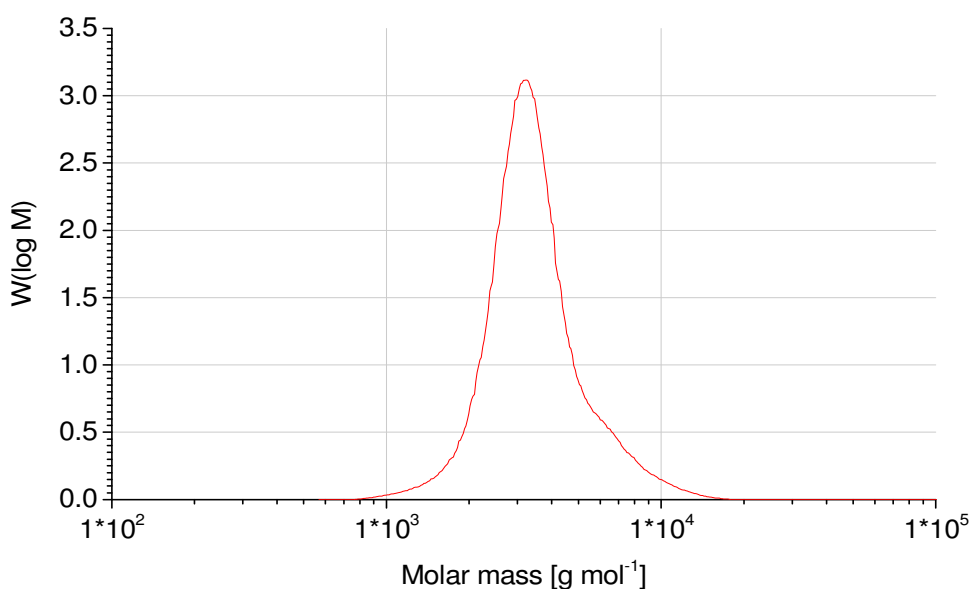


Figure 16: SEC trace of the final poly(EEGE) obtained with KOtBu as initiator at $45 \text{ }^\circ\text{C}$ and $DP = 50$ in THF. For this poly(EEGE) a M_n of 3200 g mol^{-1} and $\bar{D} = 1.17$ were obtained.

The first-order kinetics plot of the polymerization (Figure 17) with DP=50 also indicates an induction period at the beginning of the polymerization. After 3000 s (50 min, 28 % conversion) a linear increase is detected. At 18600 s (310 min, 98 % conversion) the data point slightly deviates from the linear relation and was not used for the determination of the slope with $k_{\text{app}} = 2.61 \cdot 10^{-4} \text{ s}^{-1}$. With an initiator concentration of $[I] = 0.120 \text{ M}$, a propagation rate constant of $k = 2.18 \cdot 10^{-3} \text{ L mol}^{-1} \text{ s}^{-1}$ was obtained.

Studies by Schmidt et al., using X-Ray, IR- and Raman measurements, showed that crystalline KOtBu exhibits a tetrameric cubic structure that is preserved after dissolution in THF.[141] Chisholm et al. confirmed these results and stated that the interaction of K^+ with THF is more weakly than with the alkoxide that leads to the maintenance of the cubic structure in solution.[142] The induction period of both polymerizations with DP=20 and DP=50 can be explained by this observation. Initially, at low degrees of polymerization, the K^+ -alkoxide structure are oligomeric and with growing polymer chain length the steric demand increases. This increase leads finally to a disruption of the structure. With time this leads to single K^+ -polymer alkoxide species that are then assumed to exhibit a reaction of first-order, visible as the linear region in the first-order kinetics plots. With a DP=20 this linear region starts at a conversion of 44 % (DP≈9) and for a DP=50 at 28 % (DP=14). It has to be noted that both starting points of the linear fitting were evaluated solely on the obtained data. A more detailed investigation would be necessary to define the DP at which solely single K^+ -polymer alkoxide species are present and confirm this hypothesis. These investigations would exceed the scope of this thesis.

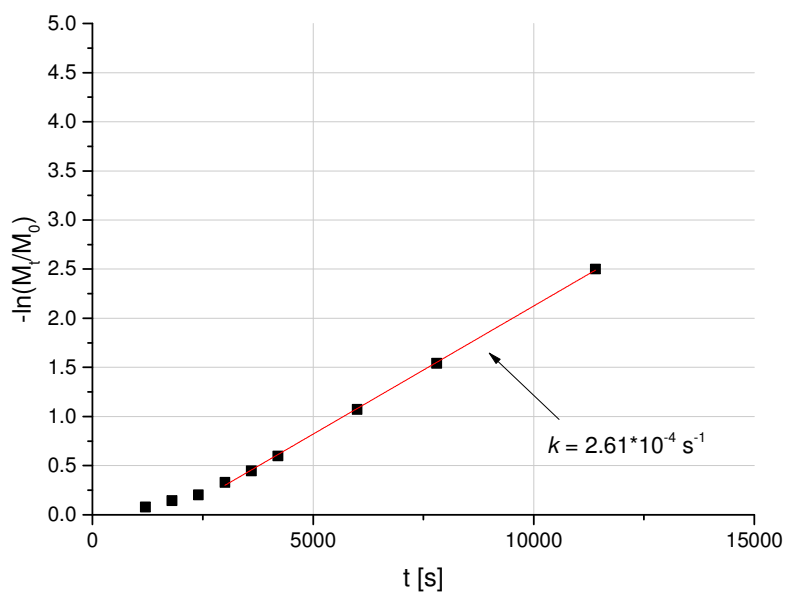


Figure 17: First-order kinetics plot of the polymerization of EEGE with DP = 50 initiated with KOtBu in THF at 45 °C. The apparent rate constant was obtained by a linear fit (red line) and the slope is inserted with $k_{app} = 2.61 \cdot 10^{-4} \text{ s}^{-1}$.

3.1.2.2. DP influence of AGE polymerization

Conversion of AGE polymerization was also determined by $^1\text{H-NMR}$ spectroscopy. As the AGE monomer shows different signals in $^1\text{H-NMR}$, the quantification by integration of the signal had to be modified. It is assumed that the overall content of allyl groups is independent on the degree of polymerization. Hence, the signal at $\delta = 5.95\text{-}5.75$ ppm in CDCl_3 , assigned to the allyl-proton $\text{CH}_2=\text{CH-CH}_2\text{-R}$, was used as reference and set to 100 (see Figure 18) for the percentage of conversion. The average value of all three epoxide-ring protons at $\delta = 3.20, 2.72$ and 2.60 ppm was used to determine the residual amount of monomers. After 50 min an example $^1\text{H-NMR}$ spectrum of poly(AGE) was recorded and is shown in Figure 18. Regarding this spectrum, the conversion is determined to be 74.9 %. This procedure was performed for all quenched Eppendorf cap contents and the results used for the determination of the conversion.

AGE was polymerized with KOtBu at 45 °C in Eppendorf caps with DP = 20. The conversion–time plot is shown in Figure 19. The conversion increases very fast at the beginning and is slowing down after approximately 75 min. The linear region starts right at the beginning of the reaction and lasts till 60 min. In contrast to EEGE polymerization (see 3.1.2.1) full conversion is reached after 200 min. This indicates a faster polymerization of AGE in contrast to EEGE.

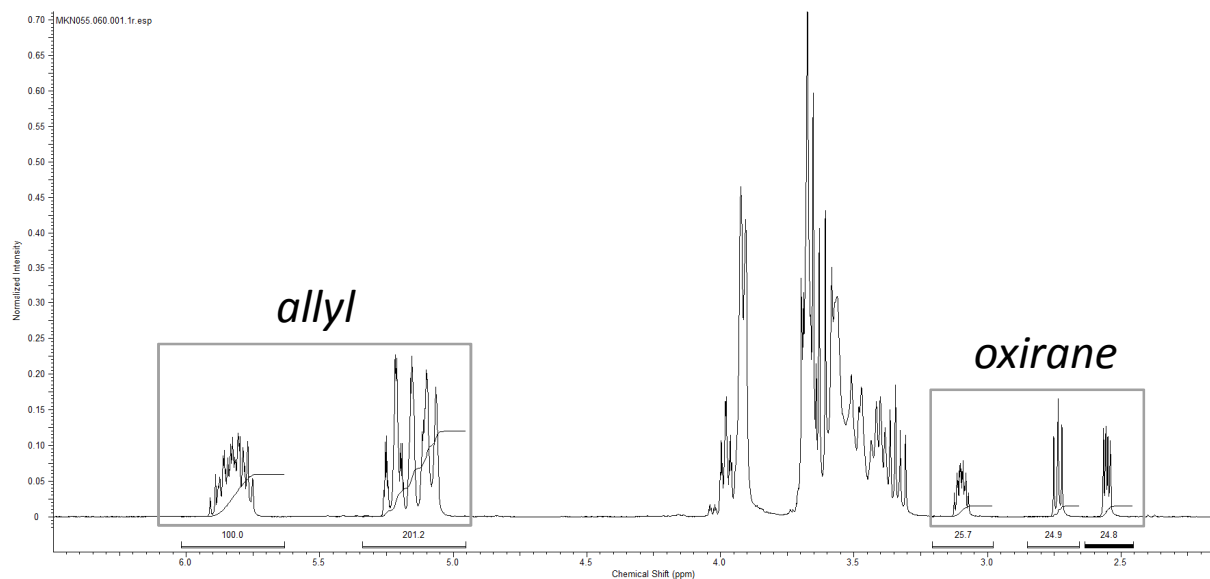


Figure 18: $^1\text{H-NMR}$ spectrum of poly(AGE) in CDCl_3 showing typical allyl signals at $\delta = 5.90\text{--}5.50$ ppm and epoxide-ring signals at $\delta = 3.20, 2.72$ and 2.60 ppm.

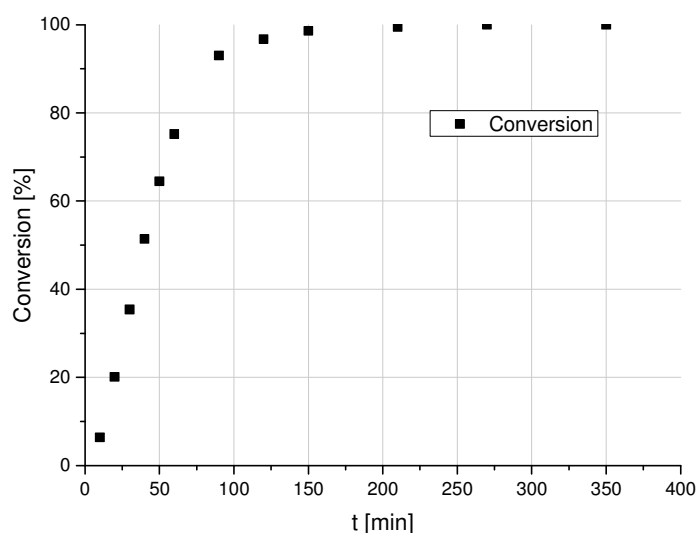


Figure 19: Conversion–time plot of AGE polymerization with DP = 20 and KOtBu as initiator at 45 °C in THF.

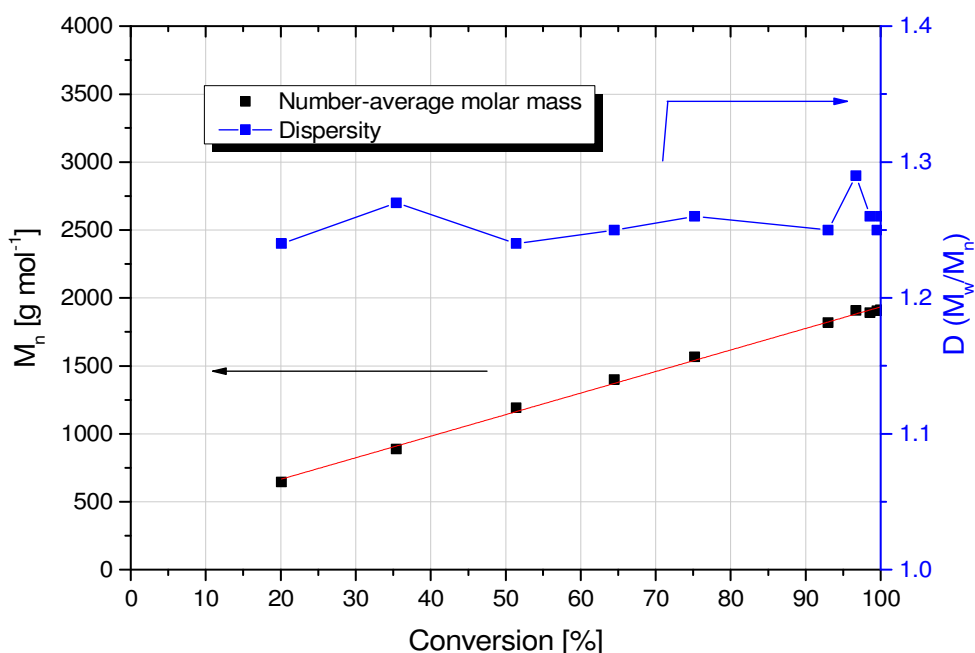


Figure 20: Molar-mass and dispersity–conversion plot for AGE polymerization with DP=20 initiated with KOtBu at 45 °C in THF. Linear relationship between molar-mass (■) and conversion (linear fit: red line) is indicated which is typical for a living polymerization. Dispersity (■) shows inconsistencies during the course of reaction.

M_n - and \bar{D} -dependencies on the conversion are given in Figure 20. The linear relation of M_n with conversion also indicates the living character of the reaction. Although the living character is indicated, the dispersity of the reaction product is too high. A dispersity of $\bar{D} = 1.26$ (with $M_n = 1912 \text{ g mol}^{-1}$) was obtained for the final product. These values are higher than 1.2 and the resulting poly(AGE) should not be determined as narrowly distributed. The SEC traces were recorded and allowed a further look into detail of the evolution of the dispersity. Figure 21 shows the elugrams of poly(AGE) after 40 min and 270 min polymerization time at 45 °C with KOtBu as initiator in THF with an aimed DP of 20. At higher conversion (100 % after 270 min) a shoulder can be observed at higher molar-masses. Although this shoulder is more pronounced in the final polymer than after 40 min (51.4 % conversion), the dispersity only slightly increases from $\bar{D} = 1.24$ to 1.26. In combination with Figure 20, dispersity is similar in course of the whole reaction. This leads to the assumption that a side-reaction occurs at the beginning of the reaction, but is not significantly changing

with time. In general, a change from colorless monomers to yellowish/brownish polymers occurs upon addition of the monomer to the initiator solution. Regarding the polymer, poly(AGE) was more intense in a yellow/brownish color than poly(EEGE). Additionally, in the case of AGE polymerization it was observed that this colour change is faster and more intense.

The first-order kinetics plot of the polymerization of AGE with DP=20 initiated with KOtBu at 45 °C also shows a non-linear increase at the beginning of the polymerization (Figure 22). After 1800 s (30 min, 35 % conversion) a linear increase was observed with a slope of $k_{app} = 5.31 \cdot 10^{-4} \text{ s}^{-1}$. After 3600 s (60 min, 75 % conversion) the slope decreases again. The initial non-linear increase was also assigned to the presence of tetrameric clusters of the initiator in the solution. With a conversion of 35 %, this corresponds to a chain length of DP = 7. From the linear increase the propagation rate constant was determined with an initiator concentration of $[I] = 0.305 \text{ M}$. For the polymerization of AGE under the given conditions, a rate of propagation of $k = 1.74 \cdot 10^{-3} \text{ L mol}^{-1} \text{ s}^{-1}$ was obtained. Although these results are similar for the polymerization of EEGE with DP = 20 ($k = 1.70 \cdot 10^{-3} \text{ L mol}^{-1} \text{ s}^{-1}$) it has to be noted that the determination of k was performed only once and no standard deviation can be given.

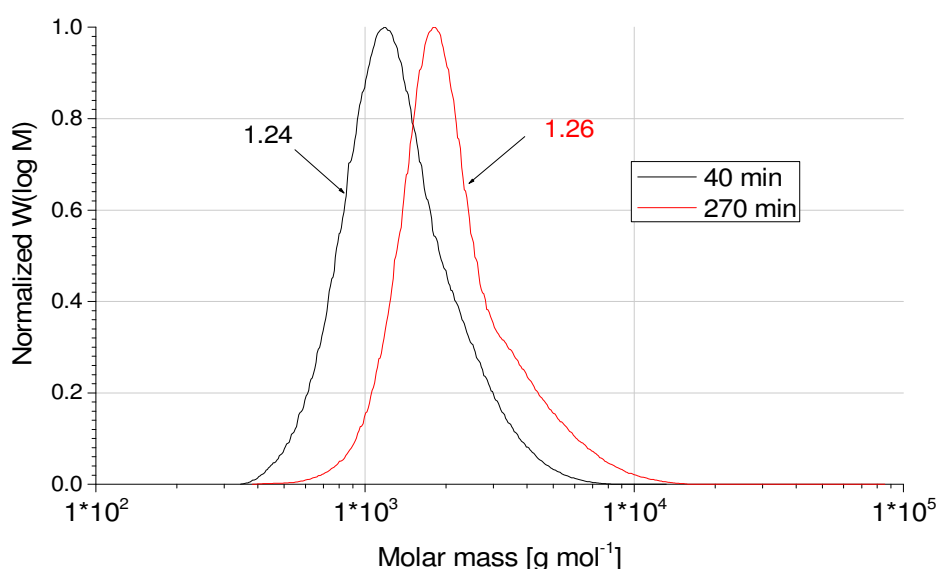


Figure 21: SEC elugram of poly(AGE) after 40 min and 270 min polymerization initiated with KOtBu at 45 °C in THF with inserted dispersities.

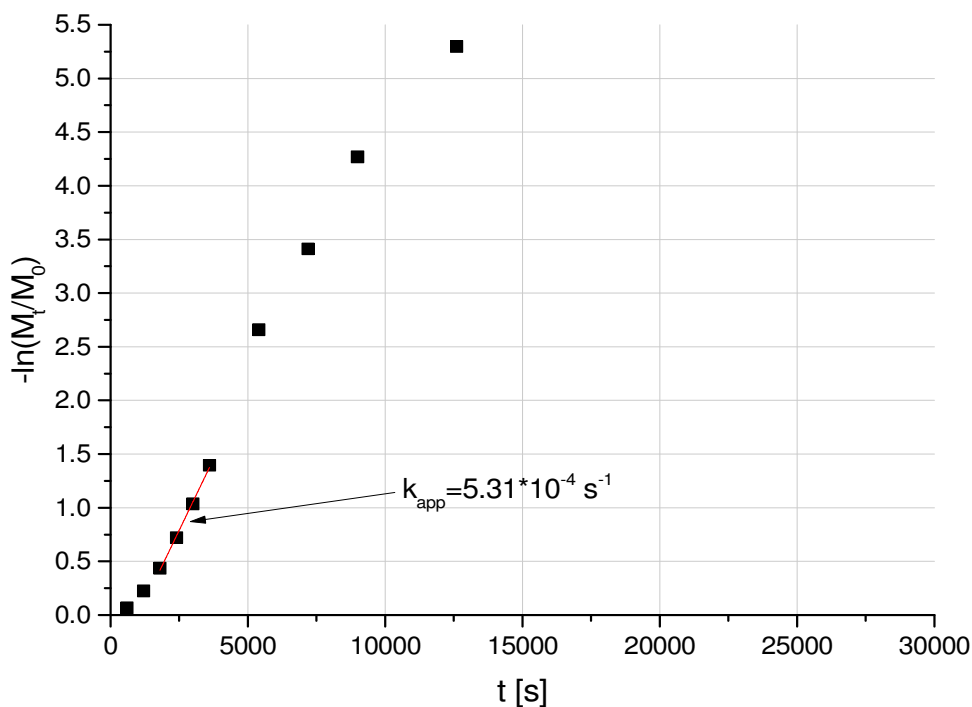


Figure 22: First-order kinetics plot of the polymerization of AGE with DP=20 initiated with KOtBu at 45 °C. A small induction period at the beginning of the reaction is observed with a subsequent linear slope. The apparent rate constant $k_{app}=5.31 \cdot 10^{-4} \text{ s}^{-1}$ (determined by a linear fitting (red line)) is inserted.

The polymerization of AGE was also investigated for DP = 50 initiated with KOtBu in THF at 45 °C. The full conversion–time plot is shown in Figure 23 and can be compared to the conversion–time plot of poly(AGE) with DP = 20 (Figure 19). This shows that the polymerization of AGE with DP = 20 is completed after 270 min, whereas polymerization for a DP of 50 takes longer with 330 min for 98 % conversion.

The M_n – and dispersity–conversion plot is shown in Figure 24. A more detailed look into the course of polymerization, regarding M_n evolution, reveals that the polymerization itself indicates a living character, whereas the dispersity of the molar-mass distribution increases from $\mathcal{D} = 1.28$ (30 %) to $\mathcal{D} = 1.36$ (98 %) with conversion (Figure 24). This increase in \mathcal{D} is not observed with DP = 20 and suggests a pronounced side-reaction that is not directly visible by the evolution of M_n .

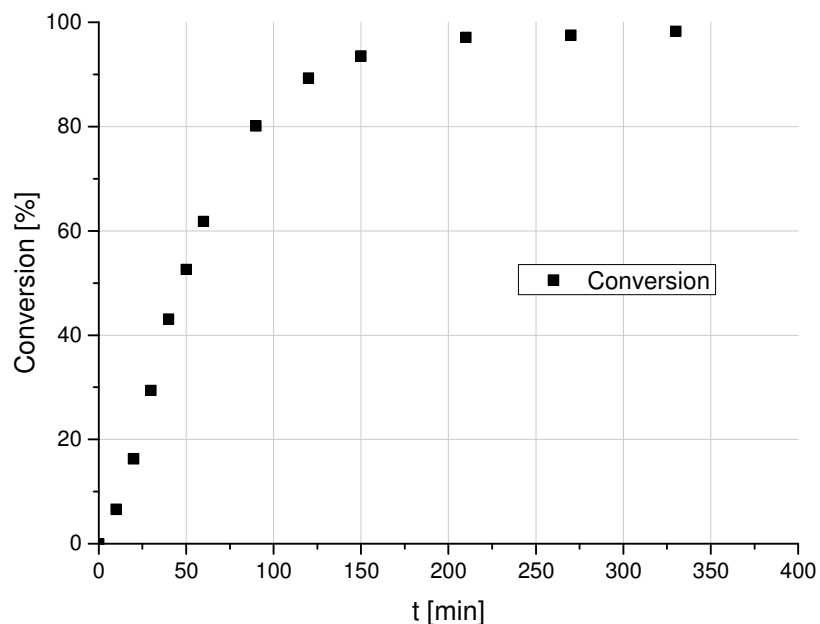


Figure 23: Conversion–time plot of AGE polymerization with DP=50 and KOtBu as initiator at 45 °C in THF. After 330 min a conversion of 98 % was obtained.

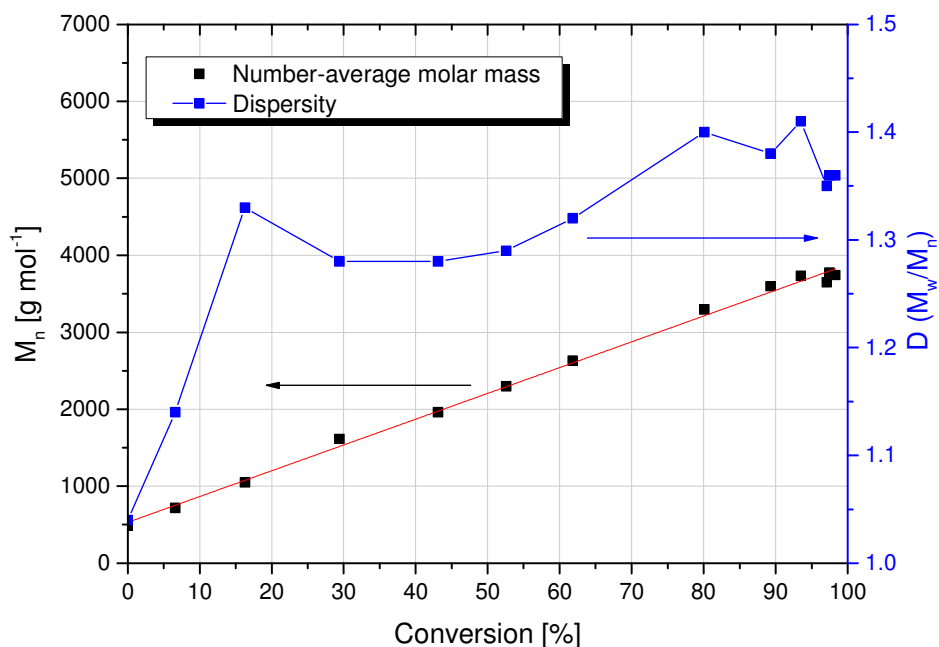


Figure 24: M_n – and dispersity–conversion plot of AGE polymerization with DP=50 initiated with KOtBu at 45 °C in THF. Linear relationship (linear fit: red line) between M_n (■) and conversion is indicated which is typical for a living polymerization. Dispersity (■) is increasing with the conversion and also shows strong variations during the polymerization.

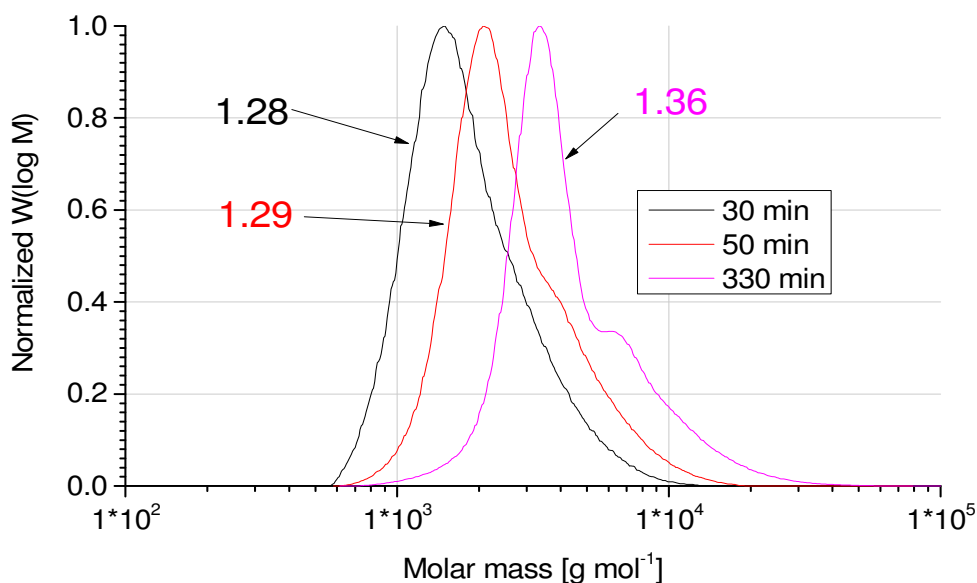


Figure 25: SEC trace of poly(AGE) polymerized with KOtBu in THF at 45 °C with DP=50. Dispersities are inserted for the corresponding SEC trace. An evolving bimodality with higher reaction times was detected with a concurrent increase in dispersity.

The evolution of SEC traces is shown in Figure 25. After 30 min polymerization at 45 °C the SEC trace is already broad and dispersity of the polymer is determined to be $\mathcal{D} = 1.28$ with a number-average molar mass of $M_n = 1614 \text{ g mol}^{-1}$. Further polymerization shifts the SEC traces to higher molar masses with $M_n = 1961 \text{ g mol}^{-1}$ ($\mathcal{D} = 1.29$) after 50 min and $M_n = 3744 \text{ g mol}^{-1}$ ($\mathcal{D} = 1.38$) after 330 min. The curve of the elugram indicates an evolution of an additional species with approximately the double molar mass. At the beginning (30 min) a broad curve and $\mathcal{D} = 1.29$ is given. The initial broad curve gets more and more defined and bimodality evolves. Together with Figure 24 the appearance of the second polymer species correlates with the increase of the dispersity reaching a final \mathcal{D} of 1.36. It has to be noted that the relationship of M_n and conversion is still linear, indicating a living character of the polymerization.

Plotting $-\ln(M_t/M_0)$ against time (Figure 26) was used to investigate the first-order kinetics of the reaction. At the beginning a small continuous increase of the slope appears up to a time point of approximately 1800 s (30 min). This was also assigned to the disintegration of the initiator tetramers at the beginning of polymerization as was described in chapter 3.1.2.1 for the polymerization of EGE with KOtBu in THF. After this small induction period, a linear

increase from 1800 s (30 min, 29 % conversion) to 5400 s (90 min, 80 % conversion) was detected. With a conversion of 29 % this corresponds to a $DP \approx 15$. This linear relation was used to determine k_{app} . Here an apparent rate constant of $k_{app} = 3.51 \cdot 10^{-4} \text{ s}^{-1}$ was obtained. The initiator concentration was $[I] = 0.146 \text{ M}$ and a propagation rate constant of $k = 2.40 \cdot 10^{-3} \text{ L mol}^{-1} \text{ s}^{-1}$ was calculated. A similar propagation rate for the polymerization of EEGE with $DP = 50$ initiated KOtBu in THF at $45 \text{ }^\circ\text{C}$ was obtained ($k = 2.18 \cdot 10^{-3} \text{ L mol}^{-1} \text{ s}^{-1}$). The slightly faster polymerization for AGE in contrast to EEGE was observed for both $DP = 20$ and $DP = 50$. The final decrease of reaction rate is assigned to the reduced content of residual monomer in the solution slowing down the conversion rate.

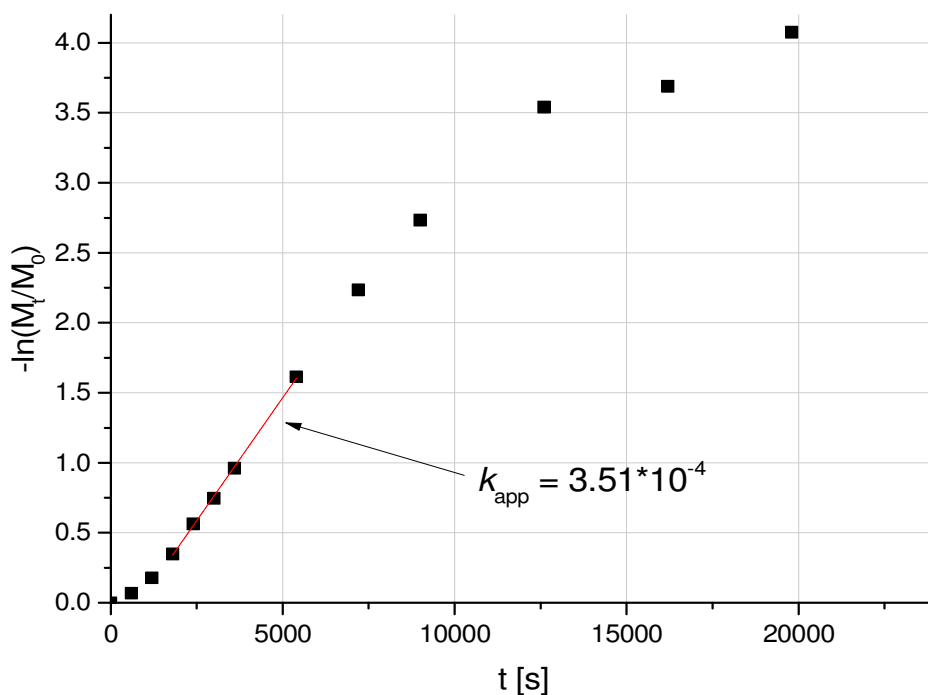


Figure 26: First-order kinetics plot of AGE polymerization with DP=50 and KOtBu as initiator at $45 \text{ }^\circ\text{C}$ in THF. The linear fit (red line) between 1800 and 5400 s was used to determine k_{app} , having a value of $k_{app} = 3.51 \cdot 10^{-4} \text{ s}^{-1}$.

3.1.2.3. EEGE and AGE copolymerization

The conversion–time plot (Figure 27) of the copolymerization of EEGE and AGE with EEGE:AGE=45:5, initiated with KOtBu at 45 °C in THF, was obtained by using $^1\text{H-NMR}$ spectroscopy as was described in the previous chapters. Here a strong increase in conversion with time can be observed at the beginning and the continuous decrease in the conversion slope after approximately 120 min. A conversion of 82 % after 60 min was declared as an outlier as it obviously does not correlate with the clearly visible relationship of conversion with time in Figure 27.

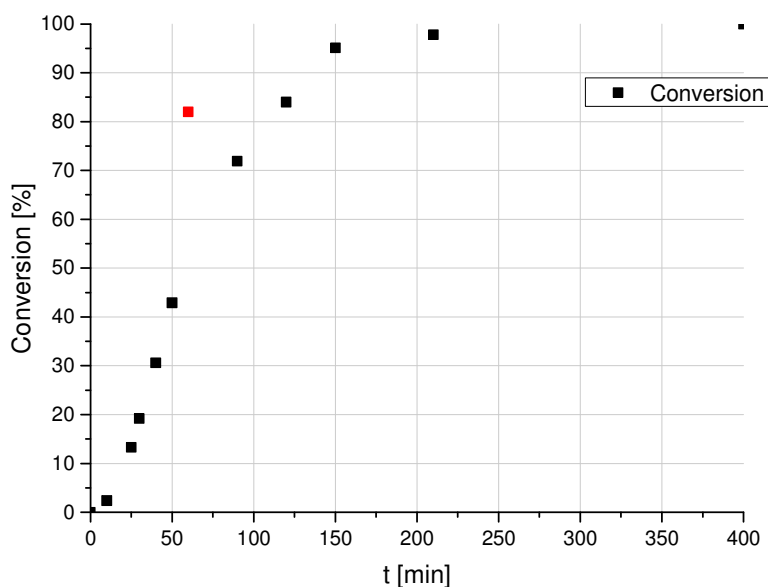


Figure 27: Conversion–time plot of EEGE:AGE=45:5 copolymerization at 45 °C initiated with KOtBu in THF. The red highlighted data point was declared as an outlier.

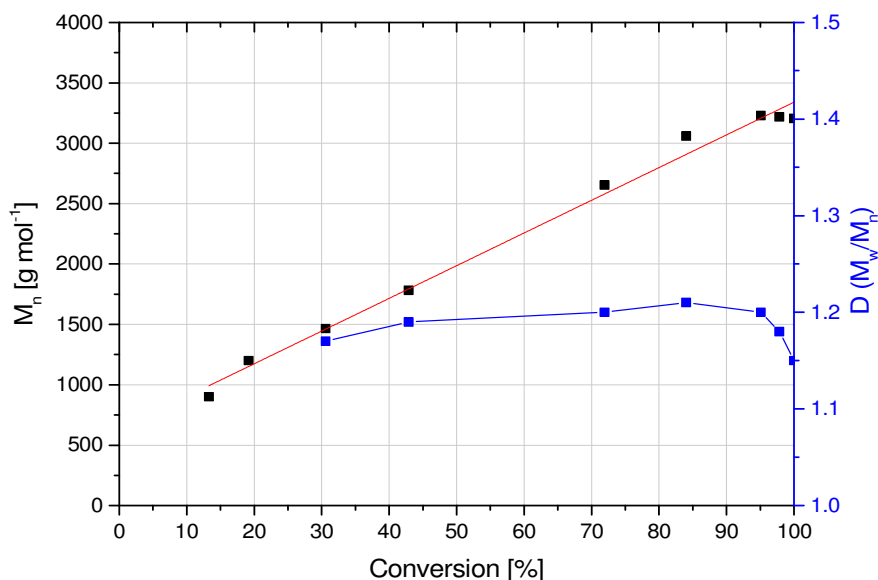


Figure 28: Molar-mass and dispersity–conversion plot of the copolymerization of EEGE and AGE with EEGE:AGE=45:5 initiated with KOtBu in THF at 45 °C. Linear relationship between molar-mass (■) and conversion is indicated with a linear fit (red line). Dispersity (■) increases with conversion and decreases upon reaching a conversion of 95 %.

The linear relationship between M_n (determined by SEC in DMF with 1.0 g L⁻¹ LiBr) and conversion indicated a copolymerization without termination and side-reactions (Figure 28). After 95 % conversion (determined by ¹H NMR) the molar mass seems to increase no further. This can be explained by analytical issues. 5 % of the reaction mixture equal approximately 2.5 repeating units with an overall DP = 50. A theoretical maximum molar-mass increase of additional 2.5 repeating units at the end would add 360 g mol⁻¹ ($2.5 \cdot M_{\text{EEGE}} = 144 \text{ g mol}^{-1}$). AGE was used with 10 % in the comonomer-mixture and the residual AGE content is 0.25 units. It is assumed that it can be neglected for further calculations. $M = 360 \text{ g mol}^{-1}$ is used with the M_n –conversion relationship in Figure 28. The slope of the M_n –conversion relationship was determined to be 27 g (mol · %)⁻¹. Theoretically, these 360 g mol⁻¹ correspond to a conversion of 13 %. This error can be assigned to the calibration of the SEC with poly(ethylene glycol) (PEG). As PEG is assumed to differently coil in DMF/LiBr compared to poly(EEGE-co-AGE), different hydrodynamic radii result for the same molar mass. Therefore molar masses determined by SEC are different from theoretical values. Additionally, copolymers might have polymeric structures other than random coils

further increasing the error. The factor between “SEC-conversion” and “NMR-conversion” was determined to be:

$$\frac{13\%}{2.5\%} = 5.2$$

If this correction factor is used for recalculating the increase in molar mass that should be visible in SEC a value of

$$\frac{360}{5.2} \cdot \frac{g}{mol} = 69 \frac{g}{mol}$$

is obtained. This order of molar mass increase is quite hard to be interpreted in SEC as the accuracy of this method is limited.

\mathcal{D} of the polymer was also determined by SEC as it is shown in Figure 28. The small increase of the dispersity from the beginning ($\mathcal{D} = 1.17$) to a conversion of 90 % ($\mathcal{D} = 1.21$) can be assigned to the presence of AGE. This monomer exhibits side-reactions at the beginning of the polymerization that might lead to a slight increase in \mathcal{D} with time as was shown before (chapter 3.1.2.2). For conversions higher 95 %, \mathcal{D} decreases again. This is also assigned to a mixture of inaccuracy and copolymer behavior in the mobile SEC phase. The final polymer had a $M_n = 3205 \text{ g mol}^{-1}$ and $\mathcal{D} = 1.21$.

A first-order kinetics plot was used to investigate aforementioned induction period and to determine the apparent rate constant (Figure 29). It should be noted that the overall rate constant was determined covering the total monomer consumption and it was not distinguished between AGE and EEGE monomer. The monomeric- and polymeric signals of the acetal-H group of EEGE in $^1\text{H-NMR}$ spectroscopy overlap and cannot clearly be separated for integration. Especially for the allyl-group signals of AGE in $^1\text{H-NMR}$ spectroscopy a separation is impossible. Furthermore, propagation rate constants determined for the homopolymerization of EEGE and AGE before indicate a similar rate that is confirmed by literature.[69] The induction period, ascribed to the tetrameric structure of the initiator in THF, was detected up to 1500 s (25 min, 13 % conversion). This corresponds to a DP of 7 although it has to be noted that the transition of the induction period to the linear region cannot be fully resolved. The apparent rate constant was determined to be $k_{\text{app}} = 3.01 \cdot 10^{-4} \text{ s}^{-1}$. With an initiator concentration of $[I] = 0.122 \text{ M}$ an overall propagation rate of $k = 2.47 \cdot 10^{-3} \text{ L mol}^{-1} \text{ s}^{-1}$ was obtained.

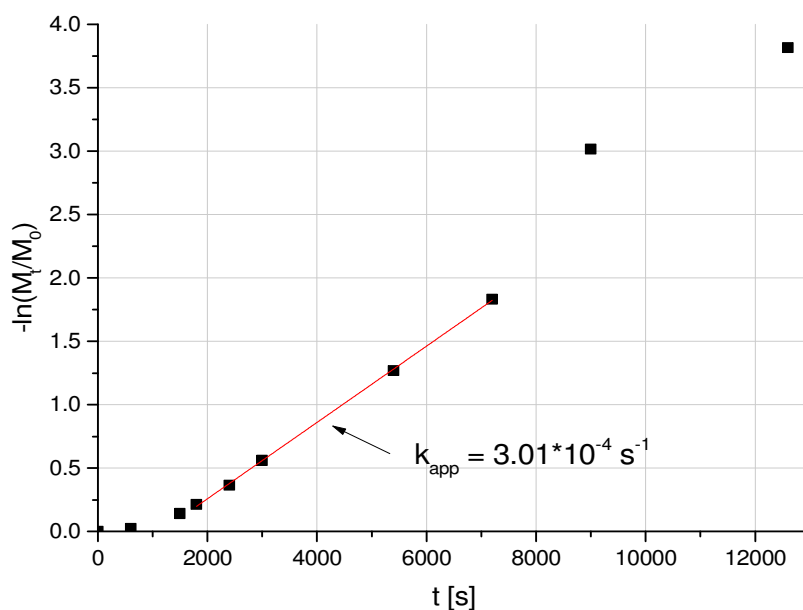


Figure 29: First-order kinetics plot for the copolymerization of EEGE and AGE with EEGE:AGE=45:5 with KOtBu in THF at 45 °C. The slope (linear fit: red line) was used to determine k_{app} having a value of $3.01 \cdot 10^{-4} \text{ s}^{-1}$.

3.1.3. Polymerization with Cs⁺ as counter ion in THF

The counter ion of IROPs plays an important role as the nature of the active species can vary, depending on the parameters. In the polymerization conditions that were investigated, potassium alkoxides and cesium alkoxides are either present as polarized covalently binding pair, contact ion pair, solvent separated ion pair or free ions mainly determining the reactivity of the active species.

KOtBu was obtained as a THF solution (1 M) by Sigma-Aldrich. In contrast to that, the cesium initiator solution was prepared before investigation of the polymerization. Phenoxyethanol, benzylic alcohol, mPEG500 and triethylene glycol monomethyl ether were investigated as initiator.

Three factors were considered to be important and advantageous for the polymerization.

1. The initiator solubility in THF.
2. Initiator signals shall not overlap with polymer signals in $^1\text{H-NMR}$ spectroscopy. This is required to determine M_n with the initiator as internal reference.
3. It should be short/small and not influence the properties of the resulting polyglycidols.

3.1.3.1. Initiator selection

Phenoxyethanol was tested as the initiator. The aromatic signal of the phenyl ring usually appears in $^1\text{H-NMR}$ spectra around 7 ppm. As there are no signals to be expected for the polyglycidols, neither poly(AGE) nor poly(EEGE), a M_n determination via $^1\text{H-NMR}$ spectroscopy should be possible. The slight excess of alcohol (1.05 eq wrt CsOH) was stirred with CsOH in benzene for 45 min at 60 °C under dry and inert atmosphere (argon). Afterwards all volatile components (benzene, water) were removed under reduced pressure (10^{-3} mbar) at 90 °C overnight. Inside the glovebox, THF as solvent was added to the initiator. Already at this time point it was visible that the solubility of Cs-phenoxyethanolate was limited. Nonetheless the polymerization was performed. The turbid solution was mixed with the monomer and 50 μL aliquots put into Eppendorf caps.

Cs-phenoxyethanolat as initiator was used at 45 °C in THF to polymerize EEGE. Plotting the conversion of the EEGE monomer (determined by $^1\text{H-NMR}$) against time indicates a polymerization that is not completed after 2880 min (91 % conversion, Figure 30). This is assumed to be caused by the limited solubility of the initiator in the solvent and a closer bonding between the Cs^+ and the alkoxide in comparison to the K^+ with the alkoxide. As a more close packing between the ions hinders the nucleophilic opening of the epoxide-ring, the reaction rate is reduced.

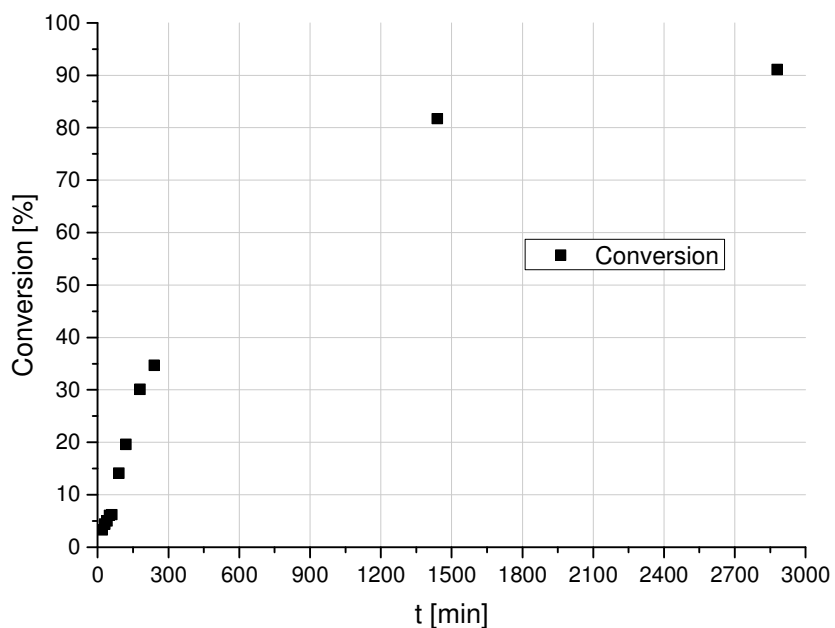


Figure 30: Conversion–time plot for the polymerization of EEGE with Cs-phenoxyethanolate in THF at 45 °C.

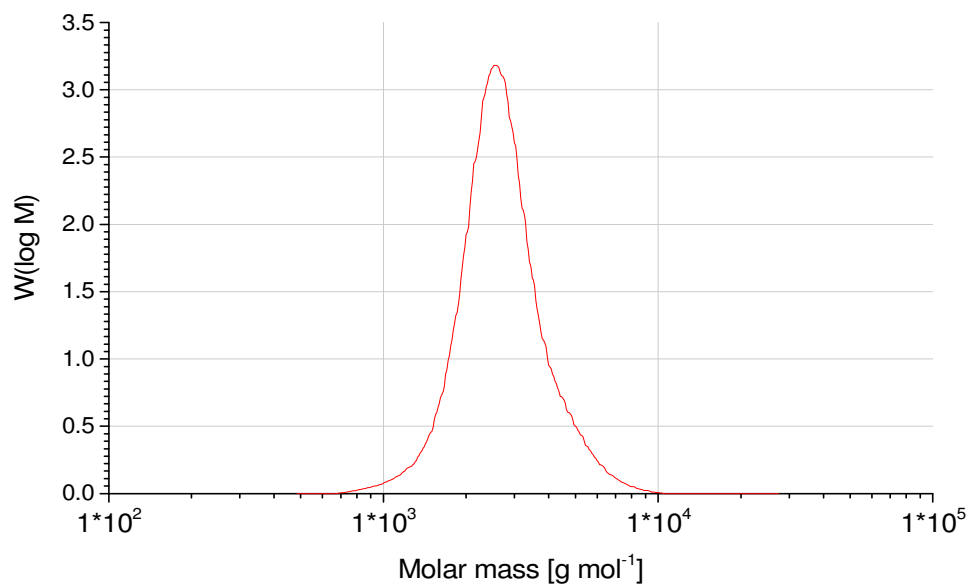


Figure 31: SEC trace of poly(EEGE) after 2880 min and 91 % conversion of EEGE with Cs-phenoxyethanolate at 45 °C in THF. The polymer had $M_n = 2500 \text{ g mol}^{-1}$ and $\mathcal{D} = 1.13$.

The molar mass was determined to be $M_n = 2500 \text{ g mol}^{-1}$ as can be seen in Figure 31. Expected molar masses of 3000-3500 g mol^{-1} for poly(EEGE) with DP=50 in DMF (with 1g/L LiBr) were not reached confirming the incomplete conversion already determined by ^1H NMR. It should be noted that a monomodal molar-mass distribution was obtained with a dispersity of $D = 1.13$.

The first-order kinetics plot of the polymerization of EEGE with DP = 50 initiated with Cs-phenoxyethanolat in THF at 45 °C was investigated (Figure 32). After 1200 s (20 min) 3 % of the monomer was converted and a linear increase in the first-order kinetics plot was observed. Here two apparent rate constants were determined by linear fits as two regions in the first-order kinetics plot showed a linear increase. The first linear fit was found between 1200 s and 3600 s. With an apparent rate constant of $1.31 \cdot 10^{-5} \text{ s}^{-1}$, and under the assumption that all initiator is active, a propagation rate of $k_1 = 1.27 \cdot 10^{-4} \text{ L mol}^{-1} \text{ s}^{-1}$ was obtained. From 5400 s (90 min, 14 % conversion) to 10800 s (180 min, 30 % conversion) a second linear increase starts with $k_{\text{app}} = 3.83 \cdot 10^{-5} \text{ s}^{-1}$ and therefore $k_2 = 3.72 \cdot 10^{-4} \text{ L mol}^{-1} \text{ s}^{-1}$. A reason for these two linear increases requires further investigation, but could be assigned to the solubility issues observed at the preparation of the initiator. Both rates of propagation are approximately one order of magnitude lower than the polymerizations initiated with KOtBu. Although a good dispersity was obtained for the final polymer, the limited solubility restricts the use of Cs-phenoxyethanolate as initiator.

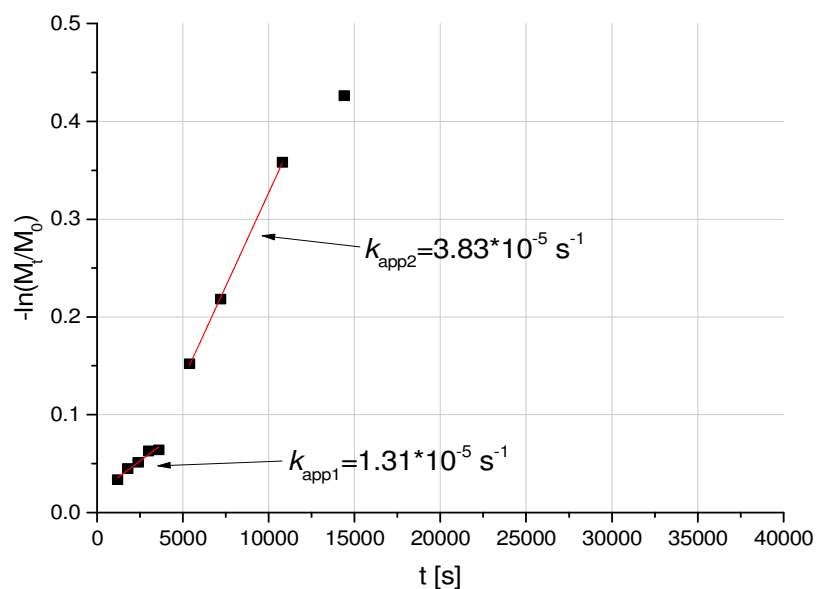


Figure 32: First-order kinetics plot of the polymerization of EEGE with Cs-phenoxyethanolate in THF at 45 °C with inserted apparent rate constants for two linear regions. Both slopes were determined by a linear fit (red line) of the data points.

Changing the alcohol from phenoxyethanol to benzylic alcohol showed the same solubility issues. Slightly turbid solutions were obtained after trying to solubilize the Cs-benzylalkoxide in THF. The solubility of the initiator is strongly influenced by the chemical composition of the alcohol. It was assumed that an increase of the chain length of the alcohol would improve the solubility of the corresponding Cs-alkoxide in THF. As PEG readily dissolves in THF, a Cs-PEG alkoxide should be a promising candidate to diminish the issues of initiator solubility. Evaluating the limit between solubility and chain length, mPEG500 was used in a first try. The PEG chain has to be as short as possible to reduced the influence of the terminal PEG-chain on the physical properties of the resulting poly(glycidol)s.

The Cs⁺/mPEG500-alkoxide initiator was prepared by the same protocol as the former Cs-alkoxides. Upon addition of THF in the glovebox the initiator readily dissolved and was used for the polymerization of EEGE and AGE. Additionally, to the inherent solubility of the PEG chain in THF, the coordination of the Cs⁺ with the PEG-ether is assumed to cause the solubility of the Cs⁺/mPEG500-alkoxide in THF. This is based on the consideration that

insoluble cesium salts, e.g. in THF, can readily be dissolved by using crown-ethers as additives that form a complex with the Cs⁺ cation.[143]

Conversion–time plots for the polymerizations of EEGE and AGE with DP = 50 with the Cs⁺/mPEG500-alkoxide as initiator in THF at 45 °C were created. Regarding the conversion–time plot, the polymerization with KOtBu is completed earlier than polymerizations initiated with Cs⁺/mPEG500-alkoxide. Using KOtBu as initiator, after 370 min a conversion of 99 % was found (chapter 3.1.2.1). For a Cs⁺/mPEG500-alkoxide initiated polymerization, after 1440 min a conversion of 92 % was obtained for the polymerization of EEGE (Figure 33). A similar observation was found for the polymerization of AGE. Initiated with KOtBu and a DP of 50, after 330 min a conversion of 98 % was obtained (chapter 3.1.2.2). If the initiation of the AGE polymerization with DP = 50 was performed with Cs⁺/mPEG500-alkoxide, after 2880 min a conversion of 88 % was obtained (Figure 34). To further investigate these differences, a detailed analysis of the propagation rates is given below.

For the polymerization of EEGE the molar mass evolution shows a linear relationship in the range of 16 – 74 % as it is indicated by a linear fit of these data (Figure 35). The data point obtained for a conversion of 9 % ($M_n = 764 \text{ g mol}^{-1}$) slightly deviated from this linear trend. For the data points at 80 % conversion (277 min) and 92 % (1440 min) higher M_n are expected regarding the linear trend. After 24 h poly(EEGE) had a molar mass of $M_n = 2696 \text{ g mol}^{-1}$ (92 % conversion) and a dispersity of $\mathcal{D} = 1.10$.

For the polymerization of AGE with DP = 50 and Cs⁺/mPEG500-alkoxide as initiator in THF at 45 °C a linear increase of M_n with conversion was observed in a range of 9 - 28 % (Figure 36). At lower conversions a linear trend can also be observed, slightly shifted to lower M_n values. This can be assigned, especially for the data points at 1 and 4 %, to the inaccuracy of the SEC as these values have M_n of 578 and 619 g mol^{-1} , respectively. These values are at the lower calibration limit of the SEC and the SEC elugrams show a partial overlap with residual monomer signals. After 24 h a conversion of 79 % was determined and a M_n of 1575 g mol^{-1} together with a dispersity of $\mathcal{D} = 1.13$ was obtained for poly(AGE). Here also a higher M_n was expected as this data point deviates from the linear trend obtained for the data points between 9 - 28 %.

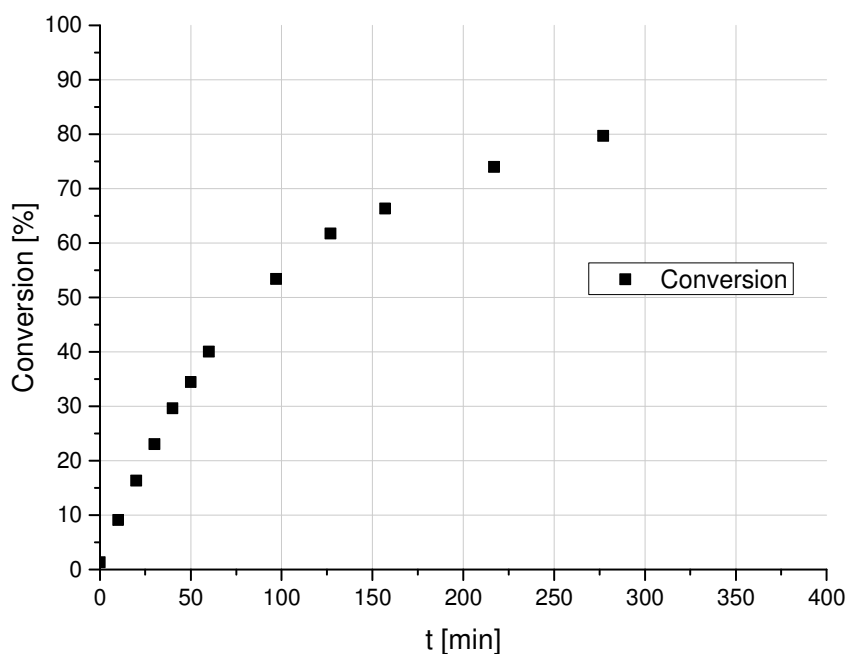


Figure 33: Conversion–time plot for EEGE polymerization with DP=50 and Cs⁺/mPEG500-alkoxide as initiator at 45 °C in THF.

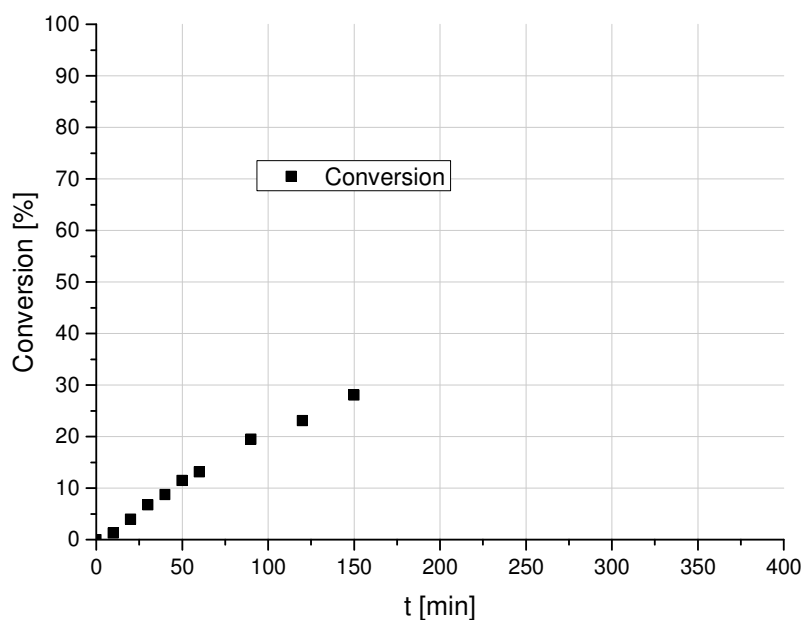


Figure 34: Conversion–time plot for AGE polymerization with DP=50 and Cs⁺/mPEG500-alkoxide as initiator at 45 °C in THF.

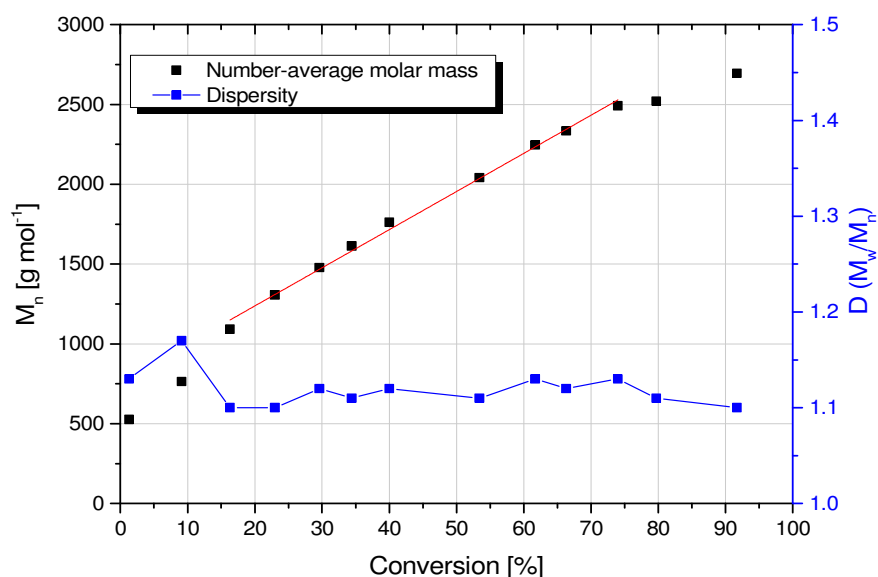


Figure 35: Molar-mass and dispersity–conversion plot of the EEGE polymerization with DP=50 and Cs⁺/mPEG500-alkoxide as initiator at 45 °C in THF. Linear fitting (red line) of the molar mass (■) is valid for the conversion range of 16-74 %. Dispersity (■) has higher values at the beginning and gets constant with increasing conversion.

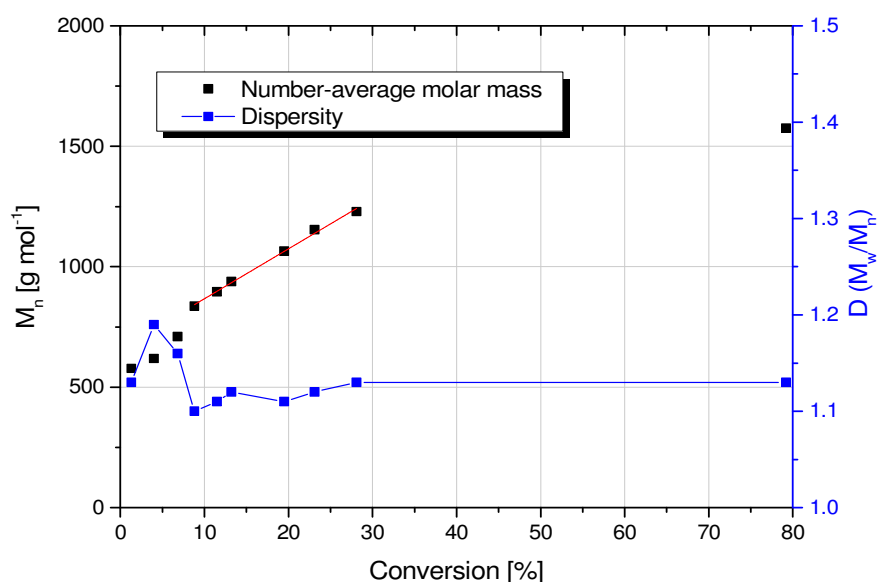


Figure 36: Molar-mass and dispersity–conversion plot of the AGE polymerization with DP = 50 and Cs⁺/mPEG500-alkoxide as initiator at 45 °C in THF. A linear fitting of M_n (■) with conversion can be obtained between 9 and 28 % (red line). Dispersity (■) is constant for conversions higher than 10 %.

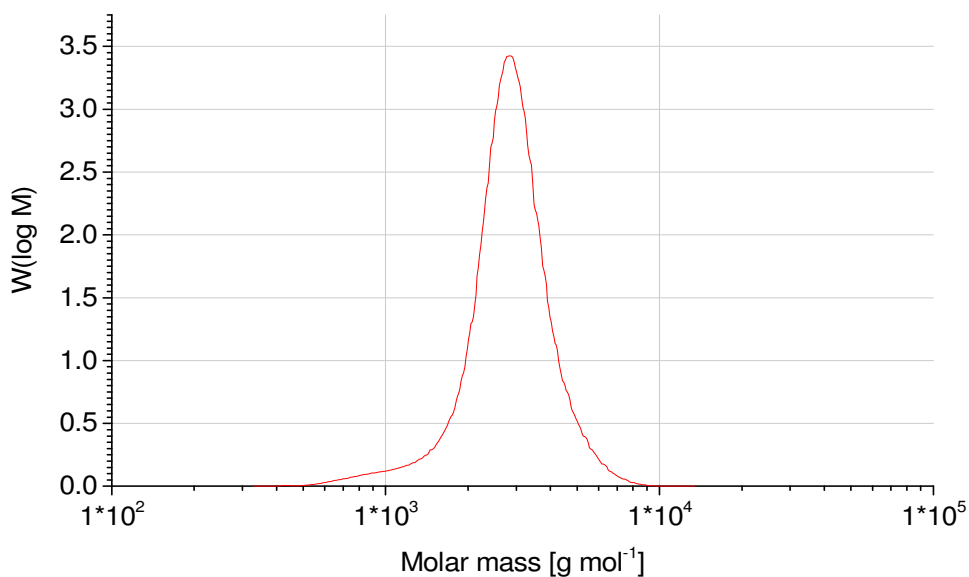


Figure 37: SEC trace of poly(EEGE) with DP=50 obtained by polymerizing EEGE with Cs^+ /mPEG500-alkoxide as initiator in THF at 45 °C. The polymer had $M_n = 2696 \text{ g mol}^{-1}$ and $\mathcal{D} = 1.10$ after 24 h polymerization (92 % conversion).

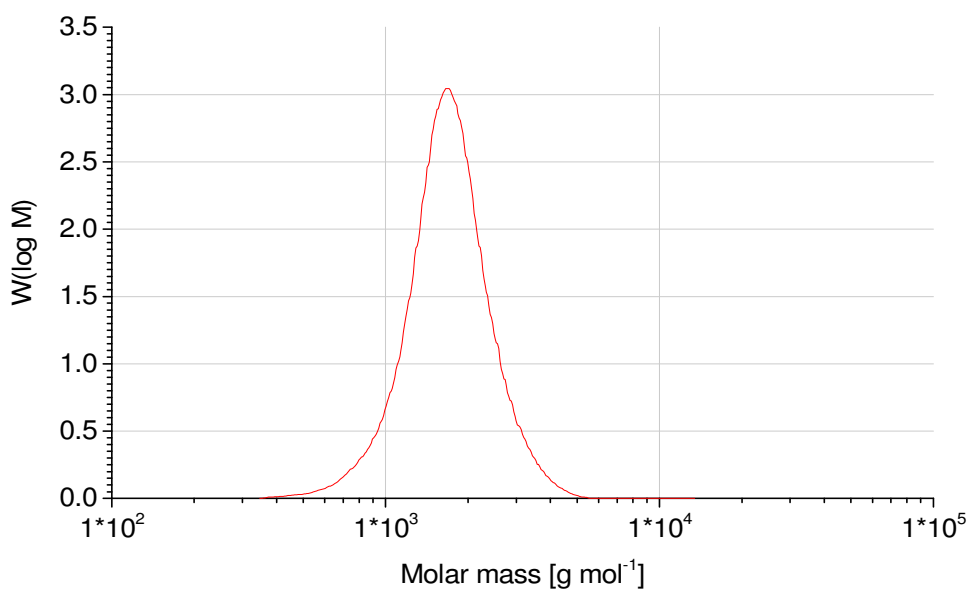


Figure 38: SEC trace of poly(AGE) with DP=50 obtained by polymerizing AGE with Cs^+ /mPEG500-alkoxide as initiator in THF at 45 °C. The polymer had $M_n = 1575 \text{ g mol}^{-1}$ and $\mathcal{D} = 1.13$ after 24 h polymerization (79 % conversion).

With respect to the molar-mass distributions, SEC analyses indicate a well control over both polymerizations (Figure 37 and Figure 38). SEC elugrams after 24 h show monomodal distributions with $\bar{D} = 1.10$ for poly(EEGE) and $\bar{D} = 1.13$ for poly(AGE) with 92 % and 79 % conversion, respectively. For both polymerizations dispersities are constant over the whole course of reaction and do not significantly increase or decrease (Figure 35 and Figure 36).

First-order kinetics plot of the polymerization of EEGE with Cs^+ /mPEG500-alkoxide in THF at 45 °C shows a good accordance with the first-order kinetics from 0 - 7620 s (0 - 127 min, 0 - 62 % conversion) (Figure 39). Here with an apparent rate constant of $k_{\text{app}} = 1.25 \cdot 10^{-4} \text{ s}^{-1}$, a rate of propagation of $k = 1.16 \cdot 10^{-3} \text{ L mol}^{-1} \text{ s}^{-1}$ was obtained. Interestingly, after 7620 s (157 min, conversions higher 62 %) a decrease in the slope was detected. A reason for this decrease could be assigned to a steric hindrance of the active chain end and reduced monomer content. The Cs^+ cation is assumed to be complexed with the synthesized polyether backbone and/or the ether backbone of the initiator. The negatively charged active chain end is attached to the complexed Cs^+ cation. With a growing polymer chain it can be assumed that the steric demand of the active center increases, concurrently reducing the overall rate of polymerization. Additionally, the reduced monomer content reduces the rate of propagation at the final stage of polymerization. It is assumed that a combination of both effects causes this reduction. No induction period is observed for the polymerization of EEGE with Cs^+ /mPEG500-alkoxide in THF at 45 °C. Polymerization starts immediately with a first-order kinetics in the monomer in contrast to polymerizations initiated with KOtBu .

First-order kinetics plot of the polymerization of AGE with Cs^+ /mPEG500-alkoxide in THF at 45 °C was performed (Figure 40). The first-order kinetics at the initial stage of polymerization was found. For a time period of 0 - 9000 s (0 - 150 min, 0 - 28 %) a linear fitting of the data points could be performed. With a slope of $k_{\text{app}} = 3.73 \cdot 10^{-5} \text{ s}^{-1}$ and $[\text{I}] = 0.135 \text{ M}$ a propagation rate of $2.76 \cdot 10^{-4} \text{ L mol}^{-1} \text{ s}^{-1}$ was determined. In general, the rate of propagation is approximately one order of magnitude lower than that for the polymerization of EEGE with Cs^+ /mPEG500-alkoxide (Figure 39). For the data point at 86400 s (1440 min) a deviation from this linear behavior was observed. As no data points were recorded for the time of 9000 - 86400 s (28 - 79 % conversion), the exact time point of k_{app} decrease could not be evaluated. Here again, the decrease of the rate of propagation can be assigned to a sterically demanding active center and a reduced content of the monomer at high conversions.

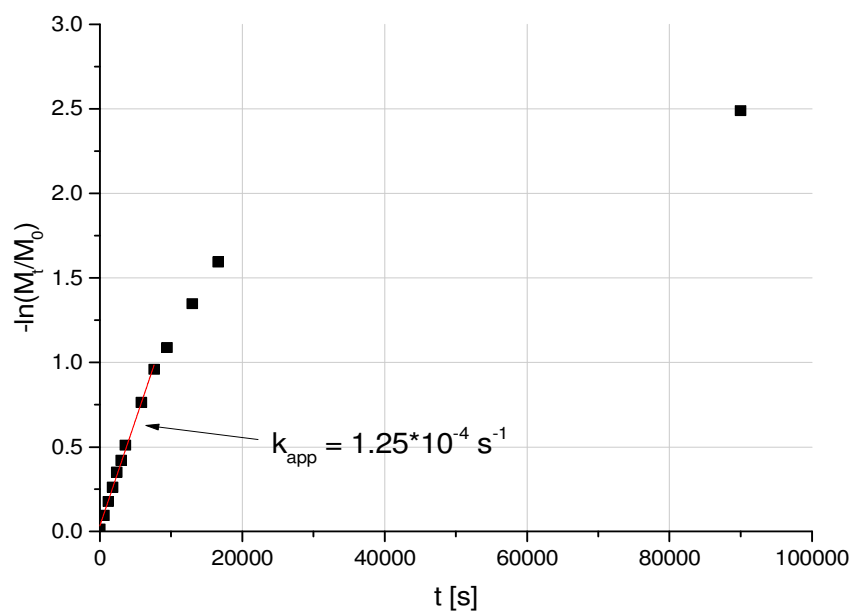


Figure 39: First-order kinetics plot of the polymerization of EEGE with Cs^+ /mPEG500-alkoxide in THF at 45 °C. For this polymerization $k_{app} = 1.25 \cdot 10^{-4} \text{ s}^{-1}$ was determined by a linear fit (red line).

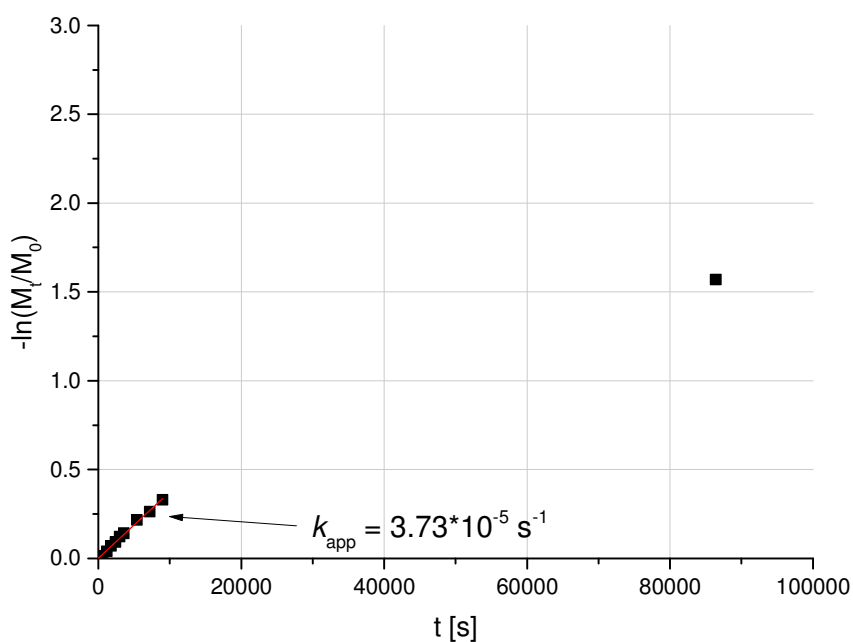


Figure 40: First-order kinetics plot of the polymerization of AGE with Cs^+ /mPEG500-alkoxide in THF at 45 °C. For this polymerization $k_{app} = 3.73 \cdot 10^{-5} \text{ s}^{-1}$ was determined by a linear fit (red line).

As mentioned above, literature describes the polymerization of EEGE and AGE with Cs⁺ as counter ion in bulk at 40 °C with DP = 20-30.[69] The authors used triethyleneglycol monomethyl ether (TEGME) as alcohol for the initiator synthesis. It was evaluated if the prepared initiator is soluble in THF to compare the obtained results with literature.

In a first try, EEGE and AGE were polymerized by the Cs⁺/TEGME-alkoxide initiator in THF. After preparation of the cesium salt, the initiator was dissolved in THF. The slightly turbid yellowish/brownish solution showed a better solubility of the initiator in THF than the Cs-phenoxyethanolate initiator but worse compared to the Cs⁺/mPEG500-alkoxide. The conversion–time plot of the EEGE and AGE polymerizations are shown in Figure 41. The direct comparison between the polymerization of EEGE and AGE shows remarkable differences with time. Whereas EEGE hardly polymerizes to completion and reaches only 96 % maximum after 70 h, AGE polymerization runs to completion within 100 min. A first-order kinetics plot was performed to directly compare the rates of propagation (Figure 42). After linear fitting of the data points (Figure 42) AGE polymerizes with an apparent rate constant $k_{app,AGE} = 1.31 \cdot 10^{-3} \text{ s}^{-1}$ in contrast to EEGE having $k_{app,EEGE} = 1.31 \cdot 10^{-4} \text{ s}^{-1}$. For these apparent rate constants, the propagation rates of $k_{AGE} = 8.68 \cdot 10^{-3} \text{ L mol}^{-1} \text{ s}^{-1}$ and $k_{EEGE} = 1.10 \cdot 10^{-3} \text{ L mol}^{-1} \text{ s}^{-1}$ were obtained. These observations show a faster polymerization of AGE in contrast to EEGE. This is in contrast to the results obtained for the polymerization initiated with Cs⁺/mPEG500-alkoxide in THF. It has to be noted that the synthesis of the initiator Cs⁺/TEGME-alkoxide was performed separately for each experiment. To rule out the error of different initiator stock solutions, the experiments were repeated using one stock solution for all experiments. The results are shown in the next chapter.

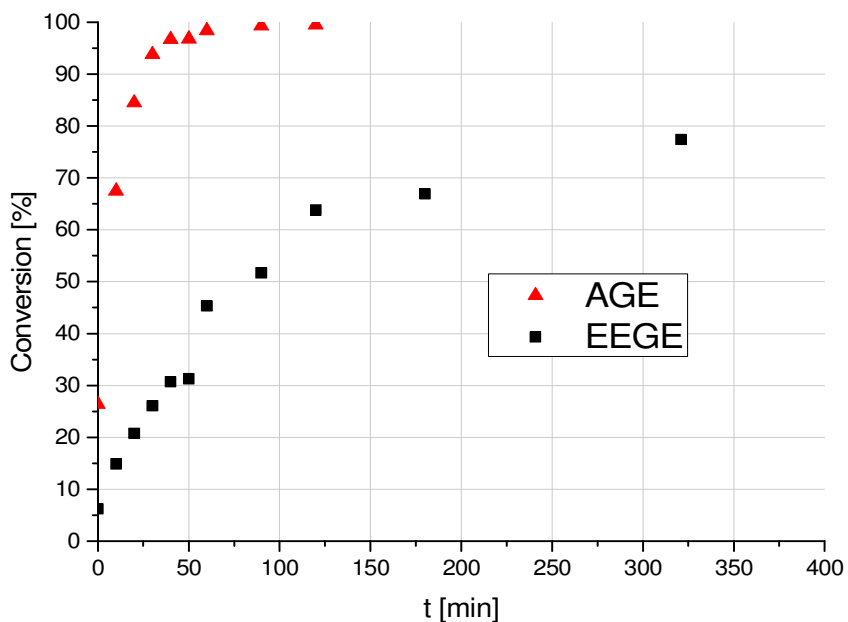


Figure 41: Conversion–time plot of the polymerization of EEGE and AGE with DP=50 initiated with Cs⁺/TEGME-alkoxide at 45 °C in THF.

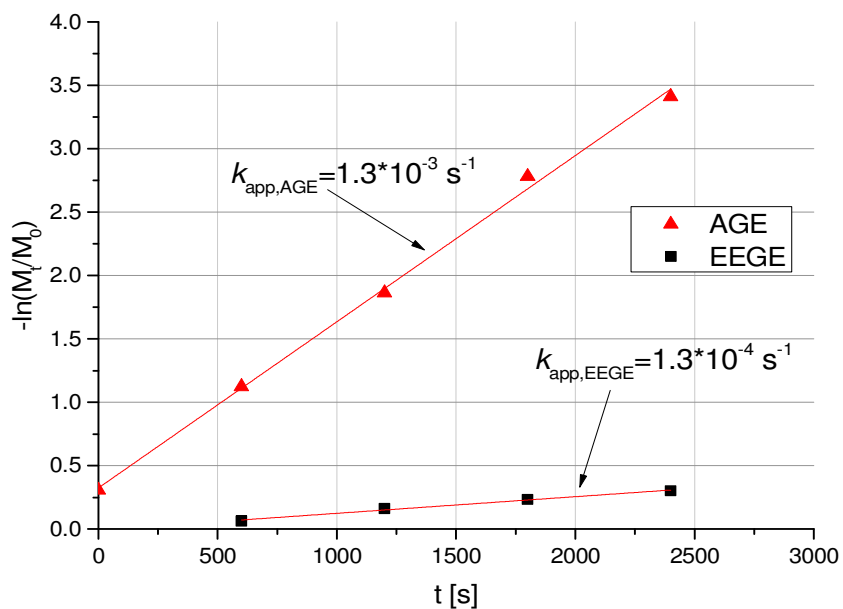


Figure 42: k_{app} determination of EEGE and AGE polymerization with DP=50 initiated with Cs⁺/TEGME-alkoxide at 45 °C in THF. The obtained values for k_{app} are inserted with $k_{app,AGE} = 1.3 \cdot 10^{-3} \text{ s}^{-1}$ and $k_{app,EEGE} = 1.3 \cdot 10^{-4} \text{ s}^{-1}$. The slopes were obtained by a linear fit (red line).

3.1.4. Polymerization with Cs⁺/TEGME-alkoxide in THF

The polymerization of EEGE, AGE and the copolymerization of both monomers with EEGE:AGE=45:5 using Cs⁺/TEGME-alkoxide in THF at 45 °C was repeated. In contrast to the experiments in chapter 3.1.3.1, one prepared stock solution of the initiator was used. This was performed ruling out an incomparable initiator formation for the following polymerization experiments. Cesium hydroxide hydrate was placed in a flame dried flask, suspended in benzene and TEGME was added. After 45 min at 60 °C all volatile compounds were removed under vacuum at 90 °C overnight. The composition of the initiator was Cs⁺:TEGME-alkoxide = 0.95:1. THF was added in the glovebox to the initiator and it was dissolved as good as possible giving a concentration of the initiator of $c_{\text{Cs}^+/\text{TEGME}} = 1.53 \text{ M}$. A slight turbidity remained. 131 μL of this initiator solution was used to prepare the stock solution of the initiator and the corresponding monomers. The turbid initiator solution was used and three solutions with EEGE:Cs⁺:TEGME-alkoxide = 50:0.95:1, AGE:Cs⁺:TEGME-alkoxide = 50:0.95:1 and EEGE:AGE:Cs⁺:TEGME-alkoxide = 45:5:0.95:1 were prepared. In Table 1 the polymerization parameters are shown. The concentrations of the monomer [M] and the initiator [I] vary, as the volume of the monomer varies due to different molar masses of the monomer. The volume of the solvent (THF) originates from the initiator solution. For investigation, 50 μL aliquots were placed into Eppendorf caps equipped with stirring bars and placed into a preheated oven at 45 °C.

Table 1: Parameters for the polymerizations of EEGE, AGE and EEGE:AGE=45:5 with DP = 50 using Cs⁺/TEGME-alkoxide as initiator in THF at 45 °C.

M	V [mL]	n_{Monomer} [mmol]	THF [μL]	$n_{\text{Initiator}}$ [mmol]	[M] [mmol mL ⁻¹]	[I] [mmol mL ⁻¹]
EEGE	1.462	10	131	0.2	6.28	0.126
AGE	1.176	10	131	0.2	7.65	0.153
EEGE:AGE (45:5)	1.316:0.118	9:1	131	0.2	6.40	0.128

Figure 43 and Figure 44 show the conversion–time plot and the first-order kinetics plot, respectively. The conversion–time plot shows an increase in conversion with time as was expected. None of the reactions are completed within 450 min, having conversions of 67 %, 54 % and 69 % for EEGE, AGE and EEGE:AGE=45:5, respectively. The molar masses of the polymers were $M_n = 2985 \text{ g mol}^{-1}$ (EEGE), $M_n = 2786 \text{ g mol}^{-1}$ (AGE) and $M_n = 3553 \text{ g mol}^{-1}$ (EEGE:AGE=45:5). The first-order kinetics plot was used to determine the apparent rate constant k_{app} (Figure 44). For this, the linear fitting was performed for all three polymerizations in a time range of 1800 s (30 min) and 5700 s (95 min). The monomer conversions for all polymerizations were similar having 23 - 49 % (EEGE), 13 - 33 % (AGE) and 19 - 45 % (EEGE:AGE =45:5). It is assumed that the initiator concentration $[I]$ equals the concentration of the active chain ends and is constant with time. From this data, EEGE polymerizes the fastest with $k_{EEGE} = 8.49 \cdot 10^{-4} \text{ L mol}^{-1} \text{ s}^{-1}$. AGE polymerizes the slowest having $k_{AGE} = 4.31 \cdot 10^{-4} \text{ L mol}^{-1} \text{ s}^{-1}$. If the overall monomer consumption of the copolymerization is used for the determination of the rate constant a value of $k_{Copoly} = 7.50 \cdot 10^{-4} \text{ L mol}^{-1} \text{ s}^{-1}$ is obtained and is clearly between k_{EEGE} and k_{AGE} .

Although the same initiator solution was used for all polymerizations a difference in polymerization rates was observed. Although stated in literature, it should not be assumed that a statistical copolymer results under these polymerization conditions.[62, 69] These results indicate that either the intrinsic reactivity of AGE compared to EEGE is lower or that the presence of EEGE influences the propagation rate. One explanation of the latter hypothesis would be a complexation of the acetal-group with the Cs^+ cation that alters the reactivity of the active species.

Table 2: Results for the polymerizations of EEGE, AGE and EEGE:AGE=45:5 with DP = 50 using Cs^+ /TEGME-alkoxide as initiator in THF at 45 °C.

M	M_n [g mol ⁻¹] (Conversion)	\bar{D}	k_{app} [s ⁻¹]	k [L mol ⁻¹ s ⁻¹]
EEGE	2985 (67%)	1.15	$1.07 \cdot 10^{-4}$	$8.49 \cdot 10^{-4}$
AGE	2786 (54%)	1.14	$0.66 \cdot 10^{-4}$	$4.31 \cdot 10^{-4}$
EEGE:AGE (45:5)	3553 (69%)	1.14	$0.95 \cdot 10^{-4}$	$7.50 \cdot 10^{-4}$

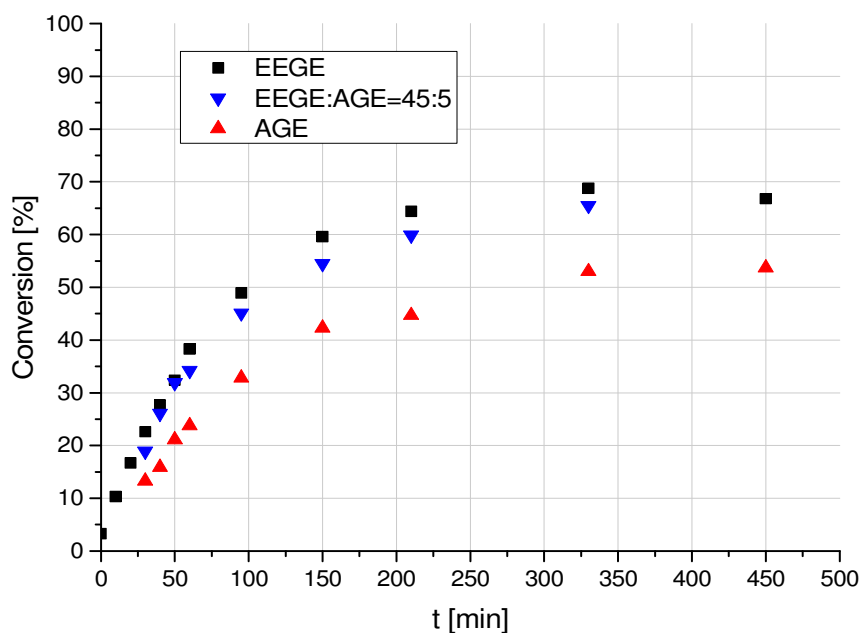


Figure 43: Conversion–time plot for EEGE, AGE and EEGE:AGE=45:5 (co)polymerization at 45 °C in THF initiated with Cs⁺/TEGME-alkoxide.

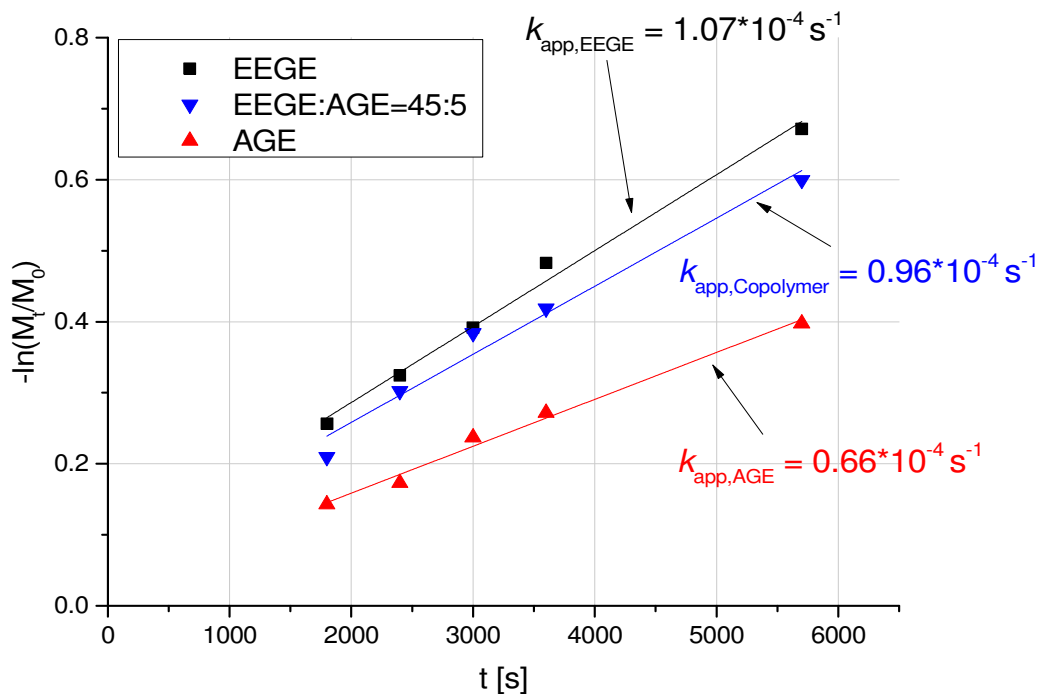


Figure 44: k determination of EEGE, AGE and EEGE:AGE=45:5 (co)polymerization at 45 °C in THF initiated with Cs⁺/TEGME-alkoxide. Linear fitting of the data revealed apparent rate constants of $k_{\text{EEGE}} = 1.07 \cdot 10^{-4} \text{ s}^{-1}$, $k_{\text{Copolymer}} = 0.96 \cdot 10^{-4} \text{ s}^{-1}$ and $k_{\text{AGE}} = 0.66 \cdot 10^{-4} \text{ s}^{-1}$.

The data obtained for the polymerizations of EEGE and AGE show that the polymerizations with Cs⁺ as counter ion, compared to K⁺ as counter ion, have lower propagation rates. Although the solubilities of Cs-alkoxide initiators were improved using THF-soluble oligoethylene glycol alkoxides, all propagation rates were lower than for the polymerizations with KOtBu in THF at 45 °C. Interestingly, no induction period was found for the polymerizations with Cs⁺ as counter ion, in contrast to all polymerizations with K⁺ as counter ion. Furthermore, more narrow dispersities were obtained for the polymerizations in THF using Cs-alkoxides as initiators, compared to KOtBu.

3.1.5. Polymerization with KOtBu in bulk

The commercially available KOtBu solution is 1 M in THF that was evaporated in the glovebox for experiments in bulk. For this a glass vial was used and the corresponding volume (153 µL) of the initiator injected. After evaporation, a white crystalline solid was obtained and it was assumed that no degradation of the initiator occurred during the THF removal. After monomer addition (see Table 3) it was shaken at RT in the glovebox until no initiator was visible anymore. 50 µL aliquots were placed in Eppendorf caps equipped with a stirring bar and placed into a preheated oven.

Table 3: Parameters for EEGE, AGE and EEGE:AGE=45:5 (co)polymerizations with DP = 50 initiated with KOtBu as initiator in bulk at 45 °C.

Monomer	Volume [mL]	Quantity [mmol]	[M]:[I]	[M] [mmol mL ⁻¹]	[I] [mmol mL ⁻¹]
EEGE	1.118	7.65	50	6.84	0.137
AGE	0.900	7.65	50	8.50	0.170
EEGE:AGE (45:5)	1.006:0.090	7.65	50	6.98	0.140

Figure 45 shows the time-dependent conversion of EEGE polymerized with KOtBu in bulk at 45 °C. After 3 h the conversion reached 76 % and after 24 h 95 % of the monomer was polymerized. No unexpected behavior of the conversion can be observed indicating a successful polymerization option of EEGE in bulk with KOtBu. The number-average molar masses and dispersities obtained for 2 % and 6 % conversion are not used for the discussion,

as both determined M_n are below the calibration level of the SEC (Figure 46). The first reliable data point obtained by SEC analytics in DMF (1 g L^{-1} LiBr) was recorded at a conversion of 23 % having a determined M_n of 1800 g mol^{-1} and a \mathcal{D} of 1.11. M_n - and dispersity-conversion plot is given in Figure 46. Between 23 % and 95 % a linear increase of M_n was recorded with $M_n = 1800 - 4800 \text{ g mol}^{-1}$. A slight increase in dispersity can be observed for the EEGE polymerization with KOtBu in bulk indicating a side-reaction. After 24 h, M_n was determined to be $M_n = 4800 \text{ g mol}^{-1}$ with $\mathcal{D} = 1.22$. Up to a conversion of 62 % the dispersity was increasing and between 62 % and 95 % constant.

Table 4: Results of EEGE, AGE and EEGE:AGE=45:5 (co)polymerization with DP = 50 with KOtBu as initiator in bulk at 45 °C.

Monomer	M_n [g mol ⁻¹] (Conversion)	\mathcal{D}	k_{app} [s ⁻¹]	k [L mol ⁻¹ s ⁻¹]
EEGE	4800 (95 %)	1.22	$1.51 \cdot 10^{-4}$	$1.10 \cdot 10^{-3}$
AGE	5416 (99 %)	1.57	$2.79 \cdot 10^{-4}$	$1.64 \cdot 10^{-3}$
EEGE:AGE (45:5)	4925 (94 %)	1.24	$1.46 \cdot 10^{-4}$	$1.04 \cdot 10^{-3}$

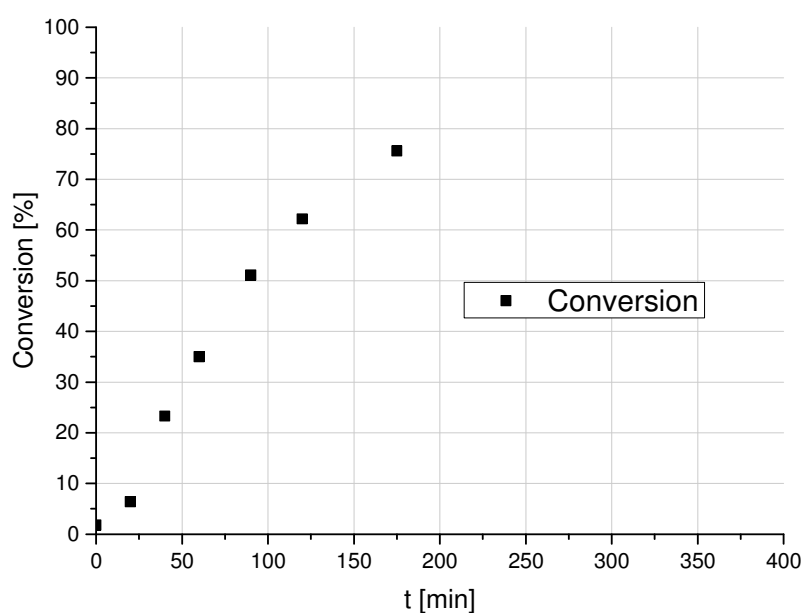


Figure 45: Conversion-time plot for the polymerization of EEGE with DP=50 and KOtBu as initiator in bulk at 45 °C.

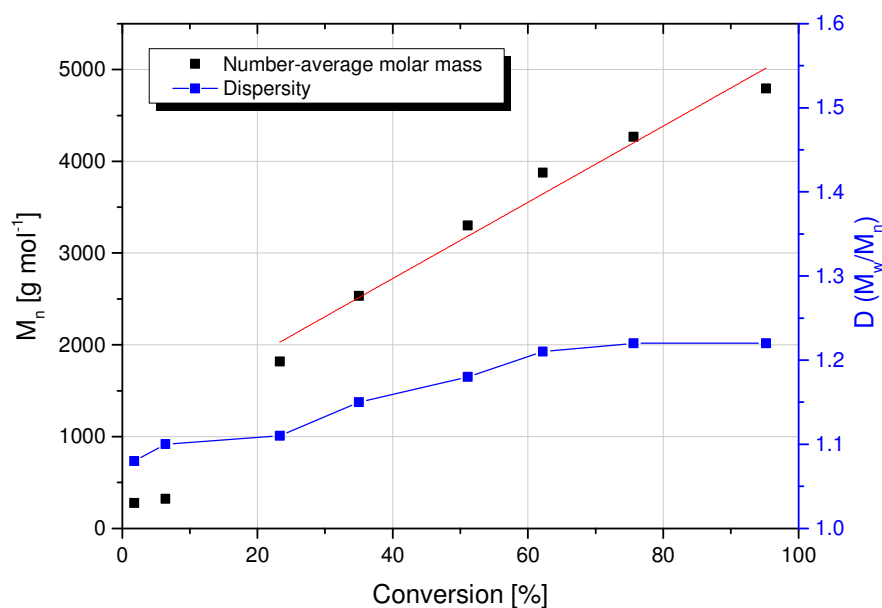


Figure 46: M_n - and dispersity-conversion plot of EEGE polymerization with DP=50 and KOtBu as initiator in bulk at 45 °C. Molar mass (■) linearly increases with conversion. The data points at 2 and 6 % conversion were not used for linear fitting (red line). Dispersity (■) continuously increases with conversion in a non-linear fashion.

The evolution of the dispersity was investigated by comparison of the SEC elugrams after 40 min and 24 h polymerization time (Figure 47). A shoulder appears at the ongoing polymerization yielding higher molar-masses and higher dispersities. After 40 min the shoulder was not detected. This can be explained by combining conclusions derived in literature and the analytics. Stolarzewicz described in 1986 the abstraction of a proton at the methylene-group at phenyl glycidyl ether.[144] As stated above, Hans et al. observed the same side-reaction for EEGE. An enolate anion forms, yielding subsequently a terminal ketone-group (see Scheme 13). As the enolate is able to initiate a polymerization, a new polymer is derived with a carbonyl-terminus. The coupling of an active chain end and the ketone results in the dimerization of the polymer with the double molar mass. The presence of the main fraction and the dimerized polymer results in a broadening of the molar-mass distribution and an increase in dispersity. Kwon et al. recently assumed that this reaction occurs at the early stage of polymerization.[72] Although the dimer should already be visible after 40 min, only one species was detected by SEC analysis. After 24 h a second species was detectable (Figure 47).

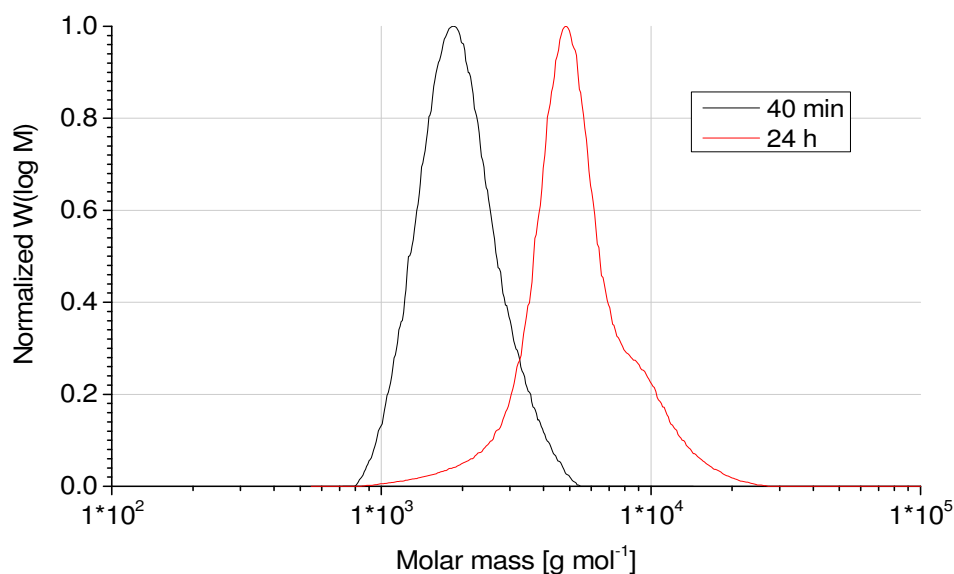


Figure 47: SEC elugrams of poly(EEGE) with DP=50 after 40 min and 24 h polymerization initiated with KOtBu in bulk at 45 °C. At 24 h polymerization time a bimodal distribution was obtained that is not detectable after 40 min.

It was assumed that the molar mass distribution of second polymer-species, initiated by the enolate, is overlapped by the main fraction in the SEC elugram after 40 min and can be separated at higher molar masses by SEC. A more detail investigation is given in chapter 3.1.8.

The polymerization of AGE shows similar results and in Figure 48 and Figure 49 are the conversion–time plot and M_n – and dispersity–conversion plots shown. After 180 min 92 % of the AGE was polymerized and after 24 h the polymerization was completed to an extent of 99 %. A linear increase in M_n with conversion was obtained with a final M_n of 5416 g mol⁻¹. Dispersity also increases with conversion and a \bar{D} of 1.57 was obtained for the polymer after 24 h (99 % conversion) (Figure 49).

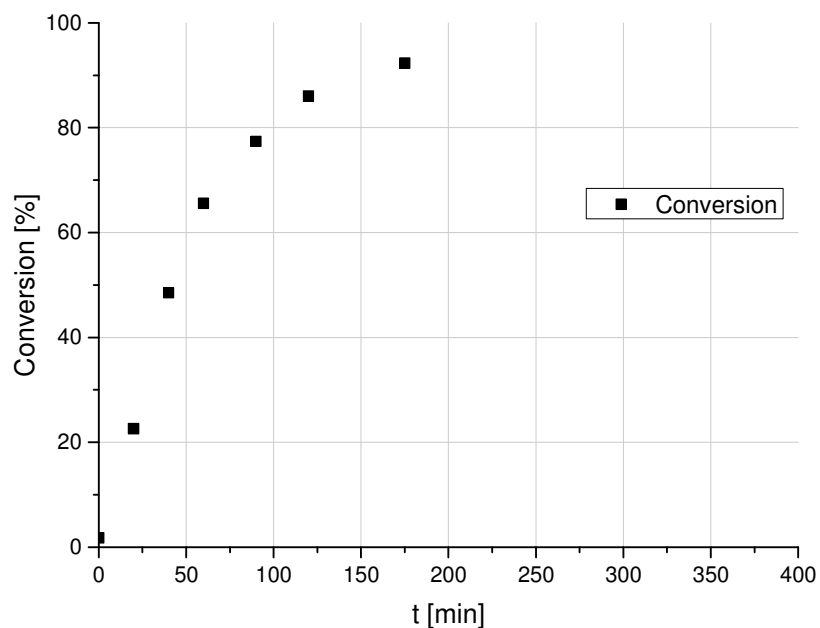


Figure 48: Conversion–time plot for the polymerization of AGE with DP=50 initiated with KOtBu in bulk at 45 °C.

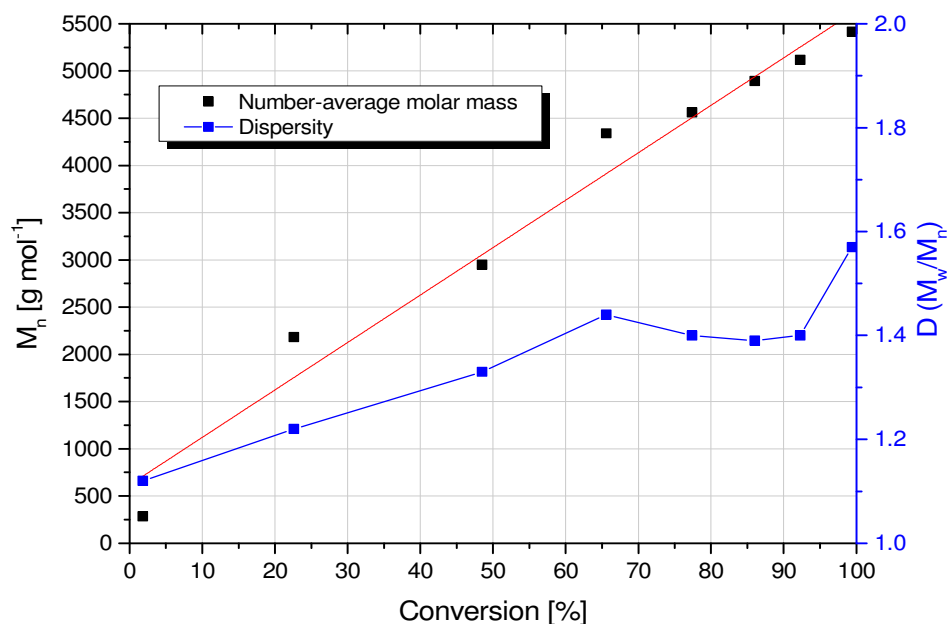


Figure 49: M_n - and dispersity-conversion plot of AGE polymerization with DP=50 initiated with KOtBu in bulk at 45 °C. Molar mass (■) linearly increases (linear fit: red line) with conversion. Dispersity (■) also increases with conversion.

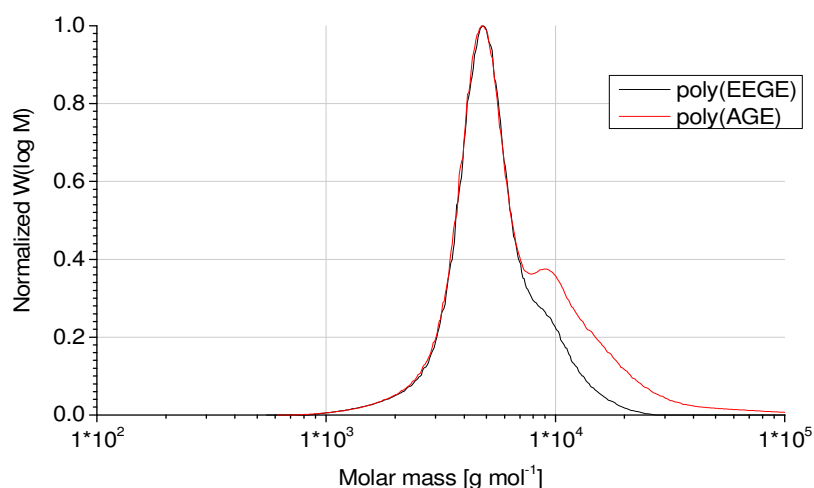


Figure 50: SEC elugram of poly(AGE) (red) and poly(EEGE) (black) with DP=50. Polymerization was initiated with KOtBu and conducted in bulk at 45 °C. The polymer species detected at higher molar masses was assigned to dimerized polymer chains for both polymers. Bimodality is more pronounced for poly(AGE) compared to poly(EEGE).

The detailed analysis of the SEC elugram indicates a side-reaction and shows a bimodal distribution (Figure 50). The second polymer species has twice the molar mass than the main fraction of the signal. A higher dispersity ($D_{AGE} = 1.57$ and $D_{EEGE} = 1.22$) of the poly(AGE) with a more pronounced bimodality indicate that the side-reaction is more likely occurring with AGE as monomer than with EEGE. For clarity both elugrams were plotted in Figure 50. If this is caused by a higher acidity of the AGE epoxide-ring or the altered environment of the active species by the monomer is unknown and requires further investigation.

For the copolymerization of EEGE and AGE in bulk at 45 °C a mixture of EEGE:AGE=45:5 was used, the conversion determined by $^1\text{H-NMR}$ spectroscopy and plotted against time (Figure 51). It has to be noted that the overall monomer consumption was determined, as it was already shown that both monomers have similar propagation rates and statistical copolymers can be obtained for EEGE and AGE.[62, 69]. Here again, the values of M_n determined by SEC were below the calibration level for conversions below 20 % and are not shown and used for discussion (Figure 52). After 24 h a conversion of 94 % is reached being almost equal to the conversion obtained for EEGE homopolymerization. A linear increase of M_n with conversion was detected with a final M_n of 4925 g mol^{-1} . Dispersity also increases with conversion and has a final value of $D = 1.24$.

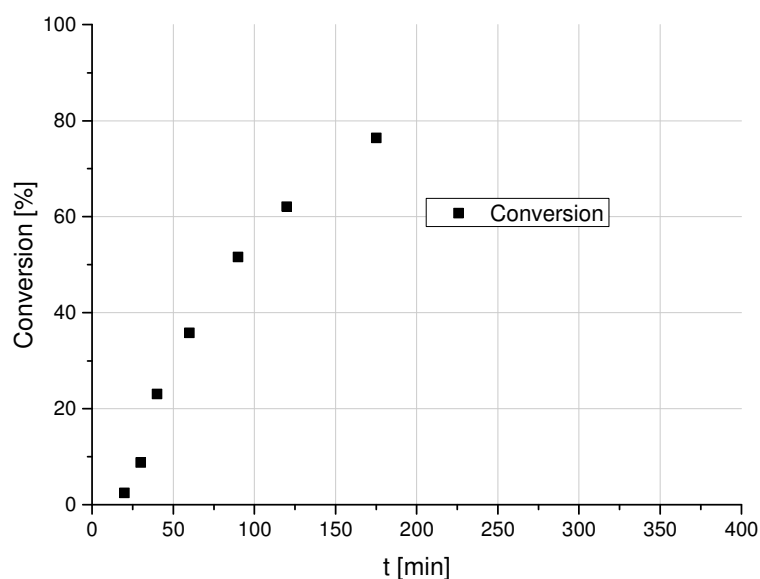


Figure 51: Conversion–time plot for the copolymerization of EEGE and AGE with EEGE:AGE=45:5 initiated with KOtBu in bulk at 45 °C.

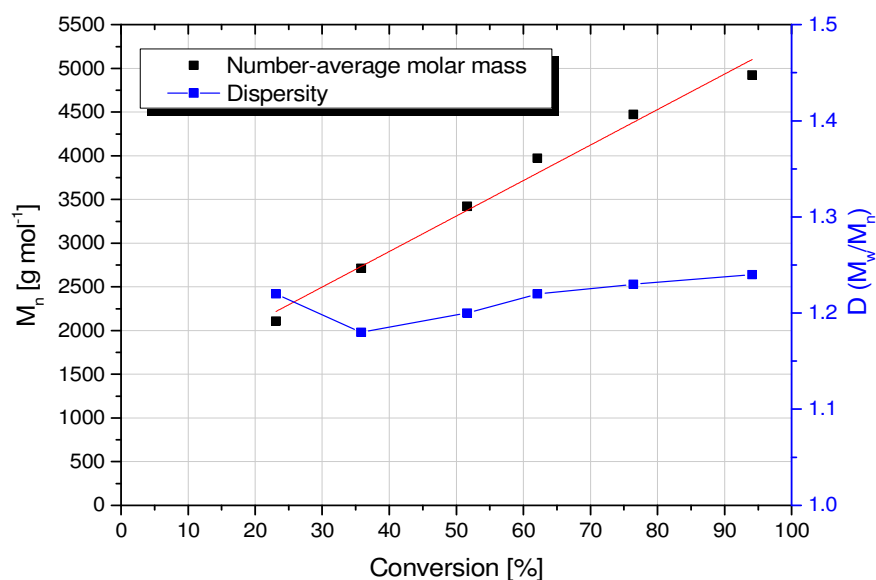


Figure 52: M_n - and dispersity-conversion plot of EEGE:AGE=45:5 copolymerization with DP=50 initiated with KOtBu in bulk at 45 °C. A linear increase of M_n (■) with conversion (linear fit: red line) is obtained with a final M_n of 4925 g mol⁻¹. Dispersity (■) initially decreases up to a conversion of 35 % and afterwards steadily increases to a final value of $\bar{D} = 1.24$.

A more detailed look into the rate constants for the homo- and copolymerizations was performed using the first-order kinetics plot (Figure 53). The apparent rate constants for the monomers were determined to be $k_{app,EEGE} = 1.51 \cdot 10^{-4} \text{ s}^{-1}$, $k_{app,AGE} = 2.79 \cdot 10^{-4} \text{ s}^{-1}$ and $k_{app,copolymer} = 1.46 \cdot 10^{-4} \text{ s}^{-1}$. Regarding the concentrations of the initiator and hence the active species, without termination reactions, propagation rate constants of $k_{EEGE} = 1.10 \cdot 10^{-3} \text{ L mol}^{-1} \text{ s}^{-1}$, $k_{AGE} = 1.64 \cdot 10^{-3} \text{ L mol}^{-1} \text{ s}^{-1}$ and $k_{copolymer} = 1.04 \cdot 10^{-3} \text{ L mol}^{-1} \text{ s}^{-1}$ were obtained. The difference obtained for the homopolymerization of EEGE and the copolymerization of EEGE and AGE can be assigned to the inaccuracy of the measurements. Statistical analysis of the results and the determination of the accuracy cannot be performed as the experiments were performed only once. Hence no standard deviation can be calculated. Similar to the results obtained for the polymerizations of EEGE and AGE with KOtBu in THF at 45 °C (chapter 3.1.2), AGE polymerizes slightly faster than EEGE. The ability of ethers, acetals- and other oxy-species to complex metals is known and special ethers, crown-ethers, are used in organic chemistry to modify the reactivity of e.g. K-alkoxides.[145, 146] For the differences in the propagation rate two reasons can be considered. Either the intrinsic reactivity of the epoxide-rings of AGE is higher, leading to a faster polymerization, or the complexation of K^+ by the EEGE acetals alters the reactivity of the active species. Analysis of the chemical environment of the active species would be necessary to investigate these hypotheses but would exceed the scope of this thesis.

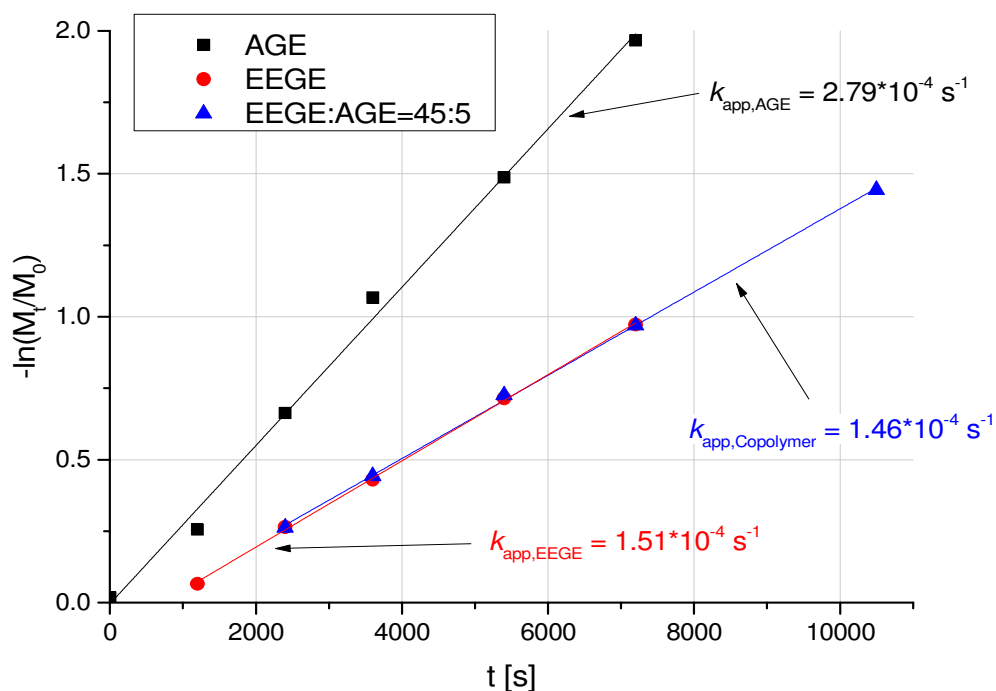


Figure 53: First-order kinetics plot for the bulk polymerization of EEGE, AGE and EEGE:AGE=45:5 initiated with KOtBu in bulk at 45 °C. Apparent rate constants k are inserted with $k_{\text{AGE}} = 2.79 \cdot 10^{-4} \text{ s}^{-1}$, $k_{\text{EEGE}} = 1.51 \cdot 10^{-4} \text{ s}^{-1}$ and $k_{\text{Copolymer}} = 1.46 \cdot 10^{-4} \text{ s}^{-1}$.

3.1.6. Polymerization with Cs⁺/TEGME-alkoxide in bulk

The polymerization of EEGE, AGE and EEGE:AGE=45:5 was performed with Cs-triethyleneglycol monomethyl ether alkoxide in bulk at 45 °C. For comparison, the same quantities of monomer and initiator as for the polymerization with KOtBu in bulk were chosen (see chapter 3.1.5).

Table 5: Bulk polymerization parameters of EEGE, AGE and EEGE:AGE=45:5 (co)polymerization initiated with Cs⁺/TEGME-alkoxide at 45 °C.

Monomer	V [mL]	n _{Monomer} [mmol]	[M]:[I]	[M] [mmol mL ⁻¹]	[I] [mmol mL ⁻¹]
EEGE	1.118	7.65	50	6.84	0.137
AGE	0.900	7.65	50	8.50	0.170
EEGE:AGE (45:5)	1.006:0.090	6.885:0.765	50	6.98	0.140

First the polymerization with EEGE is discussed. After 175 min 74 % of the monomer was polymerized. After 24 h the polymerization was not completed as only 93 % of the monomer was converted (Figure 54). A linear relationship of M_n with conversion was obtained up to a conversion of 74 % (Figure 55), whereas the M_n obtained for the final conversion of 93 % ($M_n = 3658 \text{ g mol}^{-1}$) slightly deviates from the linear fitting. The dispersity of the polymer is constant for conversions higher than 34 %, having a final value of $\mathcal{D} = 1.13$ (Figure 55). Although at a conversion of 19 % a value of $\mathcal{D} = 1.17$ was obtained, it is assumed that the accuracy of SEC analytics was inappropriate, as the RI-signal of the polymer was slightly overlapping with the monomer signals. The SEC elugram (Figure 56) shows a monomodal distribution with only a slight shoulder to higher molar masses. This shoulder was already assigned to the side-reaction described in chapters 2.4 and 3.1.5. The initial formation of ketone-terminal polymers causes a ketone–alkoxide coupling of two polymer chains yielding polymer fractions with twice the molar mass of the main polymer. A decrease of this dimerization is in accordance with the reduced polymerization rate with Cs^+ as counter ion. A tighter bonding of the alkoxide with the Cs^+ – relative to K^+ – reduces both the nucleophilic and the basic properties reducing the side-reactions and subsequent dimerization. For the determination of the propagation rate constant $-\ln(M_t/M_0)$ was plotted against time showing a linear dependency with $k_{\text{app,EEGE}} = 1.65 \cdot 10^{-4} \text{ s}^{-1}$ (Figure 57). With this a propagation rate constant of $k_{\text{EEGE}} = 1.20 \cdot 10^{-3} \text{ L mol}^{-1} \text{ s}^{-1}$ was calculated.

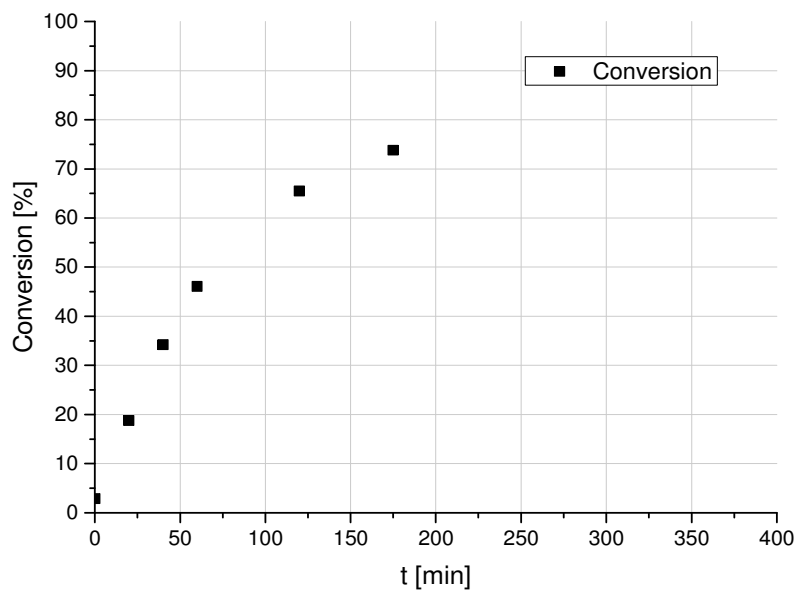


Figure 54: Conversion–time plot for the bulk polymerization of EEGE with Cs^+ /TEGME-alkoxide at 45 °C.

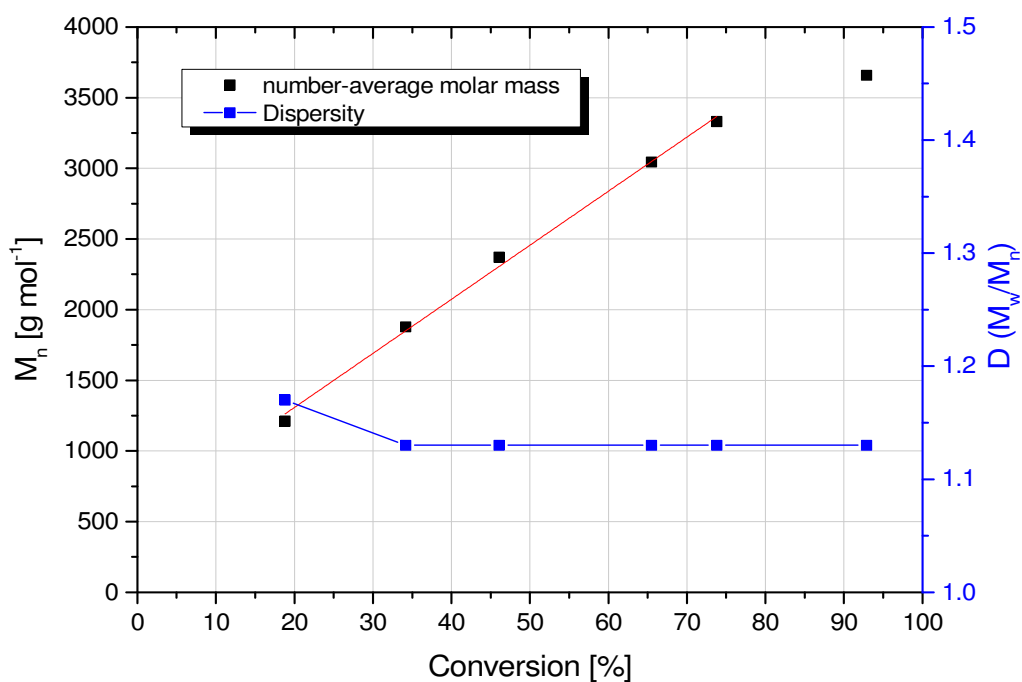


Figure 55: M_n - and dispersity–conversion plot for EEGE polymerization initiated with Cs^+ /TEGME-alkoxide at 45 °C in bulk. Molar mass (■) linearly increases with conversion from 19-74 % (linear fit: red line), whereas dispersity (■) decreases between 19 and 34 % to a value of $D = 1.13$.

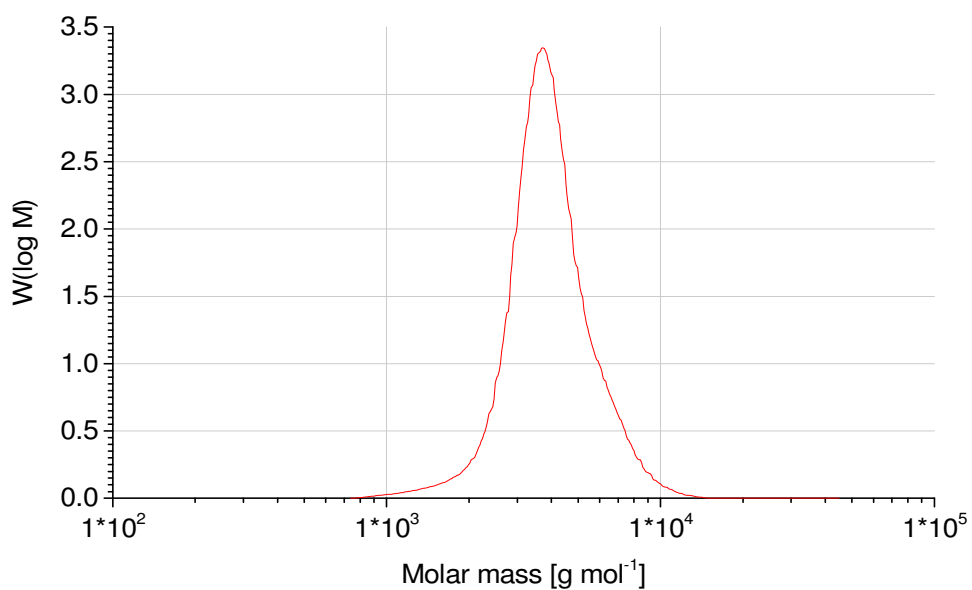


Figure 56: SEC elugram for poly(EEGE) synthesized by polymerization of EEGE with DP=50 initiated with Cs⁺/TEGME-alkoxide in bulk at 45 °C.

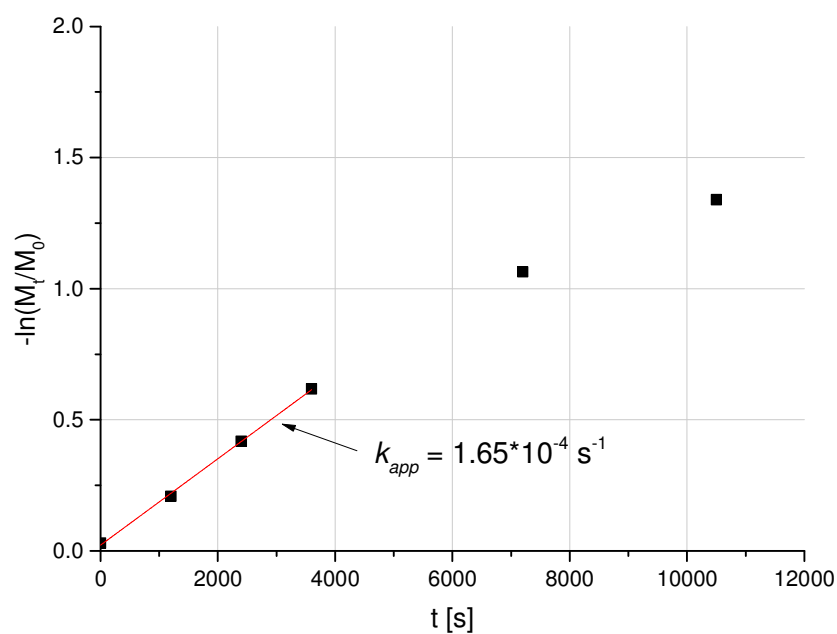


Figure 57: First-order kinetics plot for EEGE polymerization initiated with Cs⁺/TEGME-alkoxide in bulk at 45 °C. The apparent rate constant k_{app} , derived from the slope, is inserted having a value of $1.65 \cdot 10^{-4} \text{ s}^{-1}$. The slope was determined by a linear fit (red line).

The bulk polymerization of AGE with Cs⁺/TEGME-alkoxide leads to a conversion of only 27 % after 175 min (Figure 58) and only 67 % conversion of AGE after 24 h. For molar-mass progress a linear increase is observed up to a conversion of 27 % (Figure 59). The next data point obtained for a conversion of 67 % deviates from the linear relation. Unfortunately, the progress was not observable over the whole polymerization due to the reduced rate of polymerization. The dispersities were significantly lower, compared to the polymerization with KOtBu ($\bar{D} = 1.57$), having a value of $\bar{D} = 1.19$ at 67 %. As an increase in dispersity was sometimes observed, this value does not have to be the final dispersity of the polymer. Regarding this, the dispersity at 67 % ($\bar{D} = 1.19$) was compared to the dispersity of KOtBu polymerization at 65 % ($\bar{D} = 1.44$) and still indicates a better control over dispersity using Cs⁺ as counterion. The SEC elugram recorded of the polymer after 24 h shows a shoulder at higher molar masses that was assigned to the dimerization reaction of two polymers (Figure 60).

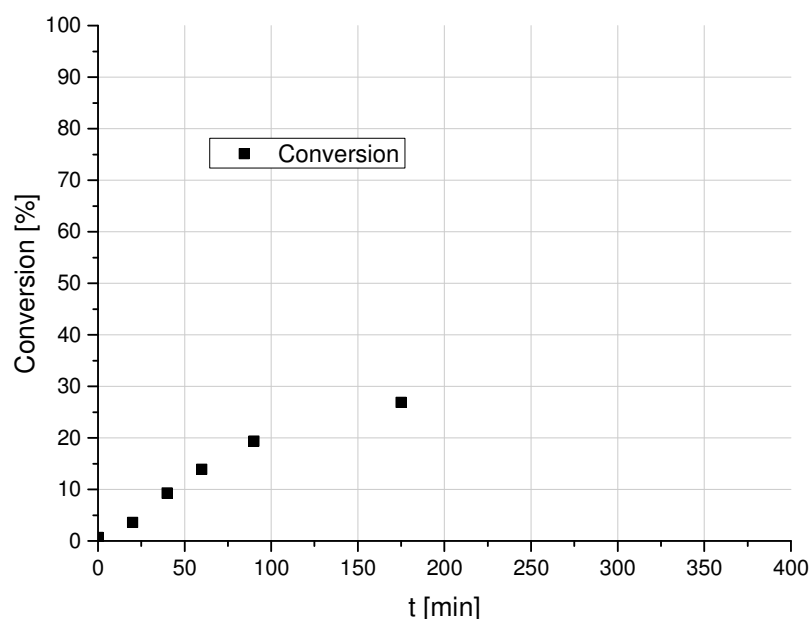


Figure 58: Conversion–time plot of the bulk polymerization of AGE with DP = 50 initiated with Cs⁺/TEGME-alkoxide at 45 °C.

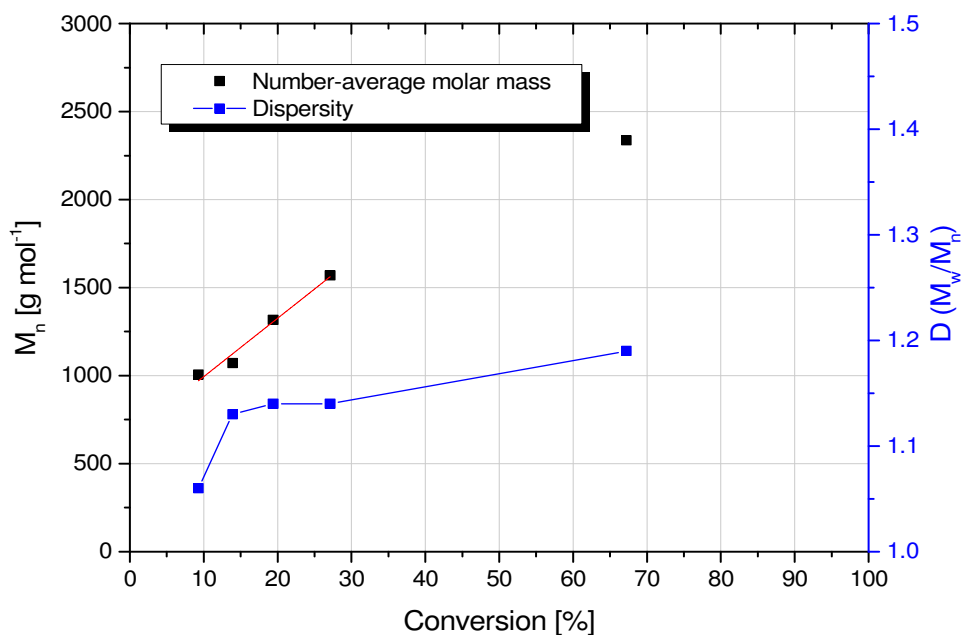


Figure 59: M_n - and dispersity-conversion plot for AGE polymerization initiated with Cs^+ /TEGME-alkoxide at 45 °C in bulk. Molar mass (■) increases in a linear fashion between 9-27 % conversion as indicated with a linear fitting of these data points (red line). Dispersity (■) steadily increases with conversion to a final value of $\mathcal{D} = 1.19$.

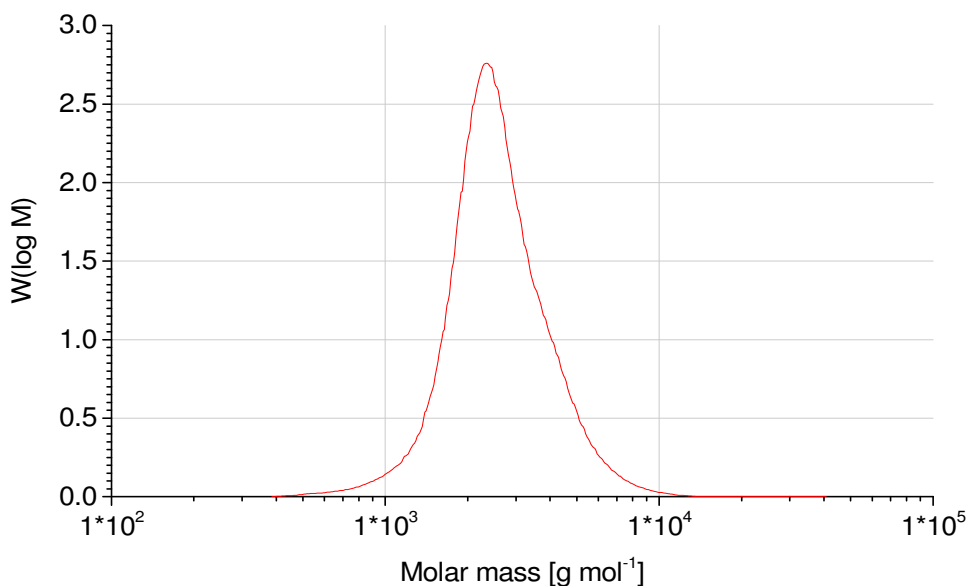


Figure 60: SEC elugram for poly(AGE). The polymerization was initiated with Cs^+ /TEGME-alkoxide in bulk at 45 °C. The polymer has $M_n = 2337 \text{ g mol}^{-1}$ and $\mathcal{D} = 1.19$ after 24 h with a conversion of 67 %.

The rate of propagation was calculated using the first-order kinetics plot (Figure 61). The data points used for the determination were between 2400 s (40 min, 9 % conversion) and 5400 s (90 min, 19 % conversion). With an apparent rate constant of $k_{\text{app}} = 0.39 \cdot 10^{-4} \text{ s}^{-1}$ a propagation rate constant of $k = 0.23 \cdot 10^{-3} \text{ L mol}^{-1} \text{ s}^{-1}$ was obtained for the polymerization of AGE with Cs^+ /TEGME-alkoxide in bulk at 45 °C, being approximately 5-times slower than the polymerization of EEGE under the same conditions.

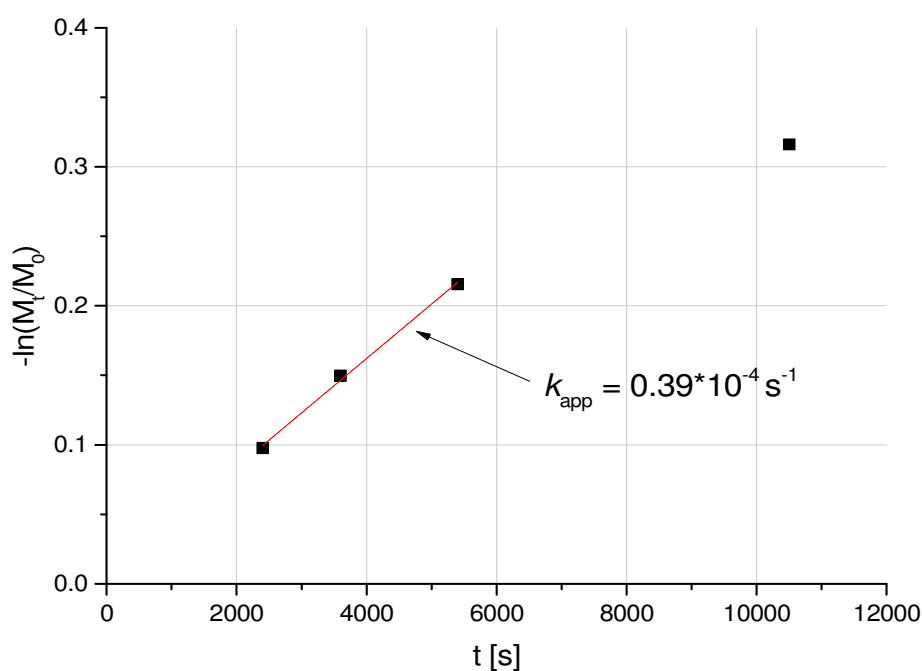


Figure 61: First-order kinetics plot for the polymerization of AGE with DP=50 initiated with Cs^+ /TEGME-alkoxide in bulk at 45 °C. Under these conditions an apparent rate constant of $k_{\text{app}} = 0.39 \cdot 10^{-4} \text{ s}^{-1}$ was determined by a linear fit (red line).

The bulk copolymerization of EEGE:AGE=45:5 initiated with Cs⁺/TEGME-alkoxide shows that the conversion reaches 87 % after 24 h (see Figure 62), similar to the homopolymerization of EEGE (93 %). A linear increase of M_n was observed for a conversion of 23 - 53 % with a slight deviation for lower conversion that can be ascribed to the accuracy of SEC measurements (Figure 63). At a higher conversion (87 %) a shift to lower M_n was found as well. The dispersity was determined to be $\mathcal{D} = 1.16$ after 24 h, having an overall small increase with conversion (Figure 63). SEC elugram shows that the curve is monomodal with a shoulder at higher molar masses giving a slightly asymmetrical curve (Figure 64). As described before this can be assigned to the initial formation of ketone-terminal polymers coupling with active chain ends yielding a polymer-dimer.

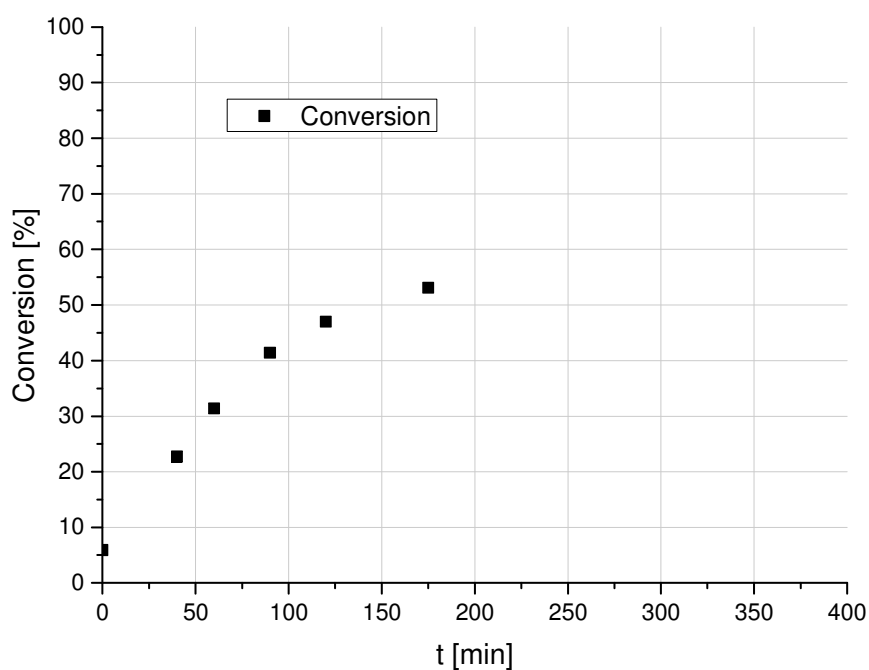


Figure 62: Conversion–time plot of the bulk copolymerization of EEGE:AGE=45:5 initiated with Cs⁺/TEGME-alkoxide at 45 °C .

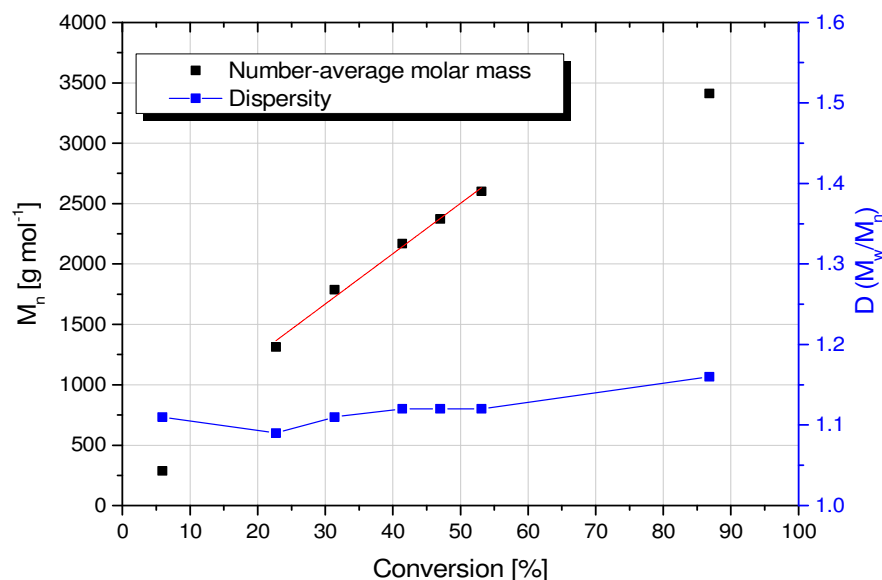


Figure 63: M_n - and dispersity-conversion plot for EEGE:AGE=45:5 copolymerization with DP=50 initiated with Cs^+ /TEGME-alkoxide at 45 °C in bulk. Molar mass (■) shows a linear relation with conversion between 23 and 53 % as indicated by a linear fitting (red line). Data points at lower and higher conversions slightly deviate. Dispersity (■) increases with conversion.

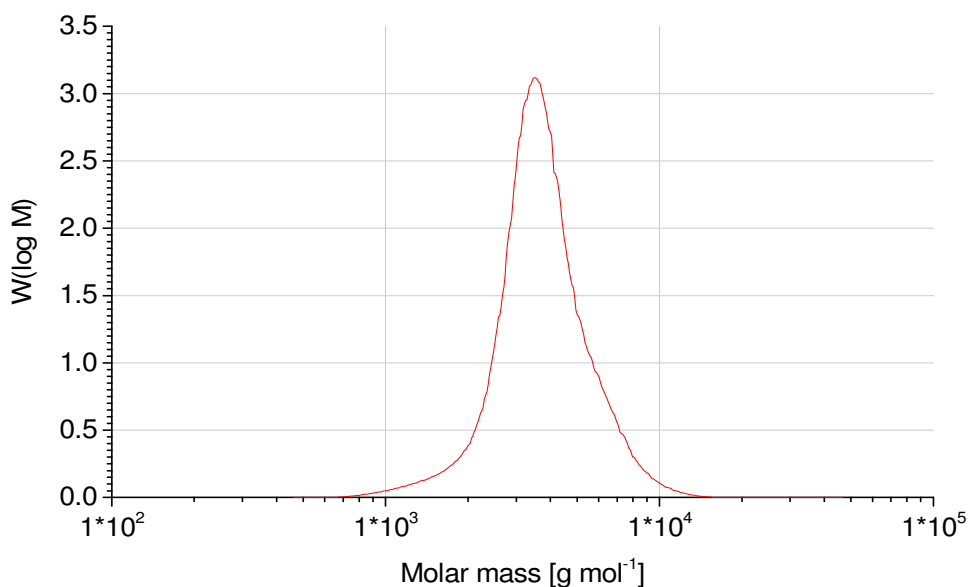


Figure 64: SEC elugram of poly(EEGE-co-AGE) with EEGE:AGE=45:5 obtained by the copolymerization of EEGE and AGE initiated with Cs^+ /TEGME-alkoxide in bulk at 45 °C.

Using the first-order kinetics plot, the apparent rate constant and hence the propagation rate can be determined (Figure 65). As the polymerization is of first order from the beginning, a linear fit of the data points from 0 - 5400 s (0 - 90 min, 6 - 41 %) was performed. It has to be noted, that a conversion of 6 % at $t = 0$ min was obtained. This can be ascribed to a polymerization already occurring at RT. For the preparation of the sample, first the monomer is added to the initiator. After this, it takes 2-3 min to completely dissolve the initiator in the monomer. Additionally, sample preparation requires approximately 10 min that is enough time to already partially polymerize the monomer. The volume to be heated in the oven (50 μ L) is assumed to be instantly warmed to 45 °C so that the first data point can also be used for the determination of the apparent rate constant. With this a linear relation was observed with a slope of $k_{app} = 0.88 \cdot 10^{-4} \text{ s}^{-1}$. With this apparent rate constant an overall propagation rate of $k_{copolymer} = 0.63 \cdot 10^{-3} \text{ L mol}^{-1} \text{ s}^{-1}$ was obtained.

In Table 6 the propagation rate constants of the homopolymerization of EEGE and AGE and the overall propagation rate constant of the copolymerization of EEGE and AGE with EEGE:AGE=45:5 are summarized. The polymerizations were conducted in bulk initiated with Cs^+ /TEGME-alkoxide at 45 °C. EEGE polymerizes the fastest with propagation a rate constant of $k_{EEGE} = 1.20 \cdot 10^{-3} \text{ L mol}^{-1} \text{ s}^{-1}$, whereas AGE polymerizes the slowest with $k_{AGE} = 0.23 \cdot 10^{-3} \text{ L mol}^{-1} \text{ s}^{-1}$. The overall propagation rate constant of the copolymerization is clearly inbetween the propagation rate constants for the homopolymerization with $k_{copolymer} = 0.63 \cdot 10^{-3} \text{ L mol}^{-1} \text{ s}^{-1}$.

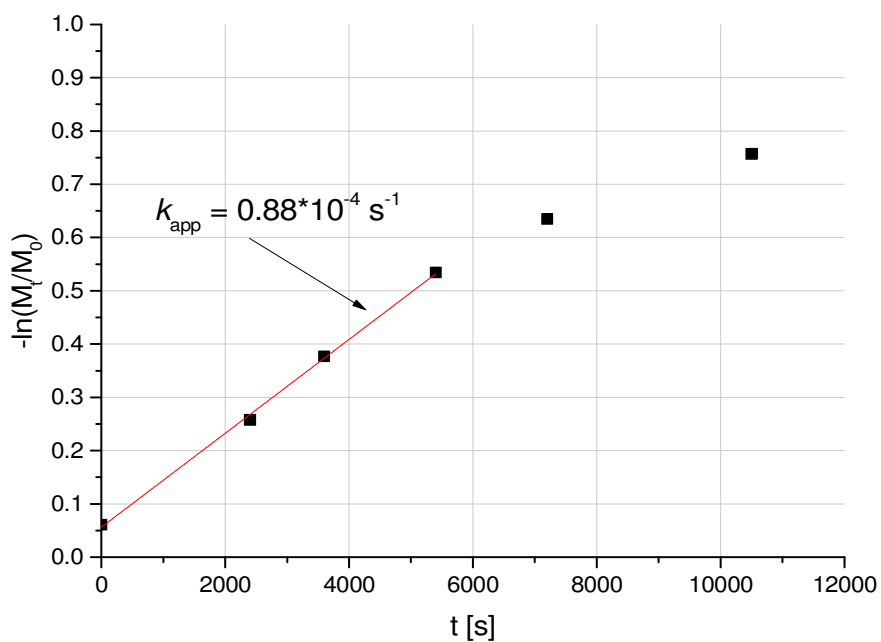


Figure 65: First-order kinetics plot for EEGE:AGE=45:5 copolymerization initiated with Cs^+ /TEGME-alkoxide in bulk at 45 °C. The rate constant k was derived from the slope with $0.88 \cdot 10^{-4} \text{ s}^{-1}$.

Table 6: Results of the bulk experiments of EEGE, AGE and EEGE:AGE=45:5 (co)polymerization initiated with Cs^+ /TEGME-alkoxide at 45 °C.

Monomer	M_n [g mol ⁻¹] (Conversion)	\bar{D}	k_{app} [s ⁻¹]	k [L mol ⁻¹ s ⁻¹]
EEGE	3658 (93%)	1.13	$1.65 \cdot 10^{-4}$	$1.20 \cdot 10^{-3}$
AGE	2337 (67%)	1.19	$0.39 \cdot 10^{-4}$	$0.23 \cdot 10^{-3}$
EEGE:AGE (45:5)	3411 (87%)	1.16	$0.88 \cdot 10^{-4}$	$0.63 \cdot 10^{-3}$

3.1.7. Discussion of the rate constants

In Table 7 all propagation rate constants used for the discussion of the polymerizations are summarized.

Table 7: Propagation rate constants of polymerizations in bulk and THF at 45 °C with DP = 50 initiated with KOtBu or Cs⁺/TEGME-alkoxide.

Initiator	Monomer	<i>k</i> (bulk)	<i>k</i> (THF)
		[10 ⁻³ L mol ⁻¹ s ⁻¹]	[10 ⁻³ L mol ⁻¹ s ⁻¹]
Cs ⁺ /TEGME-alkoxide	EEGE	1.20	0.85
	EEGE:AGE=45:5	0.63	0.75
	AGE	0.23	0.43
KOtBu	EEGE	1.10	2.18
	EEGE:AGE=45:5	1.04	2.47
	AGE	1.64	2.50

In general, it was observed that the propagation rate constants of the monomers and the mixtures therefore vary with the type of initiator. Polymerizations initiated with KOtBu are similar or faster than the polymerizations initiated with Cs⁺/TEGME-alkoxide. Regarding the choice of the initiator it was observed that the propagation rate constant differences are larger for the monomers by using Cs⁺/TEGME-alkoxide than KOtBu. Here, the polymerization of EEGE with Cs⁺/TEGME-alkoxide in bulk has a propagation rate constant of $k_{\text{Cs,bulk,EEGE}} = 1.20 \cdot 10^{-3} \text{ L mol}^{-1} \text{ s}^{-1}$ whereas the polymerization of AGE in bulk has a value of $k_{\text{Cs,bulk,AGE}} = 0.23 \cdot 10^{-3} \text{ L mol}^{-1} \text{ s}^{-1}$. On the one hand, this might be caused by an inherent lower reactivity of the AGE monomer under the given conditions. On the other hand, the acetal-group of EEGE could complex the Cs⁺ cations altering the reactivity of the active species towards all monomers present. Therefore, this would also increase the propagation rate constant of AGE in the presence of EEGE in bulk experiments. As only the overall propagation rate constant of the copolymerization was determined, no evaluation of these hypotheses can be performed by the copolymerization experiments. Interestingly, an inverse effect is observed for the monomers by using KOtBu as initiator in bulk. Here, the

propagation rate constant is higher for the AGE monomer than for EEGE. The overall propagation rate constant of the copolymerization is lower than the value obtained for the EEGE homopolymerization. Regarding the EEGE homo- and EEGE/AGE-copolymerization it has to be noted, that these values are similar and more experiments are necessary to evaluate if this difference is caused by experimental errors or by an actual propagation rate difference.

For polymerizations in the presence of THF the same trend of monomer and initiator can be observed. In general, all polymerizations have higher propagation rate constants by using KOtBu as initiator. Using Cs⁺/TEGME-alkoxide as initiator the polymerization of EEGE has higher propagation rate constants than were determined for the polymerization of AGE. Vice versa, using KOtBu as initiator leads to an increase of the propagation rate constants by changing from EEGE to AGE. Especially in the case of KOtBu, this trend has to be further proven to evaluate the experimental errors.

The propagation rate constants of the investigated experiments are shown in Figure 66 with respect to the monomer. For the experiments in the presence of THF and KOtBu as initiator the propagation rate constant is similar for the polymerization of AGE and the comonomer mixture EEGE:AGE=45:5. By using solely EEGE as monomer the propagation rate decreases. For the polymerizations in bulk and KOtBu as initiator, all propagation rate constants are lower than were obtained in the presence of THF. Here the presence of EEGE influences the propagation rate constant and k drops from $k_{\text{KOtBu,bulk,AGE}} = 1.64 \cdot 10^{-3} \text{ L mol}^{-1} \text{ s}^{-1}$ to $k_{\text{KOtBu,bulk,copolymer}} = 1.04 \cdot 10^{-3} \text{ L mol}^{-1} \text{ s}^{-1}$ and $k_{\text{KOtBu,bulk,EEGE}} = 1.10 \cdot 10^{-3} \text{ L mol}^{-1} \text{ s}^{-1}$. It has to be noted that the overall monomer consumption was used for the determination of k . With a ratio of EEGE:AGE = 45:5, EEGE is the main fraction of the monomer in the initial mixture. The observed data indicate that the influence of EEGE on the propagation rate constants is more pronounced in the absence of THF.

Polymerizations initiated with Cs⁺/TEGME-alkoxide in the presence of THF also show an influence of EEGE on the propagation rate constant. In contrast to the polymerizations initiated with KOtBu, an increase of k can be observed with this presence of EEGE. The hypothesis that the complexation of Cs⁺ with the acetal group is responsible for this increase requires further investigation. Regarding this, it has to be noted that the differences of the propagation rates are less pronounced for experiments performed in the presence of THF.

The differences of k are for the bulk homopolymerizations of EEGE and AGE $\Delta k_{\text{KOTBu,bulk}} = 0.54 \cdot 10^{-3} \text{ L mol}^{-1} \text{ s}^{-1}$ and $\Delta k_{\text{CsTEGME,bulk}} = 0.97 \cdot 10^{-3} \text{ L mol}^{-1} \text{ s}^{-1}$ in contrast to the experiments with the presence of THF $\Delta k_{\text{KOTBu,THF}} = 0.32 \cdot 10^{-3} \text{ L mol}^{-1} \text{ s}^{-1}$ and $\Delta k_{\text{CsTEGME,THF}} = 0.42 \cdot 10^{-3} \text{ L mol}^{-1} \text{ s}^{-1}$. These results need to be further investigated to evaluate the experimental error of the determined propagation rate constants.

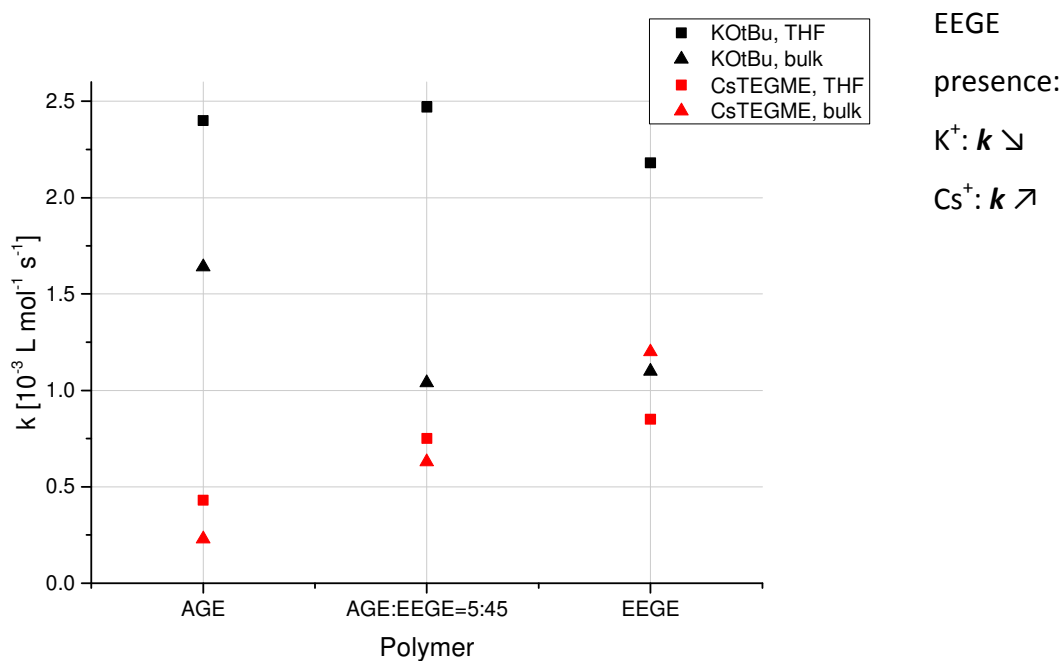


Figure 66: Dependencies of the propagation rate constants on the monomer and initiator in polymerizations at 45 °C.

3.1.8. Discussion of the dispersities

In Table 8 the dispersities of the polymers after 24 h polymerization with the corresponding polymerization parameters are summarized.

Table 8: Dispersities of the polymers after 24 h polymerization at 45 °C with DP = 50 initiated with KOtBu or Cs⁺/TEGME-alkoxide.

Initiator	Monomer	\bar{D} (bulk)	\bar{D} (THF)
Cs ⁺ /TEGME-alkoxide	EEGE	1.13	1.15
	EEGE:AGE=45:5	1.16	1.14
	AGE	1.19	1.14
KOtBu	EEGE	1.22	1.17
	EEGE:AGE=45:5	1.24	1.21
	AGE	1.57	1.36

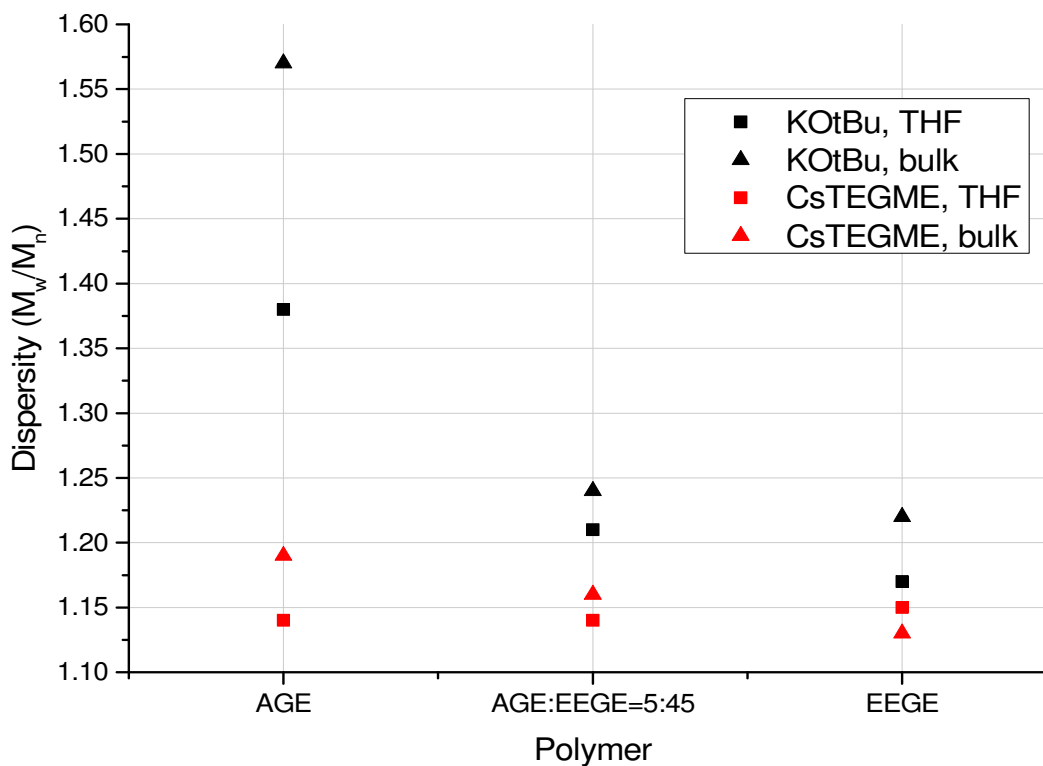


Figure 67: Dependency of the dispersity on the monomer with Cs⁺/TEGME-alkoxide and KOtBu as initiator at 45 °C.

For both monomers the polymerizations and copolymerizations initiated with Cs⁺/TEGME-alkoxide in bulk are well controlled and the dispersities are narrow and below $\mathcal{D} = 1.2$ with $\mathcal{D}_{\text{EEGE}} = 1.13$, $\mathcal{D}_{\text{Copolymer}} = 1.16$ and $\mathcal{D}_{\text{AGE}} = 1.19$ (see Table 8 and Figure 67). In contrast to that, the polymerizations in bulk with KOtBu as initiator are accompanied by a loss of control, as the dispersity increases for AGE from $\mathcal{D}_{\text{AGE,Cs}} = 1.19$ to $\mathcal{D}_{\text{AGE,K}} = 1.57$ and for EEGE $\mathcal{D}_{\text{EEGE,Cs}} = 1.13$ to $\mathcal{D}_{\text{EEGE,K}} = 1.22$. For polymerizations in THF, dispersities with Cs⁺/TEGME-alkoxide as initiator are also smaller having values of $\mathcal{D}_{\text{EEGE,Cs,THF}} = 1.15$ and $\mathcal{D}_{\text{AGE,Cs,THF}} = \mathcal{D}_{\text{Copolymer,Cs,THF}} = 1.14$. In contrast to that, the dispersities of the final polymers initiated with KOtBu in THF are $\mathcal{D}_{\text{EEGE,K,THF}} = 1.17$, $\mathcal{D}_{\text{Copolymer,K,THF}} = 1.21$ and $\mathcal{D}_{\text{AGE,K,THF}} = 1.36$. In general, the dispersities are smaller in the presence of THF instead of performing the reaction in bulk. For Cs⁺/TEGME-alkoxide in bulk $\mathcal{D}_{\text{Cs,bulk}} = 1.13$ -1.19 and for polymerizations in THF $\mathcal{D}_{\text{Cs,THF}} = 1.14$ -1.15 were obtained. For the initiation with KOtBu, the effect of THF as solvent on the dispersity is even more pronounced having values for the bulk-polymerizations $\mathcal{D}_{\text{K,bulk}} = 1.22$ -1.57 and in THF $\mathcal{D}_{\text{K,THF}} = 1.17$ -1.36. The binding of the Cs⁺ cation with the active species, i.e. alkoxide, reduces its reactivity as it is visible from the kinetic data (see chapter 3.1.7). As both the nucleophilicity and basicity are reduced, the side-reaction of deprotonation and terminal-ketone formation occurs to a lower extent. This results in both lower dispersities for the final polymers and lower propagation rate constants for the polymerization. The fast polymerizations initiated with KOtBu are usually accompanied with a high probability of the side-reaction. Bimodality evolves for these polymerizations giving dispersities with up to $\mathcal{D} = 1.57$. The higher the polymerization rate, the higher is commonly the dispersity. Furthermore the dispersities depend on the aimed number of repeating units as was investigated in chapter 3.1.2.1 and 3.1.2.2. For AGE polymerizations the dispersities increase from $\mathcal{D}_{\text{AGE,20}} = 1.26$ (DP=20) to $\mathcal{D}_{\text{AGE,50}} = 1.36$ (DP=50) and only for EEGE polymerizations they were constant with $\mathcal{D}_{\text{EEGE,20}} = \mathcal{D}_{\text{EEGE,50}} = 1.17$. The influence of the initial $[\text{M}]_0:[\text{I}]$ ratio is investigated and discussed in the following chapter.

3.1.9. Control of side-reaction by slow monomer addition

Kwon et al. recently stated that the occurrence of side-reactions is mainly occurring at the beginning of the polymerization.[72] As was already investigated at the beginning, polyglycidols with lower $[M]_0:[I]$ ratios show – especially for poly(AGE) – lower dispersities. It is therefore assumed that the initial ratio $[M]_0:[I]$ has a significant influence on the quantity of side-reactions and hence quality of the final polymer. Hans et al. also showed that the number of side-reactions increases with higher $[M]_0:[I]$ ratios.[61] It does not have to be a consequence of late-polymerization-stage side-reactions but can be caused by the excessive presence of epoxide-rings related to active chain ends at the polymerization start. As the side-reaction is in general occurring to a lower extent than the epoxide-ring opening, the probability of the side-reaction should be diminishable by keeping the ratio $[M]_0:[I]$ as low as possible. As an example, if the probability of H-abstraction is e.g. 3 %, a ratio of $[M]_0:[I] = 100$ would lead to 3 monomer units being deprotonated. These initiate a polymerization and could couple with other active chain ends. Upon reduction of the ratio, the probability of H-abstraction would be lower than unity making a side-reaction for a monomer more and more improbable. For this, a first try to reduce the side-reactions and decrease the dispersity was performed. 100 μL of the initiator 1 M KO t Bu in THF was used and stirred in a sealed flask at 45 °C. At the beginning of the reaction, 10 drops of AGE ($V_{\text{total}} = 600 \mu\text{L}$, equaling 51 repeating units in the final polymer) were added. Subsequently it was stirred for 30 min and every 10 min 10 drops were added (3x). Afterwards, every 30 min 10 drops were added. The final 100 μL were injected at once. After 24 h $^1\text{H-NMR}$ spectroscopy and SEC analytics were performed. The same procedure was done with EEGE using a total volume of $V_{\text{total}} = 730 \mu\text{L}$ due to the higher molar mass needed to obtain DP = 50, but having 30 min gaps right from the beginning. The final 100 μL were also added at once.

By $^1\text{H-NMR}$ a conversion of $x_{\text{AGE}} = 91 \%$ and $x_{\text{EEGE}} = 94 \%$ were determined corresponding to a DP = 46 and DP = 47. SEC was used to check the final molar mass and dispersities. $M_n = 1900 \text{ g mol}^{-1}$ and $M_n = 3700 \text{ g mol}^{-1}$ were obtained for poly(AGE) and poly(EEGE). The SEC elugrams are depicted in Figure 68 and do not show a pronounced peak at the higher molar mass region, i.e. twice the molar mass. Especially in the case of AGE polymerization a reduction of the side-reaction was obtained. As was shown in chapter 3.1.2.2 a dispersity of

$\bar{D} = 1.36$ was obtained, if the monomer was added at once. Here, $\bar{D} = 1.14$ was determined by SEC by adding the monomer in a step-wise fashion (Figure 69). The change of a broad molar-mass distributed poly(AGE) to a narrow molar-mass distributed poly(AGE) could be obtained by reducing the monomer feed. For EEGE polymerization only a reduction from $\bar{D} = 1.17$ to $\bar{D} = 1.13$ was possible (Figure 70). A reason for the significant difference in molar mass for poly(AGE) cannot be explained by the incomplete reaction, as the conversion of the slow addition reaction was 91%. A slight increase of M_n in poly(EEGE) using the slow addition was observed. The H-abstraction of monomers results in the decrease in monomers available for the polymerization leading to a decrease in molar-mass.

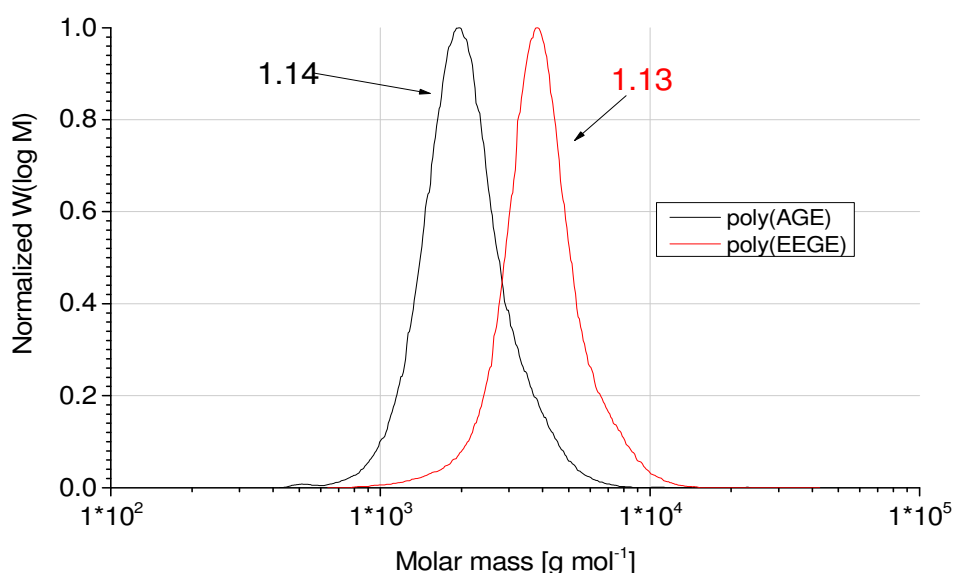


Figure 68: SEC trace of poly(EEGE) and poly(AGE) with DP=50 obtained by a slow monomer addition to a initiator solution of KOtBu in THF at 45 °C. The obtained dispersities are inserted for the corresponding polymer.

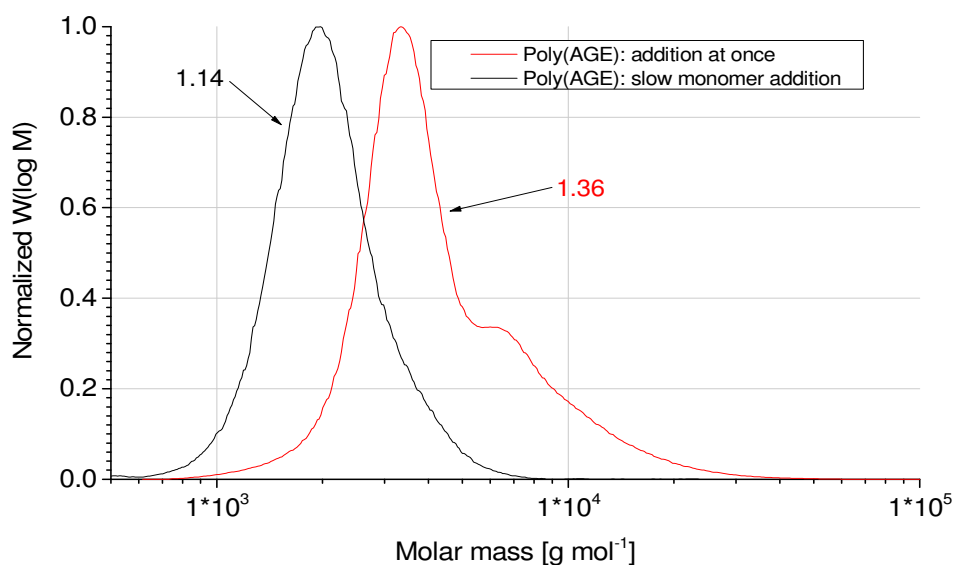


Figure 69: SEC elugrams of poly(AGE) with DP=50. The polymers were synthesized by the addition of the monomer at 45 °C to the initiator KOtBu at once (red) and by a step-wise addition (black). The obtained dispersities are inserted for the corresponding polymer.

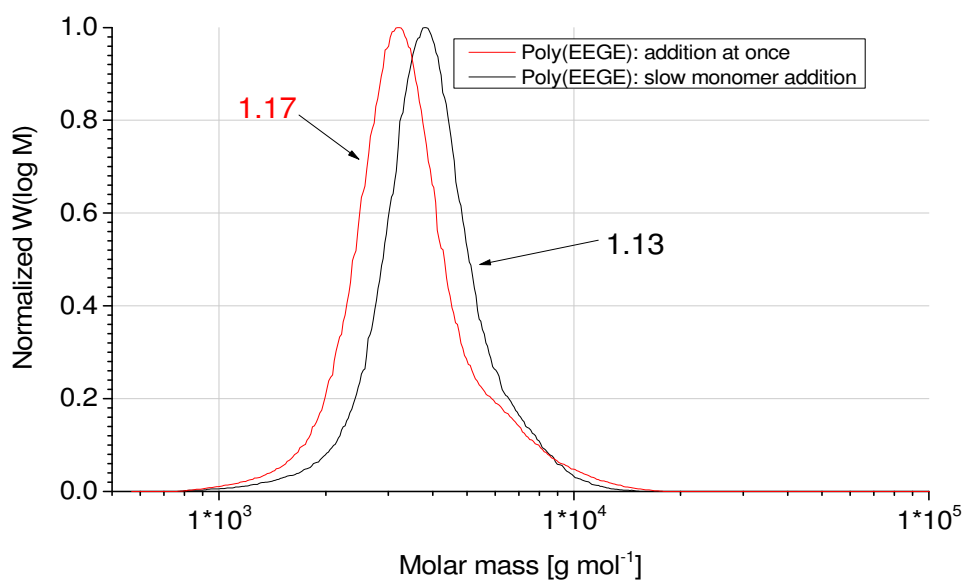


Figure 70: SEC elugrams for poly(EEGE) with DP=50 obtained by addition of the monomer to a solution of KOtBu in THF at 45 °C. The monomer was added at once (red line) and in a step-wise manner (black). Dispersities are inserted for the corresponding polymer.

Further investigation of the slow monomer addition was attempted using a syringe pump to gain more control over the volume flux of the monomer. As the initiator, commercially available KOtBu (1 M in THF) was used at 45 °C. After complete addition of the monomer the reaction was proceeded for additional 20-24 h. Experiments were conducted at different feed rates between $\dot{V}=50 - 5000 \mu\text{L h}^{-1}$ with both AGE and EEGE monomers. Briefly, in the glovebox a solution of 100 μL initiator was placed into the flask and the flask sealed with a rubber septum. The syringe was filled with the monomer and punctured through the septum. Afterwards, the syringe–flask combination was assembled in the syringe-pump and the flask placed into an oilbath. For AGE-experiments 570 μL ($[\text{M}]_0:[\text{I}]=50:1$) and for EEGE-experiments 731 μL ($[\text{M}]_0:[\text{I}]=50:1$) monomer were added by the syringe pump. After complete addition of the monomer, the flasks were either stirred in a preheated oil bath at 45 °C or inside of an incubator equipped with a multi-stirring plate to run samples in a parallel manner. The samples were directly analyzed by $^1\text{H-NMR}$ spectroscopy and SEC measurements. All experiments were performed in triplicate to determine the standard deviation of the final M_n and \bar{D} . $^1\text{H-NMR}$ spectroscopy experiments were checked for conversion but in no cases residual monomer could be observed.

Poly(AGE) was analyzed using SEC with DMF (+1 g L^{-1} LiBr) as eluent and PEG as calibration standard. All elugrams were evaluated in the same run time region (16-22 min, run time 30 min) to gain comparability. To get a better insight into molar-mass changes by the dimer, weight-average molar mass was evaluated as high-molar mass fractions strongly influence M_w . For poly(AGE), M_w and \bar{D} are shown in Table 9 and Figure 71. M_w was determined to be between 4404 – 6091 g mol^{-1} ($\dot{V} = 50 - 2000 \mu\text{L h}^{-1}$). $^1\text{H-NMR}$ analyses gave DP of 47 – 56 using the terminal *tert*-butyl group as internal reference. This is in good accordance with the theoretical DP of 50 as different coiling of poly(AGE) in DMF could cause a variation in hydrodynamic radii. Starting from 50 $\mu\text{L h}^{-1}$ feed rate a steady increase in M_w can be observed. This can be explained by an increasing content of the high molar-mass fraction, influencing the weight-average molar mass. This high-molar mass fraction is caused by the dimerization reaction between a ketone-terminal polymer with an active chain end. These results indicate that a reduction of the feed rate can reduce the side-reactions occurring at the initial phase of the polymerization.

Table 9: Dispersity and M_w values for poly(AGE) obtained by different monomer feed rates with KOtBu as initiator at 45 °C.

Feed rate [$\mu\text{L h}^{-1}$]	\mathcal{D}	M_w [g mol^{-1}]
5000	1.30 \pm 0.01	6091 \pm 212
2000	1.21 \pm 0.02	4946 \pm 695
1000	1.20 \pm 0.02	5057 \pm 481
500	1.20 \pm 0.03	5052 \pm 389
400	1.20 \pm 0.01	4889 \pm 328
250	1.19 \pm 0.01	4887 \pm 205
50	1.16 \pm 0.01	4404 \pm 143

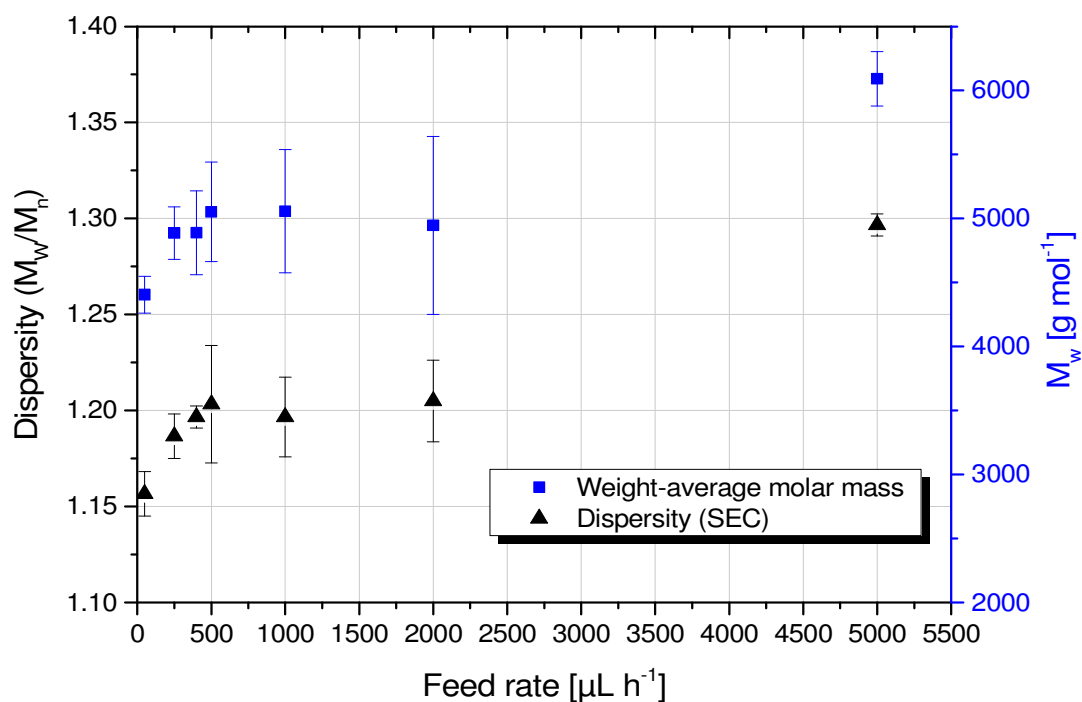


Figure 71: Dispersity (■)– and M_w (■)–feed rate plot for the synthesis of poly(AGE) initiated with KOtBu at 45 °C. All experiments were performed in triplicate and the obtained standard deviation shown as error bars.

At the lower feed rates, an evolution of the dispersity from 1.16 ± 0.01 ($50 \mu\text{L h}^{-1}$) to 1.20 ± 0.01 ($500 \mu\text{L h}^{-1}$) was observed. Between $500 \mu\text{L h}^{-1}$ and $2000 \mu\text{L h}^{-1}$ no significant dispersity alteration was observed, but it increases again from 1.21 ± 0.02 ($2000 \mu\text{L h}^{-1}$) to 1.30 ± 0.01 ($5000 \mu\text{L h}^{-1}$) for higher feed rates. Qualitatively, SEC elugrams further confirm the indicated coupling. The fraction of the dimer decreases with decreasing feed rate, leading to a more narrow molar-mass distribution (Figure 72).

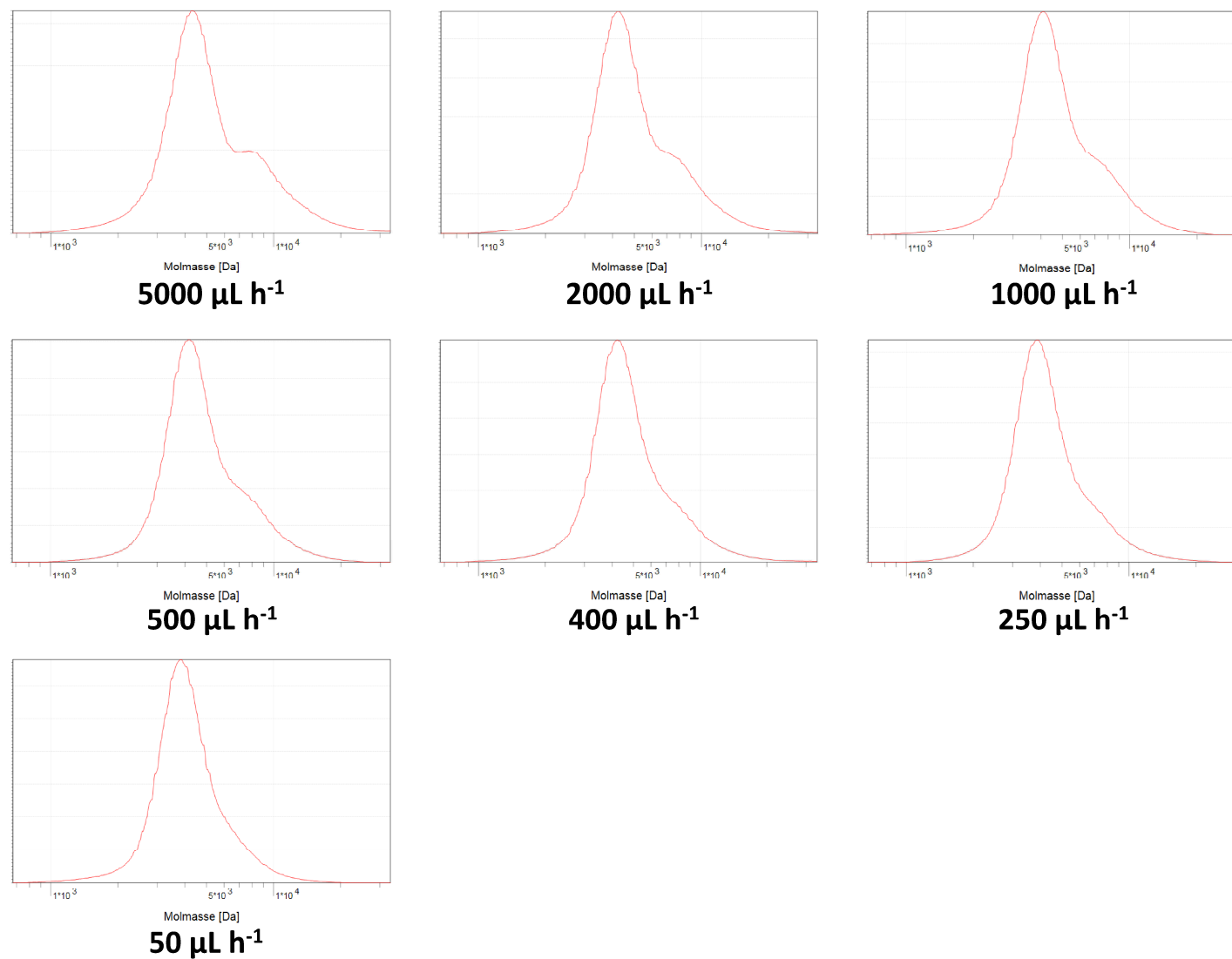


Figure 72: Elugrams obtained for poly(AGE) synthesized with KOtBu as initiator at 45 °C in THF depending on the monomer feed rate.

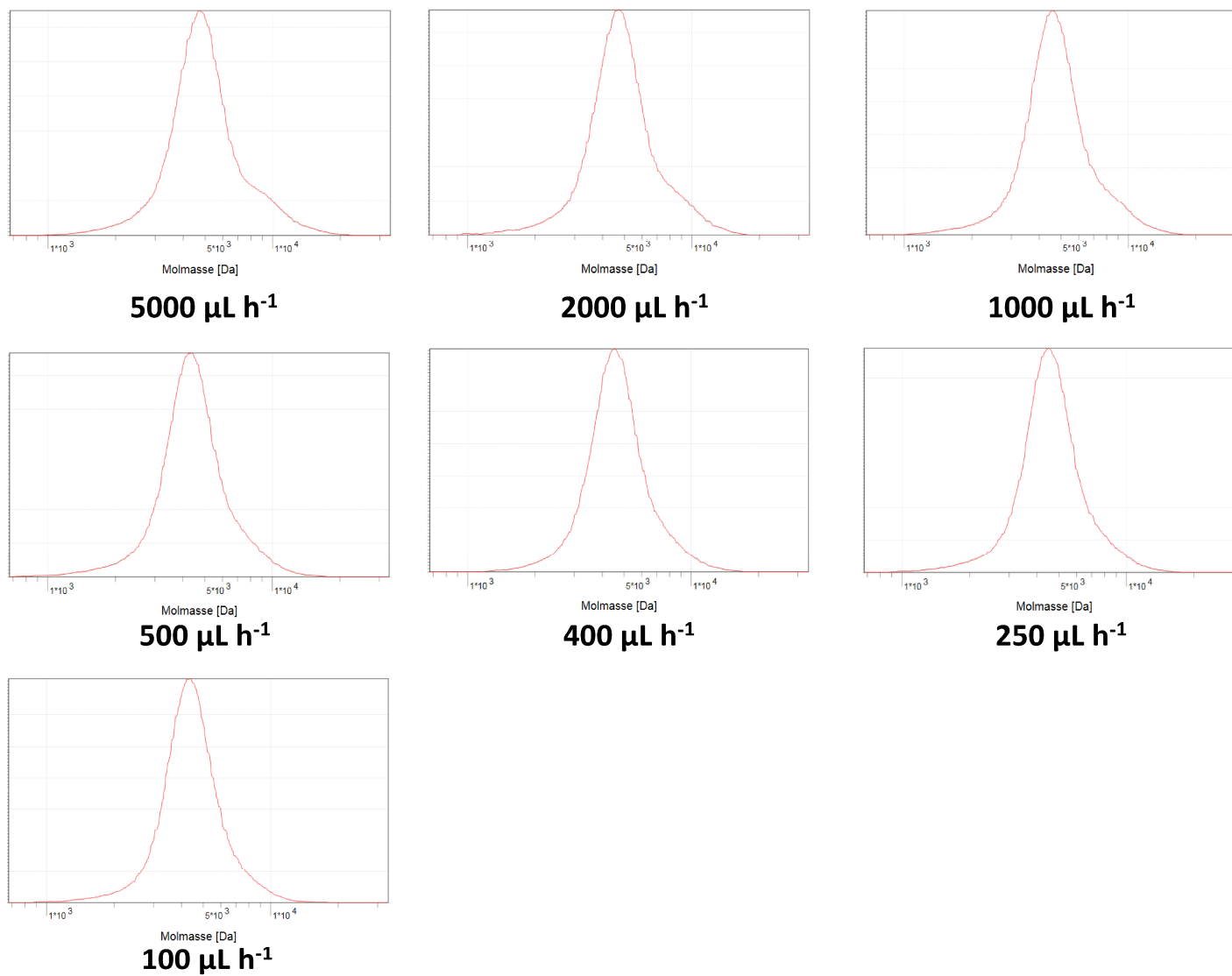


Figure 73: Elugrams obtained for poly(EEGE) synthesized with $\text{KO}t\text{Bu}$ as initiator at 45°C in THF depending on the monomer feed rate.

For poly(EEGE) experiments a DP of 50 was also chosen to compare the results of both polymers. In general, it could be observed that dispersities are lower than dispersities of poly(AGE) (Table 10 and Figure 74). Dispersities were determined to be between 1.11 ± 0.01 and 1.16 ± 0.01 with feed rates of $100 \mu\text{L h}^{-1}$ and $5000 \mu\text{L h}^{-1}$, respectively. The fraction of the dimer is less pronounced than in AGE polymerizations but visible as an asymmetry of the SEC curves for the highest feed rates (see Figure 73). Comparing the feed rates of AGE and EEGE polymerizations, Figure 71 and Figure 74, indicates a reduction in dispersity below $500 \mu\text{L h}^{-1}$ for both AGE and EEGE polymerizations. It is assumed that polymerization kinetics is responsible for this drop in dispersity for the lowest feed rates. If polymerization is too slow compared to the addition of the monomer, an inappropriate ratio of $[\text{M}]:[\text{I}]$ is present. This leads to the aforementioned higher probability of deprotonation and hence dimerization reactions. Therefore, it is necessary to balance the monomer feed rate with the polymerization rate to get an overall reduction of $[\text{M}]$. Compared to the results of the AGE polymerization, M_w increase of poly(EEGE) with increasing \dot{V} is less pronounced already indicated by a smaller difference of \mathcal{D} .

Table 10: Dispersity and M_w values for poly(EEGE) obtained by different monomer addition rates with KOtBu as initiator at 45 °C.

Flow rate [$\mu\text{L h}^{-1}$]	\mathcal{D}	M_w [g mol^{-1}]
5000	1.16 ± 0.01	5045 ± 406
2000	1.15 ± 0.01	4858 ± 284
1000	1.14 ± 0.01	5053 ± 66
500	1.14 ± 0.02	4907 ± 238
400	1.13 ± 0.01	4699 ± 237
250	1.13 ± 0.01	4877 ± 45
100	1.11 ± 0.01	4671 ± 30

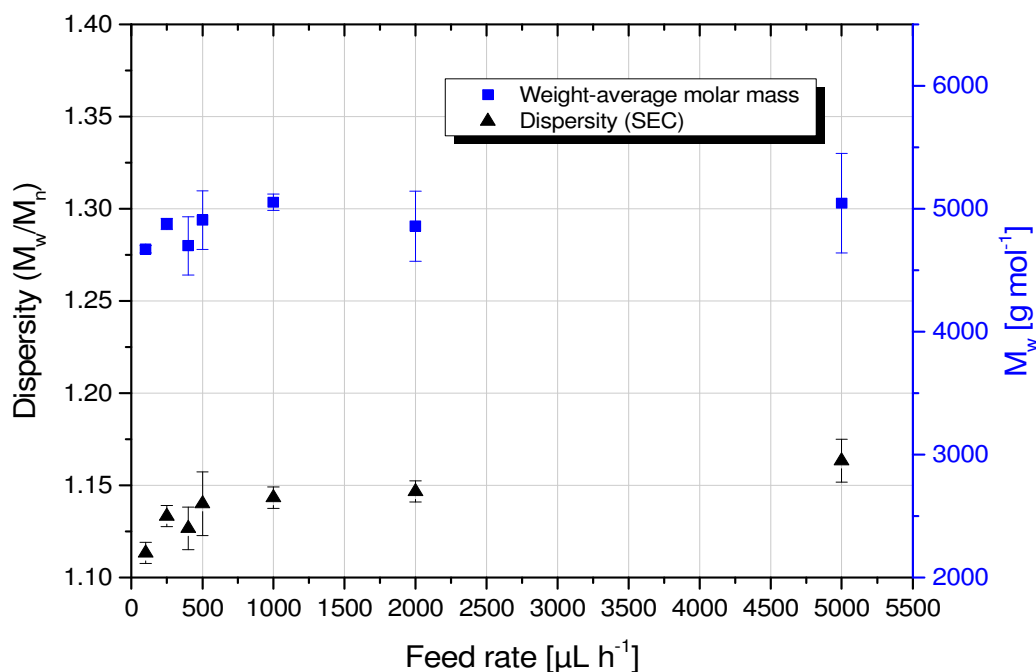


Figure 74: Dispersity (▲)– and M_w (■)–feed rate plot for the synthesis of poly(EEGE) initiated with KOtBu at $45\text{ }^\circ\text{C}$. All experiments were performed in triplicate and the obtained standard deviation shown as error bars.

To confirm the above mentioned hypothesis, the first-order kinetics plot for AGE and EEGE polymerization was determined for an initial $[\text{M}]_0:[\text{I}]$ ratio of 50:1. In these experiments all monomer was present from the beginning (“infinite feed rate”). Conversion was determined by $^1\text{H-NMR}$ spectroscopy and $-\ln(M_t/M_0)$ plotted against time (Figure 75). The apparent rate constants were determined and the propagation rate constants calculated. With these, AGE polymerizes faster than EEGE, having propagation rate constants of $k_{\text{AGE}} = 2.41 \cdot 10^{-3} \text{ L mol}^{-1} \text{ s}^{-1}$ and $k_{\text{EEGE}} = 2.20 \cdot 10^{-3} \text{ L mol}^{-1} \text{ s}^{-1}$ under the given conditions. In contrast to that, the polymerization of AGE was stated to be slower than EEGE in diglyme at $120\text{ }^\circ\text{C}$ by Erberich et al.[62] This can be assigned to the modified polymerization conditions. Both polymerizations show induction periods as was already discussed in chapter 3.1.2. The propagation rate constants were calculated using the concentration of the active species in solution. For the experiments with the slow monomer addition the quantity of the active species can be assumed to be constant, but the concentration alters with time. With this, no

calculation can be performed to determine the optimized feed rate that is probably related to the propagation speed.

Regarding the feed rate and intended DP of 50, the initial volume of the monomer has also to be considered for feed rate adjustment. As an example for AGE, with a total volume of 570 μL monomer and a feed rate of 500 $\mu\text{L h}^{-1}$, after 66 min all monomer was injected. In contrast to that with the same feed rate for EEGE polymerization (total volume 731 μL) full monomer addition is obtained not before 88 min. Therefore, as more volume of EEGE is needed for the same intended DP and polymerization is slightly slower, feed-rate influences for low dispersity poly(glycidyl ether)s are assumed to differ from monomer to monomer, depending on kinetics and monomer volume.

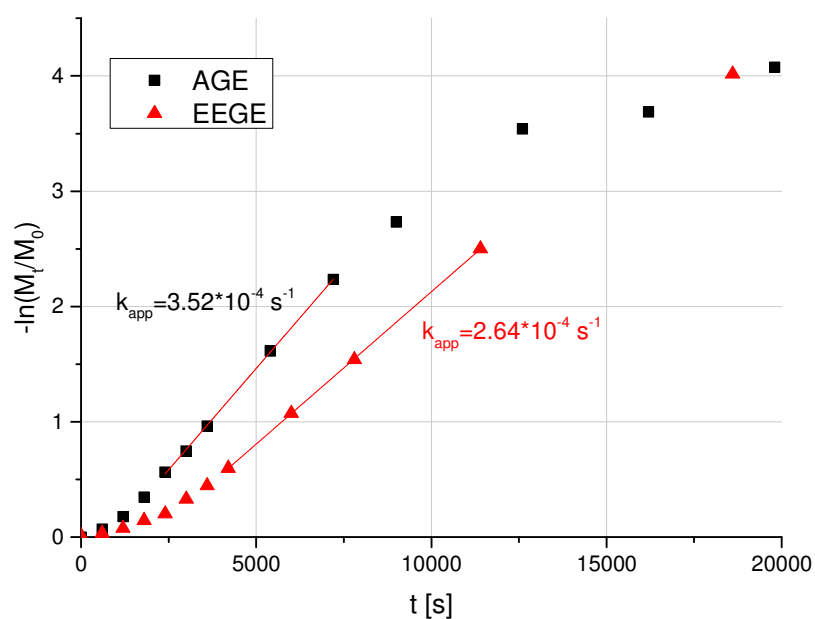


Figure 75: First-order kinetics plot for AGE and EEGE polymerization initiated with KOtBu at 45 °C. Apparent rate constants were determined by a linear fitting (red lines). The corresponding apparent rate constants are inserted with $k_{app} = 3.52 \cdot 10^{-4} \text{ s}^{-1}$ (AGE) and $k_{app} = 2.64 \cdot 10^{-4} \text{ s}^{-1}$ (EEGE).

3.2. *Synthesis of polythioglycidols*

In this chapter controlled oxyanionic ring-opening polymerizations of polyglycidols were translated a thioanionic ring-opening polymerization. For this the glycidyl-monomers were converted to the corresponding episulfides (IUPAC: thiirane) and polymerized by an anionic mechanism. Focusing on EEGE and AGE monomers, polymerization protocols were used as described in literature and slightly modified reducing side-reactions during polymerization processes. A deprotection of poly(ethoxy ethyl thioglycidyl ether) was established. Amphiphilic poly(thioglycidol)-*block*-poly(ethylene glycol) lead to the formation of aggregates in aqueous solution.

Parts of the results were already published in

M. Kuhlmann, S. Singh, J. Groll, Controlled Ring-Opening Polymerization of Substituted Episulfides for Side-Chain Functional Polysulfide-Based Amphiphiles, *Macromolecular Rapid Communications*, 33 (2012) 1482-1486.

3.2.1. Synthesis of the monomer

According to the published procedure by Spassky et al. episulfides were synthesized by stirring the epoxide with dispersed or dissolved thiocyanates.[85, 86] Allyl glycidyl ether is commercially available and ethoxy ethyl glycidyl ether was synthesized as described in the previous chapter. Stirring the epoxide with dispersed potassium thiocyanate in isopropanol for 7 days gives the ring-transformed episulfides.

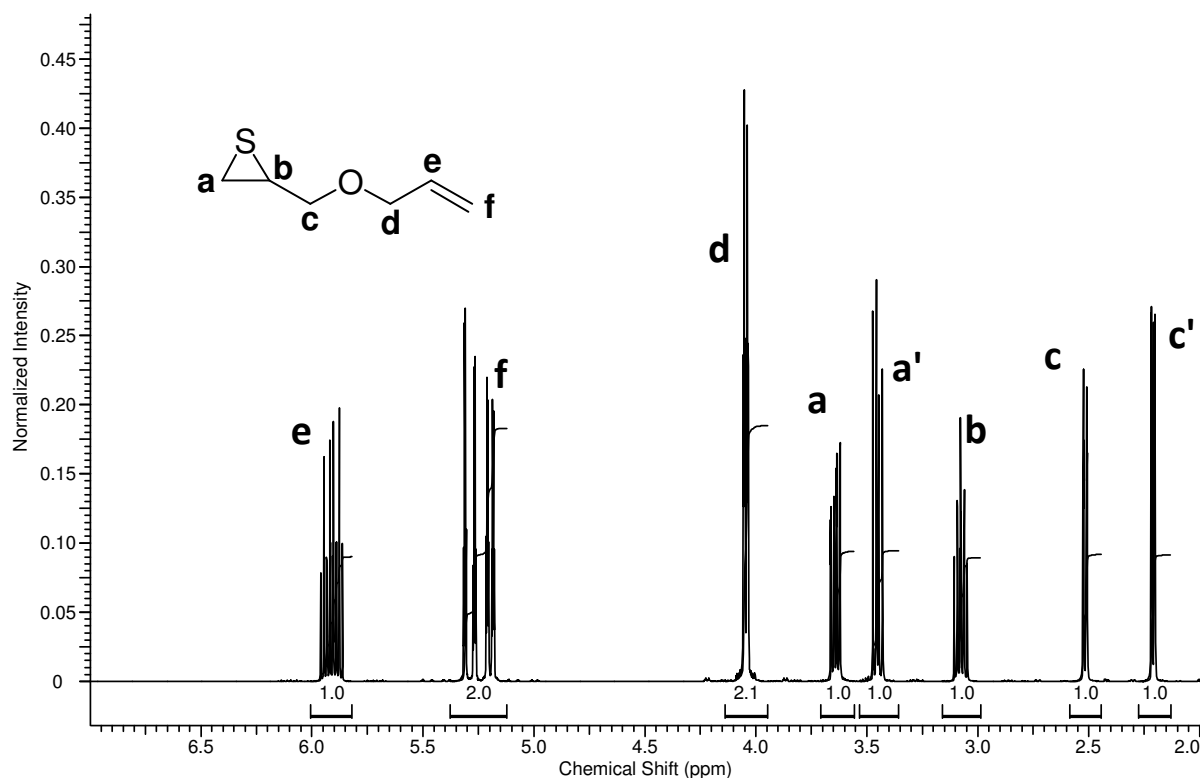


Figure 76: $^1\text{H-NMR}$ spectrum of allyl thioglycidyl ether (ATGE) in CDCl_3 .

After purification by distillation the $^1\text{H-NMR}$ spectrum of synthesized allyl thioglycidyl ether (ATGE) is shown in Figure 76. Here the signals of H^c and H^a split due to the racemic nature of the monomer. The asymmetric substituted C^b results in a different chemical shift of H^c and $\text{H}^{c'}$ with $\Delta\delta = 0.26$ ppm. Retention of the correct integration ratio between heterocycle H^a and H^b $I(\text{H}^a + \text{H}^b) = 3$ and the signals of the allyl-group H^e and H^f with $I(\text{H}^e + \text{H}^f) = 3$ clearly show the complete ring-transformation. In analogy to this, ethoxy ethyl thioglycidyl ether was prepared. In Figure 77 the purified ethoxy ethyl thioglycidyl ether is shown with the signals of the episulfide at $\delta = 3.05 - 3.17$ (H^b) ppm, $2.52 - 2.60$ (H^a) ppm and $\delta = 2.23 - 2.34$ ($\text{H}^{a'}$) ppm. The acetal- H^d can be detected at $\delta = 4.68 - 4.77$ ppm and the corresponding CH_3 -signals with a doublet at $\delta = 1.15 - 1.28$ ppm (H^e) and a triplet at $\delta = 1.02 - 1.15$ ppm (H^g).

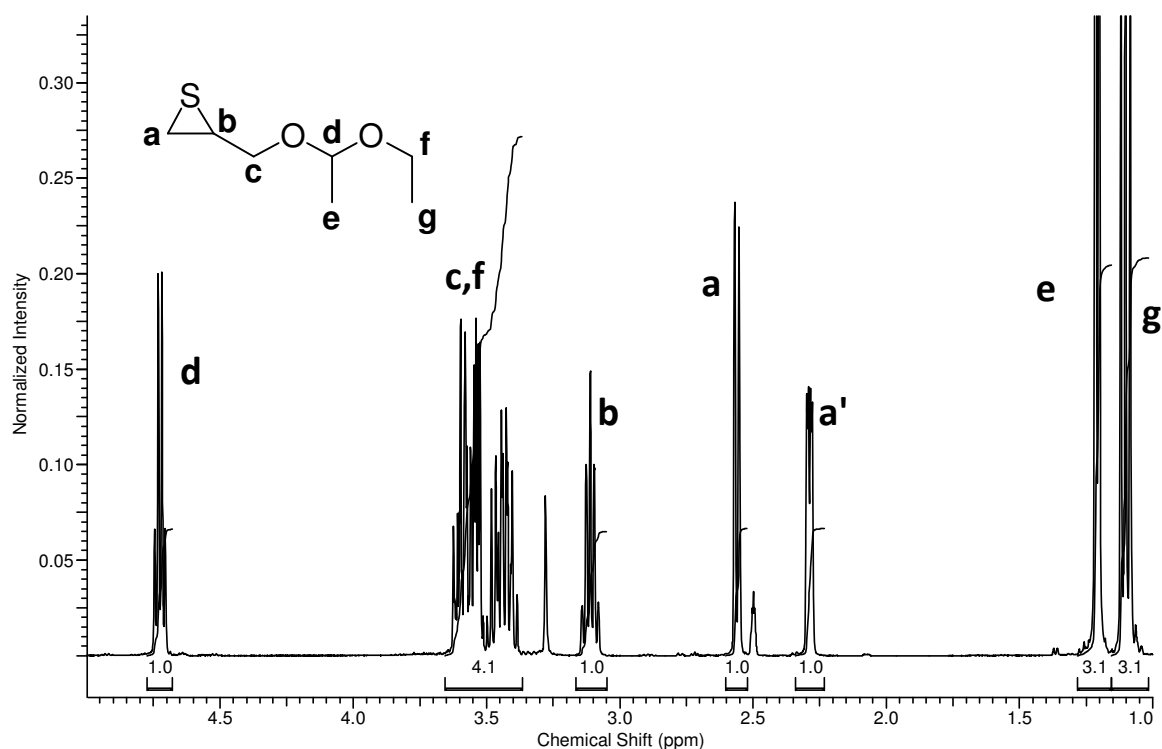
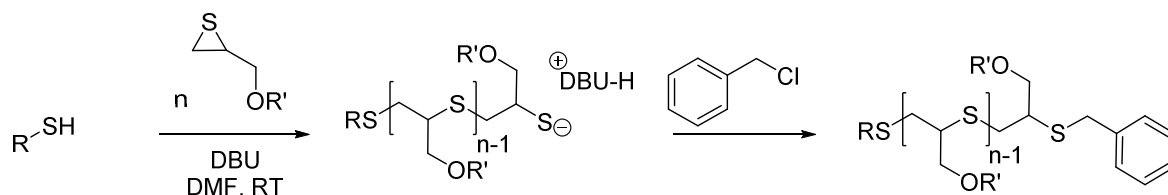


Figure 77: ¹H-NMR spectrum of ethoxy ethyl thioglycidyl ether (EETGE) in DMSO-*d*₆.

3.2.2. Homo- and copolymerization of ATGE and EETGE with thiolates

Although there is a broad spectrum of initiators mentioned in literature for episulfide polymerization, thiolates seem to be the most promising species due to published narrow molar-mass distributions, a variety of commercially available thiols, and the presence of the active species already in the initiator. Unfortunately, hints are given that possible disulfide-impurities broaden the molar-mass distribution of the resulting polymer. The polymerization of the episulfides ethoxy ethyl thioglycidyl ether and allyl thioglycidyl ether was investigated after distillation of the thiols, especially focusing on the best initiator, regarding their use as internal NMR reference.



R' = allyl, ethoxy ethyl

Scheme 26: Initiation and polymerization of episulfides with thiolates. Quenching of the thiolate as active species was achieved using benzyl chloride.

3.2.2.1. Thiophenol as initiator

Thiophenol was used as an aromatic thiolate-initiator. The advantages of thiophenol-initiated polymerizations were already described in literature using propylene sulfide as monomer and DBU as base in DMF at RT.[147] The initiation with thiophenol and termination with PEG-bromide, in the cited literature, leads to amphiphilic blockcopolymers with an aromatic end-group used for M_n -determination by $^1\text{H-NMR}$ spectroscopy. Literature states the degradation of the thioether backbone using benzyl bromides, hence it was focused on the less reactive benzyl chlorides.[101] After quenching, non-terminated thiolates undergo a fast dimerization under oxidative conditions. Bimodal SEC-curves therefore indicate an incomplete quenching, as residual thiolates are readily oxidized by O_2 and dimerize.

The polymerization of allyl thioglycidyl ether was performed with thiophenol/DBU in DMF at RT and the active species was quenched with benzyl chloride. The $^1\text{H-NMR}$ spectrum (Figure 78) shows the aromatic signal of the initiator (thiophenol) and the termination agent (benzyl chloride) at $\delta = 7.11 - 7.46$ ppm. At $\delta = 5.72 - 6.0$ ppm the ^1H -signals of the allyl-group H^h appears as a multiplet, whereas at $\delta = 5.05 - 5.35$ ppm the signals of the H^i were identified (for assignment see Figure 78). The former sharp episulfide ring-signals get blurred and were identified as the backbone signals H^e and H^d at $\delta = 2.95 - 3.09$ ppm and $\delta = 2.71 - 2.95$ ppm indicating a polymerization. At $\delta = 3.87 - 4.04$ ppm H^b was identified. At $\delta = 3.80 - 3.87$ ppm a singlet was recorded and assigned to the terminator signal H^j in benzylic position, confirmed by literature giving similar values for such a position.[148]

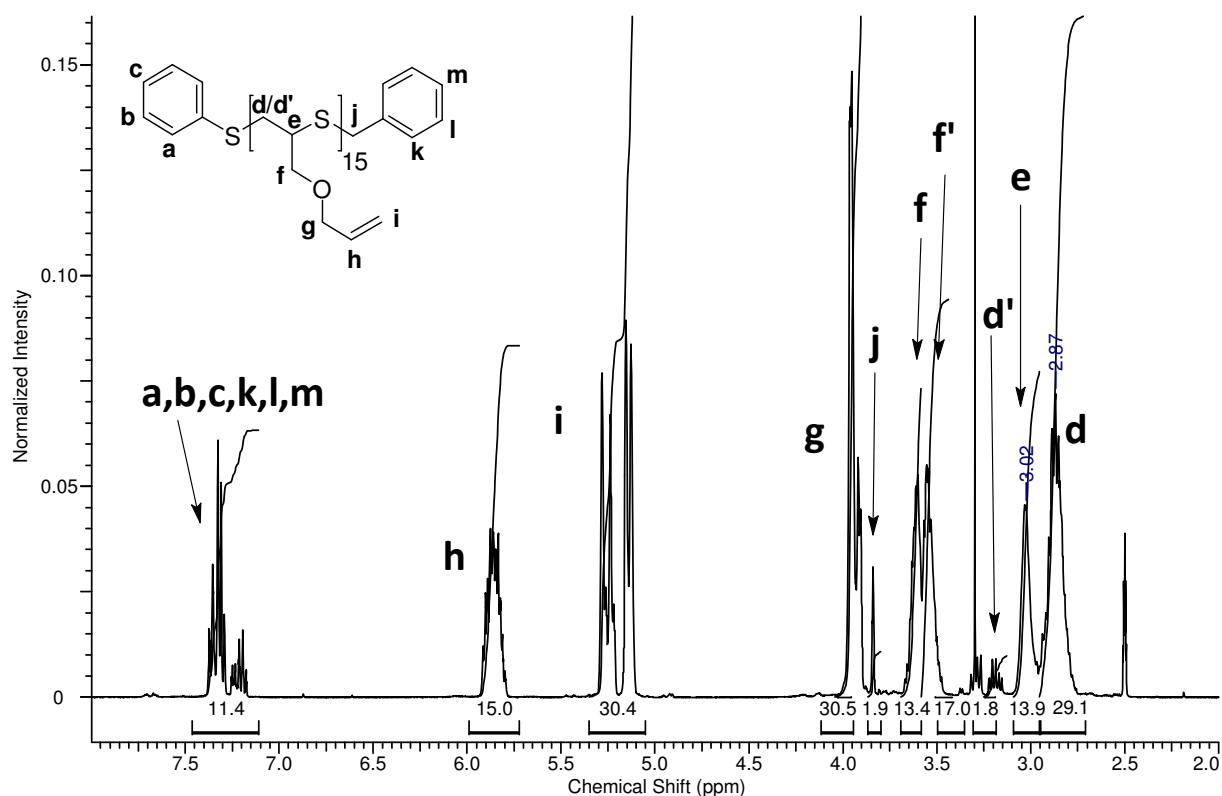


Figure 78: $^1\text{H-NMR}$ of poly(ATGE) in $\text{DMSO-}d_6$ with thiophenol as initiator and benzyl chloride as terminating agent.

The signal at $\delta = 3.13\text{-}3.25$ ppm can be ascribed to the $\text{H}^{d'}$ signal of the backbone, i.e. the first repeating unit at the initiator site. Although at both termini an aromatic ring is present, the direct chemical environment differs. This can be explained by the following argumentation. The backbone-signals H^d and H^e have all the same chemical shift, whereas the first and last repeating units are influenced by the initiator and the terminator. At the initiator site, the $\text{H}^{d'}$ signal is downfield shifted, due to the aromatic ring. At the terminator-site the H^j signal is even more affected by the aromatic ring, leading to a more pronounced downfield-shift. The side-chain signals of H^f between the ether and the poly(thioether) backbone was ascribed to the signals appearing at $\delta = 3.44 - 3.69$ ppm. It is assumed that the allyl group is not affected by the polymerization. Both, initiation and termination agent signals were used to determine the DP. Besides the determination of the DP, it allows the evaluation of the quenching reaction. The H^j signal of the initiator was used to evaluate the termination reaction. An incomplete termination reaction with benzyl chloride could be detected by a difference of the determined DP. For the polymerization of allyl thioglycidyl

ether with thiophenol/DBU as initiator and benzyl chloride as quencher the aromatic region was first used as reference. A DP = 15 was aimed using a ratio of allyl thioglycidyl ether:thiophenol = [M]:[I] = 15:1. With a fixed integral of $I = 10$ of the aromatic region a DP = 13 was obtained. Using the terminal Hⁱ-signal at $\delta = 3.84$ ppm and an integral of 2 a DP = 15 is obtained. The H^{d'} signal at $\delta = 3.13 - 3.25$ ppm was also set to 2, yielding a DP = 17. As the overall integral of the aromatic region has the highest number of H-atoms of the reference signals, the inaccuracy of this signal is the lowest, indicating the complete termination with benzyl chloride. Unfortunately, a potentially occurring insufficient quenching reaction reduces the integral and therefore falsifies the signal intensity. The only signal independent on the quenching reaction is the signal H^{d'} at $\delta = 3.13 - 3.25$ ppm. Although the inaccuracy of this signal is higher than of the aromatic region, the intensity is not influenced by an insufficient termination reaction.

SEC-analysis (THF, 1.0 mL min^{-1} , poly(styrene)-standard) of the polymer poly(allyl thioglycidyl ether) (poly(ATGE)) showed a monomodal distribution with $M_n = 2000 \text{ g mol}^{-1}$ corresponding to DP = 15 and $\mathcal{D} = 1.1$ (see Figure 79). The polymer was synthesized with an initial feed of [M]:[I] = 15:1. Therefore it can be assumed that the polymerization process can be controlled with respect to molar-mass and DP indicating a living polymerization.

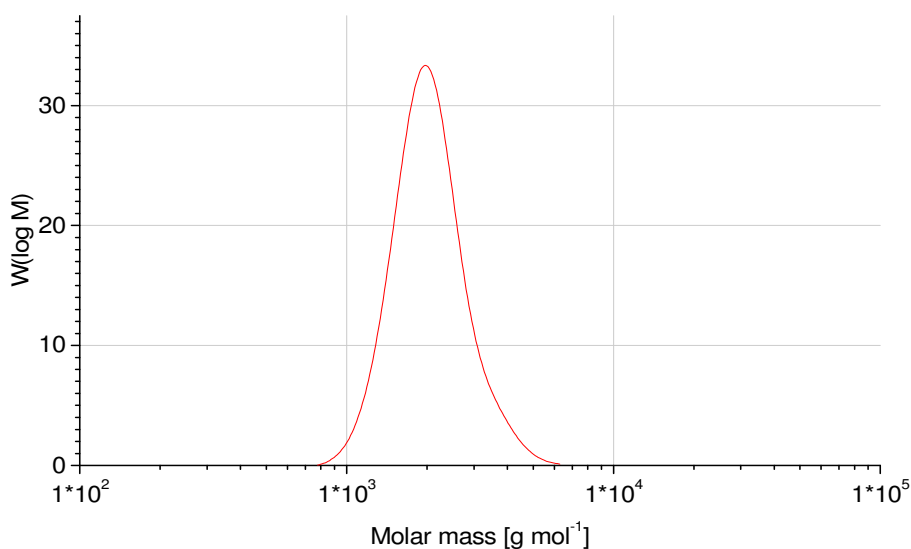


Figure 79: SEC-elugram of poly(ATGE) with DP=15 synthesized with DBU/thiophenol as initiator. A dispersity of $\bar{D} = 1.10$ and number-average molar mass of $M_n = 2000 \text{ g mol}^{-1}$ was obtained.

3.2.2.2. Butanethiol as initiator

Aliphatic thiols were also investigated as initiator for the polymerization and their use as reference in $^1\text{H-NMR}$ spectroscopy. The initiation of the polymerization of episulfides was performed with butanethiol and DBU as base. In contrast to the initiation of episulfide-polymerization with thiophenol, the aliphatic signals are expected to be separated from the signals of the terminating agent in $^1\text{H-NMR}$ spectra. Analyzing the polymerization with thiophenol showed that no polymeric $^1\text{H-NMR}$ signals appear in this region. Therefore the use of butanethiol-signals as internal reference might enhance the determination of DP and M_n . For this, the same procedure was performed as was described for the initiation with thiophenol/DBU (chapter 3.2.2.1), but butanethiol/DBU was used instead. Ratios of $[\text{M}]:[\text{I}] = 18:1$ and $54:1$ were used.

$^1\text{H-NMR}$ spectroscopy of poly(ATGE) with $[\text{M}]:[\text{I}] = 18:1$ was performed in $\text{DMSO-}d_6$ (Figure 80). The initiator signals appear as a triplet at $\delta = 0.79 - 0.95 \text{ ppm}$ for the terminal CH_3 -group H^a , a sextet at $\delta = 1.28 - 1.43 \text{ ppm}$ for H^b and a quintet at $\delta = 1.43 - 1.61 \text{ ppm}$ for H^c .

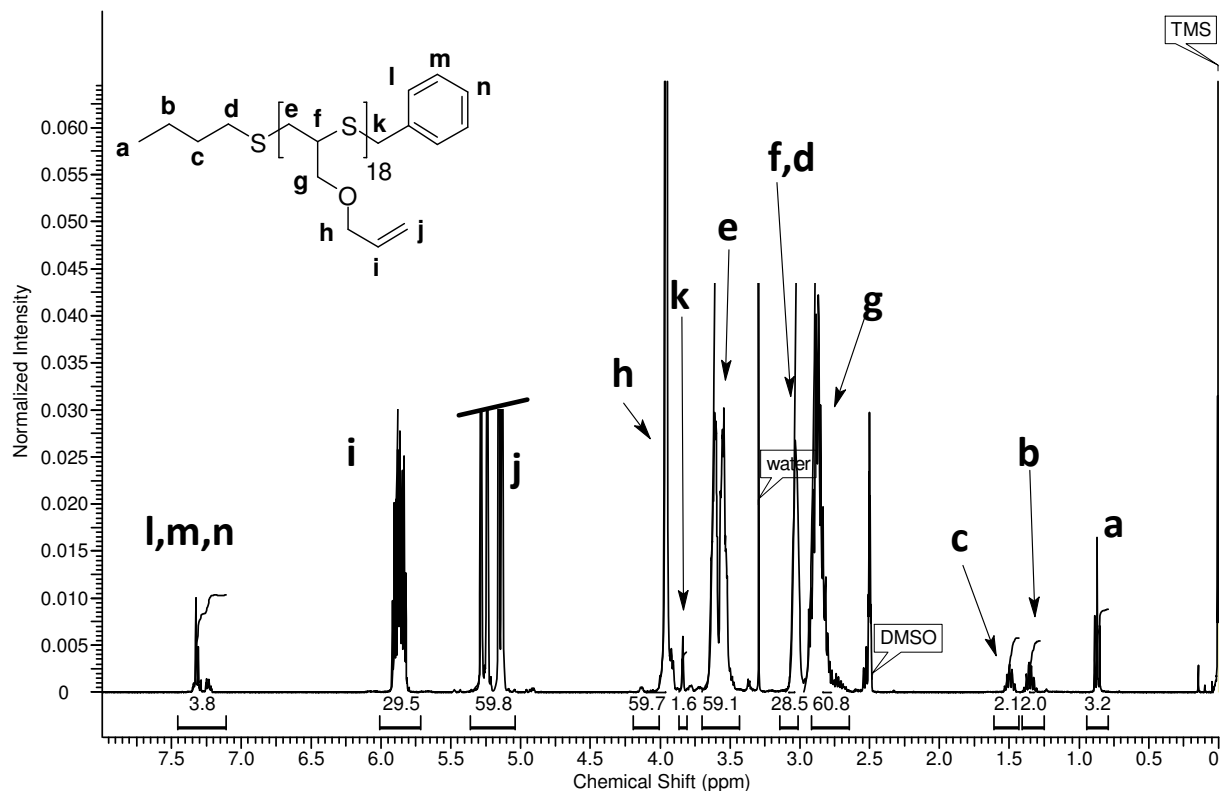


Figure 80 ^1H -NMR spectrum of poly(ATGE) initiated with butanethiol/DBU and terminated with benzyl chloride. The degree of polymerization (DP) determined by NMR was 30, although a ratio of $[\text{M}]:[\text{I}]=18$ was used for the synthesis.

The triplet expected for H^{d} overlaps with the backbone signals H^{f} . Using the initiator as reference an average DP = 30 was obtained. With the aromatic signals of the benzyl-ring as reference a DP = 39 is obtained. This inconsistency can be ascribed to an incomplete termination reaction after quenching with benzyl chloride. An integral of $I = 5$ is expected, but a value of $I = 3.8$ was obtained, indicating an incomplete termination reaction. With the benzyl-group as reference and an integral of $I = 5$ the DP is hence overestimated. The polymerization was repeated using a feed of $[\text{M}]:[\text{I}] = 54:1$ with butanethiol/DBU as initiator. The ^1H -NMR spectrum was recorded and the initiator used as reference for the determination of DP (Figure 81). Here, a DP of 52 was obtained with the use of the terminal CH_3 -group (H^{a}) as reference. This is in good agreement with the theoretical value. With the use of the CH_2 -signal H^{k} of the terminating agent a DP = 57 was calculated, indicating an insufficient termination with benzyl chloride under the used conditions.

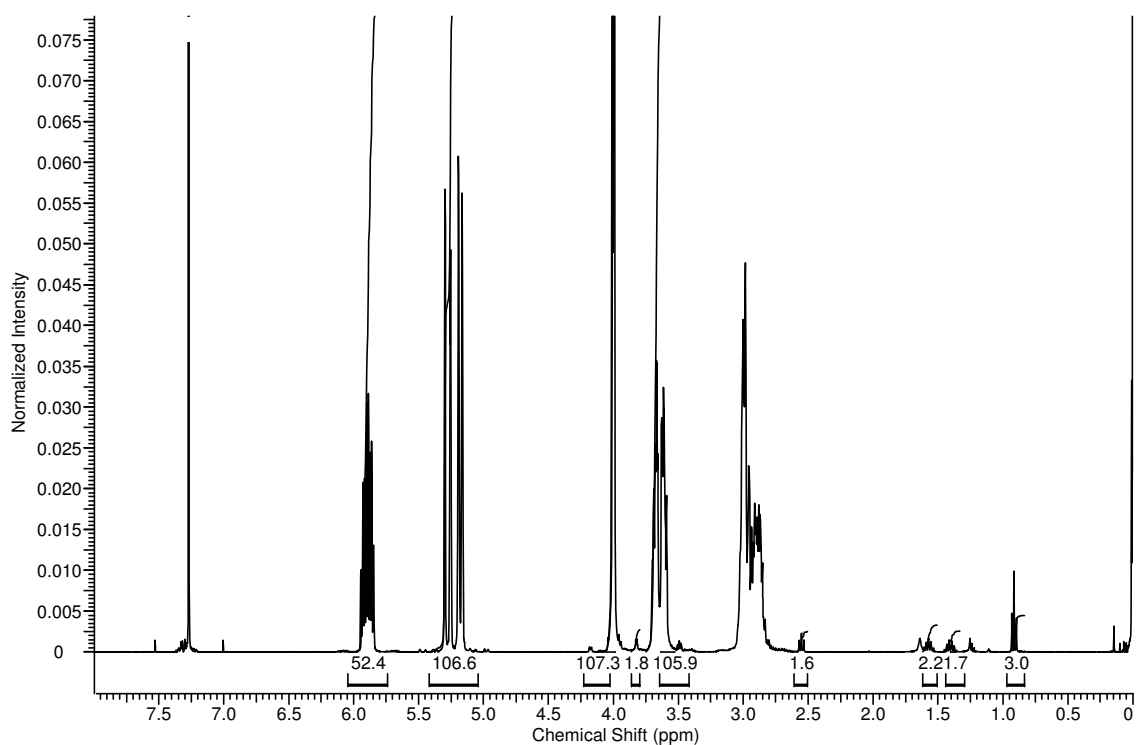


Figure 81: ¹H-NMR spectrum of poly(ATGE) ([M]:[I]=54) initiated with butanethiol/DBU and terminated with benzyl chloride.

The SEC-elugrams were determined using THF as mobile phase and poly(styrene) as calibration-standard. The polymer synthesized with [M]:[I] = 18:1 had a number-average molar-mass of $M_n = 4800 \text{ g mol}^{-1}$ (Figure 82). Poly(ATGE) obtained with [M]:[I] = 54:1 has a M_n of 7700 g mol^{-1} (Figure 83). With a molar-mass of the monomer of $M = 130.20 \text{ g mol}^{-1}$ the corresponding DPs were determined. For the measurements $DP_{SEC,18} = 37$ and $DP_{SEC,54} = 59$ were obtained. These values indicate two interesting facts. On the one hand does it show that the quantity of the monomer for the first feed ($DP = 18$) was too high, as it was already indicated by ¹H-NMR spectroscopy. On the other hand does it indicate (confirmed by the [M]:[I] = 54:1 experiment and thiophenol-initiated polymerization) that the used SEC system (solvent: THF; 1.0 mL min^{-1} , poly(styrene) as calibration-standard) is quite good for the polymers, indicating a similar hydrodynamic radius – molar-mass relationship of poly(styrene) and poly(allyl thioglycidyl ether) in THF. A shoulder at twice the molar mass of the main polymer signal was detected in both SEC elugrams, indicating a dimerization by oxidation. The obtained dispersities were $\mathcal{D} = 1.1$ and $\mathcal{D} = 1.22$ for the polymers with and initial ratio of [M]:[I] = 18:1 and [M]:[I] = 54:1, respectively.

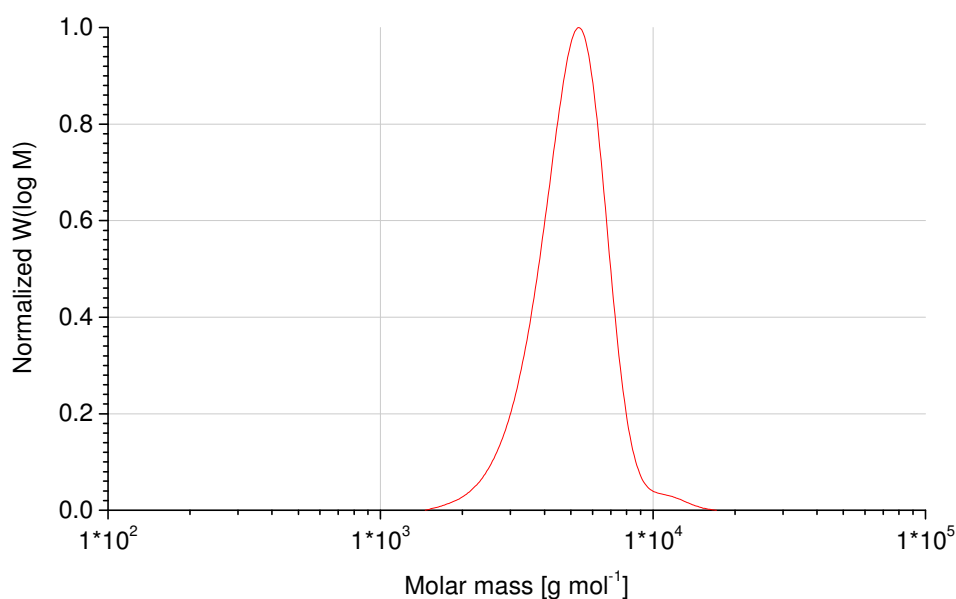


Figure 82: SEC-elugram for poly(ATGE) with DP = 18 initiated with butanethiol/DBU and terminated with benzyl chloride. Besides the main polymer fraction a second higher molar-mass polymer fraction was detected at $M > 10,000 \text{ g mol}^{-1}$.

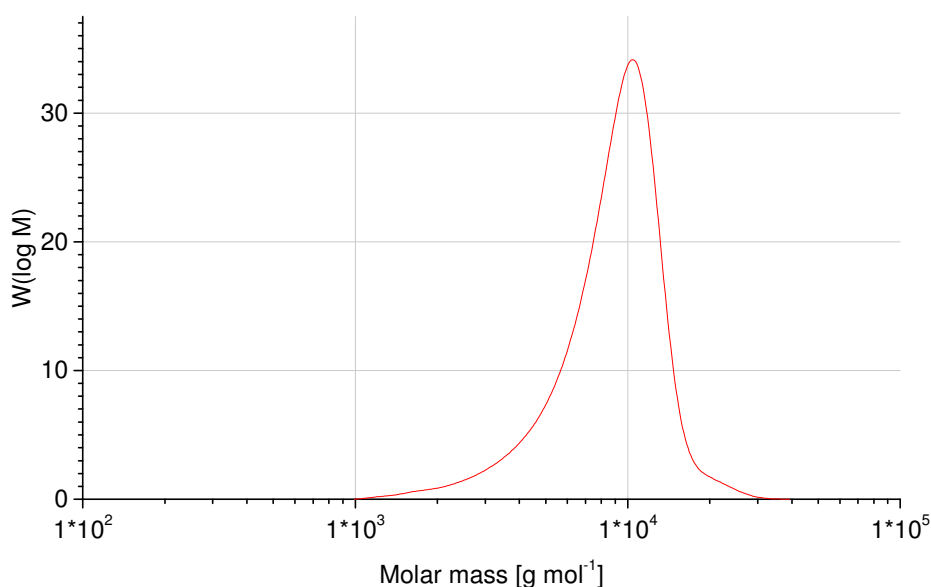


Figure 83: SEC-elugram for poly(ATGE) with DP = 54 initiated with butanethiol/DBU and quenched with benzyl chloride. A tailing of the molar mass distribution as well as a small shoulder at higher molar mass fractions were detected.

Expanding the polymerization of allyl-functional to acetal-functional episulfides, the polymerization of EETGE was performed with butanethiol/DBU with a ratio of $[M]:[I] = 31:1$. The $^1\text{H-NMR}$ spectrum (Figure 84) was recorded in CDCl_3 . At $\delta = 2.47 - 2.61$ ppm (H^d), 1.49 - 1.64 ppm (H^c) and 0.84 - 0.98 (H^a) ppm the signals of the initiator were identified. Using the integral of the initiator at $\delta = 0.84 - 0.98$ ppm (terminal CH_3 -group) a $\text{DP} = 31$ was determined. SEC-analytic (Figure 85) gives a $M_n = 6200 \text{ g mol}^{-1}$ equaling a $\text{DP} = 38$. A monomodal molar-mass distribution was recorded with a small tailing to lower molar-masses, but no indication of dimerization was observed.

The molar-mass determined by SEC-analysis and by $^1\text{H-NMR}$ spectroscopy indicates a slight deviation of the determined DP for both methods. As no side-reactions are observable in SEC elugrams, it is assumed that the ratio of the polymer- to initiator-signals in $^1\text{H-NMR}$ -spectroscopy determines the correct ratio.

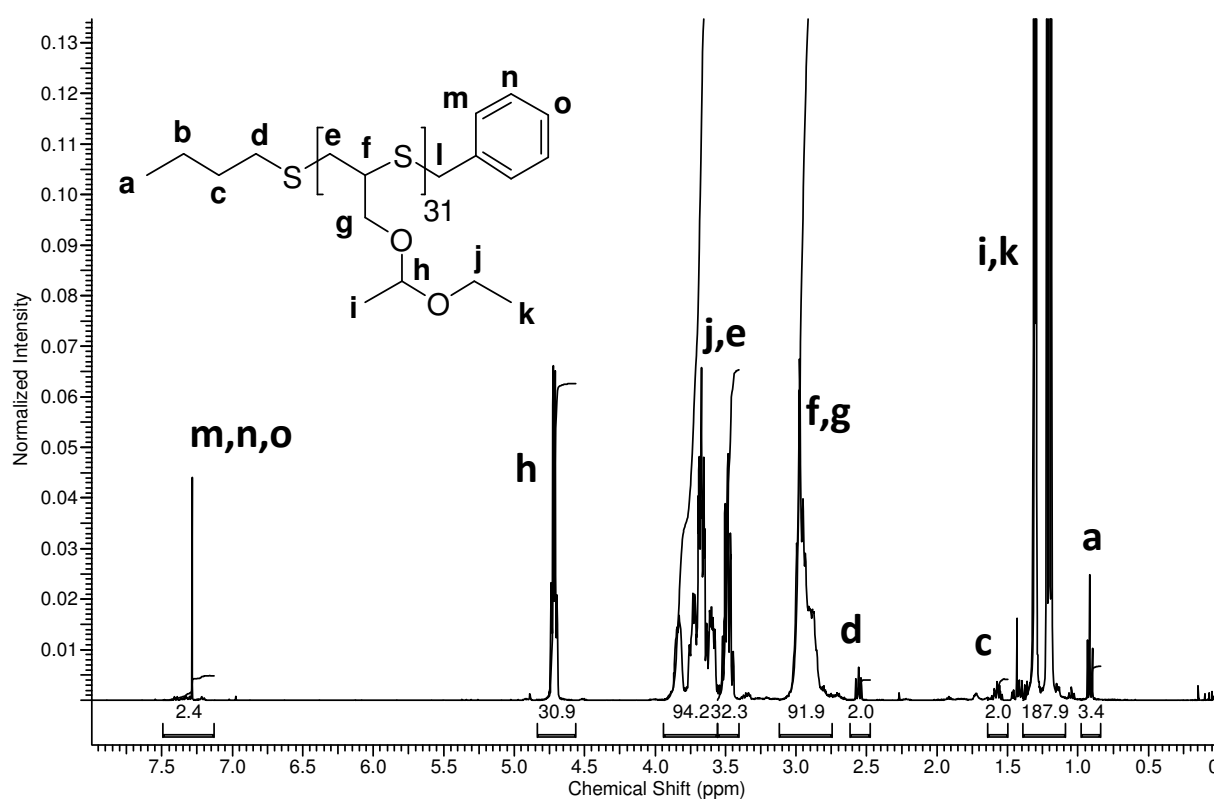


Figure 84: $^1\text{H-NMR}$ spectrum of poly(EETGE) with $\text{DP} = 31$ in CDCl_3 . Polymerization was initiated with butanethiol/DBU and quenched with benzyl chloride.

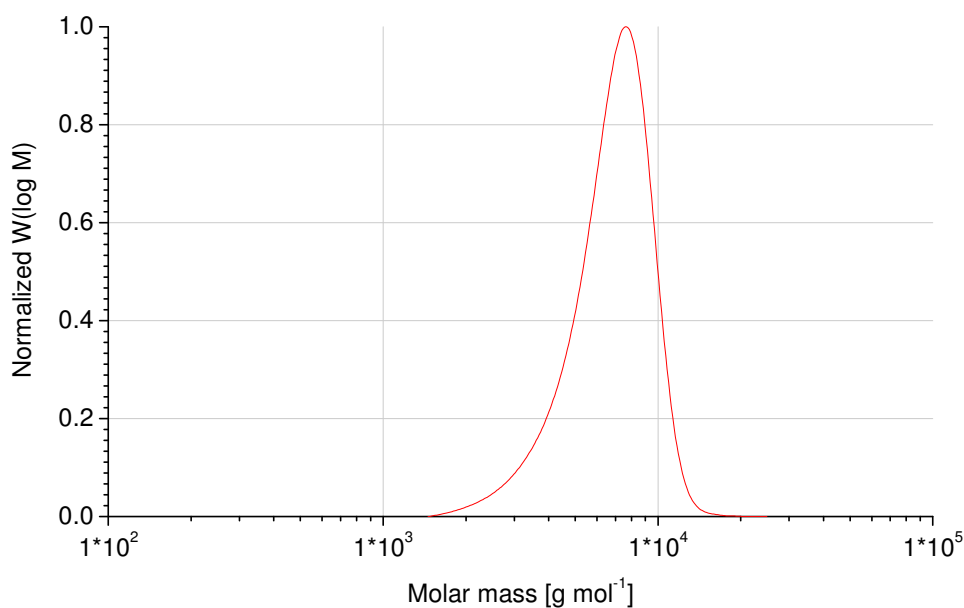


Figure 85: SEC-elugram of poly(EETGE) with DP = 30 initiated with butanethiol/DBU and quenched with benzyl chloride. A small tailing of the curve was detected.

The block-copolymerization of ATGE and EETGE was investigated as well. The ¹H-NMR spectrum of poly(ethoxy ethyl thioglycidyl ether)-*block*-poly(allyl thioglycidyl ether) is shown in Figure 86. A DP_{EETGE} = 15 and DP_{ATGE} = 15 were attempted. Using the terminal CH₃-group of butanethiol as internal reference a DP_{EETGE} = 13 and DP_{ATGE} = 16 were determined. For this, the typical allyl signals of ATGE at $\delta = 5.85$ ppm (H^p) and acetal signals of EETGE at $\delta = 4.6$ ppm (H^h) were used. The obtained DPs determined by ¹H NMR-spectroscopy are in good accordance with the initial ratios [EETGE]:[I] = [ATGE]:[I] = 15:1.

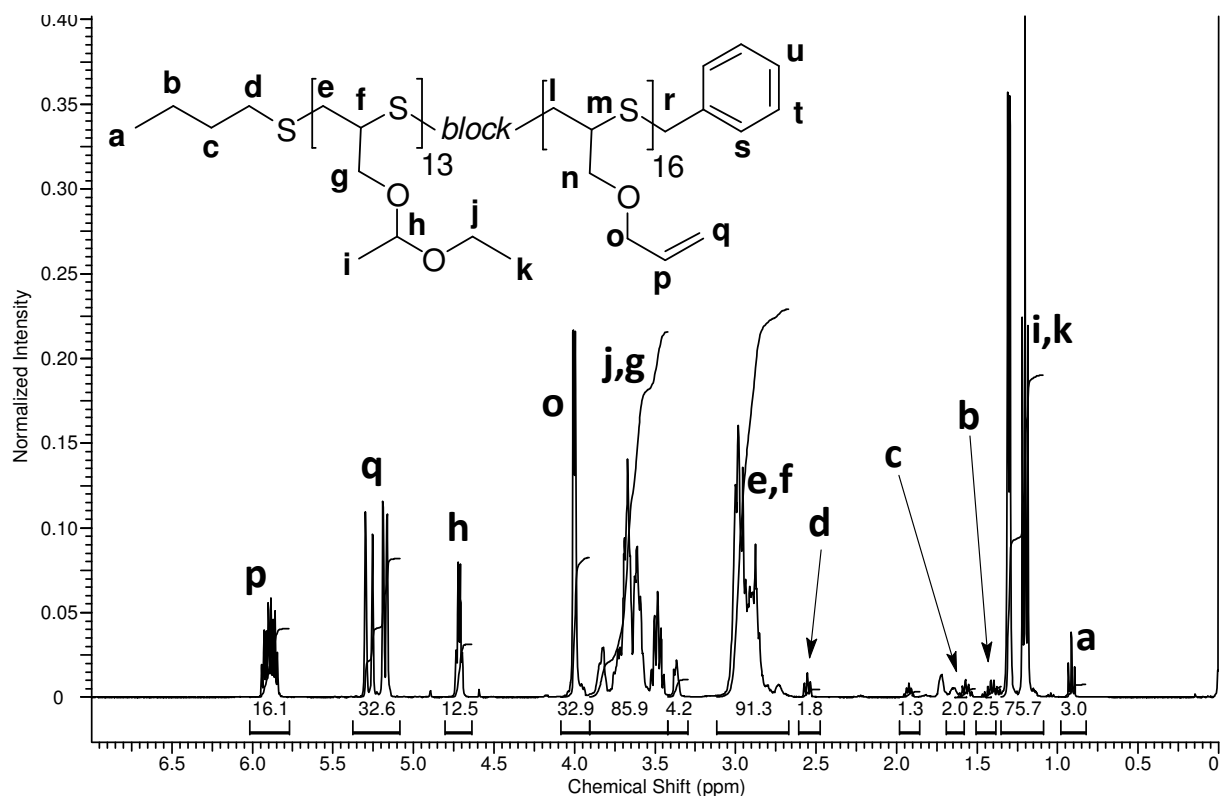


Figure 86: $^1\text{H-NMR}$ spectrum in CDCl_3 of poly(EETGE)-*block*-poly(ATGE) with EETGE:ATGE=15:15 initiated with butanethiol/DBU and quenched with benzyl chloride.

The SEC-elugram of the block-copolymer shows a pronounced bimodality (Figure 87). It is assumed that upon addition of the second monomer oxygen is introduced into the flask, leading to the oxidation of the thiolate species and hence dimerization of the poly(thioether). With a molar-mass of $M(\text{EETGE}) = 162.25 \text{ g mol}^{-1}$ and $M(\text{ATGE}) = 130.20 \text{ g mol}^{-1}$ a molar-mass of the block-copolymer of $M = 4387 \text{ g mol}^{-1}$ is calculated. The two main peaks were determined at approximately $M = 4800 \text{ g mol}^{-1}$ and $M = 9500 \text{ g mol}^{-1}$. Here the main fraction of the sample was assigned to the dimer. The appearance of the pronounced dimer peak also explains the dispersity with a value of $\mathcal{D} = 1.24$.

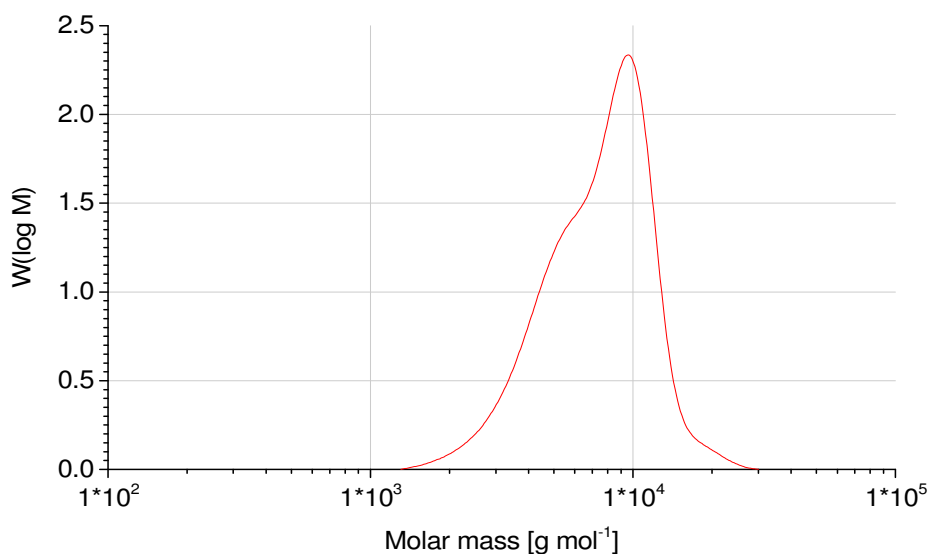


Figure 87: SEC-elugram of poly(EETGE)-*block*-(ATGE) initiated with butanethiol/DBU and quenched with benzyl chloride. The main fraction of the sample was assigned to the dimerized polymer, whereas the lower fraction was assigned to the attempted polymer.

3.2.2.3. Mercaptoethanol as initiator

The group of Bonnans-Plaisance showed that the presence of hydroxy-groups does not disturb the polymerization of episulfides due to the low acidity of alcohols ($pK_a \approx 16$) compared to thiols ($pK_a \approx 9$).^[94, 101] The polymerization of ATGE and EETGE was hence performed with mercaptoethanol/DBU as initiator. As the ^1H -spectra of the resulting polymers do not differ from previous discussed signals, they are not shown here. Using ATGE as monomer ($[M]:[I] = 18:1$), the ^1H -NMR spectrum gives a $DP = 18$, if the initiator is used as reference. The SEC of the resulting polymer showed that the polymerization proceeds without oxidation and hence without dimerization reactions of the polymer. The M_n of 2300 g mol^{-1} , determined by SEC analysis, gives a $DP = 18$ with a dispersity of $\mathcal{D} = 1.10$. This further shows that the SEC system is well suited for poly(ATGE)s as was already indicated above.

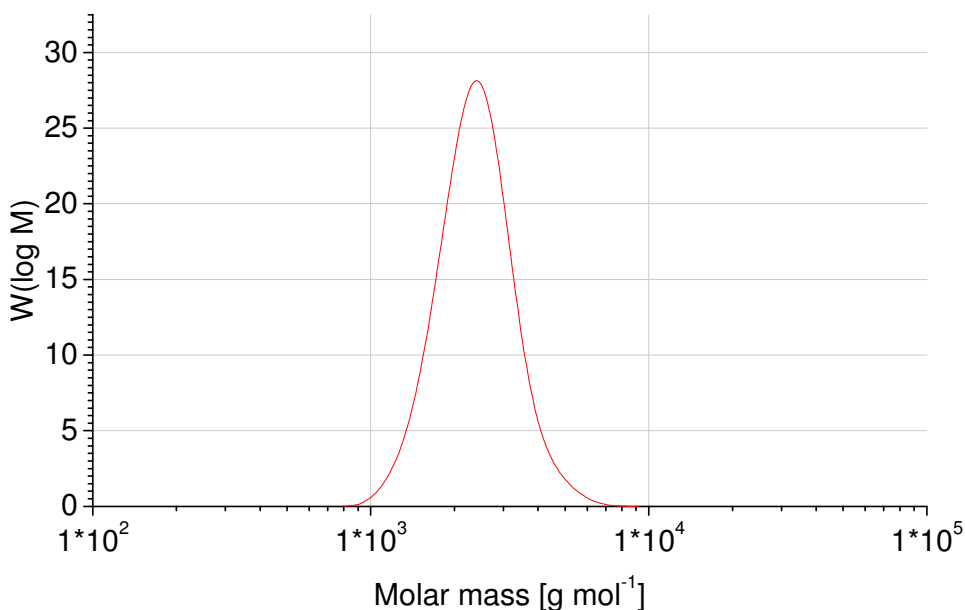


Figure 88: SEC-elugram of poly(ATGE) with DP = 18. The polymer was synthesized with mercaptoethanol/DBU as initiator and benzylchloride as quencher. For the polymer $M_n = 2300 \text{ g mol}^{-1}$ with $\mathcal{D} = 1.10$ was determined.

ATGE polymerization was repeated using a ratio of $[M]:[I] = 66:1$ and benzyl chloride as terminating agent. With this, the influence of the DP on dispersity was investigated. $^1\text{H-NMR}$ spectroscopy was used to determine the DP with the initiator mercaptoethanol as reference. Although a DP of 66 was attempted, $^1\text{H-NMR}$ spectroscopy gives a DP of 48. The SEC-elugram (Figure 89) shows a trimodality with $M_n = 7200 \text{ g mol}^{-1}$ and $\mathcal{D} = 1.48$, corresponding to a DP of 49. Although the polymerizations were performed similar, a dimerization of the polymer was obtained, compared to the polymerization with a lower DP (Figure 88). A third polymer species was detected at $M > 20000 \text{ g mol}^{-1}$, but the reason for this higher fraction is not clear.

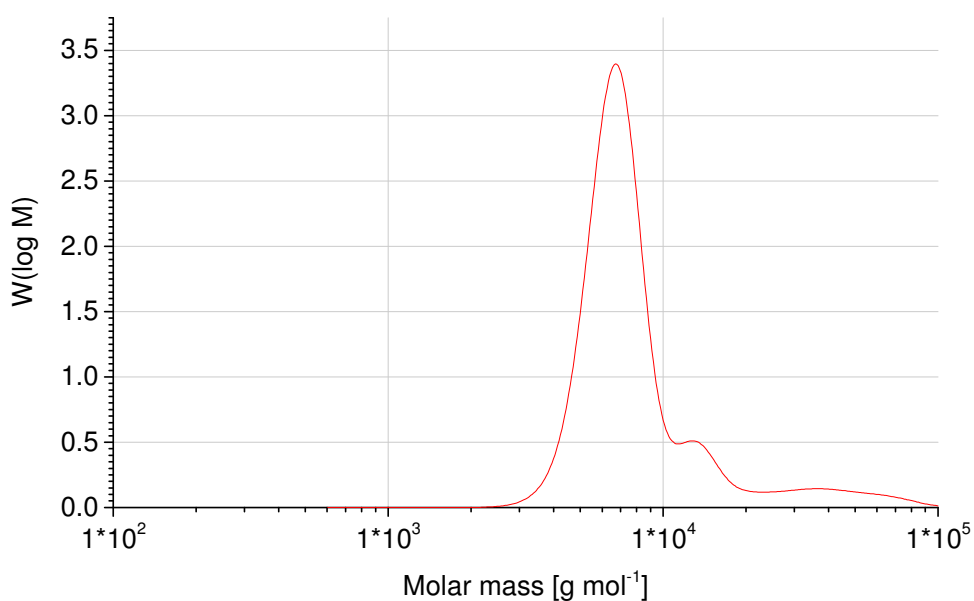


Figure 89: SEC-elugram of poly(EETGE), DP = 66, initiated with mercaptoethanol/DBU and terminated with benzyl chloride. The main fraction of the polymer is accompanied by a high molar mass fraction with twice the molar mass. This is assigned to the dimerized polymer. At molar masses $M > 20\,000\text{ g mol}^{-1}$ a third polymer species was detected. The overall number-average molar mass was $M_n = 7200\text{ g mol}^{-1}$ with a dispersity of $\mathcal{D} = 1.48$.

In general, bimodality is assumed to be caused by an insufficient termination reaction of the active chain ends with benzyl chloride. To enhance the termination reaction, acrylates were also tested due to their high reactivity towards thiolates. Additionally, poly(ethoxy ethyl thioglycidyl ether)-*block*-poly(ethylene glycol) block-copolymers can be obtained using acrylate functional poly(ethylene glycol)s as quenching agent. Using methyl acrylate as a model substance, the quenching of polymerization was investigated. The polymerization of poly(ethoxy ethyl thioglycidyl ether) with $[M]:[I] = 54:1$ was quenched with an excess of methyl acrylate. The $^1\text{H-NMR}$ spectrum of the obtained poly(ethoxy ethyl thioglycidyl ether) reveals a DP of 46 with the initiator mercaptoethanol as internal reference. The SEC-elugram (Figure 90) shows a bimodal distribution with $M_n = 8200\text{ g mol}^{-1}$ and $\mathcal{D} = 1.07$. Although bimodality was observed, the dispersity is quite narrow. The oxidative dimerization reaction of two polymer chains is assumed to cause the second polymer species at twice the molar mass of the main polymer fraction.

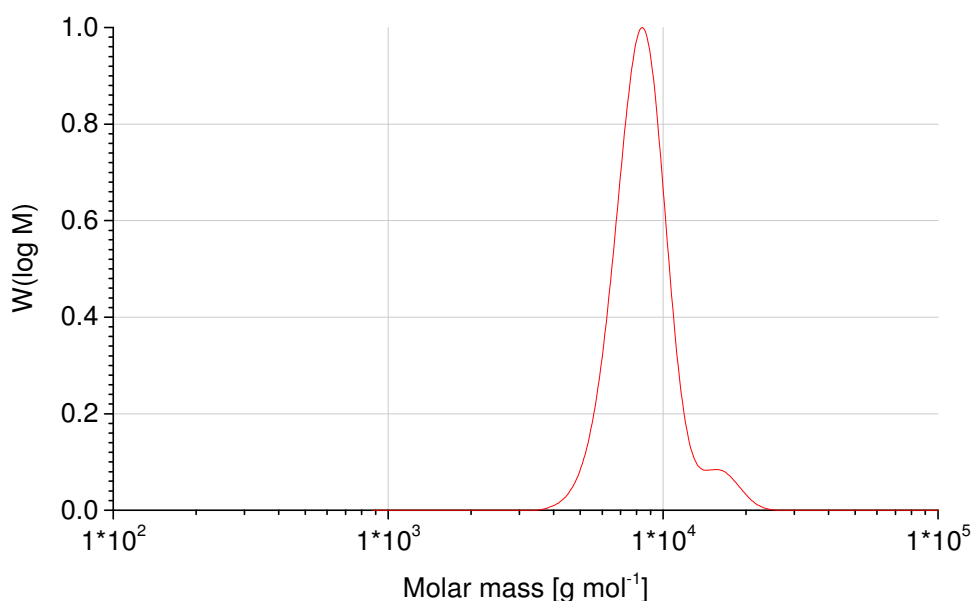


Figure 90: SEC-elugram of poly(EETGE) with DP = 54 initiated with mercaptoethanol/DBU and terminated with methyl acrylate. A second polymer species was detected at $M > 15000 \text{ g mol}^{-1}$ assigned to dimerized poly(EETGE). The sample has a M_n of 8200 g mol^{-1} with a dispersity of $\bar{D} = 1.07$.

The block-copolymer of ethoxy ethyl thioglycidyl ether and allyl thioglycidyl ether was highly bimodal with butanethiol/DBU as initiator as was shown in chapter 3.2.2.2. Mercaptoethanol/DBU was also investigated as initiator for the block-copolymerization of the two monomers. Here a polymer with $[\text{ATGE}]:[\text{I}] = 33:1$ and $[\text{EETGE}]:[\text{I}] = 32:1$ was synthesized. As oxygen was assumed to be introduced upon the addition of the second monomer, the degassing protocol was slightly modified. The initial mercaptoethanol/DMF solution was degassed, by purging N_2 through the solution. Afterwards three *freeze-pump-thaw* cycles were performed. The DBU/DMF solution was equally treated. The solutions were mixed under N_2 -atmosphere, frozen and evacuated. ATGE was added to the frozen solution and it was further evacuated. Afterwards, it was warmed up to 0°C and stirred for 30 min, mixing the initiator and the monomer and start the polymerization. For adding the second monomer, the solution was frozen, and a degassed EETGE/DMF solution added. It was further evacuated. The initially frozen layers mixed upon warming, combining the already prepared poly(allyl thioglycidyl ether) with the newly introduced EETGE monomer.

Finally, a degassed benzyl chloride/DMF solution was added to quench the polymerization. Analysis with SEC shows a bimodal distribution with $M_n = 9000 \text{ g mol}^{-1}$ and $\mathcal{D} = 1.21$. Although repetitive evacuation and degassing were performed, the SEC elugram showed a bimodal curve (Figure 91). It could be observed that the efforts of degassing decreased the content of dimers compared to the polymerization procedure performed with butanethiol (Figure 87 in chapter 3.2.2.2).

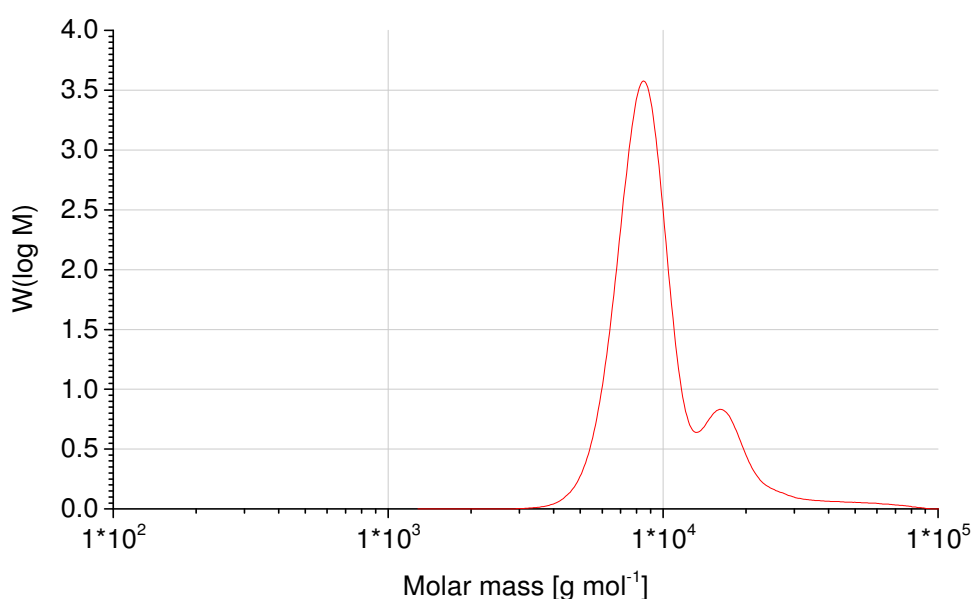


Figure 91: SEC elugram of poly(ATGE)-*block*-poly(EETGE) with ATGE:EETGE=33:32 initiated with mercaptoethanol/DBU and quenched with benzyl chloride. A bimodal elugram was observed assigned to the dimerization of the synthesized polymer. The polymer has a M_n of 9000 g mol^{-1} and a dispersity \mathcal{D} of 1.21.

3.2.2.4. Dithiothreitol as bifunctional initiator

The bifunctional dithiothreitol (DTT) was used to initiate the episulfide polymerization, rendering two vicinal hydroxy-groups exactly in the middle of the final polymer. It is assumed that disulfides introduced by the initiator are inert towards the thiol–disulfide exchange reaction as they exhibit a high enthalpic stability. Hence, all dimers observed in the final polymer were formed during polymerization and not by impurities of the initiator.

DTT/DMF-, EETGE/DMF-solutions and DMF (EETGE:DTT = [M]:[I] = 62:1) were degassed prior to the addition of the DBU/DMF solution. After addition of DBU/DMF it was evacuated for 10 min and finally warmed up to RT. After quenching the polymerization with benzyl chloride, the molar-mass distribution was investigated by SEC analysis (Figure 92). The number-average molar-mass M_n was 10400 g mol^{-1} . Regarding the aimed overall DP = 62 a molar-mass of $M = 10396 \text{ g mol}^{-1}$ was expected. The theoretical value and the obtained value match well, indicating a successful synthesis of poly(ethoxy ethyl thioglycidyl ether) with two OH-functionalities in the center. Unfortunately, the dimer-signal and a small fraction of a third species can be observed, yielding a dispersity value of $\mathcal{D} = 1.12$. As already described, the dimer occurred probably due to the formation of disulfides at the polymerization or the final termination. Due to the preliminary experiments with mercaptoethanol and literature published by Bonnans-Plaisance[94], it is assumed that the polymerization is solely initiated by the thiol groups.

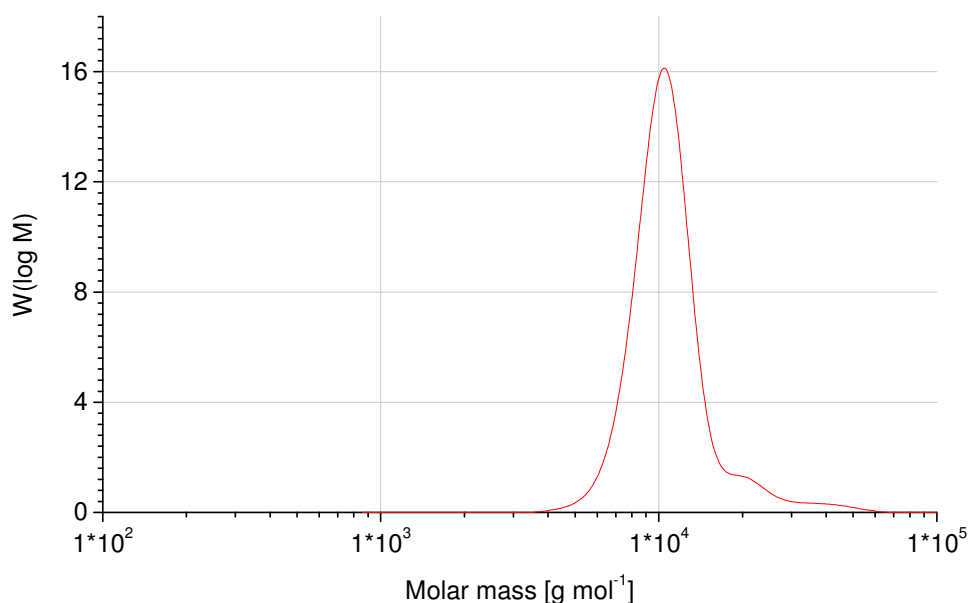


Figure 92: SEC elugram of poly(EETGE) with DP = 62 initiated with DTT/DBU. The active species was quenched benzyl chloride. A second polymer species at $M = 20000 \text{ Da}$ was assigned to the dimerized polymers.

All investigated thiols were able to polymerize the monomers in the presence of DBU. Depending on the initiator, butanethiol was judged to be the most promising initiator, regarding $^1\text{H-NMR}$ analysis, as no overlapping of the initiator- with the polymer-signals occurs. Additionally, the efficacy of the termination with benzyl chloride can be determined as no signals of the initiator overlap with the aromatic signals of the quenching agent. Experiments with thiophenol also show that thiophenol/DBU can be used as initiator for the polymerization of episulfides. Under exclusion of oxygen a living ring-opening polymerization can be assumed with the $[\text{M}]:[\text{I}]$ ratio determining the final DP. In the presence of oxygen the active species is oxidized, leading to the dimerization of the polymers. Due to the thiol-disulfide exchange reaction, oxidized chains are not completely inactivated and the polymers can further propagate. The inactivated disulfide-species can exchange with the active chain end of other polymers, regaining the activity of the chain.

3.2.2.5. Polymerization with phenol/DBU

As was shown in the previous chapter, a terminal aromatic compound can be used to determine the number-average molar-mass M_n by $^1\text{H-NMR}$ spectroscopy. An advantage of phenol, in contrast to thiophenol, would be a more robust handling with respect to oxidation and introduction of disulfides by the initiator. Additionally, the unpleasant odor could be diminished. For the polymerization, the different reactivity of the phenolate anion (alkoxide species), compared to the thiolate, has to be investigated. As the fast initiation is commonly required for narrow molar-mass distributions, especially SEC-analytics should indicate the suitability of the initiator. The polymerization was performed with the same protocol as with the thiolate-initiated polymerization with $[\text{M}]:[\text{I}] = 15:1$.

The $^1\text{H-NMR}$ spectrum was recorded in order to use the initiator as reference for the determination of DP and M_n . Under the assumption that benzyl chloride and phenol were quantitatively introduced at the termini, the aromatic signals were used as reference with $l = 10$. A DP of 68 was obtained from the $^1\text{H-NMR}$ spectrum. The high viscosity of the product already indicated a higher DP than expected and determined by $^1\text{H-NMR}$ spectroscopy.

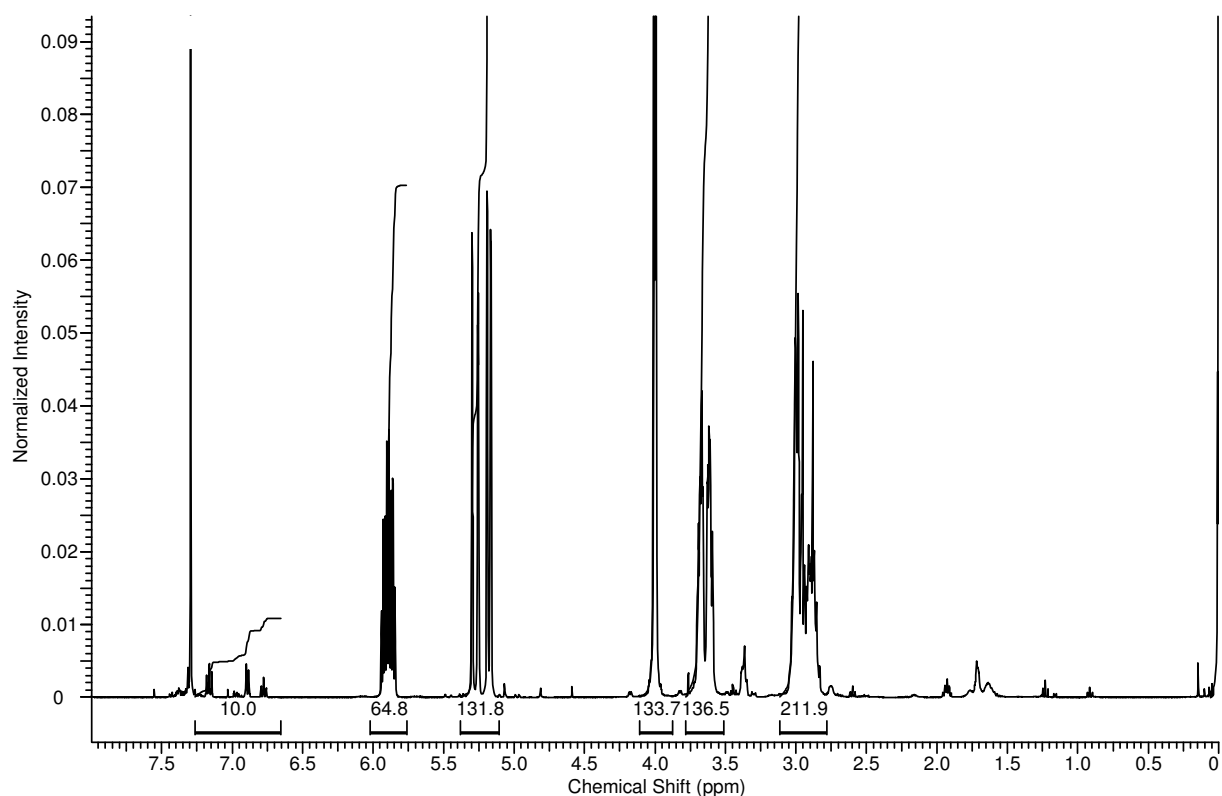


Figure 93: $^1\text{H-NMR}$ of poly(allyl thioglycidyl ether) initiated with phenol/DBU. A ratio of $[\text{M}]:[\text{I}]=15$ was used for the polymerization. The spectrum indicates a DP of 65.

The polymerization was performed using different $[\text{M}]:[\text{I}]$ ratios and the polymerizations are summarized in Table 11. For the reaction with DP = 15, DP = 30 and DP = 60 number-average molar masses of $M_n = 37000 \text{ g mol}^{-1}$ (Figure 94), $M_n = 35000 \text{ g mol}^{-1}$ and $M_n = 52000 \text{ g mol}^{-1}$ were obtained. Dispersities were high with values of $\mathcal{D} = 1.50\text{-}1.56$. Evaluation if a slow formation of the initiator is the reason for the broad molar-mass distribution and the high M_n , a longer preparation of the initiator was performed. Here the system phenol/DBU was stirred at RT for 2 h. The polymerization was performed at $0 \text{ }^\circ\text{C}$. Here, a number-average molar-mass of $M_n = 72000 \text{ g mol}^{-1}$ and $\mathcal{D} = 1.56$ was obtained. These values are too high in molar-mass and in dispersity, indicating that only a small portion of the initiator is active. Recalculation of the percentage of active species was performed for all experiments, assuming an accurate determination of the molar-mass by SEC and no termination reactions. As an example, the polymerization using $[\text{M}]:[\text{I}] = 30$ ($M_{\text{theory}} = 3966 \text{ g mol}^{-1}$) yielded a molar-mass of $M_n = 35000 \text{ g mol}^{-1}$, corresponding to a DP = 269. Assuming a living polymerization, after a successful initiation, only 11 % of the initial phenol/DBU was actively starting a

polymerization (Table 11). The initiation with phenol does not seem to be promising for synthesizing narrow-distributed poly(thioether)s, as neither the $[M]:[I]$ ratio reflects the final DP, nor dispersities can be defined as narrow.

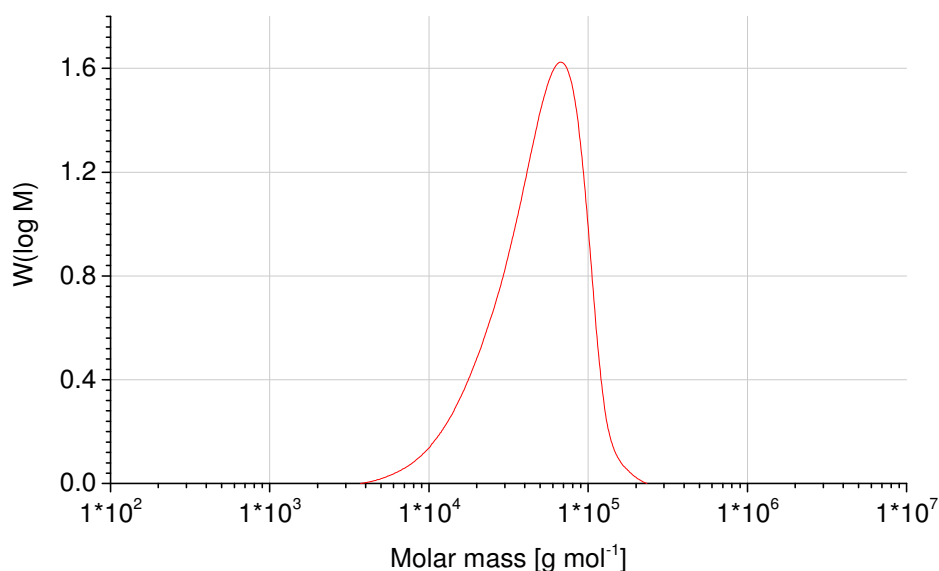


Figure 94: SEC-elugram of poly(ATGE) with $[M]:[I]=15$ initiated with phenol/DBU. A number-average molar mass of $M_n = 37000 \text{ g mol}^{-1}$ with a dispersity of $\bar{D} = 1.50$ was obtained.

Table 11: Overview of polymerizations of allyl thioglycidyl ether with phenol/DBU.

Number	$M_{n, \text{theo}}$ [g mol ⁻¹]	$M_{n, \text{GPC}}$ [g mol ⁻¹]	\bar{D}	Polymerization parameters	Active initiator (calculated)
MAK2	2000	37000	1.50	2h, RT	5 %
MAK4	4000	35000	1.56	2 h, RT	11 %
MAK3	8000	52000	1.51	2 h, RT	15 %
MAK8	2000	72000	1.56	Initiator: 2 h phenol/DBU, RT Polymerization: 2 h, 0 °C, then RT	3 %

3.2.2.6. Estimation of the disulfide-formation

Raman spectroscopy can be used to determine the presence of disulfide bonds in the products. As Raman spectroscopy is not quantitative, the quantification of the disulfide content is not possible. At $\nu = 509 \text{ cm}^{-1}$ disulfides can be observed, whereas at $\nu = 617 \text{ cm}^{-1}$ episulfides give a characteristic signal. In Figure 95 the Raman spectra of various polymers are depicted. As can be seen in some cases episulfides signals can still be observed. This can be ascribed to the high viscosity of some polymeric samples that do not run to completion and hence still contain episulfides. In no polymer analyzed via Raman spectroscopy a hint for disulfide formation can be found. The polymers used for Raman spectroscopy are listed in Table 12 with the following definition:

#	Table 12 (Entry)
1	9
2	10
3	11
4	12
5	4

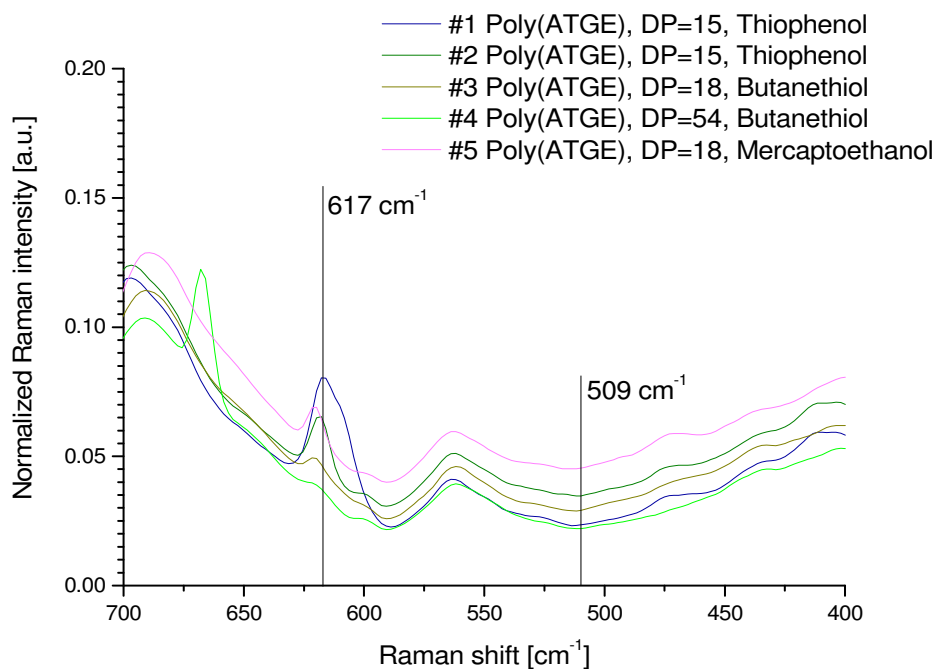


Figure 95: Raman-spectra of poly(allyl thioglycidyl ether)s polymerized with different thiols/DBU.

As most of the SEC curves show bimodality, the results from the Raman spectroscopy are not in accordance with the observations and theoretical considerations. This can either be explained by the low signal strength of disulfides or the overall content of disulfides in the polymeric samples. It is assumed that it is a combination of both effects. The signal intensity of a polymer is determined by all groups and hence sum up. To explain the considerations, a few things have to be assumed. If $DP = 18$, $1:36^{\text{th}}$ of the repeating units of a dimerized polymer are disulfides. If 10 % of all polymers are oxidized, only $1:360^{\text{th}}$ of the signals intensity is left. If the signal intensity of disulfides is not intense, the signal is probably superimposed by the large intensity of other functional groups. It is therefore assumed that Raman-spectroscopy is not a valid method to confirm the presence of disulfides.

Table 12: Polymerizations of EETGE and ATGE performed with various initiators and terminating agents.

#	Initiator	Monomer	Terminating agent	$M_c^a)$ [g mol ⁻¹]	$M_{n,SEC}^b)$ [g mol ⁻¹]	$DP_c^c)$	$DP_{NMR}^d)$	$DP_{SEC}^e)$	M_w/M_n	Modality (SEC)	Episulfides (Raman)	Disulfides (Raman)
1	HOEtSH	ATGE	BzCl	8495	9200	64	37	71	1.18	bimodal	n.d.	n.d.
2	HOEtSH	ATGE	BzCl	8215	7800	63	60	58	1.11	bimodal	n.d.	n.d.
3	HOEtSH	EETGE	BzCl	9783	6700	66	50	48	1.11	bimodal	n.d.	n.d.
4	HOEtSH	EETGE	mPEG480Ac	3000	2300	17	13	12	1.16	Slightly bimodal	n.d.	n.d.
5	HOEtSH	EETGE	MeAc	8831	8200	59	42	55	1.07	bimodal	n.d.	n.d.
6	HOEtSH	ATGE/ EETGE	BzCl	9038	9000	65	53	65	1.21	bimodal	n.d.	n.d.
7	DTT	EETGE	BzCl	9528	10400	2x31	n.d.	2x34	1.12	Slightly bimodal	n.d.	n.d.
8	HOEtSH	EETGE	mPEG480Ac	2080	2800	11	12	15	1.08	monomodal	n.d.	n.d.
9	Thiophenol	ATGE	BzCl	1953	1900	15	18	15	1.10	Shoulder	Yes	No

a) Calculated, b) Number-average molar mass determined by SEC in THF with PS as calibration standard, c) calculated DP d) DP determined by NMR, e) DP determined by SEC

#	Initiator	Monomer	Terminating agent	$M_c^{a)}$ [g mol ⁻¹]	$M_{n,SEC}^{b)}$ [g mol ⁻¹]	DP _c ^{c)}	DP _{NMR} ^{d)}	DP _{SEC} ^{e)}	M_w/M_n	Modality (SEC)	Episulfides (Raman)	Disulfides (Raman)
10	Thiophenol	ATGE	BzCl	1953	2200	15	20	17	1.13	Shoulder	Yes	No
11	Butanethiol	ATGE	BzCl	2344	4800	18	37	36	1.10	Slightly bimodal	Slightly	No
12	Butanethiol	ATGE	BzCl	7031	7700	54	53	59	1.22	Slightly bimodal	No	no
13	Butanethiol	ATGE	BzCl	2343	2300	18	16	18	1.10	monomodal	n.d.	n.d.
14	Butanethiol	EETGE	BzCl	5030	6300	31	31	39	1.13	monomodal	n.d.	n.d.
15	Butanethiol	ATGE/ EETGE	BzCl	4567	6500	30	29	32	1.24	bimodal $\Delta RI(\text{dimer}) >$ $\Delta RI(\text{polymer})$	n.d.	n.d.

a) Calculated, b) Number-average molar mass determined by SEC in THF with PS as calibration standard, c) calculated DP d) DP determined by NMR, e) DP determined by SEC

3.2.3. Deprotection of the acetal-group

As all polymers were insoluble in water, the removal of the acetal-group was attempted by acidic hydrolysis. After cleavage of the acetal-group, the hydroxy-functional poly(thioether)s should be water soluble due to H-bond formation. First the stability of the poly(thioether) chain with poly(allyl thioglycidyl ether) was tested. The allyl-groups should be inert against the acidic hydrolysis as it is described in literature for the corresponding poly(glycidol)s.[62] Investigation of the molar-mass before and after treatment of poly(ATGE) with an acid gives insight on the stability of the thioether-backbone.

Poly(allyl thioglycidyl ether) with 36 repeating units (determined by SEC in THF with poly(styrene) as calibration standard) was dissolved in THF. Addition of hydrochloric acid and stirring at RT for 2 d was performed. The $^1\text{H-NMR}$ spectrum, after hydrochloric acid-treatment, showed no visible difference compared to the initial polymer. Using the terminal butanethiol moiety as reference, the M_n was determined by $^1\text{H-NMR}$ spectroscopy, but no significant difference could be observed. SEC-measurements after deprotection and determination of M_n showed a molar-mass of $M_n = 5000 \text{ g mol}^{-1}$. Before treatment with hydrochloric acid a M_n of 4700 g mol^{-1} was determined.

Poly(ethoxy ethyl thioglycidyl ether) was used to hydrolyze the acetal side-chains and obtain poly(thioglycidol). This was also performed in THF with aqueous hydrochloric acid. After 3 d a $^1\text{H-NMR}$ spectrum of the separated oily phase was recorded (Figure 96). At $\delta = 4.44 - 5.17 \text{ ppm}$ a broad singlet can be observed. This broad signal was assigned to the OH-group, showing that the polymer was deprotected. At $\delta = 3.44 - 3.77 \text{ ppm}$ the signal was assigned to the H^g -signal of the polymer further indicating an intact polymer. The polymer backbone (Figure 96, H^e , H^f) was determined to have a chemical shift of $\delta = 2.69 - 3.01 \text{ ppm}$ with an integral of $I = 72$ if the reference (initiator-signal, H^d) at $\delta = 2.56 - 2.69 \text{ ppm}$ is set to a value of $I = 2$. The terminal aromatic signals could not be observed, assuming that a cleavage of the terminal group occurred. It is interesting to note that the polymer is insoluble in water. Although a high water-solubility was assumed for the poly(thioether)-polyol only DMSO was able to dissolve the homopolymer poly(thioglycidol). Due to the lack of analytics no SEC elugram could be recorded.

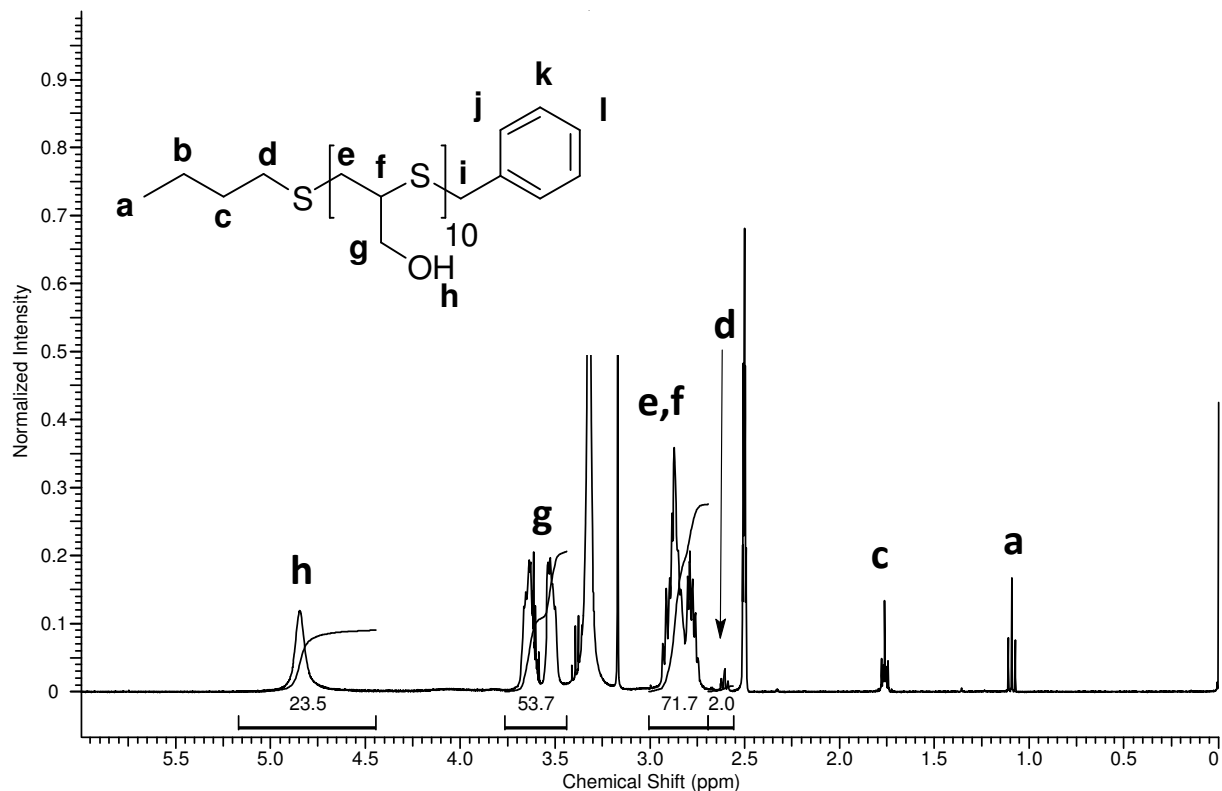


Figure 96: ^1H -NMR spectrum in $\text{DMSO-}d_6$ of poly(thioglycidol) obtained by hydrolysis of poly(ethoxy ethyl thioglycidyl ether) with hydrochloric acid in THF.

Rendering the water-solubility of the polymer, a block-copolymer of poly(thioglycidol)-*block*-poly(ethylene glycol) was attempted. This was aimed using the butanethiolate-initiated polymerization of EETGE and quenching the reaction with mPEG480-acrylate. The Michael-addition of the thiolate to the acrylate, as a Michael acceptor, couples both polymers. The symmetric block-copolymer poly(ethoxy ethyl thioglycidyl ether)-*block*-poly(ethylene glycol) with 10 thioether- and 10 ethylene glycol repeating units was treated with hydrochloric acid in THF. The ^1H -NMR spectrum of the block-copolymer is shown in Figure 97. Here the OH-functionality can be observed at $\delta = 4.81 - 4.95$ ppm. As the side-chain methylene-group splits at $\delta = 3.58 - 3.72$ ppm the CH_2 -group can be observed although the integral is only half of the expected. The other half of the signal is overlapped by the backbone signal of the ethylene glycol chain at $\delta = 3.46 - 3.58$ ppm. The reference signal for the determination of the intact backbone was the terminal CH_3 -group of the methoxy group of the poly(ethylene glycol) chain, assigned to the signal at $\delta = 3.22 - 3.27$ ppm (Figure 97, H^m).

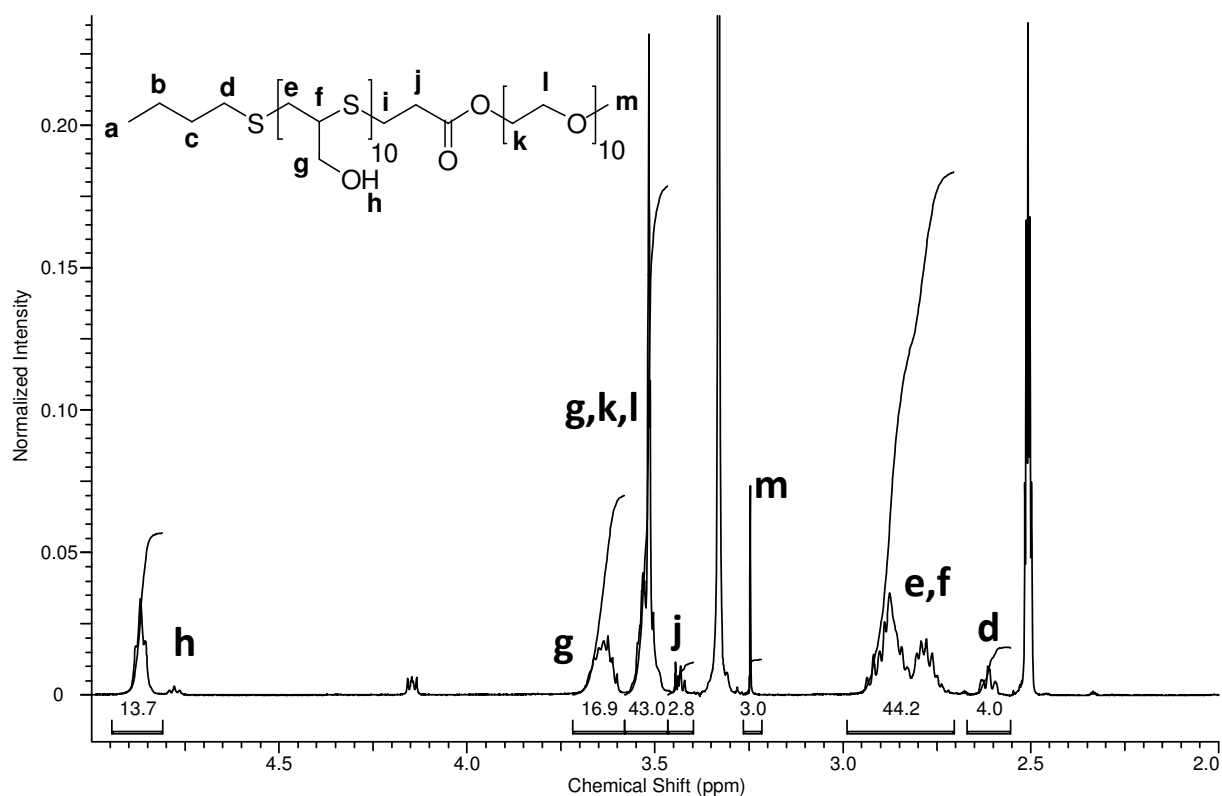


Figure 97: ^1H -NMR spectrum of poly(thioglycidol)-*block*-poly(ethylene glycol) in $\text{DMSO-}d_6$.

The poly(thioglycidol) backbone signals (3H) was identified as the broad signal at $\delta = 2.70 - 2.99$ ppm ($\text{H}^{e,f}$) corresponding to a DP of 10. The signal of the CH_2 -group of the initiator in vicinity to the thioether-unit was assigned to the signal at $\delta = 2.56 - 2.66$ ppm (H^d). The integration of the poly(ethylene glycol) region shows an integral of $I = 43$. With the overlapping signals of the methylene side-chain an integral of $I = 60$ was expected. This difference was assigned to a possible hydrolysis of the ester-bond connecting poly(ethylene glycol) with poly(thioglycidol).

SEC-analysis (Figure 98) of the protected copolymer, the block-copolymer after 18 h hydrolysis and the completely hydrolyzed polymer does not confirm this assumption. The SEC elugram of the protected poly(ethoxy ethyl thioglycidol)-*block*-poly(ethylene glycol) shows a monomodal distribution, whereas the partially acetal-deprotected polymer shows a bimodal distribution in the SEC elugram (Figure 98). The smaller fraction of this bimodal distribution was assigned to the unprotected copolymer. The ^1H -NMR spectrum (Figure 99) confirms the partial hydrolysis as the acetal-group is still present as indicated by the triplet and dublett at $\delta = 1.2$ and 1.1 ppm. Finally after a complete hydrolysis of the acetal-groups a monomodal elugram is observed indicating a fully deprotected poly(thioglycidol)-*block*-

poly(ethylene glycol). The assumption that the ester was cleaved and a mixture of the copolymer with PEG is present in the sample could not be confirmed, as no polymer signal was detected that could be assigned to PEG with $M_n = 480 \text{ g mol}^{-1}$.

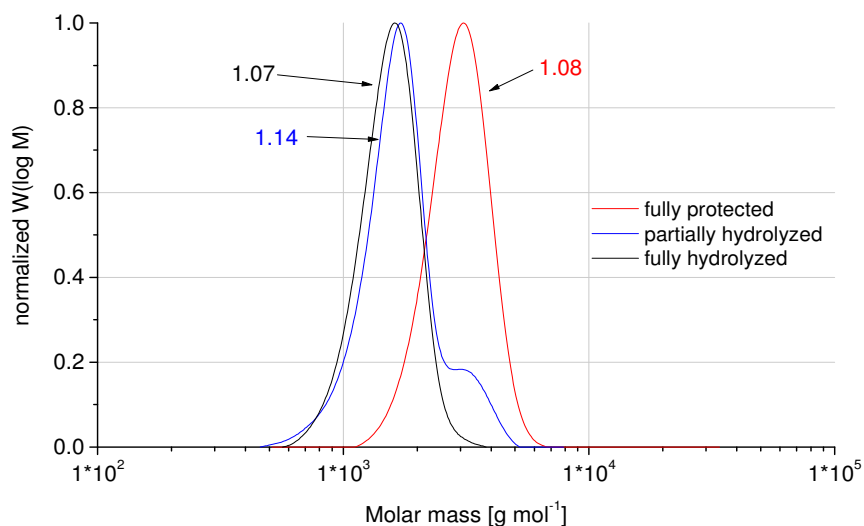


Figure 98: SEC-elugram of fully protected poly(EETGE)-*block*-poly(ethylene glycol) (red), after partial deprotection (blue) and fully deprotected poly(thioglycidol)-*block*-poly(ethylene glycol) (black).

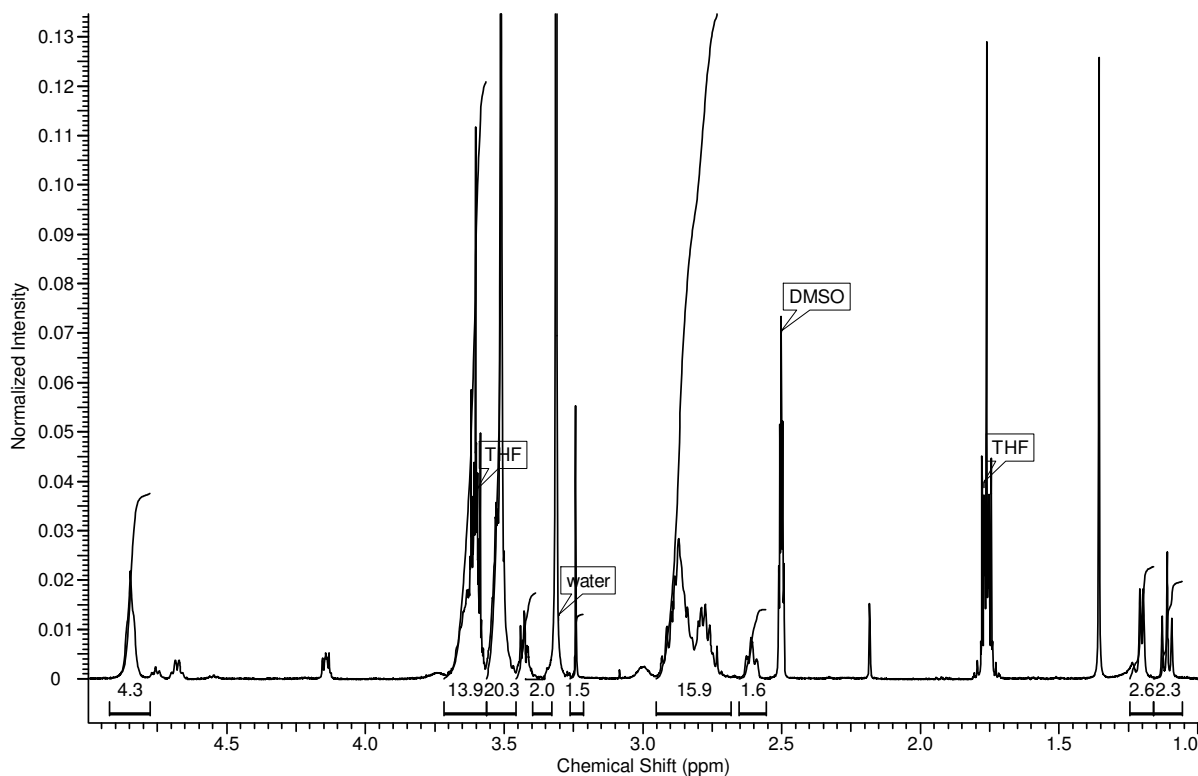


Figure 99: ¹H-NMR spectrum of partially hydrolyzed poly(ethoxy ethyl thioglycidol ether)-*block*-poly(ethylene glycol) showing residual acetal-signals at $\delta = 1.20$ and 1.10 ppm.

3.2.4. Particle formation

The turbidity of the aqueous solutions of the poly(thioglycidol)-*block*-poly(ethylene glycol) indicated an unexpected insolubility of the block-copolymer in water and implied a particle formation. The solutions were analyzed by using cryo-SEM, performed at the DWI in Aachen by Smriti Singh, and DLS measurements. In Figure 100 particles can be observed. Determination of the diameter was performed using different magnifications and manually measuring the size. For this, 9 particles were chosen from Figure 100(A), magnification 70000x, and 18 particles of Figure 100(B), magnification 25000x. An average diameter of the particles of $d = 55 \pm 9$ nm for the higher magnification was obtained. Figure 100 (B) gives a diameter of $d = 75 \pm 36$ nm. As the accuracy of the lower magnification is limited, the standard deviation is higher. For the higher magnification a better determination of the size can be obtained, although the quantity of particles is diminished as the area of the picture is reduced. With both pictures an average diameter of $d = 65 \pm 23$ nm was obtained. Confirmation of these results was attempted using dynamic light scattering (DLS). The hydrodynamic diameter was determined to be $d_h = 83$ nm with a polydispersity of PDI = 0.7 using the volume distribution. Upon changing the mode of the DLS to the intensity distribution, the main fraction of the particles was determined to be at $d_h = 2.5$ nm. This means that the main fractions of the solution are single polymers. The polymers usually have a small scattering intensity and the scattering intensity of particles is in orders of magnitudes higher.

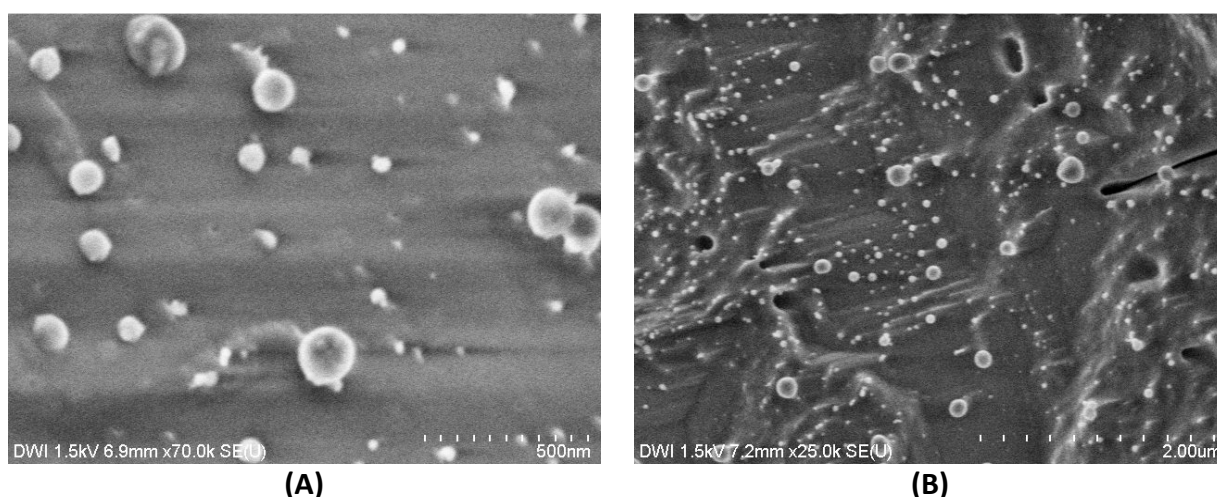


Figure 100: Cryo-SEM pictures of poly(thioglycidol)-*block*-poly(ethylene glycol) in aqueous solution at (A) 70000x magnification and (B) 25000x.

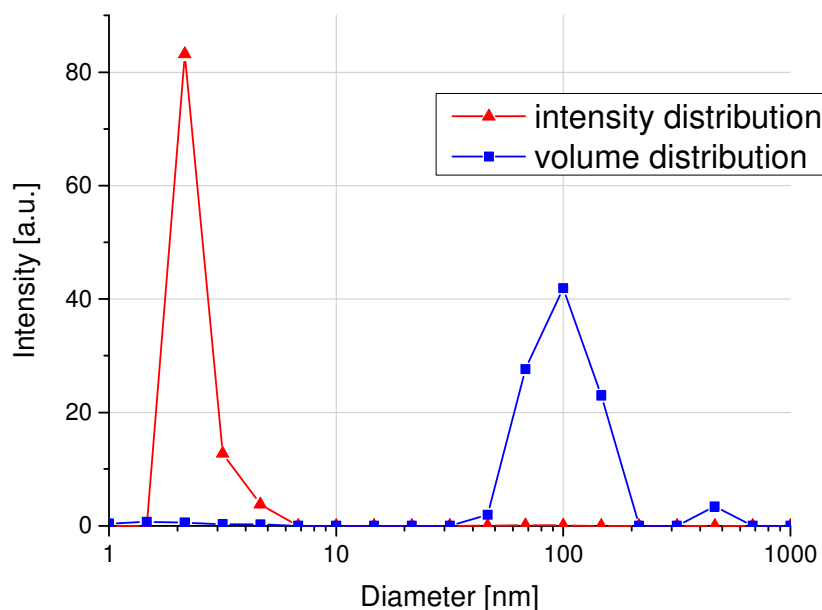


Figure 101: DLS measurement of self-assembled poly(thioglycidol)-*block*-poly(ethylene glycol) particles in aqueous solution.

The scattering intensity is higher with diameters in the polymeric region than for diameters of approximately $d = 83$ nm as expected for the particles. This means that the number of particles is small compared to the number of polymers dissolved in the solution. The calculation of the volume distribution by the DLS software shows, that the volume occupied by the particles in solution is higher than the volume occupied by the polymers.

Although the particles observed by cryo-SEM were confirmed by DLS measurements, the main scattering intensity was probably originated by the polymers dissolved in the solution. Nonetheless the limited solubility of poly(thioglycidol) in aqueous solution is further confirmed by the self-assembly of the amphiphilic poly(thioglycidol)-*block*-poly(ethylene glycol) copolymers, in which the poly(thioglycidol) represents the hydrophobic part.

3.3. *Synthesis of cysteine-functional poly(glycidol)s*

Side-chain functionalization of homo- and copolymeric poly(glycidol)(-derivatives) allows the tailor-made adoption of poly(glycidol)s, synthesized in chapter 3.1, to specific applications. In this chapter poly(glycidol) homopolymers and poly(glycidol-*stat*-allyl glycidyl ether) copolymers are functionalized with thiol-, amine-, carboxy- and cysteine-groups. Fast and efficient thiol-ene chemistry allows a complete allyl-group conversion orthogonal to OH-functional side-chains. Hence the copolymer composition predetermines the final content of SH-, NH₂-, COOH- and cysteine-groups by the fraction of allyl-groups. Furthermore the accessibility of the cysteine-residues is investigated using Native Chemical Ligation of C-terminal thioester peptides as model compound.

Parts of this chapter were already published in

M. Kuhlmann, O. Reimann, C.P.R. Hackenberger, J. Groll, Cysteine-Functional Polymers via Thiol-ene Conjugation, *Macromolecular Rapid Communications*, 36 (2015) 472-476.

This work was performed in cooperation with the group of Christian P. R. Hackenberger at Department Chemical Biology II, Leibniz-Institut für Molekulare Pharmakologie (FMP) in Berlin and Humboldt Universität zu Berlin, Department Chemie, Berlin. Oliver Reimann at the aforementioned institute performed the peptide synthesis, NCL experiments as well as MALDI-ToF and HPLC measurements. These parts are marked with a hash (#).

3.3.1. Thiazolidine formation

3.3.1.1. General

Synthesis of the 2,2,-disubstituted thiazolidines was directly accomplished by stirring acetone with cysteine. The ^1H -NMR spectrum in Figure 102 was recorded in $\text{DMSO-}d_6$ and clearly shows the signal of H^c at 4.81 - 4.98 ppm, H^b at 3.33 - 3.63 ppm and H^a at 1.61 - 1.86 ppm.

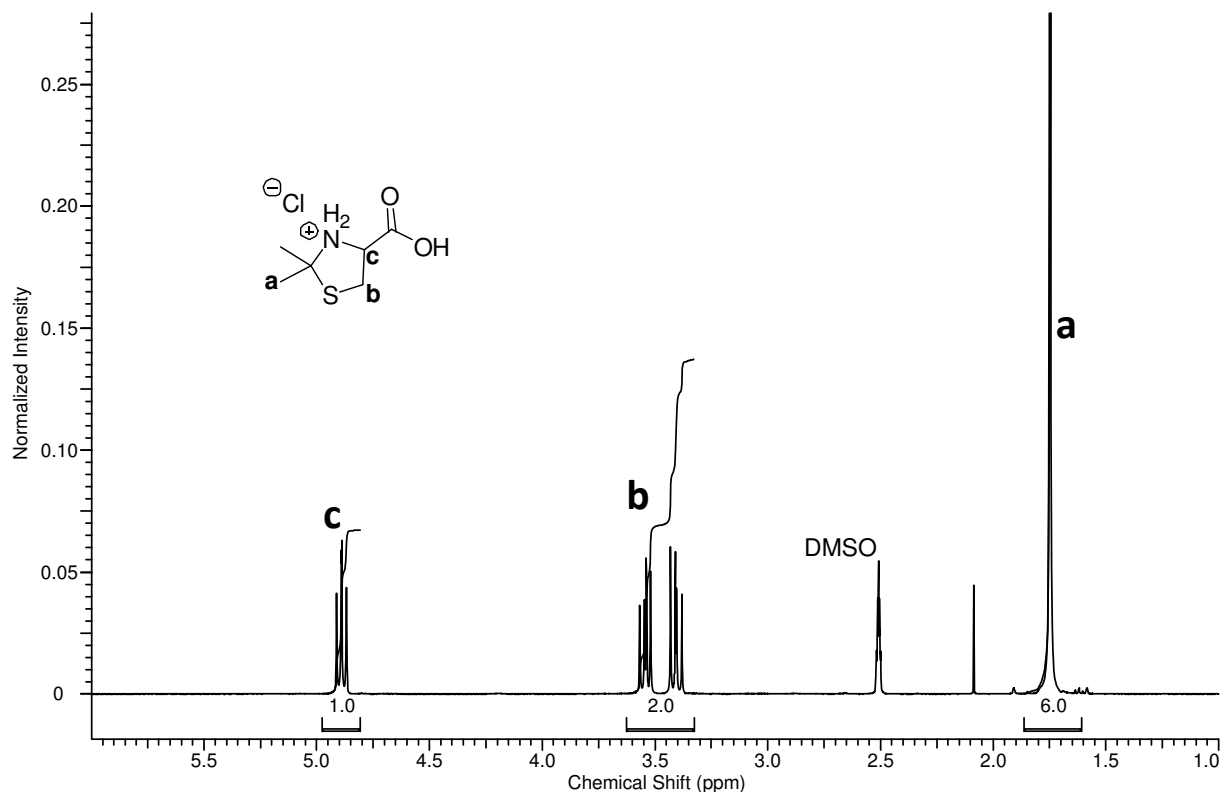


Figure 102: ^1H NMR spectrum of 2,2-dimethylthiazolidine-4-carboxylic acid.

Integration of the signals indicates no detectable impurities, overlapping with the identified signals, as the ratio $\text{H}^a:\text{H}^b:\text{H}^c = 6:2:1$ was matches the theoretical number of protons. A broad singlet at $\delta = 13 - 9.5$ ppm was determined to result from the two H-atoms bound to the amine forming the corresponding hydrochloric salt of the thiazolidine. As the functionalization of the thiazolidine for polyglycidol-modification will be executed via the carboxylic acid, the ring-amine had to be protected to avoid a coupling of the thiazolidine-amine with the activated carboxylic group. A formyl-group was chosen as the protective group. Deprotection of the thiazolidine-ring, after a potentially successful polymer-analog functionalization, has to be performed and hydrolyzed thiazolidine-rings will bear the α - β -

aminothiol, rendering the polymer sensitive towards oxidation. As the oxidation occurs under neutral to basic conditions, an acidic deprotection protocol was attempted. Additionally, polymer-analog reactions close to the backbone of polymer are sterically demanding making an acidic cleavable amine-protection most promising. The formyl-group represents the smallest possible amine-group that is cleaved under acidic conditions as well. For this the 2,2-dimethyl-thiazolidine-4-carboxylic acid was dissolved in a mixture of formic acid and sodium formate. Upon addition of acetic acid anhydride the mixed anhydride forms and results in a formylation of the amine-group. Recrystallized white powder was analyzed via $^1\text{H-NMR}$ spectroscopy and showed the expected signals that split. At $\delta = 13$ ppm the proton of the carboxylic acid H^e can be observed as a broad singlet. The aldehyde signals H^a shows a splitting, giving a singlet at $\delta = 8.41$ ppm and 8.23 ppm, as well as the H^d at 5.05 and 4.83 ppm. CH_3 -signals of the thiazolidine-ring also show a 70:30 ratio of both signals with a chemical shift of $\delta = 1.76$ and 1.74 ppm. Splitting of the signals is already known in literature for pseudo-proline (Ψ -proline) and oxazolidines.[149, 150] Confirmed by x-ray analysis of a single crystal the compound was successfully synthesized and reveals the (*R*)-configured *N*-formylated thiazolidine (Figure 104).

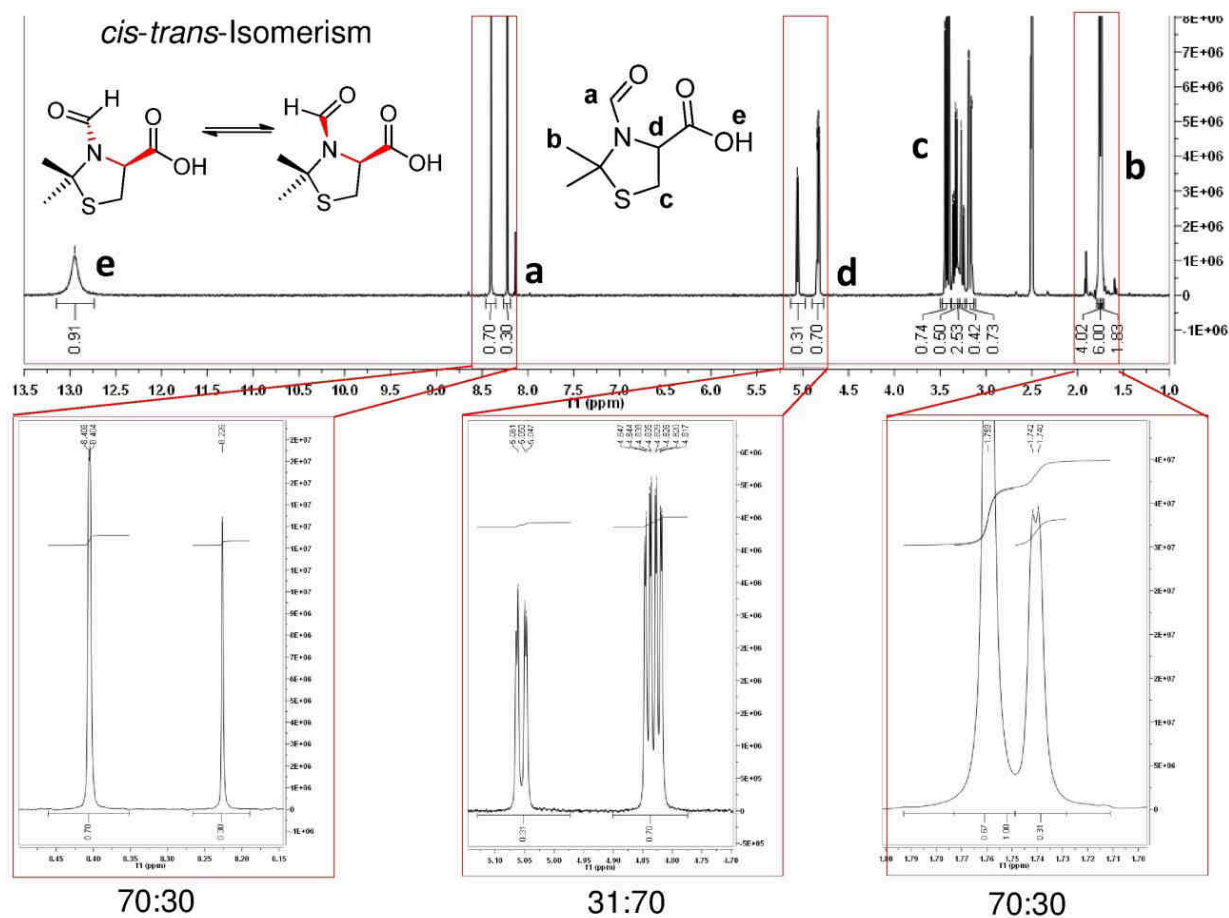


Figure 103: $^1\text{H-NMR}$ signals showing the *cis*-/*trans* splitting of the signals of formylated 2,2-dimethylthiazolidine-4-carboxylic acid.

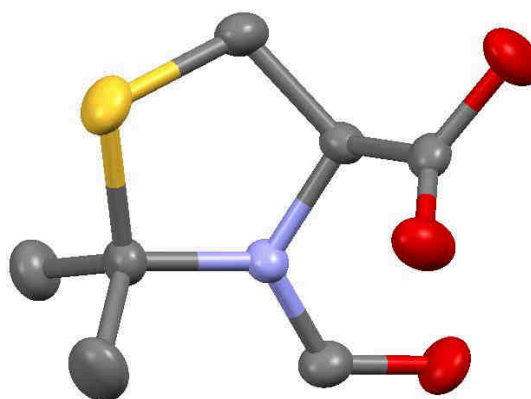
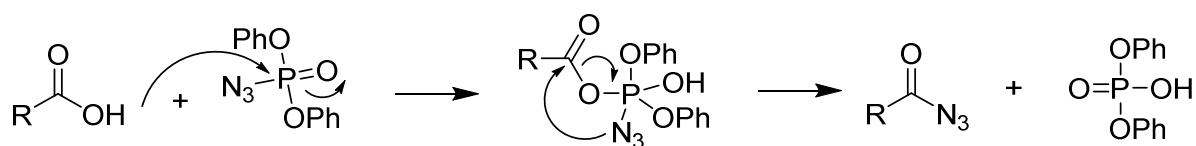


Figure 104: X-ray crystal structure of formylated 2,2-dimethyl-thiazolidine-4-carboxylic acid.

3.3.1.2. Isocyanate-functional thiazolidine

Formylated thiazolidine could directly be used for an esterification reaction with the polyol poly(glycidol). As the acidic hydrolysis of the thiazolidine-ring would probably cleave the ester-bond a more stable link between thiazolidine and poly(glycidol) is necessary. A more stable carbamate-bond can be introduced by the reaction between an isocyanate and a hydroxy-group. Isocyanate-functionalization of the formylated thiazolidine was hence attempted. Thiazolidine-functionalization via a stable carbamate-bond and subsequent hydrolysis of the thiazolidines would lead to cysteine-functional poly(glycidol). For this the Curtius rearrangement was used. Here the carboxyl-functionality of the thiazolidine was derivatized with an azide that undergoes a Curtius rearrangement under heat. Hydrolyzable isocyanates-thiazolidines can be isolated under anhydrous conditions. Diphenylphosphoryl azide (DPPA) is a commercially available compound allowing a direct and easy synthesis of the corresponding acyl azides (Scheme 27).[151]



Scheme 27: Formation of an acyl azide using DPPA.

The synthesized acyl azides undergo a rearrangement under N₂ release upon thermal treatment. Mechanistically, the release of the N₂ and the rearrangement are concerted as no nitrene was detectable as already described in 1969.[152] For the synthesis of the thiazolidine-isocyanate, the corresponding formylated 2,2-dimethyl-thiazolidine-4-carboxylic acid was treated with DPPA in DMF at RT. Deprotonation of the carboxylic acid was achieved using triethylamine as was described in literature for this type of reaction.[153] Stirring the solution overnight and removing all volatile components yielded the raw product. Attempts to extract the compound with CHCl₃ and remove the impurities with H₂O-washing failed, as the ¹H-NMR spectra always showed residual aromatic impurities. Thin-layer chromatography (tlc) with silica was used to evaluate the amounts of compounds in the mixture. Staining of the tlc plate was obtained using iodine vapor or uv-light with λ = 254 nm (for aromatic compounds). EtOAc:hexane = 1:2 as mobile phase yielded the desired product with a value of R_f = 0.17 and R_f = 0.68 for the aromatic impurity. Column chromatography was performed

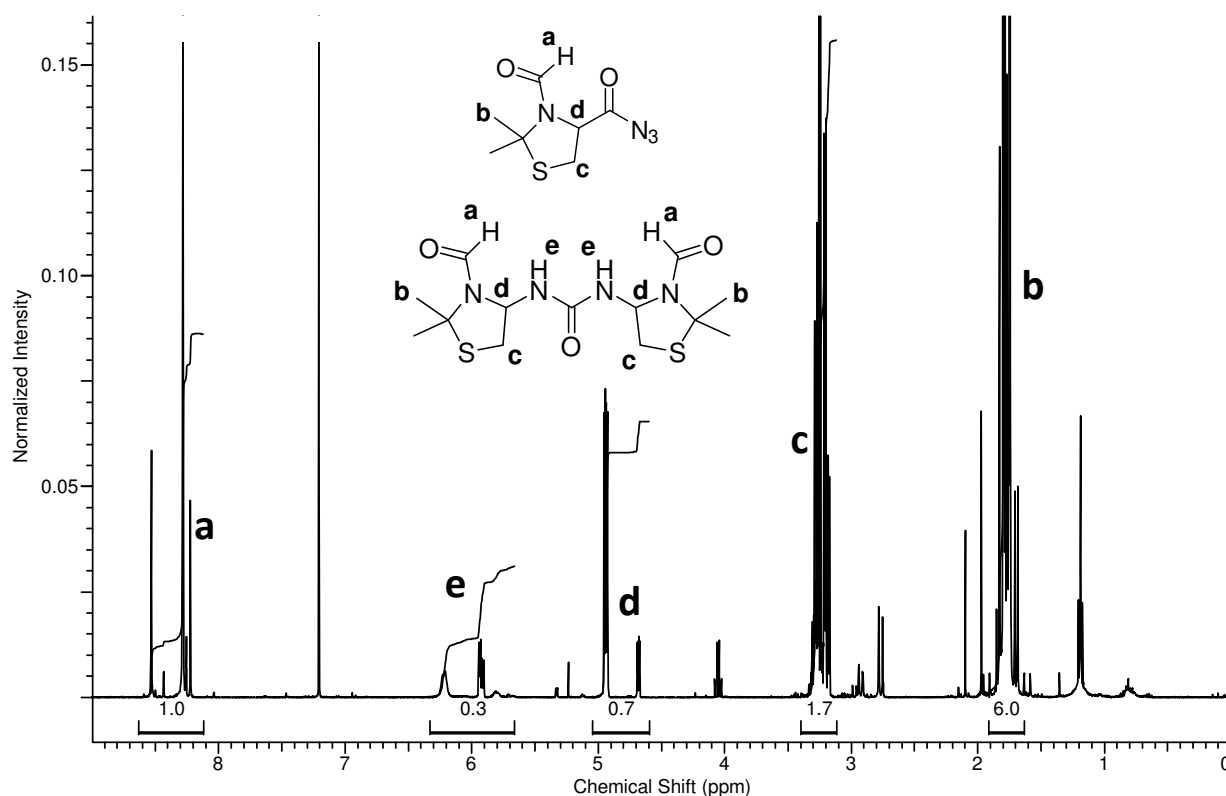
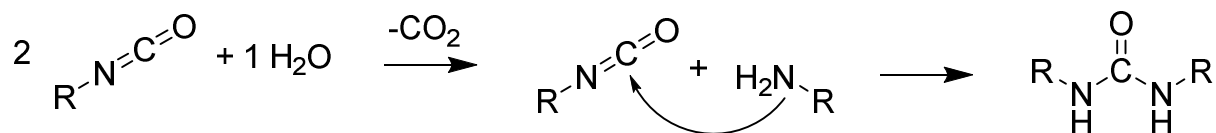


Figure 105: ^1H -NMR spectrum of acyl azide derivatized thiazolidine.

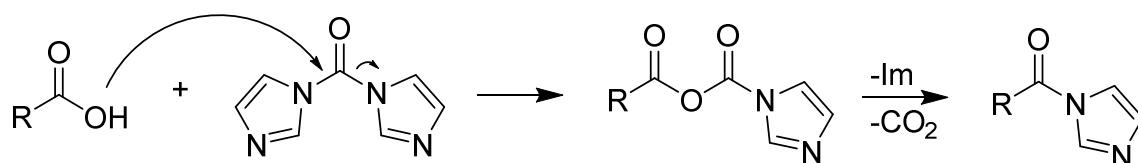
to separate the aromatic fraction from the desired product. Acyl azide-functionalized thiazolidine was analyzed by ^1H -NMR spectroscopy and is shown in Figure 105. Formyl-H H^{a} was assigned to the signal at $\delta = 8.25 - 8.5$ ppm. The strong electron withdrawing effect of the acyl azide group shifts the CH-signal downfield and assigned to the signal H^{d} at $\delta = 4.9 - 4.6$ ppm. CH_3 -signals at the thiazolidine ring were identified as the signals H^{b} at $\delta = 1.75$ ppm. Residual ethyl acetate was detected at $\delta = 2.05$ ppm (singlet), 4.1 ppm (quartet) and a triplet at 1.24 ppm. CH_2 -ring signals H^{c} were identified at $\delta = 3.25$ ppm. This leads to the assumption that the thiazolidine is intact and is not disturbed by the derivatization of the carboxylic acid to the corresponding acyl azide. But it is assumed, that a partial Curtius rearrangement and hydrolysis of the isocyanate occurred, as the signals at $\delta = 6.25 - 5.8$ ppm were assigned to amide-H signals H^{e} . The partial hydrolysis of the product leads to a carbamic acid that decarboxylates to the corresponding amine, able to attack a further isocyanate building a urea-bond (Scheme 28). Synthesized isocyanate-functional thiazolidine was used for polymer-analog functionalization of the poly(glycidol) homopolymer.



Scheme 28: Hydrolysis of isocyanates and the subsequent formation of a urea bond, dimerizing the initial isocyanate-moieties.

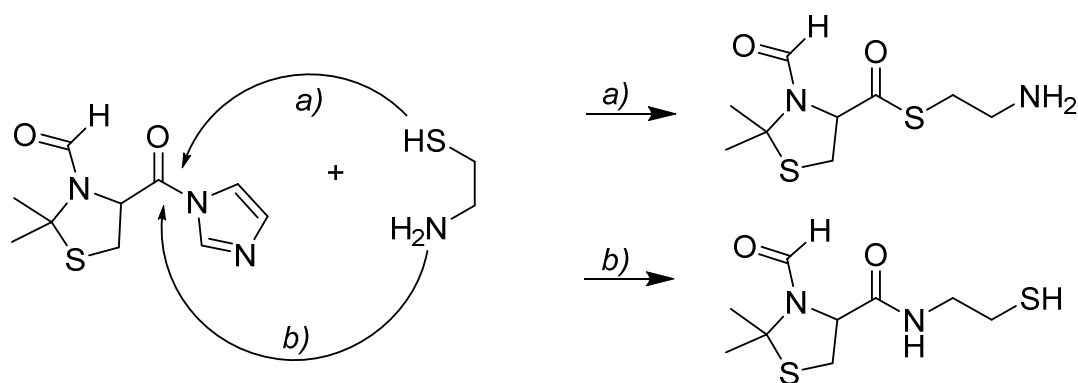
3.3.1.3. Thiol-functional thiazolidine

The carboxyl-group was attempted to be activated with activating agents. Usually carboxylic acid groups are less reactive towards nucleophiles e. g. amines. Activation of carboxylic acids can be performed by transformation of these to their halides or active esters. Carbodiimide-activated amide-formation is commonly performed in peptide-synthesis, but initial formed *o*-acylisoureas can easily be hydrolyzed by the aqueous environment. Water-soluble sulfo-NHS or NHS is added to prevent this hydrolysis and give activated esters. *N,N'*-Carbonyldiimidazol is an alternative zero-length approach for the linkage of carboxylic acids and amines. A pronounced advantage of the CDI-method is the high driving force of the reaction as CO₂ is formed. Unfortunately, hydrolysis in H₂O is even more pronounced.[154]



Scheme 29: Carboxyl acid activation with CDI under formation of the imidazol-amide.

Activated imidazole-amide was reacted with cysteamine in pyridine in situ. Degassed pyridine is used as solvent to deprotonate the commercially available cysteamine hydrochloric salt. Double-nucleophilic cysteamine is able to attack the imidazole-amide with the amine and with the thiol, producing a mixture of path a) and path b) shown in Scheme 30.



Scheme 30: Imidazol-amide of the formylated-thiazolidine reacts either with the thiols of cysteamine or via the cysteamine amine.

As it is known in literature, and is especially a key step in Native Chemical Ligation, the formed amine-functional thioester is able to perform a N→S acyl shift and form the more stable thiol-functional thiazolidine. The shift is reversible, but requires synthetic methods that usually deal with an excess of the desired thiol moiety.[155-157] An excess of the thiol moiety is not used as cysteamine is equipped with a 1:1-ratio of both functional groups. For the synthesis, the cysteamine/thiazolidine-imidazol amide solution, in a mixture of DMF/pyridine, was stirred at RT overnight. Removal of all volatile components and extraction of an acidified aqueous solution with CHCl_3 yielded a white residue that could be recrystallized in ethyl acetate yielding white fine needles. HRMS showed $m/z = 249.0694$ $[\text{M}+\text{H}]^+$ (calculated $m/z = 249.0736$).

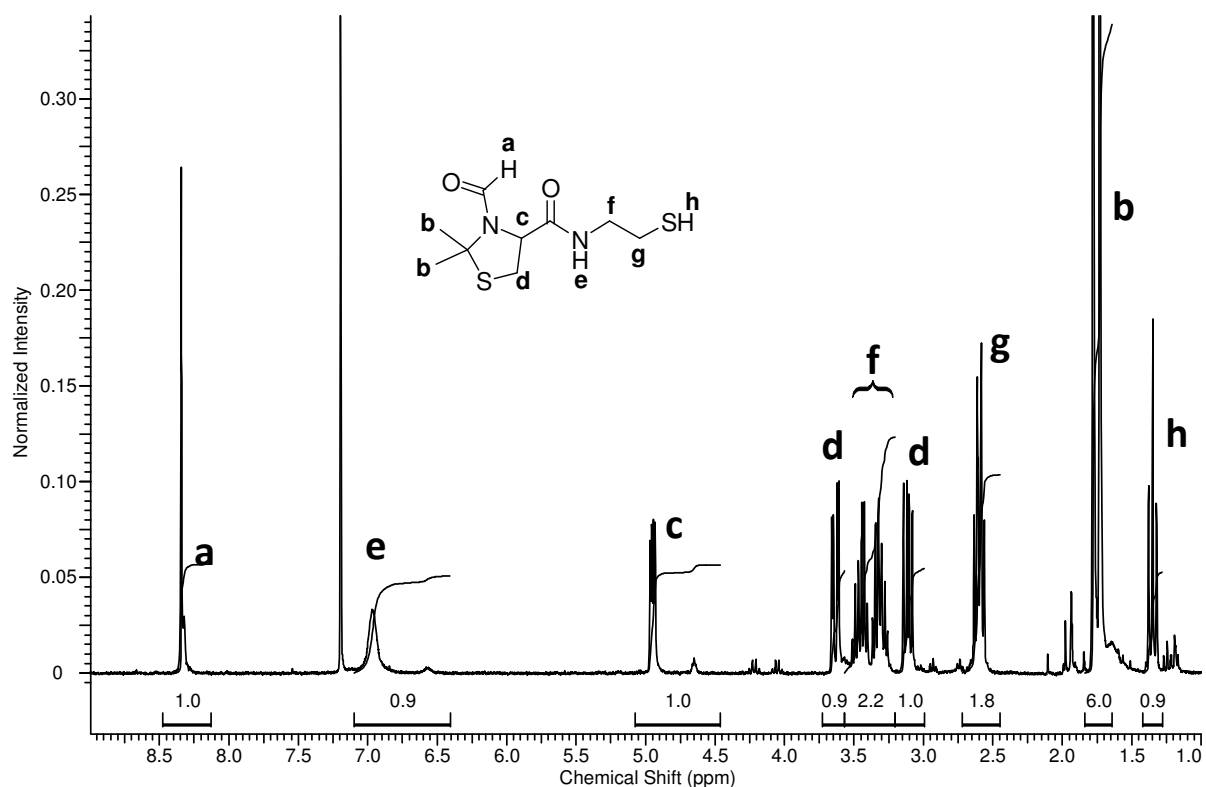


Figure 106: ^1H -NMR spectrum of 3-formyl-N-(2-mercaptoethyl)-2,2-dimethylthiazolidine-4-carboxamide (mercaptothiazolidine).

^1H -NMR spectrum was recorded, showing an intact ring system with the protective group at $\delta = 8.13 - 8.48$ ppm, H^{a} , as well as the CH_3 -groups H^{b} at $\delta = 1.75$ ppm. Newly formed amide-signal H^{e} was detected at $\delta = 7.0 - 6.6$ ppm with a splitting due to the *cis* and *trans*-isomers (discussed in 3.3.1.1). The CH_2 group, H^{d} , of the thiazolidine-ring can be observed at $\delta = 3.57 - 3.72$ ppm and $\delta = 2.99 - 3.20$ ppm. H^{f} was detected at $\delta = 3.20 - 3.57$ ppm, whereas H^{g} was determined to be at $\delta = 2.45 - 2.72$ ppm. Data given in literature matches well with the thiol detected as a triplet at $\delta = 1.28 - 1.42$ ppm. Thiol-H-coupling with the H^{g} signal has a coupling constant of $^3J = 8.1$ Hz.[158] ^1H -signal assignment was further proven with ^{13}C -NMR spectroscopy and a recorded HSQC spectrum. For confirming the thiol-functionalization, Raman spectroscopy was performed. In contrast to IR spectroscopy the signal strength of thiols and disulfides is intense and allows the qualitative detection of both groups. Figure 107 depicts the recorded Raman spectrum. A clear valence vibration signal at $\nu = 2537$ cm^{-1} can be detected that is typical for thiol-functionalities. Interestingly, no signal at 508 cm^{-1} can be observed indicating a non-detectable quantity of disulfides. In Raman spectrum both, amide and carbonyl, signals are detectable at $\nu = 1690$ cm^{-1} and $\nu = 1638$ cm^{-1} , respectively.

This further confirms the functionalization of the formylated thiazolidine-ring with cysteamine.

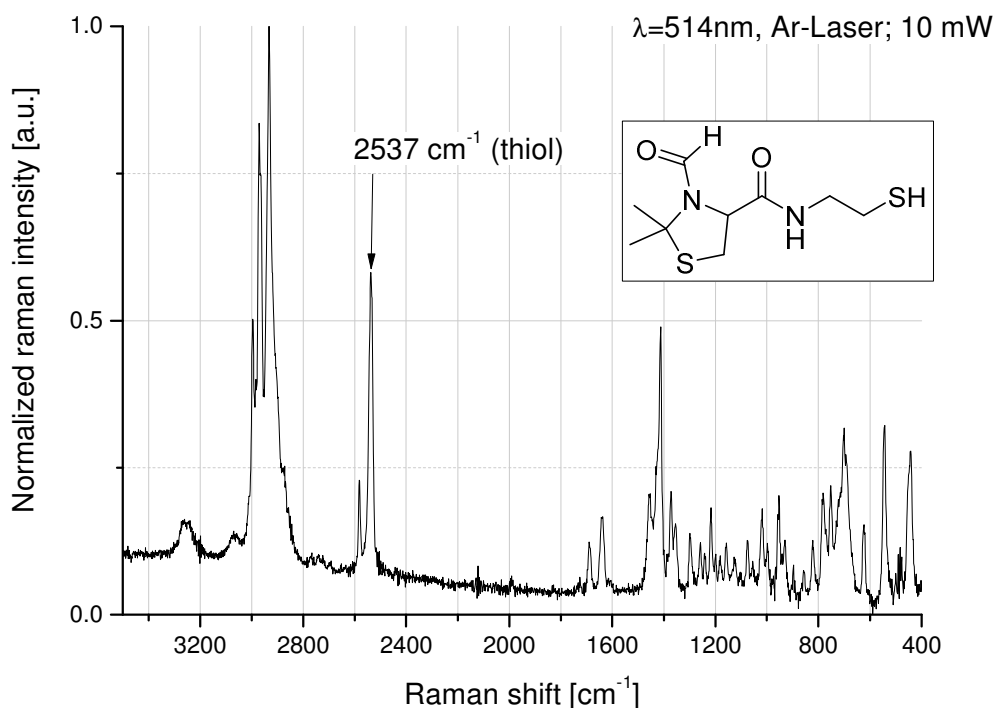


Figure 107: Raman spectrum of mercaptothiazolidine, showing a strong thiol signal at 2537 cm⁻¹, but no disulfides at 508 cm⁻¹.

3.3.2. Polymer-analog functionalization via isocyanates

The reaction between alcohols and isocyanates yields carbamates that are highly stable. For this a isocyanate was synthesized as was described in the previous chapter. To obtain a fast kinetics catalysts are added, such as organo-tin compounds.[159, 160] Here poly(glycidol-*stat*-allyl glycidyl ether) was used as the polyol. Presence of allyl-functional groups was used as an internal reference for the determination of the efficiency. Acyl-azide synthesized in chapter 3.3.1.2, was dissolved in DMF and stirred for 1 h at 90 °C. The polymer, dissolved in DMF, was added subsequently and dibutyl tin dilaurate (DBTDL) was added and stirred at RT for 20 h. After workup, the product was analyzed via ¹H-NMR spectroscopy.

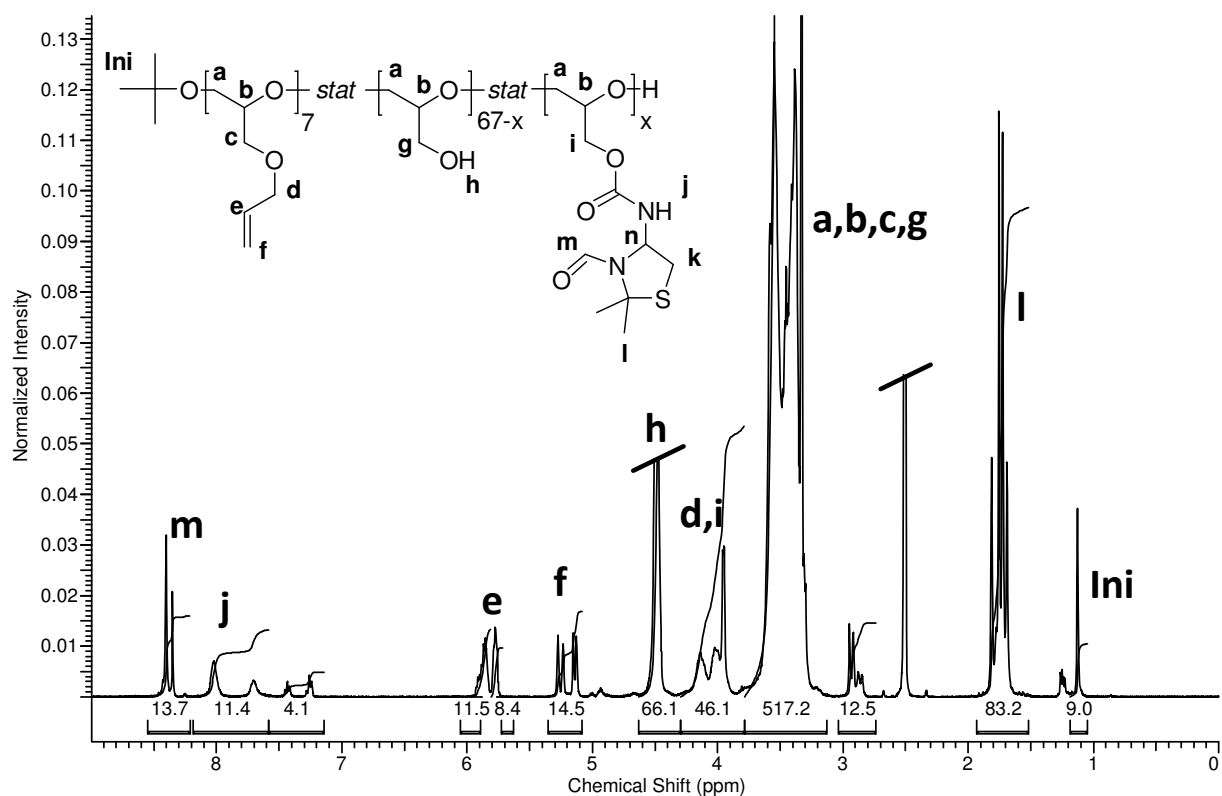


Figure 108: ^1H NMR of thiazolidine-functionalized poly(G-stat-AGE) obtained by isocyanate-functional thiazolidines and poly(G-stat-AGE).

A polymer with $\text{DP}_{\text{glycidol}} = 67$ and $\text{DP}_{\text{allyl}} = 7$ was used for the reaction. For the determination of the efficiency the terminal tert-butyl group was set to a value of 9. Allyl groups were assumed to be inert towards the reaction and the allyl-signal at $\delta = 5.6$ ppm was yielding an integral of 14 ($\text{CH}_2=\text{CH-R}$), confirming the inertness. 14 hydroxy-groups were attempted to be modified with the isocyanate. The signal of the formyl-group can be observed with a chemical shift of $\delta = 8.21 - 8.55$ ppm, the carbamate-signals at $\delta = 7.58 - 8.19$ ppm. Both signals indicate a functionalization of approximately 11-14 repeating units. Signal at $\delta = 5.65 - 6.05$ ppm were assigned to the signal H^n of the thiazolidine-ring, with the allyl-signal $\text{CH}_2=\text{CH-R}$, H^e in direct vicinity at $\delta = 5.7 - 5.81$ ppm. Hydroxy-groups are detected at $\delta = 4.5$ ppm, whereas the signal strength does not seem to be significantly diminished in comparison to the theoretical initial value of 67, as the resulting integral gives at value of $I = 66$. This is assigned to the inaccurate signal determination of alcohols in general, as the H-D-exchange can occur, potentially falsifying the signals intensity. The signal of H^d and H^i overlap at $\delta = 3.79 - 4.30$ with an integral of 46. As 7 repeating units of allyl should show a signal integral of 14 in this region, the actual value for H^i is $I = 46 - 14 = 32$, corresponding to a

number of Hⁱ groups of 16 and hence 16 attached thiazolidine-units per polymer. With an integral of $I = 83$ both CH₃ groups of the thiazolidine can be assigned to the signal at $\delta = 1.52 - 1.93$ ppm. This corresponds to a degree of functionalization of $DF = 13$. Additionally, due to the initiator assigned to the singlet at $\delta = 1.1$ ppm and an integration of $I = 9$ the degree of functionalization is proven with a second reference usable.

In a repetition experiment the poly(glycidol) homopolymer was used for the synthesis. Thiazolidine acyl azide was dissolved in DMF, heated to 90 °C to generate the isocyanate and subsequently at RT the polymer-solution in DMF was added. DBTDL was added in catalytic amounts and it was stirred at RT overnight with a ratio of OH:NCO = 60:13. After workup ¹H-NMR analysis revealed an efficiency of 15 %. The discrepancy of the efficiency was surprising and the experiment was repeated. Again the homopolymer was used for the polymer-analog functionalization. A ratio of OH:NCO = 60:20 was used and resulted in a conversion of two repeating units, i.e. an efficiency of 10 %.

The functionalization in general with isocyanate-functional thiazolidine is possible, but not always successful. Additionally, the use of tin in the functionalization procedure for cysteine-functional polymers is inappropriate. Organo-tin compounds are commonly known to be potentially toxic due to their interaction with sulfur-groups, denaturing cysteine-containing proteins. Conscientious workup would be necessary before cell studies could be performed. Circumventing this potential issue triethylamine was used as a catalyst to perform the reaction.

Table 13: Attempts to functionalize polyglycidols with NCO-thiazolidine with Et₃N as base.

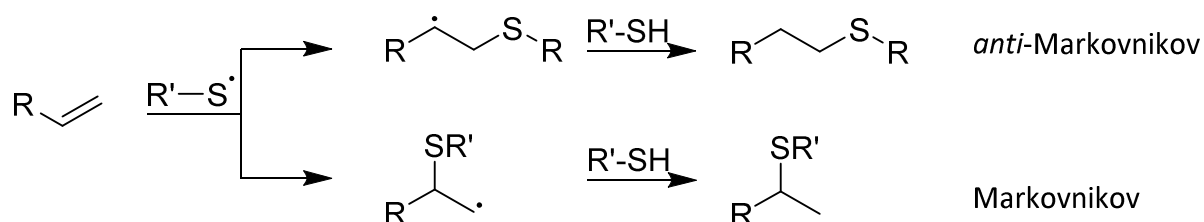
Entry	Glycidol (repeating units)	Allyl (repeating units)	NCO	Et ₃ N:NCO	time	T [°C]	Efficiency [%]
1	67	7	18	1.13:1	overnight	RT	5
2	60	-	8	0.5:1	5 d	RT	50
3	60	-	9	0.4:1	overnight	90	11

In Table 13 all attempts to functionalize poly(glycidol) with NCO-thiazolidine are summarized. Here a maximum of 50 % efficiency was obtained. Entry 2 indicates that a long reaction time is necessary to obtain higher conversions. Regarding the reaction of NCO-thiazolidine with the hydroxy-groups a high efficiency is necessary to predict the final degree

of functionalization. Assuming a variation in the polymer-length it has to be further investigated if the conversion is 50 % or if the efficiencies are polymer-length dependent. It is therefore concluded that the functionalization of polyglycidols with NCO-thiazolidines is ineffective and hence an alternative strategy was evaluated.

3.3.3. Polymer-analog functionalization via thiol-ene chemistry

Synthesized mercaptothiazolidine from 3.3.1.3 was used to functionalize allyl-functional poly(glycidol) in analogy to Koyama- and Frey-group. Thiol-ene chemistry is a promising approach for the reaction between an unsaturated double-bond and thiols, hence sometimes called hydrothiolation of a double bond. Here the abstraction of H·-radicals of the thiols are initiated using either UV-light with or without a photosensitive compound or thermal production of radicals by thermally labile compounds e.g. peroxides or azo-compounds. Thiyl-radicals $RS\cdot$ attack the unsaturated bonds under formation of the more stable carbon-radical. The carbon-radical can abstract an $H\cdot$ of a further thiol under formation of the hydrothiolated *anti*-Markovnikov product. If no substituents alter the stability of the intermediate radical-species, the *anti*-Markovnikov product is obtained for e.g. alkyl substituted unsaturated compounds.



Scheme 31: Markovnikov and *anti*-Markovnikov products possible by thiol-ene chemistry.

A second thiol necessary to transfer the $H\cdot$ species from the thiol to the carbon-centered radical is transformed to the corresponding thiyl-radical attacking further unsaturated bonds.

3.3.3.1. Thiazolidine-functionalization of poly(glycidol)

Successful thiol-ene chemistry was already shown in literature with poly(ethylene oxide-*stat*-allyl glycidyl ether) with various thiols under thermal conditions using AIBN as the radical source.[68] Polymers were dissolved in DMF and all components added subsequently. Solutions were degassed by purging through the solutions with N_2 for 30 min. AIBN:allyl

ratios were varied from AIBN:allyl = 0.69:1 to 1.47:1 and 17-21 equivalents of the thiol were used with respect to the allyl-group. After workup the internal reference (terminal *tert*-butyl group of the initiator) was not always giving the correct integral for the groups that are supposed to be inert towards the reaction, as the backbone signals or the acetal-CH- group. In this case no quantification of the conversion can be performed. This can be caused by the cleavage of the *tert*-butyl group under acidic conditions. Here only the qualitative determination is possible. For entry 1 and 3 (Table 14) no quantification was possible, but the ¹H NMR analysis showed no residual allyl-signals. Unfortunately, the first entry also does not show a residual thiazolidine ring, either caused by a cleavage of the thiazolidine ring from the polymer or the thiazolidine-ring opening upon work up. Entries of 2 and 4 (Table 14) show that upon decrease of the content of AIBN the conversion increases. If the thiol-content is increased from 17 eq to 22 eq a full conversion can be obtained. Increasing the temperature and using 19 eq. of the thiol and 1.47 eq of AIBN, with respect to the allyl-group, a conversion of 97 % can be obtained. It has to be noted that a full conversion of the allyl-groups is possible, however only with an excess of 22 equivalents of the thiol with respect to the allyl-group. In this case, with a polymer of 67 glycidol and 7 allyl-groups, 154x the quantity of the polymer had to be used to let the reaction run to completion. This reaction is therefore assumed to be inefficient. Literature often calls this type of reaction “click” chemistry. Regarding a recent publication about the term “click”-chemistry in polymer science this definition is inappropriate for such an extent of equivalents.[161]

The use of a light induced generation of radicals is an alternative approach for the Thiol-Ene reaction. For this two apparatus were available. First a photoreactor (PR) was available using 16 lamps with each having 24 W ($\lambda = 365$ nm). Second, 4 UV-LED cubes (LED), each with 11 W ($\lambda = 360$ nm), were used with 2,2-dimethoxy-2-phenylacetophenon as light-sensitive initiator.

Table 14: Thiol-ene chemistry of mercaptothiazolidine and allyl-functional poly(glycidol) initiated with AIBN at elevated temperature.

Entry	Allyl [mmol]	Acetal [mmol]	AIBN [mmol]	FTz4CySH [mmol]	Polymer [mol L ⁻¹]	T [°C]	t [h]	AIBN [eq]	AGE [eq]	Thiol [eq]	Conversion [%]
1	0.252	2.412	0.20	4.2	$6.00 \cdot 10^{-3}$	75	12	0.81	1.00	17	no CH ₃ signal
2	0.264	2.531	0.18	4.4	$6.30 \cdot 10^{-3}$	75	21	0.69	1.00	17	86
3	0.254	2.432	0.22	5.6	$6.05 \cdot 10^{-3}$	75	19	0.85	1.00	22	no allyl
4	0.259	2.481	0.22	4.3	$6.17 \cdot 10^{-3}$	75	22	0.84	1.00	17	14
5	0.166	1.588	0.24	3.1	$5.27 \cdot 10^{-3}$	85	22	1.47	1.00	19	97

Table 15: Thiol-ene chemistry of mercaptothiazolidine and allyl-functional poly(glycidol) initiated via UV-irradiation.

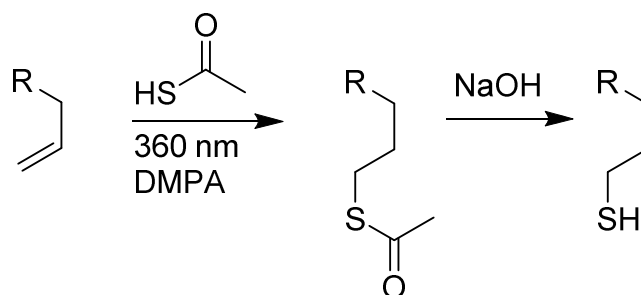
Entry	Source	Solvens	Glycidol	Allyl:DP	Polymer [mg mL ⁻¹]	t [min]	DMPA [eq]	AGE [eq]	Thiol [eq]	Conversion [%]
1	PR	EtOH	OH	7:74	22.7	70	0.10	1.0	5.5	100
2	PR	EtOH	OH	7:74	8.8	10	0.66	1.0	5.2	100
3	PR	EtOH	OH	7:74	10.8	15	0.46	1.0	3.5	100
4	PR	EtOH	OH	7:49	18.4	15	0.49	1.0	3.5	100
5	PR	EtOH	OH	7:49	18.4	25	0.52	1.0	3.4	100
6	UV-LED	EtOH	OH	7:49	19.2	150	0.50	1.0	3.3	100
7	UV-LED	MeOH	Acetal	11:79	22.3	<10	0.90	1.0	6.2	100
8	UV-LED	MeOH	Acetal	11:79	50	60	0.59	1.0	2.3	100
9	UV-LED	MeOH	Acetal	11:79	27.6	120	0.52	1.0	1.9	100
10	UV-LED	MeOH:EtOH =1:2	Acetal	5:50	76.1	30	0.50	1.0	3.3	100
11	UV-LED	MeOH	Acetal	5:50	59.7	30	0.5	1.0	3.1	100

Table 14 and Table 15 summarize the experiments performed with AIBN and elevated temperature as well as DMPA as initiator and UV-irradiation to perform Thiol-Ene chemistry with mercaptothiazolidine and allyl-functional poly(glycidol). Table 15, entries 1-5 were performed with a photoreactor using 16x24 W lamps. Entries 6-11 were performed with UV-LED cubes having 4x11 W. It shall be noticed that the intensity of the two light sources vary. More important than the intensity is the fact the lamps as well as LEDs are used. Whereas the spectra of lamps are usually giving an intensity *maximum* at the specified wavelength, other wavelengths are also radiated. LEDs radiate one specific wavelength, here 360 nm, and no other wavelength is radiated by that source. As the photoinitiator also absorbs at various wavelengths, the initiation of DMPA with the more intense and more radiative photoreactor is supposed to be more efficient. Using a photoreactor, ethanol as solvent and a ratio of DMPA:allyl:thiol = 0.66:1.0:5.2 the reaction is completed within minutes. The reaction is also able to proceed within a wide range of polymer concentrations, i.e. $c = 8.8 - 76.1 \text{ mg mL}^{-1}$. Allyl-allyl coupling can also proceed, as was mentioned by ten Brummelhuis et al.[162] No signals in $^1\text{H-NMR}$ spectrum can be observed indicating the presence of this side-reaction. A higher spatial separation of the groups allows the avoidance of this reaction, i.e. a longer side-chain, tacticity or a side-chain "dilution" by comonomers, as was stated by the authors. As only up to 14 % of the monomers bear allyl side-chains and the statistical copolymerization is assumed (see chapter 3.1) the theoretical considerations confirm the experimental observations. This leads to the assumption that the *anti*-Markovnikov addition happens without any detectable side-reactions. In all experiments the allyl-content was varied between 9.5 - 14 % of the polymer. The lowest ratio of thiol:allyl = 1.9:1 was used to assure a full conversion and a suppression of the side-reaction. Table 15 also indicates that the use of ethanol and methanol is possible for this reaction. In general the reaction is always fast. It was noticed that a slight turbidity at the beginning, due to the restricted solubility of mercaptothiazolidine in ethanol, beginning to clear as the reaction proceeds. Mercaptothiazolidine solubility is assumed to increase as the substrate is removed during the course of reaction, and the solubility-equilibrium is shifted. Furthermore the reaction slightly warms up during irradiation and hence increases solubility. Nonetheless the reaction is well performed although an incomplete solubility was initially observed. The solubility of mercaptothiazolidine in methanol is better, as no turbidity could be observed during preparation of the reaction. In summary a procedure for the thiol-ene chemistry of the

mercaptothiazolidine and allyl-functional poly(glycidol) should be performed with 3-3.5 eq thiol with respect to the allyl-group. With this ratio it is assumed that a suppression of a potentially occurring side-reaction can be diminished with concurrently reducing the use of mercaptothiazolidine. A ratio of DMPA:allyl = 0.5:1 can be used to let the reaction run to completion. Entry 11, Table 15 was performed with ca. 3 g polymer indicating a potential process to synthesize thiazolidine- and hence cysteine-polymers in a gram scale batch.

3.3.3.2. Thiol-, amine- and carboxyl-functionalization

A successful functionalization of the polymer with Thiol-Ene chemistry was transferred to other functional groups promising with respect to biomaterials. Thiol-functionalization of poly(glycidol)s was already demonstrated to yield redox-sensitive nanogels for a potential drug-delivery.[83] Here esterification of the synthesized poly(glycidol)s was demonstrated. Ester-free thiol-functional poly(glycidol)s should be obtainable using thioacetic acid and allyl-functional poly(glycidol). Attached thioacetates should be cleavable by hydrolysis.



Scheme 32: Synthesis of thiol-functional poly(glycidol)s via Thiol-ene chemistry.

In analogy to the functionalization of allyl-functional poly(glycidol) a solution of thiol:allyl:DMPA = 3.5:1:0.5 in ethanol was irradiated with 360 nm (LED-cubes) for 2.5 h. After work-up a ¹H-NMR spectrum was recorded (Figure 109). Here a polymer with DP_{glycidol} = 42 and DP_{allyl} = 7 was used. Typical signals of the new formed thioacetate are assigned to the triplet at δ = 2.93 ppm (H^g), the singlet at δ = 2.35 ppm (H^h) and the quintet at δ = 1.84 ppm (H^f). The procedure was performed with a maximum of 7 g polymer initially used for the synthesis. This also shows the gram-scale opportunity using this modification protocol. A polymer with 10 % thioacetate-functionalities was acetal-protected in THF with HCl and yielded the thioacetate-functional water-soluble poly(glycidol).

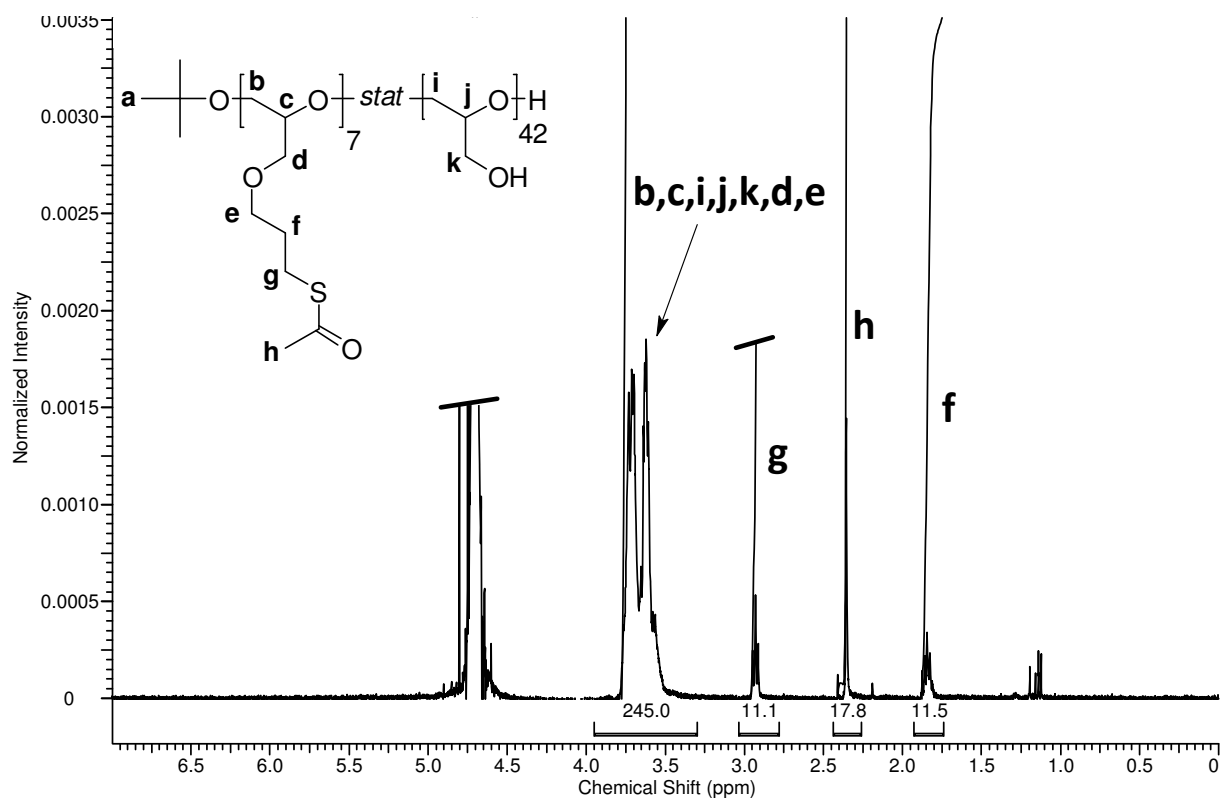
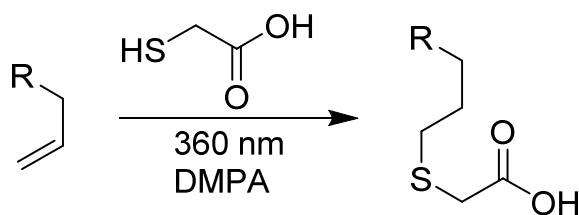


Figure 109: ^1H -NMR spectrum of thioacetate-functional poly(glycidol).

Thioacetate side-chains were hydrolyzed with $c = 30 \text{ g L}^{-1}$ and a solution of 1.44 M NaOH in an ethanol/water solution (EtOH:H₂O = 4:1). Subsequently the oxidized polymer was reduced with TCEP under inert atmosphere and dialyzed against water. An Ellmann assay was used to determine the content of thiol-functionalities. The synthesized polymer was analyzed and yielded a overall content of 0.439 mM in the initial solution. With a theoretical value of 0.44 mM thiols in the analyzed solution this matches very well and confirms the ^1H -NMR spectrum giving a number-averaged value of 4 - 4.5 thiols per polymer, using the polymerization initiator as reference.

The amine-functionalization of poly(glycidol)s are of interest, as the positive charge of protonated amines under neutral conditions should be able to complex (poly)anions as e.g. DNA. As was already shown by the Koyama-group, thiol-ene reaction can be performed with cysteamine hydrochloric salt, giving amine-functional poly(glycidol)s as could be confirmed with ^1H -NMR.

As well as amine-functionalization, carboxyl-functionalization of poly(glycidol) was achieved using thioglycolic acid with a ratio of SH:allyl:DMPA = 3.5:1:0.5 equivalents. Here it was also possible to directly obtain carboxylic acid functional poly(glycidol).



Scheme 33: Allyl-functionalization with carboxylic acid via thiol-ene reaction with thioglycolic acid.

3.3.3.3. Thiazolidine-hydrolysis of thiazolidine-functional polyglycidols

For deprotection of the thiazolidine-ring the following aspects have to be considered. In aqueous solution thiazolidines are in equilibrium with the corresponding cysteine and aldehyde or ketone. In non-aqueous solution it is stable. Ring-stability can be enhanced by modification of the ring-amine. Formylation was performed in the previous chapter leading to a stabilized ring, enabling a purification of thiazolidine-functional polyglycidol by dialysis against water. Cleavage of the formyl-group can be done by the following substrates as it is stated in literature[163]:

1. Acidic cleavage with HCl in H₂O or dioxane.
2. Transfer of the formyl-group to strong nucleophiles.
3. Hydrogenolysis with H₂ and Pd.
4. H₂O₂
5. Acylchloride/benzyl alcohol.
6. UV-irradiation at 254 nm in acetonitrile.
7. Alkaline cleavage with NaOH.

Various opportunities of deprotection will be considered. The first two deprotection-routes are promising as the cleavage under acidic conditions hinders the oxidation of the obtained thiols towards oxygen, possibly using open-flask conditions. Hydrogenolysis is promising, as potentially oxidized thiols will be reduced, in parallel to the deprotection. Unfortunately, regarding the potential use of the polymers for biomaterials, the use of palladium is

inappropriate as it has to be removed completely, that might be problematic due to the complexation of Pd with cysteine-ligands, either reducing the yield or making work-up difficult.[164] Oxidative cleavage of the formyl-group with H₂O₂ does not seem to be efficient by the value given in literature (15 %). Additionally, a possible over-oxidation to the corresponding sulfones and sulfoxides is possible. Furthermore, the subsequent reduction had to be performed increasing synthetic efforts. Reaction of acyl chloride and benzyl alcohol forms HCl leading to the acidic cleavage of the reaction in analogy to the reaction with HCl in H₂O or dioxane. Here the electrophilic acyl chloride might interact with the ring-thioether as the free electron pairs of the sulfur are highly nucleophilic. Removal of the formyl-group with UV-light might be an option. As it is known for thiol-ene reactions, the formation of thiyl-radicals can be performed by irradiation with UV-light without photosensitizer if wavelengths of 254 nm are used. After deprotection, the formation of thiyl-radicals could possibly lead to side-reactions. For these reasons the cleavage of the thiazolidine-rings seemed to be most promising with hydrochloric acid.

Table 16: Deprotection of the formylated thiazolidine-ring attached to poly(glycidol).

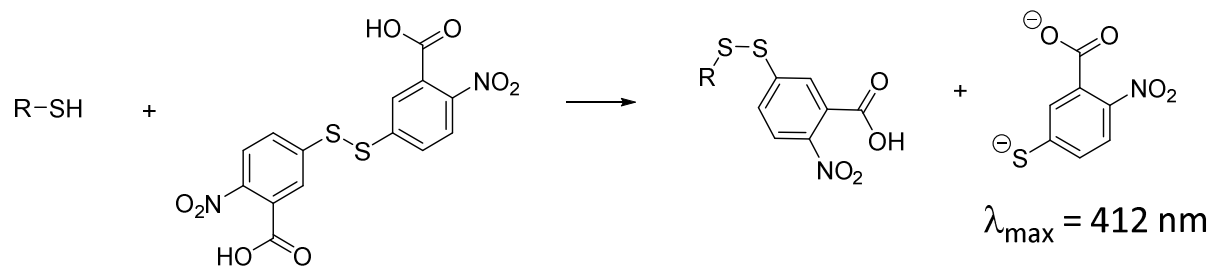
Entry	Substrate	T [°C]	Time [h]	Result
1	0.1 M HCl	RT	24	No deprotection
2	0.1 M HCl	70	66	78 % deprotected
3	0.1 M HCl	70	114	Fully deprotected
4	0.1 M HCl	80	24	66 % deprotected
5	0.1 M HCl	80	48	73 % deprotected
6	0.1 M HCl	90	5	49 % deprotected
7	0.1 M HCl	120	3	Side-chain cleavage
8	pTsOH	RT	Overnight	No deprotection
9	2.5 M NaOH	Reflux	Overnight	Side-chain cleavage
10	Hydroxylamine	RT	Overnight	No deprotection
11	Hydrazine	65	4	No deprotection

Different temperature and times were evaluated, whereas it was always focused on 0.1 M hydrochloric acid, as a higher concentration might be too acidic, being able to cleave the

thioether connecting the polymer with the thiazolidine. At room temperature no deprotection could be observed using $^1\text{H-NMR}$ spectroscopy to investigate the disappearance of the CH_3 -groups of the thiazolidine-ring at 1.75 ppm. Upon increasing the temperature to 70 - 90 °C a deprotection can be observed. Upon further increasing the temperature side-chain cleavage occurs, being inappropriate for the thiazolidine-deprotection. As the heating plates used in the laboratory usually fluctuate in the range of 5-10 °C, and 70 °C seems to be valuable for the deprotection, this temperature was chosen. Time was further investigated to reach a full deprotection of the thiazolidine-ring. Entry 5 in Table 16 reveals that 48 h at 80 °C is not enough to hydrolyze the thiazolidine-ring. Hence it was stirred for 66 h at 70 °C, whereas with these parameters only 78 % were converted to the corresponding cysteines. It takes approximately 5 d at 70°C with 0.1 M HCl to fully deprotect the thiazolidine-ring and obtain cysteine-functional polyglycidol. Using other deprotection agents lead either to a cleavage of the side-chain from the backbone or no deprotection. This was observed e.g. for hydroxylamine, p-toluene sulfonic acid or hydrazine.

3.3.3.4. Thiol-quantification of cysteine-functional poly(glycidol)

Ellman published in 1958 and 1959 results offering a good opportunity to quantify thiols.[40, 41] Using the aromatic disulfide 5,5'-dithiobis(2-nitrobenzoic acid) one mole thiol reacts with the disulfide and sets free one mole of an aromatic water soluble thiolate.



Scheme 34: Reaction mechanism of Ellmann reagent with thiols.

First the non-carboxylated compound was used, but the application was limited due to the little solubility in water. In 1959 the determination with a carboxylated aromatic disulfide was published. The reason for the introduction was on the one hand the solubility and on the other hand the application of the assay in slightly basic media, deprotonating the carboxyl group to the corresponding carboxylate. Oxidation of thiols to the corresponding

disulfides is performed under neutral to basic conditions and cannot be excluded while performing the assay.

For calibration of the assay, cysteamine and cysteine were tried as a standard testing the variation of the method with the substrate.

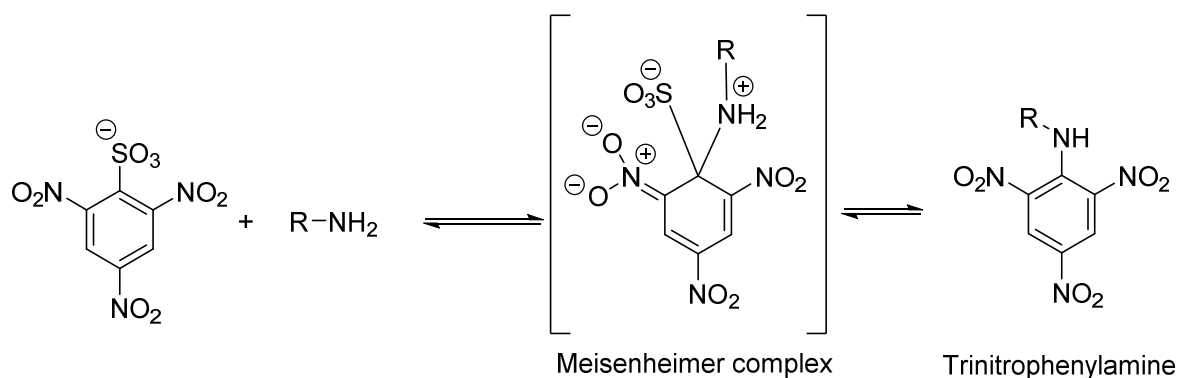
Measurements of the cysteine functional poly(glycidol) are summarized in Table 17, indicating a strong variation in the result. As all polymers shall have 5 thiols none of the polymers gives a “good” value. Depending on ¹H-NMR studies the values of the expected thiols are five, but Ellman gave values between 1.5 and 2.4. A specific reason for this deviation is not known. It could either be caused by the ¹H-NMR measurements with its inaccuracy, or the efficiency of the assay. In general, Ellman assay gives only the value of free thiols. Already oxidized thiols during or before the assay cannot be determined, allowing no accurate determination of the efficacy of the cysteine-functionalization via click chemistry. To sum up, the Ellman assay, in our case, proves the existence of thiol, but for an accurate determination are further methods necessary to prove or disprove the obtained results.

Table 17: Results of the Ellman assay of some thiomers and cysteinomers.

Polymer	Theory	Analysis	Analysis
	SH	NMR	Ellman
MAK331	4	n.d.	1.5
MAK336	5	3.5	2.4
MKN012	5	4	1.8

3.3.3.5. Amine-quantification of cysteine-functional poly(glycidol)

Nucleophilic properties of amines and thiols can be used to convert colourless compounds to a colored complex being analysed via UV-Vis spectroscopy. Besides other the trinitrobenzosulfonic acid (TNBSA) is a reagent used for the quantification of amines in biochemistry. The sulfonic acid group can act as a good leaving group, making the aromatic ring accessible for a nucleophilic substitution reaction. An appropriate electron deficiency is obtained by the threefold functionalization of the ring with NO₂-group. Isolation of the Meisenheimer complex proved this reaction to be via the addition-elimination mechanism with an intermediate and not via a transition state.[165]



Scheme 35: Mechanism for the quantification of primary amines and thiols with TNBSA.

As thiols and primary amines can react with the TNBSA reagent the determination of cysteines should result in the double determination of both functional groups. For this the assay was performed with cysteine (NH₂ SH), cysteamine (NH₂, SH), mercaptoethanol (SH) and ethanolamine (NH₂).

As can be seen in Figure 110 there is a linear dependence of the absorbance and the concentration. For both substances the absorbance–concentration dependence is similar, indicating that the absorption of the assay substrate is independent on the actual species, i.e. thiol or amine.

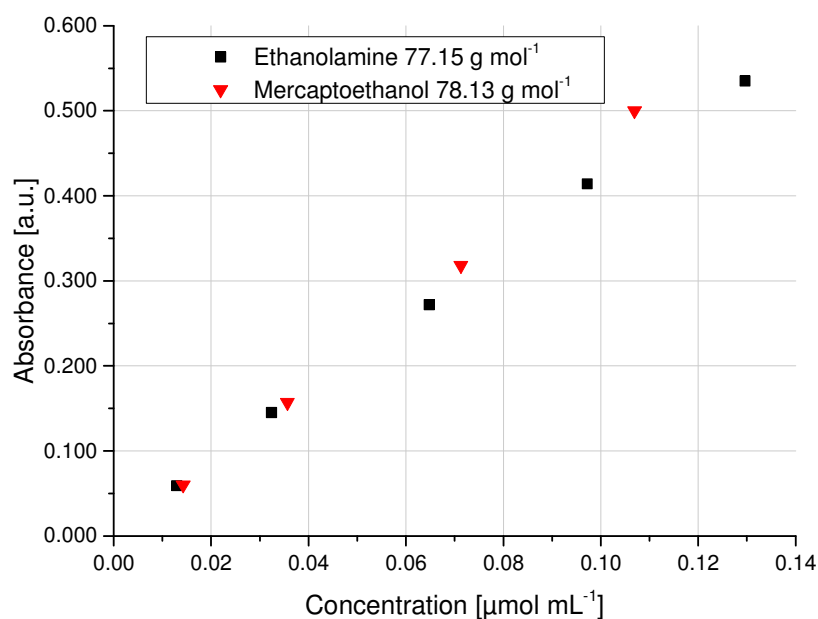


Figure 110: Absorbance–concentration dependence for TNBSA assay with mercaptoethanol and ethanolamine.

Investigating the steric demand of TNBSA two groups in vicinity to each other was analyzed. Figure 111 shows that monofunctional and difunctional compound show the more or less exact calibration line. Linear fitting reveals the data for the slope and intercept shown in

Table 18: Linear fitting parameters of the absorbance measurements for the TNBSA-assay with different calibration standards. A strong deviation of cysteamine, in contrast to oxidized cysteamine, ethanolamine and mercaptoethanol, is found.

Calibration standard	Slope	Intercept
Cysteamine*HCl	6.17	0.015
Cysteamine*HCl + H ₂ O ₂	4.19	0.018
Ethanolamine	4.09	0.009
Mercaptoethanol	4.71	-0.001

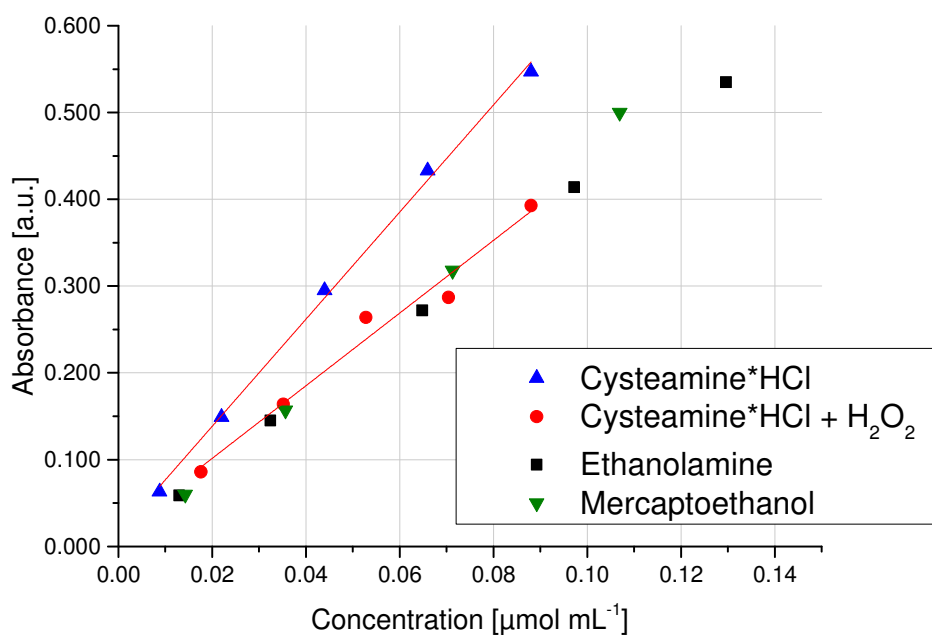


Figure 111: Comparison of mono- and di-reacting compounds with TNBSA. Mono and difunctional compound seem to react only once.

If it is assumed that cysteamine reacted with both groups and the amount of cysteamine molecules is calculated, it has to be divided the amount by the factor of two. This recalculation varies a lot from the other calibration lines. As the concentration of the compound is in μmol and cysteamine reacts similar to mercaptoethanol and ethanolamine this means either the reaction of both termini in all cases (NH_2 , SH , OH), making the alcohol group reactive towards the TNBSA, too. This could also mean that although both termini of cysteamine can react, only one does. The alcohol reactivity can be a reason, but as the solution is delivered in methanol (Thermo Scientific) it is assumed that the possible reaction with alcohol groups can be neglected although the pH is changed from neutral (pure methanol as solvent for TNBSA) to pH 8 for the assay. A theoretical consideration is performed with ethanol, having a $\text{pKa} = 16$, and mercaptoethanol, having a $\text{pKa} = 9.6$, leading to the following calculation in the equilibrium:

$$pK_s = \frac{[\text{EtO}^-][\text{H}^+]}{[\text{EtOH}]}$$

$$\frac{10^{-16}[\text{EtOH}]}{[\text{H}^+]} = [\text{EtO}^-]$$

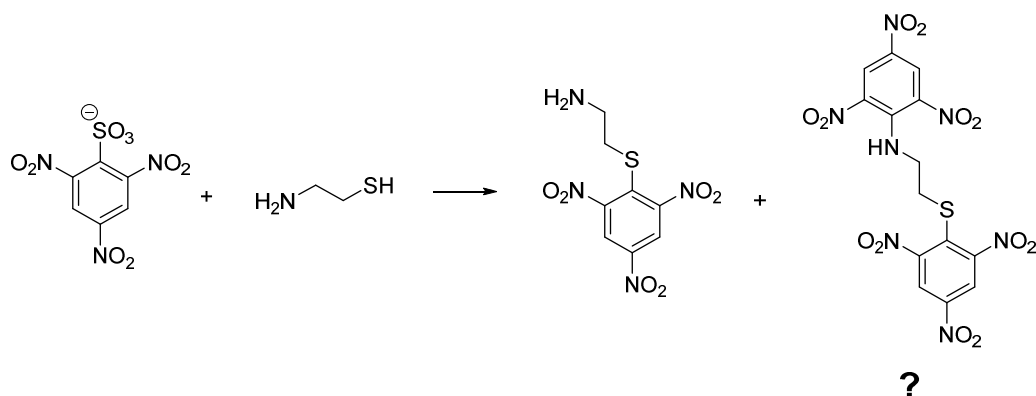
$$\frac{10^{-16}[\text{EtOH}]}{10^{-8}} = [\text{EtO}^-]$$

$$10^{-8} = \frac{[\text{EtO}^-]}{[\text{EtOH}]} = 0.00000001 = 0.000001\%$$

$$\frac{10^{-9.6}[\text{EtSH}]}{10^{-8}} = [\text{EtS}^-]$$

$$10^{-1.4} = \frac{\text{EtS}^-}{\text{EtSH}} = 0.04 = 4\%$$

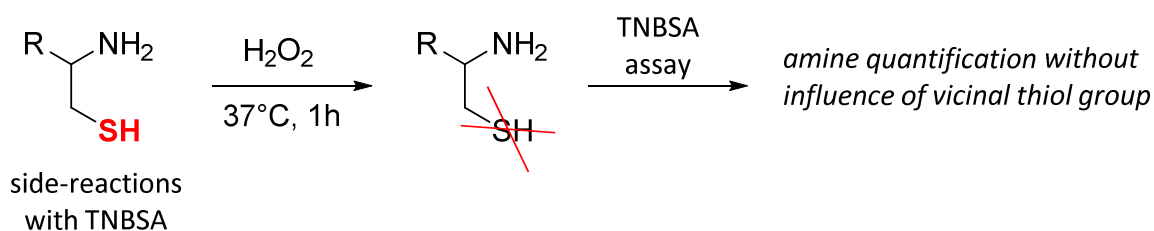
Whereas ethanol is only deprotonated at a pH of 8 to 10^{-6} %, mercaptoethanol is deprotonated of about 4 %. As TNBSA removes the thiolate anion out of the equilibrium, more and more thiols will be deprotonated as the trinitrophenylation proceeds. It can therefore be assumed that the alcohol does not significantly participate in the TNBSA assay. Upon addition of TNBSA solution to the calibration standards a fast color change appeared at the cysteamine solution in contrast to ethanolamine. Usually the color change (colorless to yellow) can be seen up to the 2 $\mu\text{g}/\text{mL}$ solution. An observable color change took longer (30 min - 1h) for the cysteine-solution. This indicates a fast reaction of the thiol compared to the amine. Why the thiol of the cysteamine compared to the cysteins' thiol reacts fast can be explained by the structure. As the cysteamine-amine is able to deprotonate the thiol and with pH 8 is directly available for the nucleophilic attack on the TNBSA, with cysteine the carboxylic acid can additionally protonate the thiol. On the other hand it is probable that although the thiol can be protonated by the carboxylic acid, the excess of NaHCO_3 additionally deprotonated the thiol again making the amine and thiol available for TNBSA reaction. Charge- and steric- reasons can also explain the slow and incomplete conversion of the TNBSA assay with cysteine. The amine of cysteine is close to the deprotonated carboxylate group so that an electrostatic repulsion might occur slowing down the reaction. Additionally the assay is said to be specific for primary amines. Therefore it is assumed, that the thiol of cysteine can react but shall not be used for calibration.



Scheme 36: TNBSA can potentially react with the amine- or the thiol-terminus. A single and double trinitrophenylation is possible.

As the uncertainty with the monoreaction with cysteamine and TNBSA persists it was tested if the TNBSA assay can be performed under oxidative conditions. Therefore the assay was performed with H_2O_2 to see if there is any side-reaction with TNBSA. The standard protocol was performed but instead of using an amine or a thiol H_2O_2 was used in the concentration range of 10 $\mu\text{g}/\text{mL}$ to 1 $\mu\text{g}/\text{mL}$. Maximum of absorbance at $\lambda = 335 \text{ nm}$ of H_2O_2 can be neglected and therefore does not disturb the measurement.

Mercaptoethanol was used for the determination of the necessary oxidation time to completely remove thiols from the solution to be investigated. For this a 50 μL sample solution, with a sample concentration of 10 mg mL^{-1} , was added to a solution containing 4.950 mL 0.1 M NaHCO_3 and 50 μL $\text{H}_2\text{O}_2/\text{NaHCO}_3$ (10 mg mL^{-1} , NaHCO_3 0.1 M). Oxidation was performed for 1 h at 37 °C. Afterwards the standard TNBSA assay was performed with this stock solution.



Scheme 37: Oxidation of thiol-groups in cysteine-functionalities leads to the single quantification of the primary amine using the TNBSA assay.

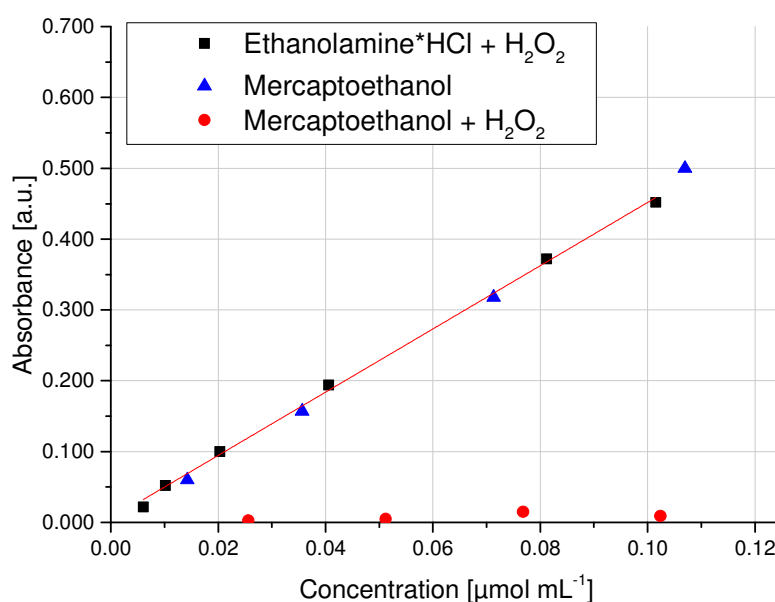


Figure 112: TNBSA assay performed with mercaptoethanol, oxidized mercaptoethanol and ethanolamine. The oxidized mercaptoethanol does not react with the TNBSA.

Figure 112 shows the absorbance at $\lambda = 335$ nm recorded for different concentrations. Ethanolamine, also attempted to be oxidized, does not show an influence of H₂O₂ on the quantification of the primary amine. Measurements with mercaptoethanol show that thiols react equally to amines and the quantification of thiols and amines are hence possible. Upon oxidation of the thiols with H₂O₂ no reaction of mercaptoethanol with TNBSA can be observed, indication that the quantification of cysteines solely via the amine is possible using a prior oxidation of the thiols.

Cysteine-functional poly(glycidol)s were oxidized prior to the determination with the TNBSA assay. Hence the thiols were oxidized and solely the amines were used to quantify the overall quantity of the cysteines attached to the poly(glycidol). Table 19 summarizes the values obtained for the quantification of the amine-content of the polymer. Ethanolamine was used for calibration, measured and a linear fit was performed. The slope m and the intercept b were determined to be $m = 4.466$ and $b = 0.0053$. using this equation the μmol of the calibration were recalculated and are shown in column 5 in Table 19. Entries 1-4 indicate that the values obtained for the absorbance are too small for the quantification as e.g. for entry 1 and 2 the values obtained for the calibration are negative due to the inaccurate measurement. Values of entry 5 - 11 are similar for different concentrations indicating a

constant value obtained for the amine content. Number-average amine-functionality was determined calculating the average value from entry 5 - 11, yielding 4.2 ± 0.5 amines and hence cysteines per polymer. A polymer with $DP_{\text{glycidol}} = 45$ and $DP_{\text{allyl}} = 5$ was used prior to the cysteine-functionalization. This indicates a good synthetic approach for the cysteine-functionalization via Thiol-Ene chemistry using the synthesized mercaptothiazolidine and a good quantification method of cysteines using an oxidative TNBSA assay.

Table 19: TNBSA of cysteine-functional poly(glycidol) with prior oxidation with H_2O_2 .

Entry	Polymer		Calibration		Ratio
	$\mu\text{g mL}^{-1}$	$\mu\text{mol mL}^{-1}$	Abs. [a.u.]	NH_2 [μmol]	Calibration/Polymer $\text{NH}_2\text{:polymer}$
1	0.59	0.00012	0.003	-0.00122	-10.5
2	0.99	0.00019	0.006	-0.00053	-2.7
3	1.98	0.00039	0.009	0.00016	0.4
4	3.96	0.00078	0.017	0.00200	2.6
5	7.92	0.00155	0.034	0.00591	3.8
6	9.90	0.00194	0.044	0.00820	4.2
7	11.88	0.00233	0.054	0.01050	4.5
8	15.84	0.00311	0.070	0.01418	4.6
9	19.80	0.00388	0.087	0.01808	4.7
10	49.50	0.00971	0.157	0.03417	3.5
11	99.00	0.01941	0.333	0.07461	3.8

3.4. Native Chemical Ligation with cysteine-functional poly(glycidol)#

Proofing the functionality of cysteine side-chains, NCL was performed. The group of Christian P. R. Hackenberger at Department Chemical Biology II, Leibniz-Institut für Molekulare Pharmakologie (FMP) in Berlin and Humboldt Universität zu Berlin, Department Chemie, Berlin performed the NCL experiments, MALDI-ToF measurements and HPLC measurements. The polymer was synthesized with $DP_{\text{glycidol}} = 45$ and $DP_{\text{cysteine}} = 5$ (stored as the acetate salt). C-terminal thioester peptide of the sequence 390-410 of the tauprotein (Thz-EIVYKSPVVS GDTSPRHLSN, Thz: Thiazolidine protected cysteine) was synthesized by Oliver Reimann in the group of Hackenberger. Oliver Reimann performed the experiments allowing the thioester-peptide to react with the cysteine-functional poly(glycidol) under reductive condition at pH 6.9 and 4-mercaptophenylacetic acid (MPAA) as an aromatic catalyst. Reaction was run for 3 h and peptide:polymer (pep:pol) = 1:1, 3:1 and 5:1 ratios were used to check the peptide distribution and the saturation-functionalization of the 5 kDa polymer with a comparably large 2 kDa peptides. After dialysis with a MWCO 3,500 dialysis tube, to remove unbound peptide, MALDI-TOF experiments were performed. Best MALDI spectra were obtained with sinapinic acid that is often used for peptide analytics in MALDI experiments. This indicates a strong influence of the peptide on the desorption properties of the conjugate. The main signal of conjugates is obtained for disubstituted conjugates (if mass discrimination can be neglected) making the conjugate already a more or less mass:mass = 1:1 compound of peptide:polymer (Figure 113). With higher degrees of conjugation the influence of the peptide further increases.

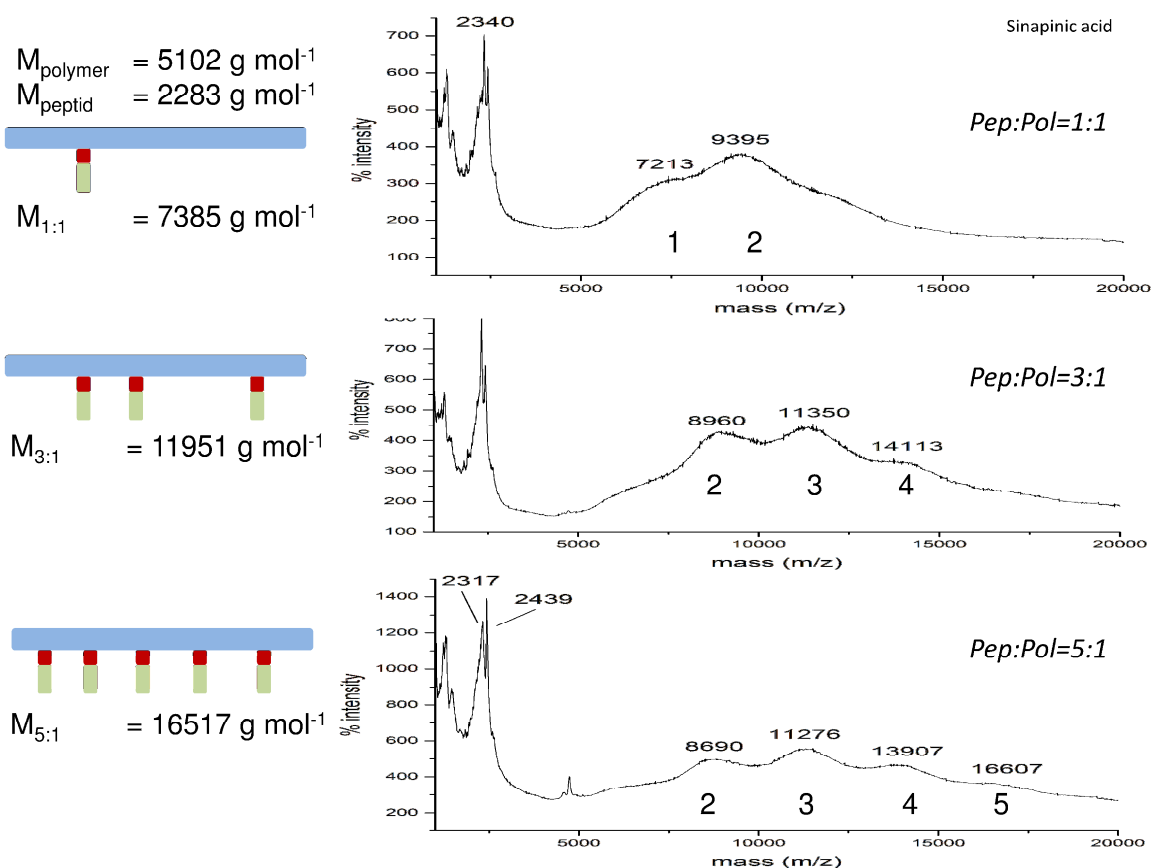


Figure 113: MALDI-TOF experiments of polyglycidol–peptide conjugates with peptide:polymer feed ratio of 1:1 (top), 3:1 (middle), 5:1 (bottom) with the corresponding estimated maxima of the signals and the amount of peptides at each polymer.

When the feed ratio thioester:cystein=1:5 was chosen for the NCL, three species, pep:pol=1:1, 2:1 and 3:1 occur in the MALDI spectrum. As up to five peptides can be added (in average) to every polymer a higher degree of substitution is valid with respect to the intended ratio.

Table 20: Native Chemical Ligation experiments. Polyglycidol with five cysteine functionalities was used and modified with three different peptide:cysteine ratios, i.e. 1:1, 3:1 and 5:1. The conjugates were dialyzed and analyzed by MALDI-TOF experiments.

Ratio peptide:polymer (thioester:cysteine)	Peptide [g mol ⁻¹]	Conjugate ¹⁾ [g mol ⁻¹]	Mass ²⁾ [g mol ⁻¹]		
			1:5	3:5	5:5
0:1 (0:5)		5102			
1:1 (1:5)	2283	7385	7213	-	-
2:1 (2:5)	4566	9668	9395	8960	8690
3:1 (3:5)	6849	11951	-	11350	11276
4:1 (4:5)	9132	14234	-	14113	13907
5:1 (1:1)	11415	16517	-	-	16607

1) Theoretical molar mass

2) Determined by MALDI-TOF experiments. Peak maximum was used.

Table 20 shows the results of three experiments with feed ratios of thioester:cysteine = 1:5, 3:5 and 1:1. The higher the amount of thioester-peptide with respect to the amount of cysteine-units, the higher degrees of conjugation can be obtained. All experiments show the same conjugates with an inaccuracy in determined molecular weight determined by MALDI-TOF experiments (peak maximum) due to the overlap of all degrees of conjugation with the overall overlap of polymeric molecular mass distribution (see Figure 113). The molecular-weight distribution of the original polymer can be observed resulting in a broad multimodal signal ranging from 4.8 kDa to 18 kDa (Figure 113). Additionally, possible polymer fractions of small molecular weight might be considered having no cysteine attached caused by copolymerization feed and might therefore exist as “homopolymeric impurities” in the sample. With approximately 10 % AGE in the copolymer, all polymers with DP < 10 bear no allyl group. As these fraction have molecular weights smaller than MWCO of post-NCL dialysis, MALDI-TOF experiments are assumed to be recorded of the pure peptide–polymer conjugates. Increasing the amounts of peptide up to an equimolar ratio of peptide:polymer = 5:1 (thioester:cysteine = 1:1), gives a higher degree of peptide-conjugation. Only a small almost negligible fifth peptide condensation at the polymer can be observed, indicating a saturation of the polymer with the peptide at a ratio of

peptide:polymer = 4:1. Considering the molar masses of 5100 g mol^{-1} of the polymer a peptide with 2283 g mol^{-1} and the increasing bulkiness of the conjugates, with increasing degree of conjugation, the fifth functionalization might be too hindered. Furthermore a discrimination of higher molar masses in MALDI might also be a valid explanation for the small occurrence of the five-fold conjugate. Nonetheless MALDI-TOF experiments confirm the multiple conjugation of peptides along the polyglycidol backbone varied by the peptide:polymer ratio.

Further proofing the higher degree of substitution a Tricin SDS-PAGE was performed according to the literature.[166] A 16 % gel was used with urea and finally stained with silver having a high sensitivity towards peptide. Figure 114 shows one example of a couple of gels that were performed. Although a standard coomassie staining, silver staining and a commercial zinc staining were used the pure reference peptide could not be observed. Literature indicates an influence of the coomassie stain on the quite sensitive silver stain.[167] Staining with silver is more pronounced if sulfonic acids are present either by oxidation of thiols or the sulfonic acid in coomassie blue. As there is no visible complexation of coomassie with the reference peptide the lack of silver staining might be explained by this, too. Reasons for the non-staining of the peptide are still unknown. Gels run with no urea also did not lead to a visible band of the pure peptide. Fortunately, polymer bands and conjugate bands are visible showing a strong smearing due to the molecular-weight distribution of the polymer. Furthermore the molecular-weight increase of the conjugates can be seen in the gel by decreasing the length of the bands from the pure polymer to the conjugates. With thioester:cysteine = 1:5 to 3:5 and 1:1 a stepwise increase in molecular-weight and a reduced migration in the gel can be observed. As the difference of the thioester:cysteine = 3:5 and 1:1 experiments is not significant in the gel a conclusion about a saturation of the polymer with the conjugates cannot be drawn by this method.

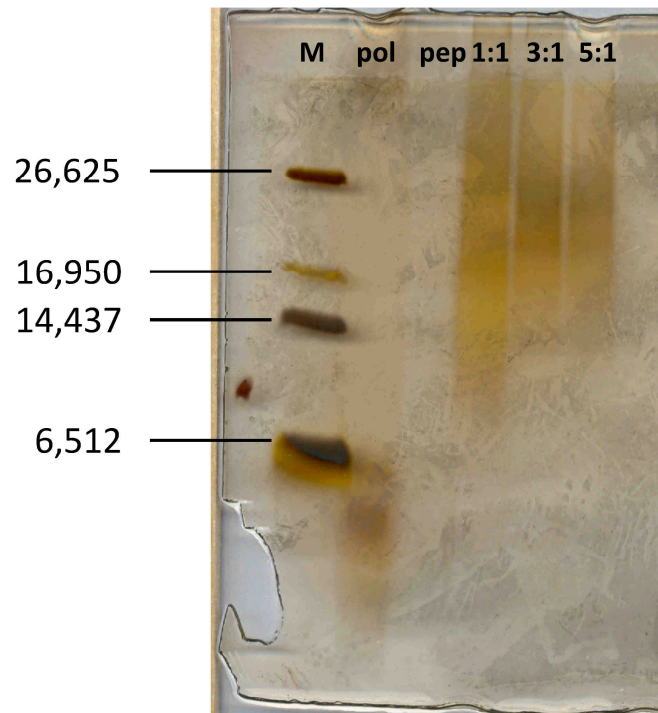


Figure 114: Tricin SDS-Page with marker (M), cysteine-functional poly(glycidol) (pol), peptide (pep) and the conjugates synthesized with a ratio of thioester:cysteine=1:5, 3:5 and 1:1 (peptide:polymer = 1:1; 3:1, 5:1).

4. Summary/Zusammenfassung

Summary

Aim of this thesis was to combine the versatility of sulfur-chemistry, regarding redox-sensitivity as well as chemo- and site-specific conjugation, with multifunctionality of poly(glycidol)s as an alternative to poly(ethylene glycol). For this, first the poly(glycidol) synthesis was evaluated and optimized. With this knowledge, the oxidation-sensitive thioether-analogs of poly(glycidol)s, i.e. poly(thioglycidol)s, were developed. Finally, water-soluble poly(glycidol)s derivatized with thiols, amines carboxylic acids and cysteines were prepared. The cysteine-functionality combines redox- and pH-sensitivity with the possibility of chemically orthogonal coupling via Native Chemical Ligation.

Poly(glycidol) synthesis and process optimization. First the homo- and copolymerization of EEGE and AGE were performed with respect to molar-mass distribution and reaction kinetics. A detailed study was given, varying the polymerization parameters such as DP, counter ion, solvent and monomer influence. It can be concluded that in general the rates for all polymerizations are higher using K^+ , in contrast to Cs^+ , as counter ion for the active alkoxide species. Additionally, the solubilities of the respective K^+ -salts are better in a variety of solvents. Unfortunately, K^+ as counter ion commonly leads to a reduced control over polymer dispersity. Especially the polymerization of AGE is problematic giving generally dispersities higher $\mathcal{D} = 1.2$. The development of bimodal molar-mass distributions was assigned to the dimerization of polymer chains. In this thesis it was shown that the broad molar-mass distributions might be reduced by adding the monomer in a step-wise manner. In experiments with a syringe pump, for continuously adding the monomer, a significant reduction of the dispersities especially for AGE polymerizations could be found using K^+ as counter ion.

In the future, a more detailed investigation of the slow monomer addition would be promising as this type of side-reaction is not only occurring at the investigated monomers but other epoxide- and glycidyl-monomers are also known to exhibit these side-reactions. Furthermore, optimization of EEGE synthesis is necessary, currently hindering the large-scale synthesis of poly(glycidol)s and hence the transfer of the polymer system “from bench to bedside”. A possible route would be a continuous-flow reactor approach having a fixed-bed acid catalyst that might reduce work-up procedures.

Synthesis of poly(thioglycidol)s: In analogy to the oxyanionic polymerization of epoxides, the polymerization of episulfides via a thioanionic mechanism with various DPs was successful with thiols/DBU as initiator. In most experiments bimodality could be observed due to the dimerization, caused by oxidation processes by introduced oxygen during synthesis. Reducing this was successful by a modified degassing procedure. For this, either continuously reduced pressure and temperature (-15 °C) conditions or repeated degassing cycles after each step, i.e. initiation, monomer addition and quenching, are required. Unfortunately, it was not always possible to completely avoid the dimerization due to oxidation. Thiophenol, butanethiol, mercaptoethanol and dithiothreitol were used as thiol initiators, all being capable to initiate the polymerization and predetermine the resulting molar-mass in the range of DP = 18-66 for ethoxy ethyl thioglycidyl ether and allyl thioglycidyl ether. With the prediction and the narrow molar-mass distributions, the living character of the polymerization is therefore indicated. Attempts to use other initiators, to avoid the introduction of disulfides by these, failed using phenol/DBU as initiating system. Successful removal of the acetal-groups under acidic conditions lead to hydroxy-functional poly(thioglycidol)s that were almost negligible water-soluble. For this a poly(thioglycidol)-*block*-poly(ethylene glycol) copolymer was synthesized to increase water solubility and the resulting amphiphilic copolymer self-assembled in aqueous solution.

Reduced water-solubility of poly(thioglycidol) hinders the direct use of these polymers. However, block-copolymers (with PEG) formed particles that should be examined towards oxidative conditions and compared to the results of literature given PEG-PPS copolymers. Furthermore, it would be interesting grafting PEG or poly(glycidol) on the poly(thioglycidol)s as the thioethers are assumed to strongly attach to gold surfaces. This would lead to the multi-thioether fixation of the polymers on the gold exhibiting a strong coating.

Cysteine-functionalization of poly(glycidol)s: Homo- and copolymers of poly(glycidol) were used to functionalize these polymers with side-chains bearing amines, thiols, carboxylic acids and cysteines. The cysteine side-chains were obtained using a newly synthesized thiol-functional thiazolidine (mercaptothiazolidine, FTZ4Cys). For this, cysteine was protected using a condensation reaction with acetone yielding a dimethyl-substituted thiazolidine. Protection of the ring-amine was obtained via a mixed-anhydride route using formic acid and acetic anhydride. Attaching the thiazolidine to the polymer was first attempted by forming

an isocyanate-functional thiazolidine. This was reactive towards the poly(glycidol) hydroxy-groups, but reactions were not accurately reproducible. An alternative route for functionalization was hence followed that turned out to be more successful by activating the carboxylic acid of 2,2-dimethylthiazolidine-4-carboxylic acid with CDI and attach cysteamine. The obtained crystalline mercaptothiazolidine (FTz4Cys) was subjected to thiol-ene click chemistry with allyl-functional poly(glycidol). A systematic comparison of thermal- versus photo-initiation showed a much higher yield and reaction rate for the UV-light mediated thiol-ene synthesis with DMPA as photo-initiator. Using UV-LEDs, a ratio of only 3.5:1:0.5 = thiol:allyl:DMPA was necessary to reproducibly obtain thiazolidine-functional poly(glycidol)s with a full conversion after 30 minutes. Hydrolysis of the protected thiazolidine-functionalities was obtained upon heating the samples for 5 d at 70 °C in 0.1 M HCl. Dialysis against acetic acid lead to cysteine-functional poly(glycidol)s, storable as the acetate salt even under non-inert atmosphere. An oxidative TNBSA assay was developed to quantify the cysteine-content without the influence of the thiol-functionality. A cooperation partner coupled C-terminal thioester peptides with the cysteine-functional poly(glycidol)s and showed the good accessibility and reactivity of the cysteines along the backbone. SDS-PAGE, HPLC and MALDI-ToF measurements confirmed the successful coupling.

In the future, cysteine-functional poly(glycidol)s are promising candidates for the oxidative coupling to form hydrogels. As it is shown in literature for thiol-functional poly(glycidol)s,[83, 111] this allows the formation of particles. With the new thiol-ene based route, ester-free nanogels are available for targeted drug-delivery with a potential longer stability. Additionally, amine-functionalities are prone to protonation and are hence able to form complexes with polyanions, such as DNA, also interesting for drug-delivery applications. Poly(glycidol)s with α,β -aminothiols allow a redox-sensitive behavior of the nanogels via the thiols and an additional pH-sensitivity via the amines. Furthermore, positively charged amino-groups induce enhanced repulsive forces between the chains that potentially improve the disintegration of the particles. More reductive- and acidic-tumor sites are hence targets to be addressed. Native Chemical Ligation accessible cysteine-functional poly(glycidol)s could also be promising candidates for the chemoselective and stable conjugation of peptides studying multivalency effects with desired peptides.

Zusammenfassung

Ziel der Arbeit war es die Vielseitigkeit der Schwefelchemie, hinsichtlich der Redoxsensitivität und chemo- und seitenspezifischer Konjugation, mit der Funktionalisierbarkeit von Poly(glycidol)en, als multifunktionale PEG-Alternative zu kombinieren. Zuerst wurde die Poly(glycidol) Darstellung untersucht und optimiert. Im Anschluß wurden die oxidationsempfindlichen Thioether-Analoga der Poly(glycidol)e, die Poly(thioglycidol)e, synthetisiert. Zu guter Letzt wurden wasserlösliche Poly(glycidol)-Derivate mit Thiol-, Amin-, Carbonsäure- und α,β -Aminothiolfunktionen dargestellt. Letztere erlauben die Kombination aus Redoxsensitivität und chemisch orthogonaler Kopplung mittels Native Chemical Ligation.

Poly(glycidol)-Synthese und die Prozessoptimierung. Zunächst wurden die Homo- und Copolymerisationen von EEGE und AGE hinsichtlich der Molmassenverteilung und der Reaktionskinetik untersucht. Durch die Variation der Polymerisationsparameter, wie angestrebter Polymerisationsgrad, Gegenion, Lösungsmittel und Monomer, wurde der Einfluss dieser untersucht. Allgemein konnte gezeigt werden, dass die Polymerisationen schneller ablaufen, wenn K^+ , im Gegensatz zu Cs^+ , als Gegenion zum aktiven Alkoxidkettenende verwendet wird. Die K^+ -Salze, im Vergleich zu den Cs^+ -Analoge, sind zusätzlich in einer größeren Anzahl an Lösungsmitteln löslich. Nachteilig bei der Verwendung von K^+ als Gegenion ist der Kontrollverlust der Polymerisation, welcher mit einer Erhöhung der Dispersität einhergeht. Insbesondere die Polymerisation von AGE ist problematisch, sodass gewöhnlich Dispersitäten von \bar{D} größer 1.2 erhalten wurden. Bei dieser Kombination ist eine besonders ausgeprägte Bimodalität beobachtet worden, verursacht durch die Dimerisierung der Polymerketten. Es konnte gezeigt werden, dass die Breite der Molmassenverteilung, das Ausmaß der Bimodalität, durch die Geschwindigkeit der Monomerzugabe kontrolliert werden kann. Tatsächlich konnte die Dispersität durch die Verwendung einer Spritzenpumpe verbessert werden, da das Monomer mit einer konstanten angepassten Flussrate hinzugefügt wurde. Besonders bei der Polymerisation von AGE mit K^+ als Gegenion konnte eine bessere Kontrolle der Molmassenverteilung erreicht werden.

In Zukunft wäre die weitere Ausarbeitung der langsamen Monomerzugabe sinnvoll, da diese Nebenreaktion ebenfalls für andere Epoxid- und Glycidolmonomere bekannt ist. Ebenfalls ist die EAGE Monomersynthese ansich optimierungsbedürftig, da die Menge und Verfügbarkeit der Monomer die Anwendbarkeit stark beeinflusst. Eine großtechnische Darstellung der Monomere und Polymere wäre ein Schlüsselaspekt des Transfers aus der universitären Forschung hin zur klinischen Anwendung. Eine mögliche Route wäre die Untersuchung der Synthese des EAGE im Durchflussreaktor mit einem sauren Festbettkatalysator, sodass die Aufreinigungsprozedur minimiert würde.

Synthese der Poly(thioglycidol)e. Analog zur oxyanionischen Polymerisation von Epoxiden, war die Polymerisation von Episulfiden mittels thioanionischer Polymerisation ebenfalls möglich. Hierzu wurden verschiedene Polymerisationsgrade von EETGE und ATGE angestrebt und mittels Thiol/DBU als Initiator auch erreicht. In den meisten Fällen war jedoch eine Dimerisierung der Polymere zu beobachten, welche durch die Oxidation der aktiven Thiolatspezies verursacht wurde. Der Sauerstoff wurde vermutlich während der Polymerisation mit eingeschleppt. Eine Reduktion der Dimerisierung konnte dadurch erreicht werden, dass ein durchgehend verminderter Druck und eine verringerte Temperatur (-15 °C) verwendet wurde. Eine weitere Möglichkeit zur Dimerisierungsunterdrückung war die wiederholte Durchführung von Entgasungszyklen nach jedem Arbeitsschritt, z.B. nach Zugabe des Initiators, des Monomers oder nach dem Quenchen. Trotz dieses experimentellen Aufwandes konnte nicht immer ein vollständiger Ausschluss der Dimerisierung erreicht werden. Thiophenol, Butanthiol, Mercaptoethanol und Dithiothreitol wurden als Thiolinitiatoren (in Kombination mit DBU) verwendet und waren alle in der Lage die Polymerisation zu starten. Bei allen Thiol/DBU-Systemen war eine Kontrolle über den Polymerisationsgrad im Bereich von DP = 18-66 für beide Monomere, EETGE und ATGE, möglich. Die Kontrolle des Polymerisationsgrades und die enge Molmassenverteilung der Polymere verdeutlichen, dass die thioanionische Polymerisation ebenfalls lebend verläuft. Eine mögliche Verunreinigung der Thiolinitiatoren durch Disulfide wurde angenommen und daher ein Alternativinitiator untersucht. Die Verwendung von Phenol/DBU als Initiator führte jedoch zu keiner Kontrolle der Polymerisation. Die erfolgreiche Entfernung der Acetalgruppen unter sauren Bedingungen lieferte multihydroxyfunktionales Poly(thioglycidol). Trotz erfolgreicher Entschützung wurde eine geringe Wasserlöslichkeit des

Poly(thioglycidol)s beobachtet. Dies wurde als Anlass genommen, um ein Poly(thioglycidol)-*block*-poly(ethylene oxid) Copolymer zu synthetisieren, welches als Amphiphil Partikel in wässrigen Lösungen ausbildete.

Die Anwendbarkeit des reinen Poly(thioglycidol)s ist durch die geringe Wasserlöslichkeit eingeschränkt. Eine Untersuchung der oxidativen Responsivität der Partikel aus dem amphiphilen Blockcopolymer Poly(thioglycidol)-*block*-poly(ethylene oxid) im Vergleich zu literaturbekannten PEG-PPS Partikeln wäre interessant. Weiterhin wäre die Derivatisierung der Poly(thioglycidol)e an den Hydroxyfunktionen mit PEG oder Poly(glycidol) interessant, beispielsweise für die PEGylierung oder PGylierung von Goldoberflächen. Das thioetherhaltige Rückgrat der Poly(thioglycidol)e sollte eine starke Adhäsion der Polymere an die Goldoberfläche ausüben.

Cysteinofunktionalisierung synthetisierter Poly(glycidol)e. Glycidol Homo- und Copolymere wurden verwendet und die Seitenketten mit Amin-, Thiol-, Carbonsäure- und Cysteingruppen funktionalisiert. Die Cysteinseitenketten wurden durch ein neues thiofunktionales Thiazolidin (Mercaptothiazolidin, FTz4Cys) erhalten. Ausgehend von Cystein und Aceton wurde zunächst das Dimethyl-substituierte Thiazolidin erhalten, welches daraufhin am Ring-Amin mit Essigsäureanhydrid und Ameisensäure formyliert wurde. Eine Verknüpfung wurde zunächst mit Isocyanat-funktionalem Thiazolidin an das Polyol Poly(glycidol) versucht. Dies war zwar möglich, jedoch wenig reproduzierbar. Als Alternativroute wurde die Carbonsäurefunktion des Thiazolidins mittels CDI aktiviert und anschließend mit Cysteamin umgesetzt. Hierbei bildete sich das niedermolekulare kristalline thiofunktionale Thiazolidin (FTz4Cys), welches mittels Thiol-En-Click Chemie an allyl-funktionales Poly(glycidol) geknüpft werden konnte. Eine systematische Untersuchungen der thermischen und UV-induzierten Thiol-En-Click Chemie zeigte, dass wesentlich höhere Umsätze und Geschwindigkeiten bei der photoinduzierten Reaktion erhalten werden. Bei der Verwendung der photosensiblen Substanz DMPA reichte die Bestrahlungszeit von 30 min mit den eingesetzten UV-LEDs aus um bei einem Verhältnis von Thiol:Allyl:DMPA = 3.5:1:0.5 einen vollständigen Umsatz der Allylgruppen zu erhalten. Mittels 0.1 M HCl konnte bei 70 °C innerhalb von 5 d die Hydrolyse der Thiazolidine im Anschluss erreicht werden. Nach der anschließenden Dialyse der Polymere gegen 0.1 M Essigsäure wurde erfolgreich das Acetatsalz der cysteine-funktionalen Poly(glycidol)e erhalten. Diese waren hinsichtlich der

Thioloxidation unter atmosphärischen Bedingungen stabil. Ein oxidativer TNSBA-Assay wurde entwickelt, um die Menge der Cysteine zu quantifizieren und gleichzeitig den störenden Einfluss der Thiole zu unterbinden. Ein Kooperationspartner setzte die cysteinfunktionalisierten Poly(glycidol)e mit C-terminalen Thioestern um und konnte die gute Zugänglichkeit und Aktivität der Cysteine entlang des Polymerrückgrats nachweisen. SDS-PAGE, HPLC und MALDI-ToF Messungen bestätigten die erfolgreiche Konjugation im Anschluss.

In der Zukunft sind die cysteinfunktionalen Poly(glycidol)e vielversprechende Kandidaten für die Bildung von Hydrogelen mittels Oxidation. Wie bereits für thiolefunktionale Poly(glycidol)e gezeigt wurde, können durch Oxidation Nanogele gebildet werden.[83, 111] Hierbei sollten die nun darstellbaren esterfreien Nanogele eine potentiell längere Stabilität aufweisen und für den zielgerichteten Wirkstofftransport anwendbar sein. Die zusätzlichen Aminfunktionen erlauben weiterhin eine Protonierung und somit die Ausbildung von Komplexen mit Polyanionen, wie beispielsweise DNA. Diese Komplexe sind ebenfalls interessant für den zielgerichteten Wirkstofftransport. Poly(glycidol)e mit α,β -Aminothiolfunktionen erlauben die Kombination aus redoxsensitivem Verhalten durch die Thiole in Kombination mit dem pH-sensitiven Verhalten der Amine innerhalb der Nanogele. Hierdurch könnte es zu einem schnelleren Gelabbau durch die repulsiven Wechselwirkung der geladenen Amine kommen. Reduktivere und saurere Tumorumgebungen sind daher vielversprechende Ziele der Partikel. Native Chemical Ligation-zugängliche cysteinfunktionale Poly(glycidol)e sind ebenfalls vielversprechende Kandidaten für die chemoselektive und stabile Konjugation mehrerer Proteinen entlang eines Polymers um beispielsweise Multivalenzeffekte mit relevanten Peptiden zu untersuchen.

5. Experimental Section

5.1. Materials and Methods

Acetic acid (VWR, p.a.), acetic acid anhydride (>98%, VWR), benzyl chlorid (BzCl) (Merck Schuchardt, for synthesis), cesium hydroxide monohydrate (Sigma-Aldrich), chloroform (VWR, p.a.), deuterated chloroform CDCl₃ (Deutero GmbH, Kastellaun, Germany), cysteamine·HCl (AppliChem), 1,8-diazabicyclo[5.4.0]undec-7-ene (DBU) (Merck Schuchardt, for synthesis), 2,2-dimethoxy-2-phenyl acetophenone (99%, Sigma-Aldrich), N,N-dimethylformamide (>99.8 %, anhydrous, Sigma-Aldrich), diphenylphosphoryl azide (97 %, Sigma-Aldrich), dipotassium phosphate (p.a., Merck), 5,5'-dithiobis(2-nitro-benzoic acid) (99 %, Sigma-Aldrich), dithiothreitol (DTT) (Sigma-Aldrich, >99 %), DMSO-*d*₆ (Deutero GmbH, Kastellaun, Germany), D₂O (Deutero GmbH, Kastellaun, Germany), ethanol (absolute, >99.8 %, Sigma-Aldrich), ethyl acetate (>99.5 %, Merck, Darmstadt, Germany), formic acid (≥98 %, Sigma-Aldrich), HCl (32%, Merck), isopropanol (Sigma-Aldrich, puriss, p.a.), methanol (p.a., VWR), magnesium sulfate (Merck, p.a.), methyl acrylate (BASF, stab.), N,N-carbonyldiimidazol (reagent grade, Sigma-Aldrich), poly(ethylene glycol) methyl ether acrylate (mPEG480Ac) (Sigma-Aldrich), potassium chloride (p.a., Merck), potassium dihydrogen phosphate (p.a., Merck), potassium *tert*-butoxide (1 M in THF, anhydrous, Sigma-Aldrich), potassium thiocyanate (KSCN) (Grüssing, anal. grade), pyridine (≥99.8%, anhydrous, Sigma-Aldrich), sodium chloride (p.a., Merck), sodium formate (>99.0%, Sigma-Aldrich), thioacetic acid (96 %, Sigma-Aldrich), thioglycolic acid (≥99 %, Sigma-Aldrich), 2,4,6-trinitrobenzene sulfonic acid (TNBSA, Thermo Scientific, 5 w/v in methanol), were used without further purification. Tetrahydrofuran (Fisher Scientific, Schwerte, Germany) for polymerizations was dried over molecular sieve (3 Å). Ethyl vinyl ether (99%, KOH stabilized, Sigma-Aldrich), Glycidol (96 %, Sigma-Aldrich) and *p*-Toluene sulfonic acid monohydrate (>98.5%, Sigma-Aldrich) were used for the synthesis of EEGE according to Fitton et al.[58] EEGE was purified by distillation and dried over CaH₂ (92 %, ABCR, Karlsruhe, Germany). Allyl glycidyl ether (≥99 %, Sigma-Aldrich) was also dried with CaH₂ (ABCR). Thiophenol (Sigma-Aldrich, ≥ 99 %), butanethiol (Sigma-Aldrich), mercaptoethanol (Acros, 99 % extra pure) were recondensed under argon atmosphere before use and stored under argon.

NMR-spectroscopy: ¹H and ¹³C spectra were recorded on two different spectrometers. First, ¹H and ¹³C spectra were recorded on a Bruker Fourier 300 at 300 MHz and 75 MHz, respectively. Deuterated chloroform (CDCl₃), dimethyl sulfoxide (DMSO-*d*₆) and deuterated

water (D₂O) spectra were recorded with non-deuterated solvent signals as internal reference. Second a Bruker Avance 400 was used for ¹H and ¹³C-measurements at 400 MHz and 100 MHz, respectively. Deuterated chloroform (CDCl₃) and dimethyl sulfoxide (DMSO-*d*₆) were used with tetramethylsilane (TMS) as internal reference. Deuterated water (D₂O) spectra were recorded without internal reference. The following abbreviations were used: s: singlet; d: doublet; t, triplet; q: quartet; quin: quintet; sex: sextet; br: broad; m: multiplet.

SEC-measurements: Two SEC-systems were used. First THF was used as solvent with a flow rate of 1.0 mL/min and a high-pressure liquid chromatography pump (Jasco PU-2080Plus), refractive index detector (Jasco RI-2031Plus) and PSS SDVlinear M column (length = 300 mm, width = 8 mm, particle size = 5 μm). For calibration, polystyrene standards (PSS) were used. A concentration of ca. 5 mg mL⁻¹ was prepared and filtered through a syringe filter (PTFE) with 0.02 μm pore size. Second SEC measurements were performed on a *Polymer Standard Service System* (PSS, Mainz, Germany) based on the Agilent Infinity 1260 SEC-System equipped with MDS RI detector (used) and MDS viscometer (not used). The columns were an 80 mm GRAM precolumn; GRAM column 1: 300x8 mm, 10 μm particle size, 30 Å porosity, 100 – 10 000 Da; Column 2: 300x8 mm, 10 μm particle size, 1000 Å porosity, 1000 – 1 000 000 Da. The columns were heated to 40 °C in a column oven. DMF equipped with 1 g/L LiBr was used as eluent and the flow rate was 1 ml/min. Calibration was performed using PEG standards between 982 g mol⁻¹ and 220,000 g mol⁻¹. Sample concentrations were ca. 5 mg/mL in the eluent and filtered through a syringe filter (0.2 μm PTFE) prior to analysis.

Dynamic light scattering experiments were performed with a N5 Submicron Particle Size Analyzer from Beckmann Coulter, Miami, FL, USA. The light source was a He-Ne Laser with 632.8 nm wavelength and an intensity of 25 mW with a detection angle of 90 °C at RT.

Cryo-SEM measurements were performed in Aachen, Germany at the DWI – Leibniz Institute for Interactive Materials (former: DWI), Forckenbeckstr. 50. The measurements were performed by Dr. Smriti Singh with a HITACHI S-4800 instrument in a cryo-mode with secondary electron image resolution of 1.0 nm at 15 kV, 2.0 nm at 1 kV and 1.4 nm at 1 kV with beam. The material was fixed on a holder and rapidly frozen with liquid nitrogen. It was then transferred to the high vacuum cryo-unit, the Balzers BF type freeze etching chamber. The cryo-chamber equipped with a knife can be handled from outside by means

of a lever to cryo etch the sample. The cryo etching enables the imaging of inner surface structures in water. In order to remove humidity, the sample was sublimated from 5 to 15 min at 95°C and then the entire material was further inserted into the observation chamber.

X-Ray crystal structure measurements were performed by Ana-Maria Krause in the group of Prof. Frank Würthner, University of Würzburg, Germany. The data were recorded on a Bruker X8 APEX diffractometer with a CCD area detector, using graphite monochromatized MoK α radiation. The structure was solved with Direct Methods, and expanded by means of Fourier techniques with the SHELX software package.

Raman Spectroscopy: Raman spectra were recorded at DWI, Leibniz-Institute for Interactive Materials, Forckenbeckstr. 50, Aachen, Germany on a Bruker RFS 100/S spectrometer. The laser used was Nd:YAG at 1064 nm wavelength at a power of 250 mW. On an average 1000 scans were taken at a resolution of 4 cm⁻¹. For sample holding, aluminium pans of 2 mm bore were used. Software used for data processing was OPUS 4.0.

UV irradiation for thiol-ene reactions were either performed with UV-LEDs obtained by Polymerschmiede (Aachen, Germany) having 4 UV-LED cubes with 11 W (each) and a wavelength of 365 nm or with a Rayonet RMR-200 photoreactor having 16 UV-lamps with each having 35 W.

UV-Vis absorbance measurements were performed on a Genesys 10S Bio Spectrophotometer at room temperature using a wavelength of 335 nm for TNBSA assay and 412 nm for Ellman assay.

MALDI measurements[#] were performed with an AB SCIEX 5800 TOF/TOF System (Applied Biosystems) with nanoLC (Dionex) and robotic system for spotting (Probot, Dionex) and 4700 Proteomics Analyzer (Applied Biosystems). A saturated solution of sinapinic acid in TA30 solvent (30:70 [v/v] acetonitrile:0.1% TFA in water) was prepared and 1 μ l of this solution added to 1 μ l water with 0.1% TFA and 1 μ l of sample. Subsequently the mixture was carefully mixed by pipetting and spotted. Analysis was performed in the linear positive ion mode. For each spectrum 5000 consecutive laser shots were accumulated and data was analyzed by Data Explorer software (Applied Biosystems).

Analytical HPLC measurements[#] were conducted on a Waters™ 600S controller system (Waters Corporation, Milford, Massachusetts, USA) with a 717 plus autosampler, 2 pumps 616 and a 2489 UV/Visible detector connected to a 3100 mass detector using a Kromasil C18 5 μm, 250 x 4.6 mm RP-HPLC-column with a flow rate of 1.0 mL/min. The following gradient of solvents was used: Method A: (A = H₂O + 0.1% TFA, B= MeCN + 0.1% TFA) 5 min at 10% B, 10 – 90% B from 5-36 min, 90% B from 36-45 min, 90-10% B in 45-50 min. HPLC chromatograms were recorded at 220 nm.

Preparative HPLC[#] was carried out on a JASCO LC-2000 Plus system (JASCO, Inc., Easton, Maryland, USA) using a reversed phase C18 column (Kromasil material) at a constant flow of 32 ml/min using water and acetonitrile with 0.1% TFA. This system was equipped with a Smartline Manager 5000 with interface module, two Smartline Pump 1000 HPLC pumps, a 6-port-3-channel injection valve with 1.0 mL loop, a UV detector (UV-2077) and a high pressure gradient mixer (All Knauer, Berlin, Germany). Purification was carried out after Method B: (A = H₂O + 0.1% TFA, B= MeCN + 0.1% TFA) 10% B 0-5 min, 10-70% B 5-70 min.

High resolution mass spectra[#] (HRMS) were measured on an Aquity UPLC system and a LCT Premier™ (Waters Micromass, Milford, MA, USA) time-of-flight (TOF) mass spectrometer with electrospray ionization (ESI) using water and acetonitrile (10-90% gradient) with 0.1% formic acid as eluent.

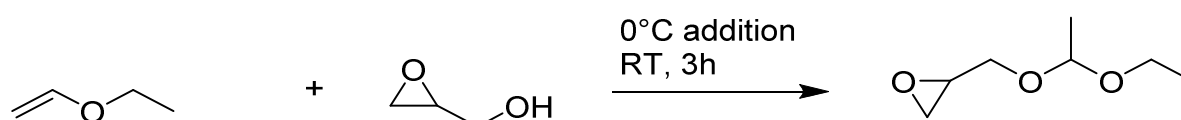
Tricin-SDS-Gelelectrophoresis was prepared according to [166].

Controlled-monomer addition was performed using the syringe pump Aladdin from World Precision Instruments, Sarasoto, FL, USA.

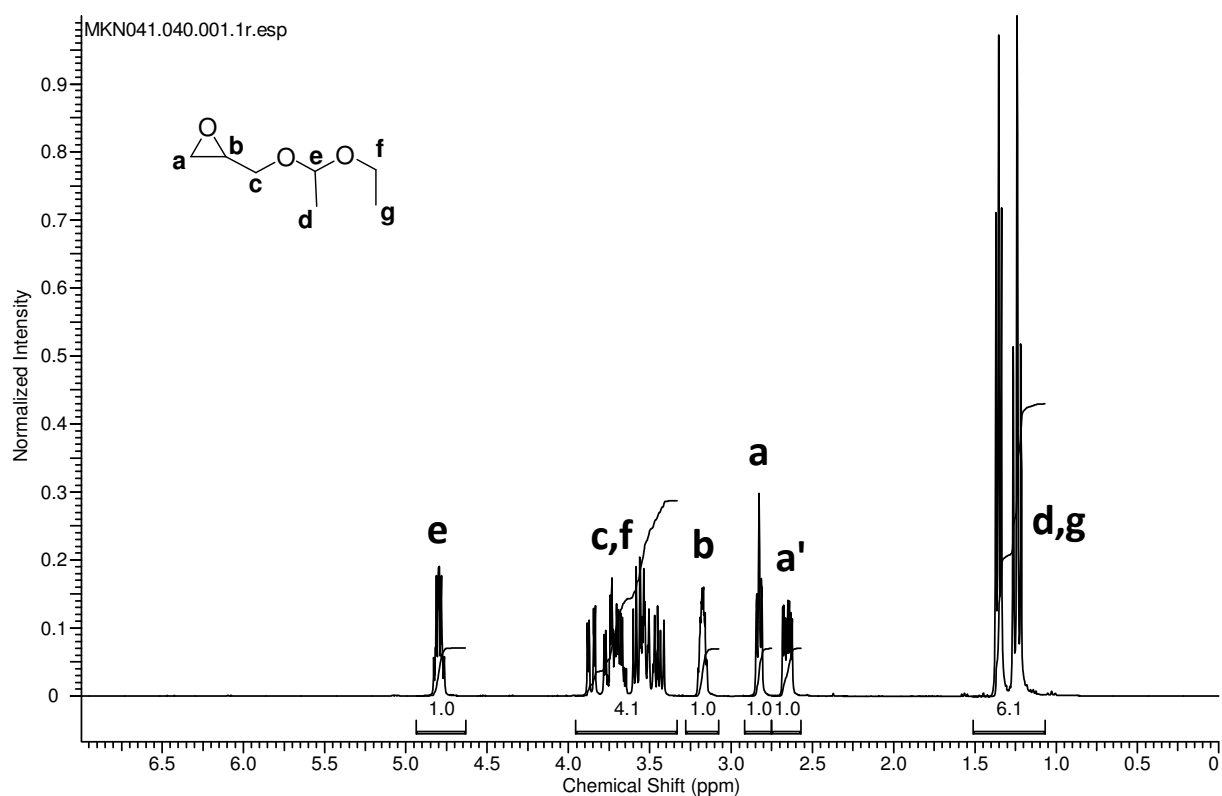
5.2. Syntheses

Parts of this chapter were already submitted for publication, but are neither yet accepted, nor published.

5.2.1. Ethoxy ethyl glycidyl ether



Glycidol (100 mL, 1.5 mol, 1.0 eq) was mixed with ethyl vinyl ether (600 mL, 6.2 mol, 4.1 eq) in a 1 L Erlenmeyer flask and cooled with an ice bath. *p*TsOH (2.058 g, 10.8 mmol) was slowly added, it was paid attention to keep the T inside of the solution below 20 °C. It was stirred 2 h at RT. Afterwards it was washed with saturated NaHCO₃ solution (3 x 100 mL). The organic phases were collected and dried with MgSO₄. It was filtered and starting with 45 °C and 900 mbar (finally at 45 °C and 150 mbar, membrane pump) the residual ethyl vinyl ether removed. Only small amounts of ethyl vinyl ether were left after evaporating with 100 °C and 20 mbar. Distillation was continued starting at 60 °C and 10⁻³ mbar. The first 10 mL of the distilled product were disposed. The following fractions were collected, dried with CaH₂ over night in flamedried flasks under argon atmosphere. A condensation bridge was used to condensate in a dried Schlenk-flask equipped with molecular sieve. For this the CaH₂/EEGE mixture was heated to 50 °C and reduced pressure applied (10⁻³ mbar). The collecting Schlenk-flask was cooled with N₂l.



^1H NMR (400 MHz, CDCl_3 , δ): 4.8 (1 H, m, e), 3.9-3.4 (4 H, m, c + f), 3.17 (1 H, m, b), 2.83 (1 H, m, a), 2.65 (1 H, m, a'), 1.4-1.2 (6 H, 2xt, d+g) ppm.

5.2.2. Cesium initiator preparation for IROP of glycidyl ethers

Argon flushed dried Schlenk-tube was used for the preparation of the initiator. CsOH (28.6 mg, 0.170 mmol, 0.95 eq.) was placed in the Schlenktube. Benzene (354 μL) was added. It was stirred under argon for 5 min. Triethyleneglycol monomethylether (TEGME, 28 μL , 179 mmol, 1.0 eq) was added under argon stream. The flask was sealed and it was heated to 60 $^\circ\text{C}$ for 60 min. The solution turned slightly brownish/yellowish. The flask was frozen with N_2 to reduced splashing upon applying vacuum. 10^{-3} mbar vacuum were applied, the flask slowly heated to RT and finally inserted into a 90 $^\circ\text{C}$ oil bath. The flask was evacuated at 90 $^\circ\text{C}$ overnight. The flask was sealed and stored into a glovebox. Depending on the initiator system, a different alcohol was used.

5.2.3. Kinetics of glycidyl ether polymerizations

THF (117 μL , dry) were added to the initiator and the initiator was dissolved as good as possible. Cs^+ /TEGME-alkoxide was almost completely dissolvable and slightly yellow. EEGE (1.308 mL, 8.95 mmol, 50 eq.) was added and shaken for 2 min at RT. 50 μL samples were

placed into each of the 13 Eppendorf caps (intended for 13 data points) equipped with stirring bars. The caps were placed into a 45 °C warm oven equipped with a magnetic stirrer. To quench the content of a cap, CDCl₃ (650 μL, 1% EtOH) was added and ¹H NMR measurements performed.

For bulk reactions, the monomer was directly added in the glovebox after drying of the initiator overnight. The initiator was dissolved in the monomer inside of the fridge, to slow down polymerization. After dissolution of the initiator the aliquotation of the solution was performed into the Eppendorf caps.

All experiments performed with the Eppendorf-caps for investigation of the kinetics are given below in Table 21 and Table 22.

For SEC measurements the whole content of the NMR tube was used, the solvent evaporated at RT in the fumehood and the residual mixture dissolved in 2 mL DMF (1 g/L LiBr; mobile phase of SEC system). SEC measurements were performed in DMF (1 g/L LiBr) on a *Polymer Standard Service* (PSS, Mainz, Germany)-SEC system (MDS RI Detector) with a 8 cm Gram pre-column (10 μm particle size) and two 30 cm (10 μm particle size) Gram columns. The column oven was at 40 °C. All samples were filtered through a 0.2 μm syringe filter prior to SEC analysis. The SEC-system was calibrated with PEG (PSS, Mainz, Germany) standards.

Table 21: Polymerizations performed with potassium as counter ion.

#	Monomer	Volume [mL]	Quantity [mmol]	[M]:[I]	THF [mL]	Initiator [mmol]	C _{Monomer} [mmol/mL]	M _n [g mol ⁻¹] (Conversion)	Đ (M _w /M _n)	k [10 ⁻⁴ s ⁻¹]
MKN054	EEGE	1.600	10.62	20	0.530	0.53	6.4	1838	1.17	4.3
MKN050	EEGE	2.000	13.68	50	0.274	0.274	6.0	3186 (92 %)	1.17	2.6
MKN051	EEGE	2.000	13.68	50	0.374	0.274	5.8	2451 (41 %)	1.18	<i>n.d.</i>
MKN055	AGE	1.570	13.8	20	0.690	0.69	8.4	1912	1.26	4.5
MKN053	AGE			50	THF			3744 (98 %)	1.38	3.4
MKN059	EEGE:AGE (45:5)	1.600:0.143	10.95:1.22	50	0.243	0.243	6.1	3205	1.21	3.3
MKN068KE	EEGE	1.118	7.65	50	<i>bulk</i>	0.153	"6.8"	4794 (95 %)	1.22	1.45
MKN068KA	AGE	0.900	7.65	50	<i>bulk</i>	0.153	"8.5"	5416 (99 %)	1.57	2.77
MKN068KEA	EEGE:AGE (45:5)	1.006:0.090	7.65	50	<i>bulk</i>	0.153	"7.0"	5039 (94 %)	1.24	1.4

Table 22: Polymerizations performed with cesium as counter ion.

#	Monomer	Volume [mL]	Quantity [mmol]	[M]/[I]	solvent [mL]	Initiator [mmol]	C _{Monomer} [mmol/mL]	M _n [g mol ⁻¹] (Conversion)	Đ (M _w /M _n)	k _{app} [10 ⁻⁴ s ⁻¹]
MKN044	EEGE:AGE =50:5	1.920:0.150	14.3	50:5	bulk	Cs ⁺ /benzyl alkoxide (Cs:Bz=0.97:1)	6.9			<i>n.d.</i>
MKN046	EEGE	2.123	15	50	bulk	Cs ⁺ /benzyl alkoxide (Cs:Bz=1:1.05)	7.1			<i>n.d.</i>
MKN049	EEGE	1.721	11.8	47	bulk	Cs ⁺ /benzyl alkoxide (Cs:Bz=1:1.05)	6.9	3947	1.17	5.8
MKN056	AGE	1.900	16.15	50	bulk	Cs ⁺ /benzyl alkoxide (Cs:Bz=1:1.05)				<i>n.d.</i>
MKN057	EEGE:AGE =45:5	1.848:0.157	13.99	45:5	bulk	Cs ⁺ /benzyl alkoxide (Cs:Bz=1:1.05)		4931 (95 %)	1.28	1.65
MKN058	EEGE:AGE =45:5	1.987:0.169	15,03	45:5	THF 0.294	Cs ⁺ /benzyl alkoxide (Cs:Bz=1:1.05)	6.1	3377 (91 %)	1.22	0.78
MKN060	AGE	1.485	12.62	50	DMF 0.450	Cs ⁺ /benzyl alkoxide (Cs:Bz=1:1.05)	6.5	2597 (78 %)	1.26	1.1 than 0.4

#	Monomer	Volume [mL]	Quantity [mmol]	[M]/[I]	solvent [mL]	Initiator [mmol]	C _{Monomer} [mmol/mL]	M _n [g mol ⁻¹] (Conversion)	Đ (M _w /M _n)	k [10 ⁻⁴ s ⁻¹]
MKN061	EEGE	2.134	14.60	53	THF	Cs ⁺ /mPEG500-alkoxide (Cs:mPEG500=1:1.05)	5.65	2696 (92%)	1.11	1.25
MKN062	AGE	1.330	11.30	50	THF	Cs ⁺ /mPEG500-alkoxide (Cs:mPGE500=1:1.05)	7.0	1575 (79%)	1.13	0.37
MKN064	EEGE	1.849	12.65	50	THF	Cs/phenoxyethanolate (Cs:phenoxyethanolate=1:1.05)	5.4	2500	1.13	<i>n.d.</i>
MKN065	EEGE	1.308	8.95	50	THF	Cs ⁺ /TEGME-alkoxide (Cs:TEGME=0.95:1)	6.3	3013	1.13	0.95
MKN066	AGE	1.127	9.87	50	THF	Cs ⁺ /TEGME-alkoxide (Cs:TEGME=0.95:1)	7,9	2790	1.21	13
MKN067	EEGE	1.462	10	50	THF	Cs ⁺ /TEGME-alkoxide (Cs:TEGME=0.95:1)		2985 (67%)	1.15	
MKN067	AGE	1.176	10	50	THF	Cs ⁺ /TEGME-alkoxide (Cs:TEGME=0.95:1)		2786 (54%)	1.14	
MKN067	EEGE:AGE 45:5	1.316:0.118	9:1	50	THF	Cs ⁺ /TEGME-alkoxide (Cs:TEGME=0.95:1)		3553 (69%)	1.14	
MKN068	EEGE	1.118	7.65	50	<i>bulk</i>	Cs ⁺ /TEGME-alkoxide (Cs:TEGME=0.95:1)	6.8	3658 (93%)	1.13	1.26
MKN068CsA	AGE	0.900	7.65	50	<i>bulk</i>	Cs ⁺ /TEGME-alkoxide (Cs:TEGME=0.95:1)	8.5	2337 (67%)	1.19	0.3
MKN068CsEA	EEGE:AGE 45:5	1.006:0.090	6.885:0.765	50	<i>bulk</i>	Cs ⁺ /TEGME-alkoxide (Cs:TEGME=0.95:1)	7.0	3411 (87%)	1.16	0.7

5.2.4. Synthesis of the polymers via slow monomer addition

5, 10 or 25 mL flask were used for all syntheses. The flask were equipped with a stirring bar and heated with a heating gun ($T=400\text{ }^{\circ}\text{C}$). Hot flasks were introduced into the glovebox double-door system and evacuation started. Evacuation–flushing (N_2) cycle was repeated twice and the last evacuation proceeded for 30 min. Afterwards, the flask were introduced into the glovebox. KOtBu ($100\text{ }\mu\text{L}$, 1 M in THF) was introduced into the flask and sealed with a rubber septum. A 1 mL syringe (inner diameter 4.7 mm) was equipped with a needle ($100\text{ Sterican}^{\circledR}$, $0.4\times 25\text{ mm}$, $27\text{G } \times 1''$, B. Braun) and filled with monomer. All atmospheric bubbles in the syringe were removed and the syringe filled with approx. $100\text{ }\mu\text{L}$ more monomer than calculated. It was paid attention that the needle and syringe are completely filled with monomer to rule out dead volume. Assembled flask and syringe, by puncturing the septum with the needle, were wrapped with parafilm[®] to fix the syringe and needle to the flask and enhance air-tightness. The syringe was assembled in the syringe pump and the syringe pump programmed from $50 - 5000\text{ }\mu\text{L h}^{-1}$ with an inner syringe diameter of 4.7 mm and total addition volume of $731\text{ }\mu\text{L}$ (EEGE) or $570\text{ }\mu\text{L}$ (AGE). After complete monomer addition the syringe was removed and the parafilm[®] used to cover the punctured site. Either in an oil bath ($45\text{ }^{\circ}\text{C}$) or an incubator ($45\text{ }^{\circ}\text{C}$) it was stirred for at least 20 h without termination and workup the samples were directly analyzed by $^1\text{H-NMR}$ (confirming full conversion) and SEC (determination of M_n , and Đ). All $^1\text{H-NMR}$ and ^{13}C were in accordance with the literature.[69]

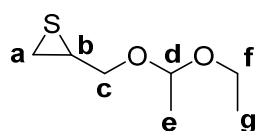
Parts of the following syntheses were already published in

M. Kuhlmann, S. Singh, J. Groll, Controlled Ring-Opening Polymerization of Substituted Episulfides for Side-Chain Functional Polysulfide-Based Amphiphiles, *Macromolecular Rapid Communications*, 33 (2012) 1482-1486.

5.2.5. Ethoxy ethyl thioglycidyl ether

The group of Spassky already described the synthesis of EETGE.[7] Briefly, EEGE (20 mL , 137 mmol) was dissolved in isopropanol (400 mL). KSCN (20 g , 206 mmol) was crushed prior to use and suspended. It was stirred for 7 days at room temperature (RT). Filtration and removal of the solvent gave a yellow liquid. If the transformation of the epoxide to the

episulfide was incompletely, determined by ^1H NMR, the EEGE/EETGE mixture was again dissolved in isopropanol and treated with an excess of KSCN until EEGE could no longer be detected by ^1H -NMR spectroscopy. After filtration, the solvent was removed under reduced pressure, taken up in DCM (50 mL) and filtered again. After removal of the solvent, the slightly yellow solution was further fractionally distilled (main fraction 90 °C, 5 mbar) to obtain a colourless and clear monomer. 7.0 g, Yield 31 %.



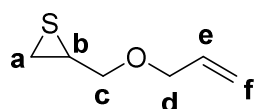
^1H NMR (400 MHz, CDCl_3 , δ): 4.56 - 4.82 (1H, m, H^{d}), 3.31 - 3.77 (4H, m, H^{c} , H^{f}), 2.92 - 3.10 (1H, quin, H^{b}), 2.38 - 2.51 (1H, d, H^{a}), 2.07 - 2.21 (1H, m, H^{a}), 1.19 - 1.33 (3H, d, H^{e}), 1.05 - 1.19 (3H, t, H^{g}) ppm.

$M = 162.25 \text{ g mol}^{-1}$

^{13}C NMR (100 MHz, CDCl_3 , δ): 98.98 (C^{d}), 69.42 (C^{c}), 60.17 (C^{f}), 33.22 (C^{b}), 23.73 (C^{a}), 19.80 (C^{e}), 15.14 (C^{g}) ppm.

5.2.6. Allyl thioglycidyl ether

ATGE was synthesized via the same procedure as was described for ethoxy ethyl thioglycidyl ether. After removal of the main fraction of isopropanol the crude product was fractionally distilled. The main product was obtained at 90 °C, 9 mbar. Yield: 35 % (Literature: 59 °C, 4 mmHg \approx 5 mbar, 54 % yield.[89])



$M = 130.20 \text{ g mol}^{-1}$

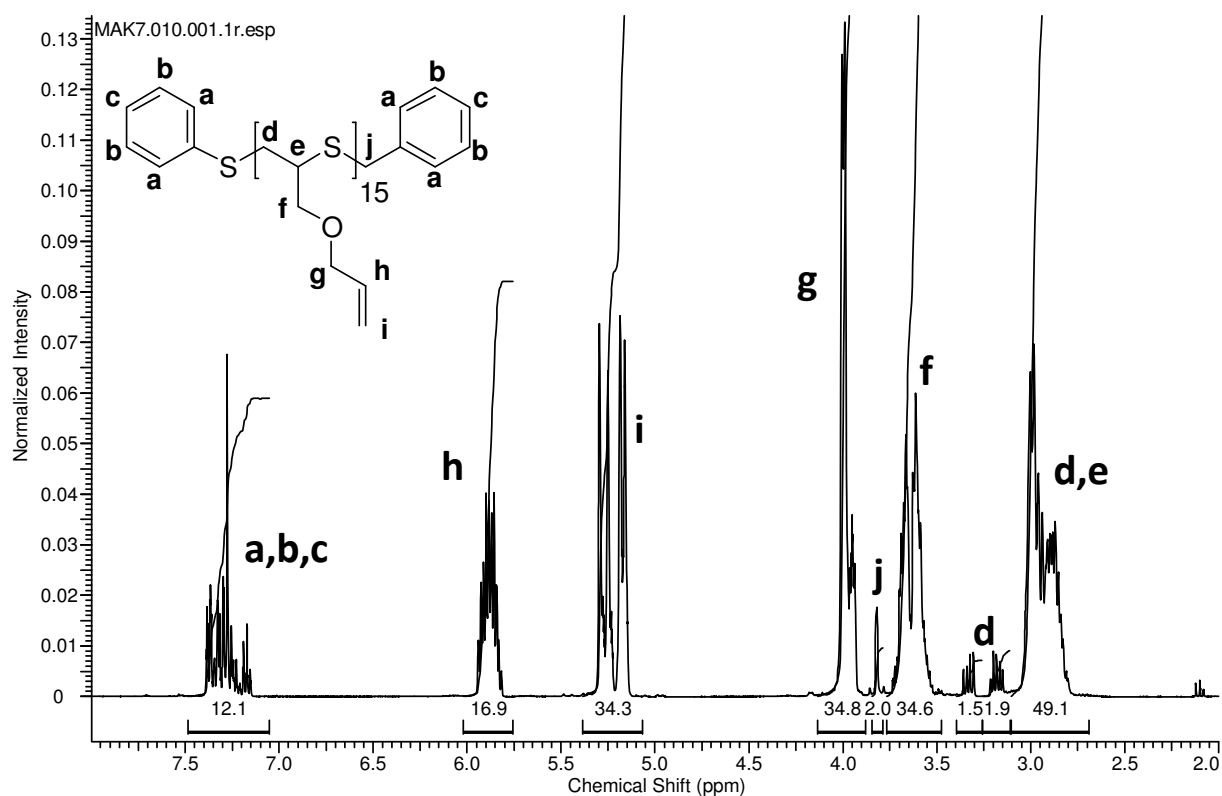
^1H NMR (400 MHz, CDCl_3 , δ): 5.84 - 5.98 (1H, m, H^{e}), 5.15 - 5.34 (2H, m, H^{f}), 3.99 - 4.10 (2H, d, H^{d}), 3.59 - 3.69 (1H, ddd, H^{b}), 3.40 - 3.51 (1H, dd, H^{a}), 3.02 - 3.13 (1H, m, H^{a}), 2.47 - 2.56 (1H, d, H^{c}), 2.16 - 2.25 (1H, d, H^{c}) ppm.

^{13}C NMR (100 MHz, CDCl_3 , δ): 134.5 (C^{e}), 117.4 (C^{f}), 74.7 (C^{c}), 72.0 (C^{d}), 32.1 (C^{b}), 23.8 (C^{a}) ppm.

5.2.7. Homopolymerization of ATGE with thiophenol/DBU.

A Schlenk flask, flushed with N_2 , was equipped with a degassed solution of 1,8-diazabicyclo[5.4.0]-undecen (DBU) in DMF (0.5 M, 2 mL, 1 mmol, 1.0 eq). The solution was frozen. Under N_2 -atmosphere thiophenol (0.1 mL, 1 mmol, 1.0 eq) was added. Afterwards the solution was further frozen with liquid N_2 and the flask evacuated ($5.6 \cdot 10^{-2}$ mbar, 1 h). The flask was flushed with N_2 and warmed up to RT. The flask was frozen again with liquid

nitrogen and evacuated for 1 h. This *freeze-pump-thaw* cycle was repeated again and finally the flask warmed up to RT under nitrogen atmosphere. ATGE (2 mL, 15 mmol, [M]:[I]=15) was added. The solution immediately warmed up and after 30 min no further heating was observed. It was stirred for 3 h. A degassed solution of benzyl chloride in DMF (1M, 2 mL, 2 mmol, 2 eq. wrt. initiator) was added and stirred for 2 h. Removal of DMF with vacuum and an external cooling trap was performed. The residual oil was dissolved in CHCl₃ and precipitated in MeOH (2x, each 400 mL). The precipitate was dissolved in CHCl₃ and the solvent removed under reduced pressure at 40 °C (Rotovap).



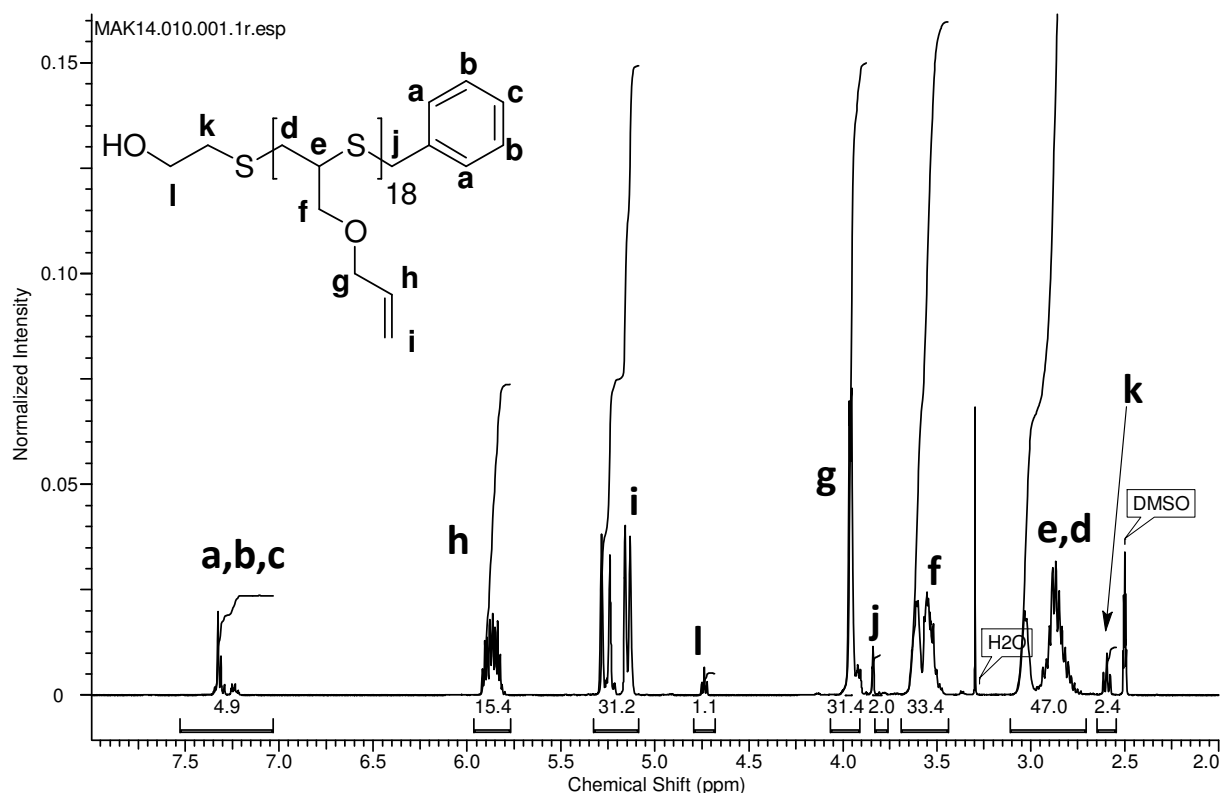
¹H NMR (400 MHz, CDCl₃, δ): 7.07 - 7.49 (10H, m, H^{a,b,c}), 5.72 - 6.02 (17H, m, H^h), 5.01 - 5.40 (34H, m, Hⁱ), 3.88 - 4.11 (34H, m, H^g), 3.75 - 3.88 (2H, s, H^j), 3.47 - 3.75 (34H, br, H^f), 3.25 - 3.40 (1H, dd, H^d, 1st repeating unit), 3.11 - 3.25 (1H, dd, H^e, 1st repeating unit), 2.70 - 3.11 (51H, br, H^d+H^e) ppm.

SEC (THF, poly(styrene)) M_n = 2200 g mol⁻¹, M_w = 2500 g mol⁻¹, Đ = 1.1, shoulder at twice the molar-mass.

M_{calc} = 2413.7 g mol⁻¹

5.2.9. Homopolymerization of ATGE with mercaptoethanol/DBU

A DBU solution (0.05 M in DMF, 7 mL, 0.35 mmol, 1.0 eq.) was degassed by purging 30 min N₂ through the solvent. A degassed mercaptoethanol solution (0.1 M in DMF, 3.5 mL, 0.35 mmol, 1.0 eq) was added. It was stirred for 10 min at RT. Degassed ATGE (1 mL, 6.3 mmol, 18 eq.) was added. It was stirred overnight and a benzyl chloride solution (1.4 M in DMF, 0.4 mL, 0.7 mmol, 2 eq) was added. It was stirred for 1 d and all volatile components removed under reduced pressure. It was dissolved in a small amount of EtOH and precipitated in MeOH.



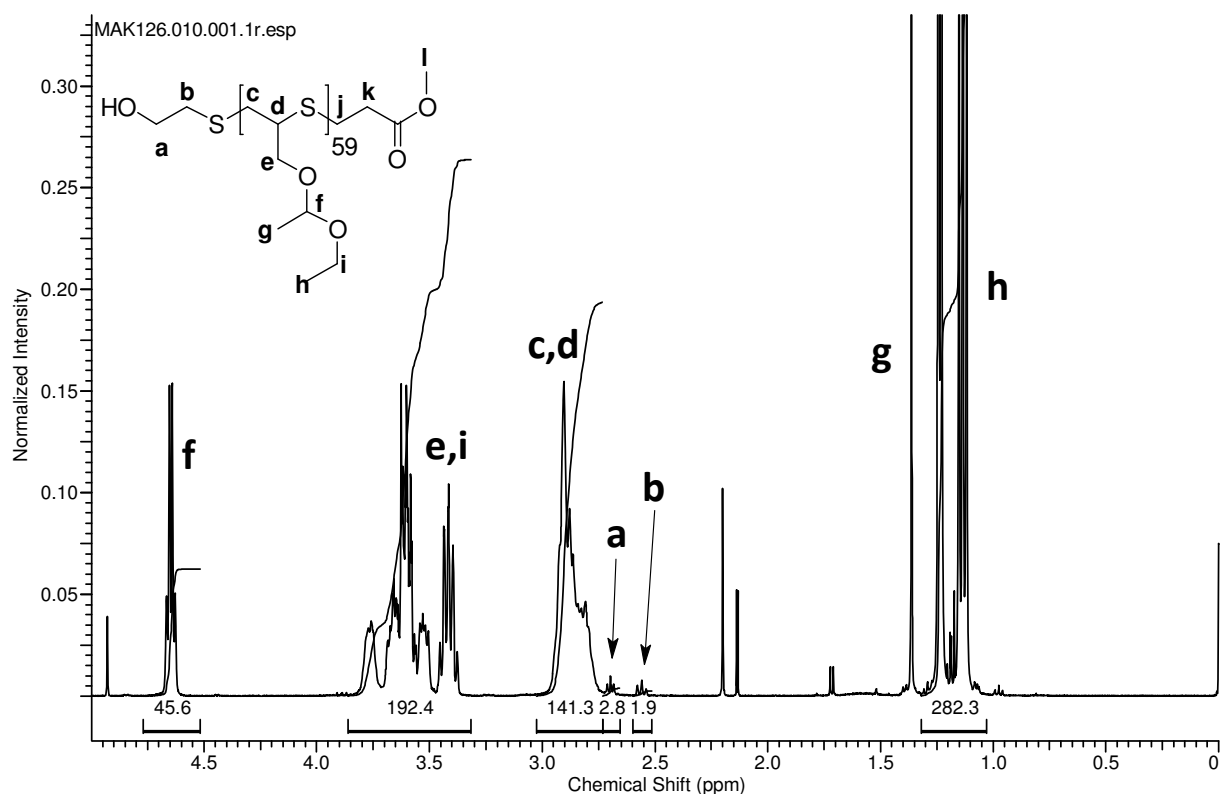
¹H NMR (400 MHz, DMSO-*d*₆, δ): 7.14 - 7.43 (5, m, H^{a,b,c}), 5.73 - 5.98 (15, m, H^h), 5.01 - 5.35 (30H, 2xd, Hⁱ), 4.66 - 4.79 (2H, t, H^l), 3.88 - 4.05 (30H, m, H^g), 3.79 - 3.88 (2H, s, H^j), 3.42 - 3.69 (30H, m, H^f), 3.24 - 3.34 (2), 2.70 - 3.10 (45H, m, H^{e,d}), 2.55 - 2.65 (2H, t, H^k) ppm.

SEC (THF, poly(styrene)) M_n = 2300 g mol⁻¹ (DP=35), M_w = 2500 g mol⁻¹, Đ = 1.1, monomodal.

M_{calc} = 2920 g mol⁻¹

5.2.10. Poly(EETGE) terminated with methyl acrylate.

DBU was dissolved in DMF (8 μL DBU, 0.053 mmol, 0.9 eq., 5 mL DMF) cooled down to $-20\text{ }^{\circ}\text{C}$ and evacuated ($9 \cdot 10^{-3}$ mbar) for 1 h. EETGE was dissolved in DMF (0.5 mL, 3.08 mmol, 54 eq., 5 mL DMF) cooled down to $-20\text{ }^{\circ}\text{C}$ and evacuated for 1 h. DMF was degassed by purging N_2 through the solution and afterwards mercaptoethanol was added (4 μL , 0.057 mmol, 1.0 eq.). It was cooled down to $-20\text{ }^{\circ}\text{C}$ and evacuated for 1 h. The three solutions were combined and stirred at RT for 2 h. DMF was degassed and methyl acrylate added (0.3 mL, 3.31 mmol, 58 eq.). It was cooled down to $-20\text{ }^{\circ}\text{C}$ and evacuated for 5 min. The flask was sealed and it was stirred over night at RT. All volatile components were removed under reduced pressure, dissolved in a few mL THF and precipitated in methanol/ H_2O (3:1). It was decanted, dissolved in THF and the THF was removed under reduced pressure.



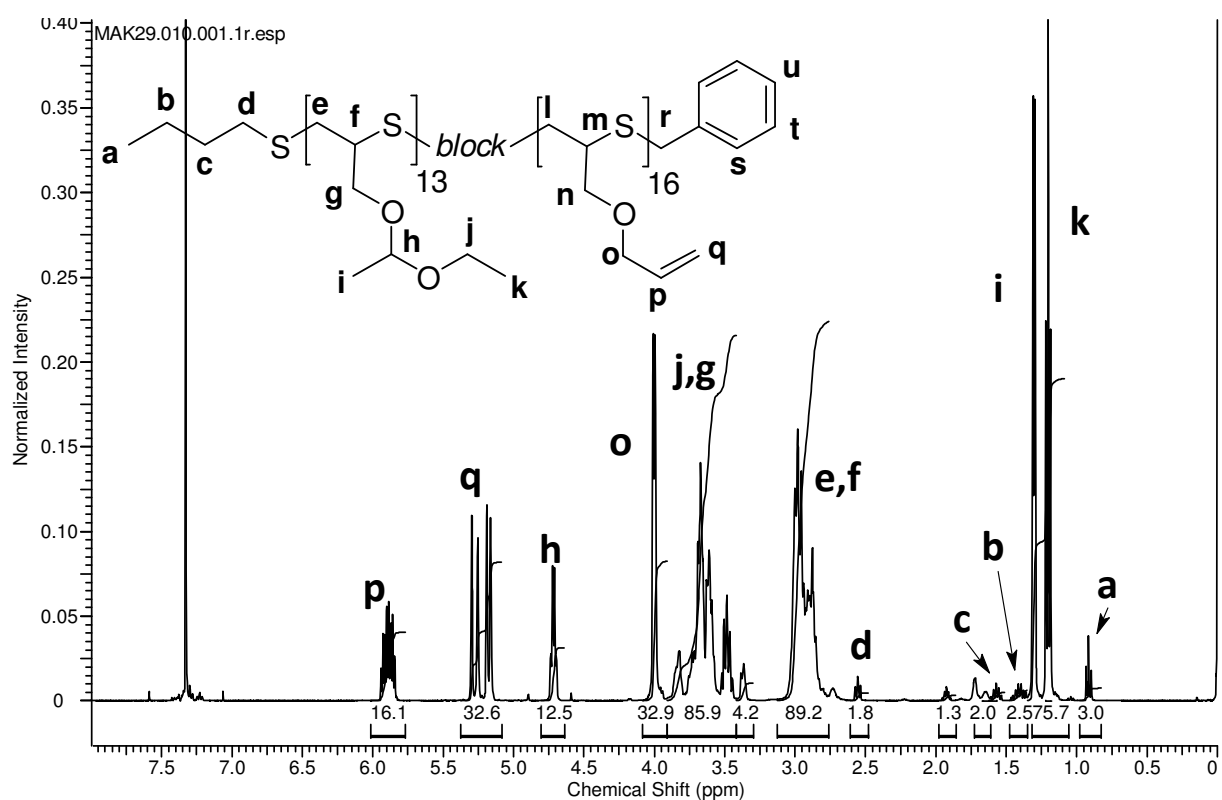
^1H NMR (400 MHz, CDCl_3 , δ): 4.52 - 4.77 (46H, m, H^f), 3.32 - 3.86 (192H, m, $\text{H}^{e,i}$), 2.73 - 3.03 (141H, $\text{H}^{c,d}$), 2.66 - 2.73 (3H, t, H^a), 2.51 - 2.60 (2H, t, H^b), 1.03 - 1.32 (282H, $\text{H}^{g,h}$) ppm.

SEC (THF, poly(styrene)) $M_n = 8200\text{ g mol}^{-1}$ (DP=51), $M_w = 8800\text{ g mol}^{-1}$, $D = 1.07$, bimodal.

$M_{\text{calc}} = 8926\text{ g mol}^{-1}$

5.2.11. Blockcopolymerization of EETGE and ATGE with butanethiol/DBU.

A degassed DBU solution (1M in DMF, 0.6 mL, 0.6 mmol, 1.0 eq) was placed in a flask flushed with N₂. A butanethiol solution was added (1M in DMF, 0.6 ml, 0.6 mmol, 1.0 eq.) and it was degassed by purging N₂ through the solution. Degassed DMF (3 mL) was added. EETGE (1.2 mL, 7.4 mmol, 12 eq) was added. It was stirred at RT for 3 h and ATGE (1.2 mL, 9 mmol, 15 eq) was added. It was stirred at RT for 2 h and a benzyl chloride solution (2 M in DMF, 0.6 mL, 2 eq.) added and stirred overnight. All volatile components were removed under reduced pressure and the polymer precipitated in THF:H₂O = 3:1 (400 mL).



¹H NMR (400 MHz, CDCl₃, δ): 5.77 - 6.01 (16H, m, H^j), 5.08 - 5.38 (33H, dd, Hⁱ), 4.64 - 4.80 (12H, q, H^h), 3.91 - 4.08 (33H, d, H^o), 3.42 - 3.91 (86H, br, H^{j,g}), 2.76 - 3.13 (89H, br, H^{e,f}), 2.48 - 2.61 (2H, H^d), 1.51 - 1.62 (2H, quin, H^c), 1.35 - 1.47 (3H, sex, H^b), 1.09 - 1.35 (76H, d + t, H^{i,k}), 0.82 - 0.98 (3H, h^a) ppm.

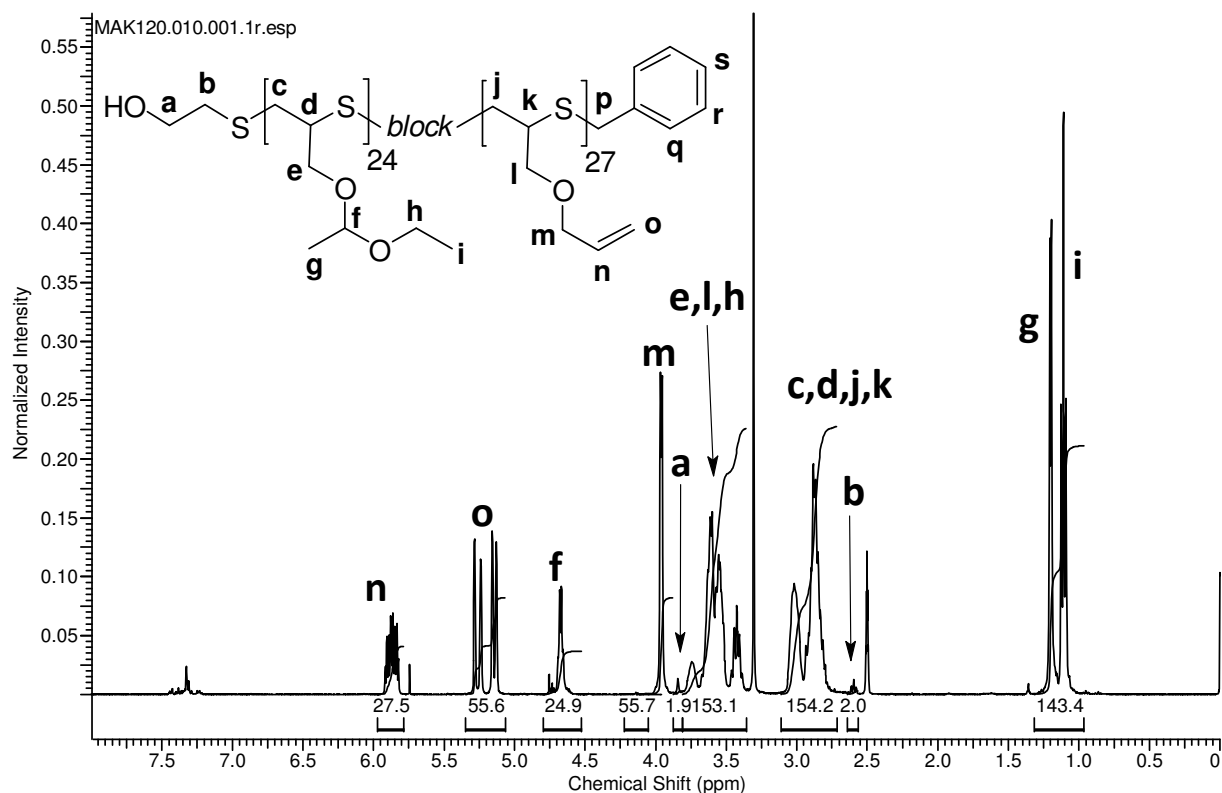
SEC (THF, poly(styrene)) M_n = 6500 g mol⁻¹ (DP=51), M_w = 8000 g mol⁻¹, Đ = 1.24, bimodal.

M_{calc} = 4586 g mol⁻¹

5.2.12. Blockcopolymerization of ATGE and EETGE with mercaptoethanol/DBU

Mercaptoethanol (5 μ L, 0.071 mmol, 1.0 eq) was dissolved in degassed DMF (purging with nitrogen, 2 mL). DBU (11 μ L, 0.074 mmol, 1.04 eq) was dissolved in degassed DMF (purging with nitrogen, 2 mL).

The mercaptoethanol solution was frozen with liquid N₂ and evacuated for 30 min. It was warmed up to RT under N₂ atmosphere, frozen again and evacuated for 30 min. The DBU solution was degassed again using 3 freeze-pump-thaw cycles. The DBU and mercaptoethanol solutions were mixed under N₂ atmosphere. It was stirred for 2 min, frozen and evacuated. ATGE (degassed, 0.3 mL, 2.31 mmol, 33 eq) was added, frozen and evacuated for 10 min. It was warmed up to 0 °C and stirred for 30 min. EETGE was added (0.33 mL, 2.03 mmol, 29 eq.), frozen and evacuated for 10 min. Cooled with an icebath it was stirred for 45 min under N₂ atmosphere. Degassed benzyl chloride (0.3 mL, 37 eq.) was added and stirred overnight. All volatile components were removed with vacuum and the polymer precipitated in MeOH.



¹H NMR (400 MHz, DMSO-*d*₆, δ): 5.79 - 5.97 (27H, m, Hⁿ), 5.07 - 5.34 (56H, dd, H^o), 4.53 - 4.80 (25H, q, H^f), 3.88 - 4.05 (56H, d, H^m), 3.81 - 3.88 (2H, t, H^a), 3.36 - 3.81 (153H, br, H^{e,l,h}),

2.72 - 3.11 (154H, br, H^{c,d,i,k}), 2.56 - 2.64 (2H, t, H^b), 0.96 - 1.32 (143H, d + t, H^{g,i}) ppm.

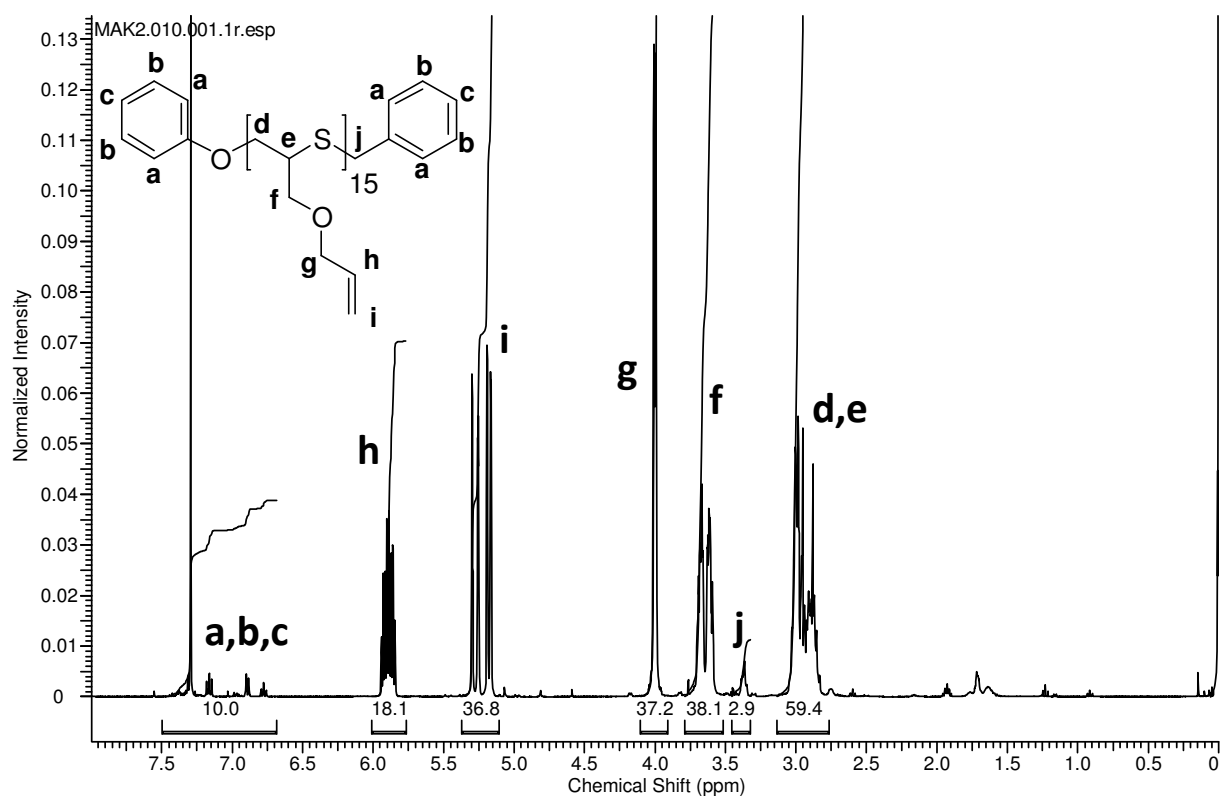
SEC (THF, poly(styrene)) $M_n = 9000 \text{ g mol}^{-1}$ (DP = 52), $M_w = 11000 \text{ g mol}^{-1}$, $\mathcal{D} = 1.21$, bimodal.

$M_{\text{calc}} = 7572 \text{ g mol}^{-1}$

5.2.13. Homopolymerization of ATGE with phenol/DBU as initiator.

Phenol (0.941 g, 10 mmol, 1 eq) was placed in a dry flask under N₂ atmosphere and was dissolved in DMF (10 mL), It was purged with N₂ for 10 min. DBU (0.75 mL, 5 mmol) was dissolved in DMF (9.25 mL) and purged with N₂ for 10 min. ATGE was purged with N₂ for 10 min and frozen with liquid nitrogen. It was evacuated to remove oxygen from the atmosphere. 3 *freeze-pump-thaw* cycles were performed with all flasks.

DBU solution (2 mL, 1 mmol, 1 eq), was placed in a dry flask with nitrogen atmosphere. Phenol solution (1 mL, 1 mmol, 1.0 eq) was added and stirred for 5 min at RT. It was shortly degassed by evacuating the solution until the solution started to bubble, than it was purged with nitrogen. ATGE (2 ml, 15 mmol) was added. It was stirred for 10 min at 0 °C and then at RT for 1 h. Degassed benzyl chloride solution (0.8 M in DMF, 1.2 mL, 9.6 mmol, 10 eq.) was added and stirred overnight. All volatile components were removed under reduced pressure and the oil dissolved in CHCl₃ (10 mL). It was precipitated in MeOH (400 mL).



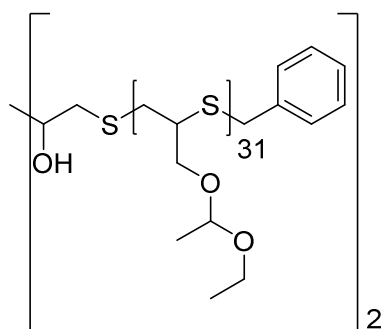
$^1\text{H NMR}$ (400 MHz, CDCl_3 , δ): 6.68 - 7.50 (10H, $\text{H}^{\text{a,b,c}}$), 5.76 - 6.01 (18H, H^{h}), 5.11 - 5.37 (37H, H^{i}), 3.91 - 4.11 (37H, H^{g}), 3.51 - 3.79 (38H, H^{f}), 3.32 - 3.45 (3H, H^{j}), 2.76 - 3.13 (59H, $\text{H}^{\text{d,e}}$) ppm.

SEC (THF, poly(styrene)) $M_n = 37300 \text{ g mol}^{-1}$ (DP=286), $M_w = 56200 \text{ g mol}^{-1}$, $D = 1.50$, bimodal.

$M_{\text{calc}} = 2132 \text{ g mol}^{-1}$

5.2.14. Homopolymerization of EETGE with DTT/DBU as initiator.

DTT (11.7 mg, 0.076 mmol, 0.152 mmol thiol, thiol: 1.0 eq), EETGE (0.7 mL, 4.72 mmol, 31 eq wrt thiol) and DMF (4 mL) were mixed and degassed. DBU (1M in DMF, 0.1 mL, 0.1 mmol, 0.7 eq wrt thiol) was added, frozen with liquid N_2 and evacuated to remove residual oxygen. It was warmed up to RT and stirred for 3 h and benzyl chloride solution (2.1 M in DMF, 0.1 mL, 0.2 mmol, 1.3 eq wrt thiol) added. It was stirred overnight. All volatile components were removed under reduced pressure and it was dissolved in CHCl_3 and precipitated in MeOH.

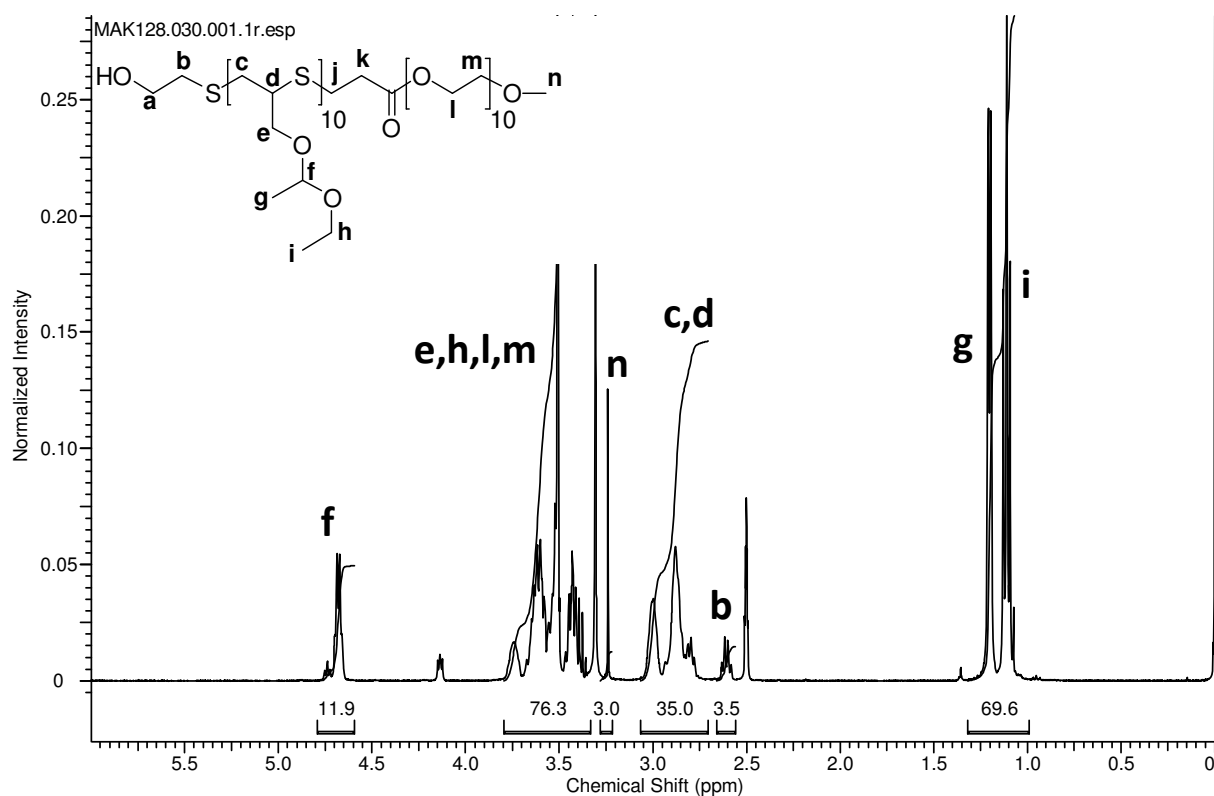


SEC (THF, poly(styrene)) $M_n = 10400 \text{ g mol}^{-1}$ (DP=64),
 $M_w = 11600 \text{ g mol}^{-1}$, $D = 1.12$, bimodal.

$M_{\text{calc}} = 10396 \text{ g mol}^{-1}$

5.2.15. Synthesis of PEETGE-*block*-mPEG480

DBU (44 μL , 0.294 mmol) dissolved in DMF (3 mL), EETGE (0.5 mL, 3.37 mmol) dissolved in DMF (3 mL) and mPEG480Ac (1.5 mL, 3.13 mmol) dissolved in DMF (3 mL) were separately cooled to $-20 \text{ }^\circ\text{C}$ and degassed under reduced pressure ($6\text{--}8 \cdot 10^{-3}$ mbar) for 1.5 h. DMF (3 mL) was predegassed purging the solution with N_2 (30 min) and mercaptoethanol (22 μL , 0.313 mmol) was added. The thiol-solution was evacuated for 1.5 h at $-20 \text{ }^\circ\text{C}$. Under N_2 -atmosphere the thiol-solution was added to the $-20 \text{ }^\circ\text{C}$ DBU-solution and it was immediately evacuated. The solution was stirred for 20 min at $-20 \text{ }^\circ\text{C}$ and under N_2 -atmosphere the monomer-solution was added at $-20 \text{ }^\circ\text{C}$. The solution was evacuated again and stirred for 1 h at $-20 \text{ }^\circ\text{C}$. Under N_2 -atmosphere the acrylate-solution was added at $-20 \text{ }^\circ\text{C}$, it was evacuated again and stirred for 1 h at $-20 \text{ }^\circ\text{C}$. The solution was purged with N_2 , the flask sealed and stirred at RT overnight. The volatile compounds were removed under reduced pressure and the residual oil taken up in diethyl ether (30 mL). All impurities could be removed by washing with saturated brine ($3 \times 40 \text{ mL}$) and water ($2 \times 40 \text{ mL}$). The solvent was dried with MgSO_4 and removed under reduced pressure.



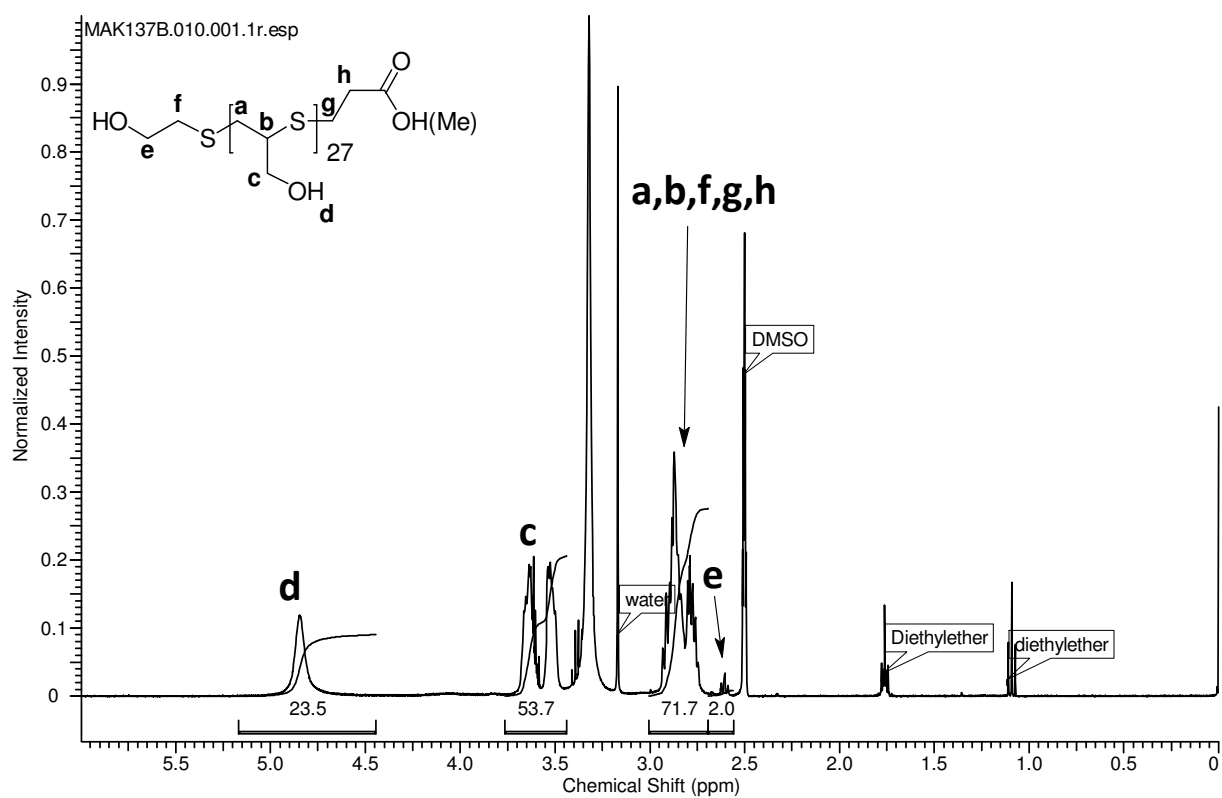
¹H NMR (400 MHz, CDCl₃, δ): 4.59 - 4.79 (12H, q, H^f), 3.33 - 3.81 (76H, H^{e,h,l,m}), 3.22 - 3.28 (3H, Hⁿ), 2.70 - 3.07 (35H, H^{c,d}), 0.99 - 1.32 (70H, H^{g,i}).

SEC (THF, poly(styrene)) M_n = 2800 g mol⁻¹ (DP = 11(PEG) + DP = 10 (P(EETGE))), M_w = 3100 g mol⁻¹, Đ = 1.08, monomodal.

M_{calc} = 2174 g mol⁻¹

5.2.16. Acetal-cleavage for the synthesis of PTG.

PEETGE (40 mg) were dissolved in THF (5 mL) and treated with aqueous HCl (0.1 M, 10 drops). It was stirred for two days at RT. Methanol (100 mL) was added. It was concentrated at 40 °C under reduced pressure. During evaporation of the solvent, the colorless oil separated from the organic phase. Addition of Et₂O (50 mL) leads to a turbid solution. The turbid solution was stored at RT for 24 h. The organic (still turbid) phase was decanted and the oily product on the bottom collected for analysis.

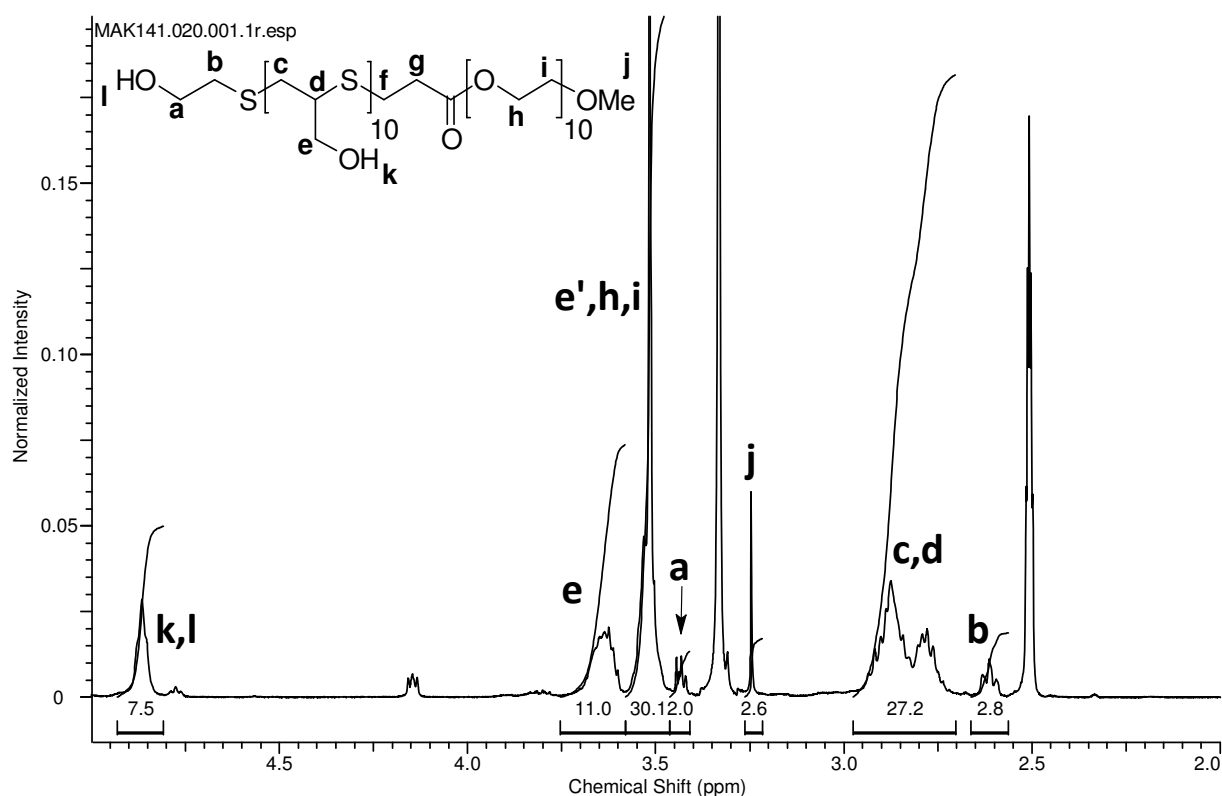


¹H NMR (400 MHz, DMSO-*d*₆, δ): 4.44 - 5.17 (24H, br, H^d), 3.44 - 3.77 (54H, br, H^c), 2.69 - 3.01 (72H, H^{a,b,f,g,h}), 2.56 - 2.69 (2H, t, H^e) ppm.

SEC: not performed

5.2.17. Acetal-cleavage for the synthesis of PTG-*block*-mPEG.

PEETGE-*block*-mPEG (100 mg, DP(poly(EETGE)) = 10, DP(PEG) = 10) was dissolved in THF (5 mL). Aqueous HCl (0.1 M, 0.8 mL) was added dropwise. It was stirred for 24 h, and hexane (100 mL) was added. A small portion of NaCl-solution (saturated) was added and the organic layer decanted. It was extracted with CHCl₃ (80mL). The aqueous phase was made slightly basic with saturated NaHCO₃ solution and subsequently with CHCl₃ (2x 80 mL) extracted. The organic phase was dried with MgSO₄. All volatile compounds of the aqueous phase were removed under reduced pressure and the white residue taken up in DCM (50 mL), crushed in solution and it was filtered. The organic solvent was removed under reduced pressure and a colorless, partially white highly viscous oil was obtained.



¹H NMR (400 MHz, DMSO-*d*₆, δ): 4.81 - 4.93 (8H, H^{k,l}), 3.58 - 3.75 (8H, H^e), 3.46 - 3.58 (48H, H^{e',h,i}), 3.41 - 3.46 (2H, H^a), 3.22 - 3.26 (3H, H^j), 2.70 - 2.98 (24H, H^{c,d}), 2.56 - 2.66 (2H, H^b) ppm.

SEC (THF, 1.0 mL min⁻¹, poly(styrene)): M_n = 1300 g mol⁻¹, M_w = 1300 g mol⁻¹, Đ = 1.08

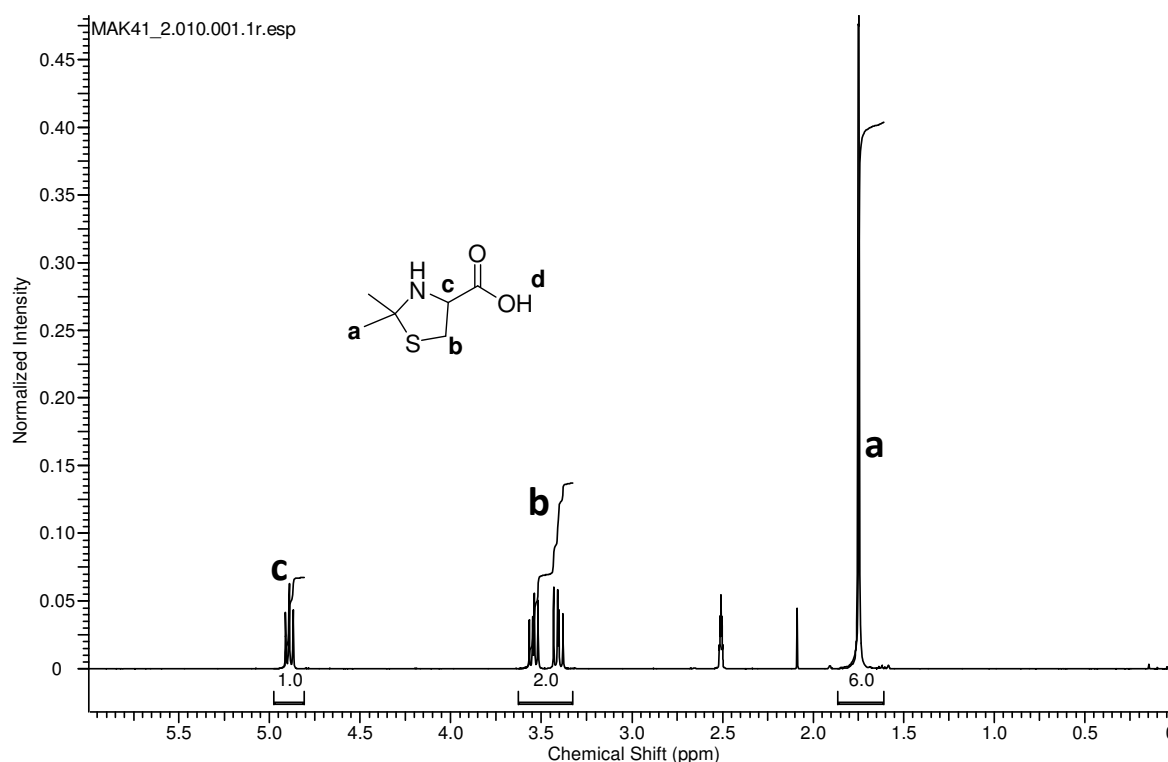
M_{calc} = 1457 g mol⁻¹

Parts of the following syntheses were already published in M. Kuhlmann, O. Reimann, C.P.R. Hackenberger, J. Groll, Cysteine-Functional Polymers via Thiol-ene Conjugation, *Macromolecular Rapid Communications*, 36 (2015) 472-476.

This work was performed in cooperation with the group of Christian P. R. Hackenberger at Department Chemical Biology II, Leibniz-Institut für Molekulare Pharmakologie (FMP) in Berlin and Humboldt Universität zu Berlin, Department Chemie, Berlin. Oliver Reimann at the aforementioned institute performed the peptide synthesis, NCL experiments as well as MALDI-ToF and HPLC measurements. These parts are marked with a hash (#).

5.2.18. Synthesis of 2,2-dimethyl-4-carboxyl-thiazolidine

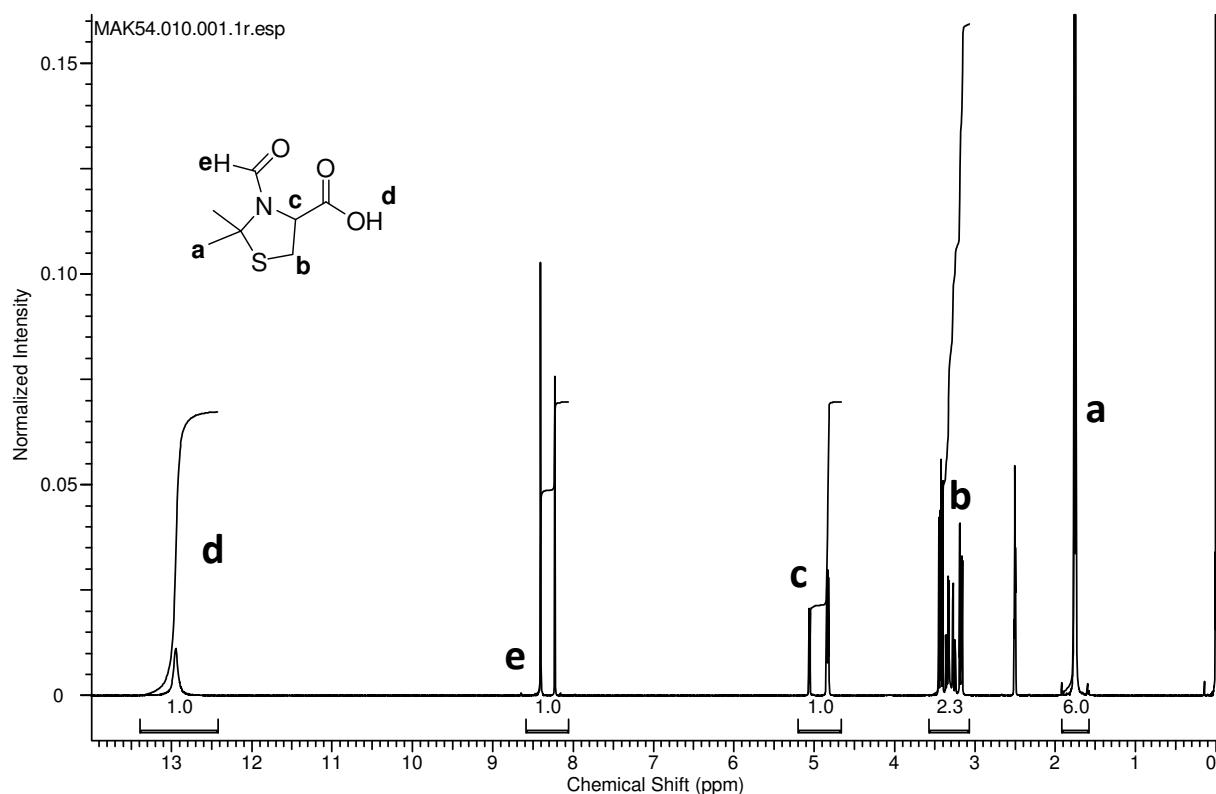
Cysteine*HCl*H₂O (13.56 g, 77.2 mmol) was suspended in acetone (300 mL) and refluxed for 4 h. The white turbid solution was filtered and the white crystalline compound collected. It was dried under vacuum to remove residual acetone.



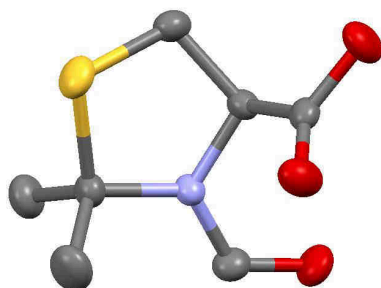
¹H NMR (400 MHz, DMSO-d₆, δ): 4.81 - 4.98 (1H, t, H^c), 3.33 - 3.63 (2H, 2x dd, H^b), 1.61 - 1.86 (6H, s, H^a) ppm.

5.2.19. Formylation of 2,2-dimethyl-4-thiazolidine

Sodium formate (1.3 g, 19 mmol) was dissolved in formic acid (25 mL). At 0 °C Tz4CA was dissolved. Over a period of approx. 1 h acetic anhydride (9.6 mL, 102 mmol) was added dropwise. It was stirred at room temperature (RT) for 1 h with a white precipitate appearing. Ice water (50 mL) was added, filtered and the white powder washed a little with ice cold water. The dried powder was recrystallized in EtOH:H₂O = 1:1. Colourless plates were obtained. Yield: 1.5 g, 7.9 mmol, 43 %. Abbreviation: FTz4CA.



¹H NMR (400 MHz, DMSO-d₆, δ): 12.42 -13.39 (1H, br, H^d), 8.06 - 8.58 (1H, 2 x s, H^e), 4.66 - 5.20 (1H, m, H^c), 3.07 - 3.57 (2H, m, H^b), (1.58 - 1.91 (6H, H^a) ppm.



X-ray analysis:

Formula: C₇H₁₁NO₃S

Space group P2₁2₁2₁

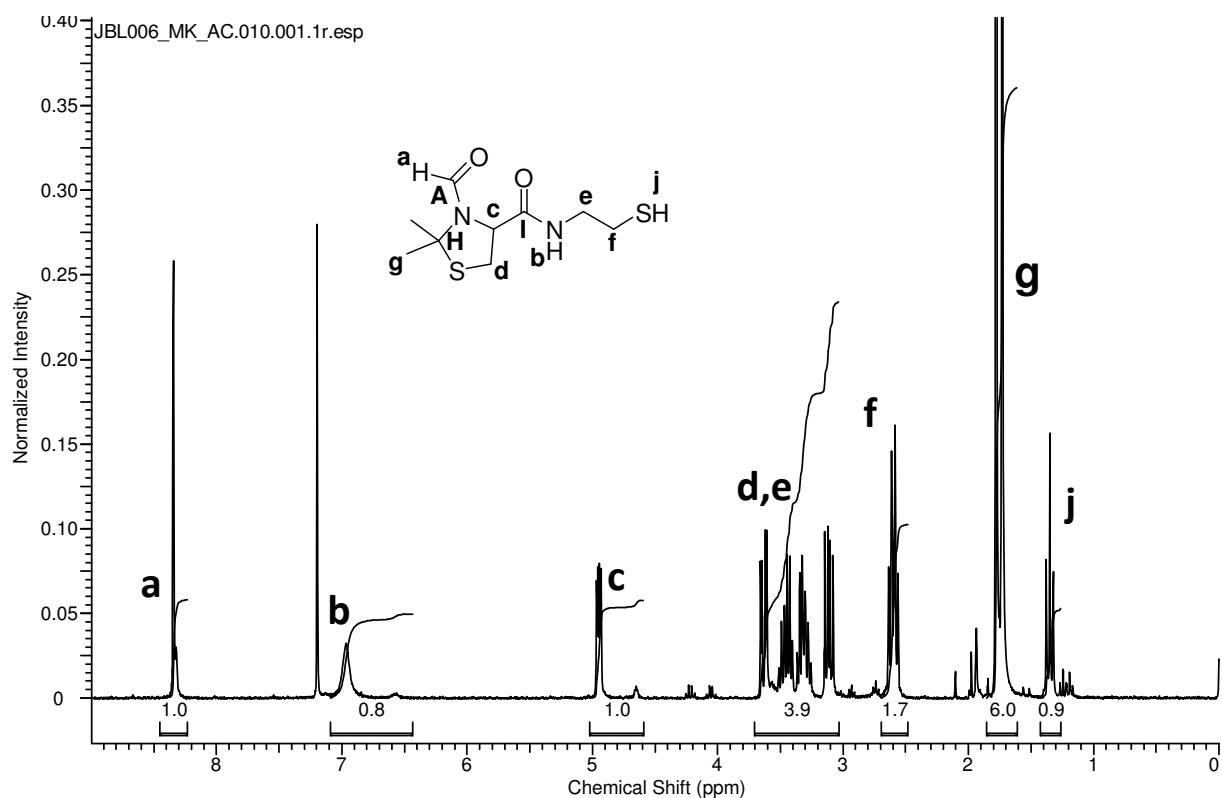
a = 7.122(3); b = 10.884(5); c = 11.339(5) Å

α = 90.00°, β = 90.00°, γ = 90.00°

V = 878.952 Å³

5.2.20. Synthesis of mercaptothiazolidine

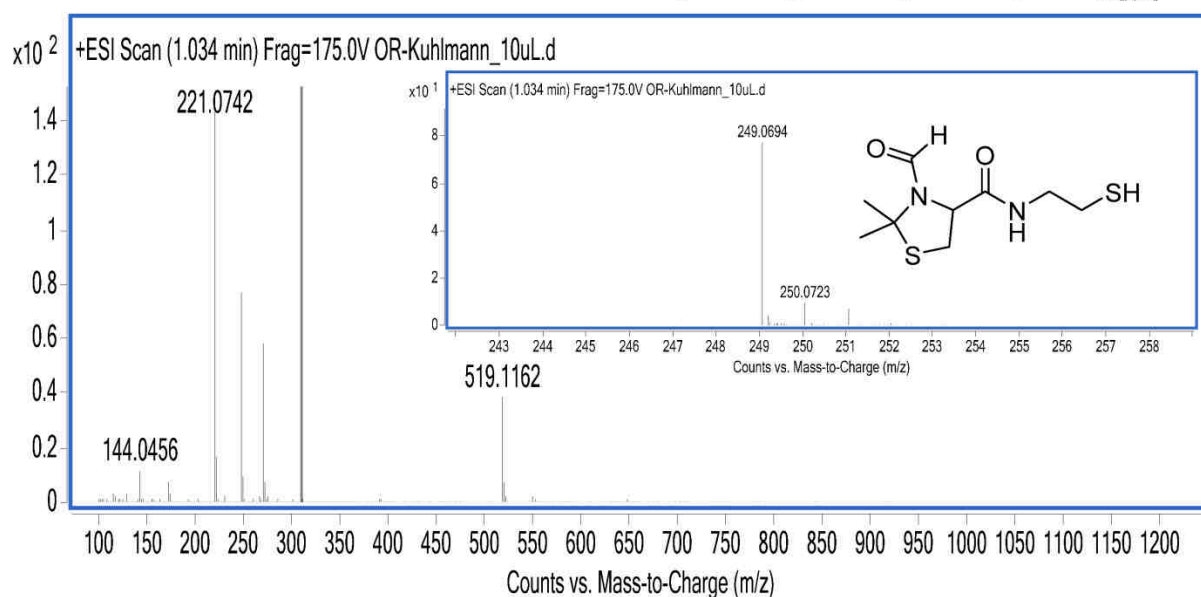
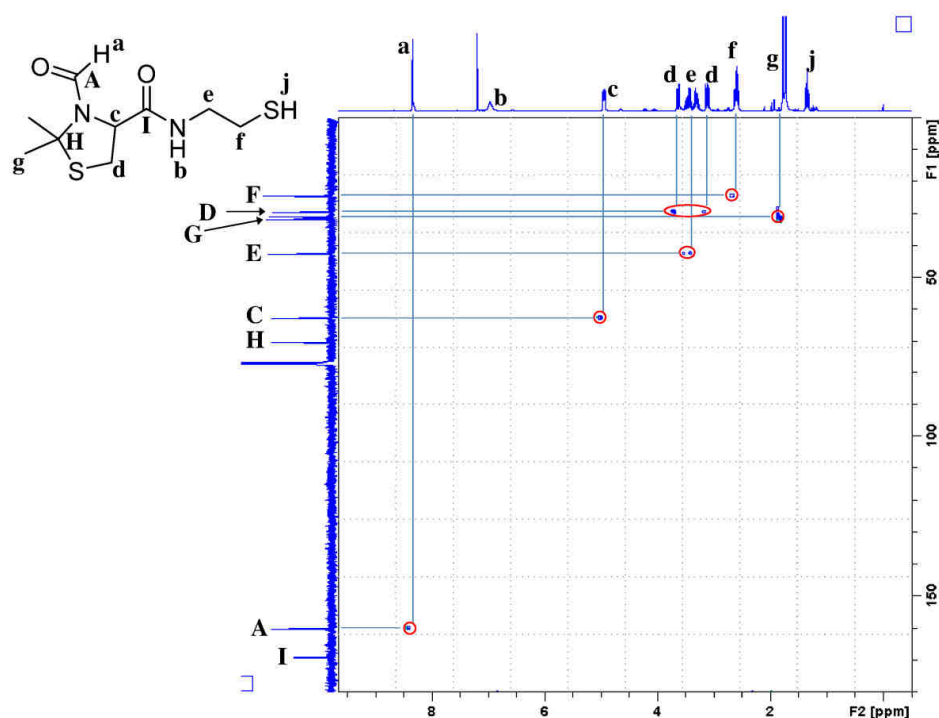
Dry FTz4CA (1.55 g, 8.2 mmol, 1.0 eq) was dissolved in dry DMF (10 mL) under argon. *N,N*-Carbonyldiimidazol (1.5 g, 9.3 mmol, 1.1 eq) was added at RT and it was stirred for 90 min at RT. Cysteamine*HCl (1.04 g, 9.2 mmol, 1.1 eq) was dissolved in dry pyridine (8 mL) under argon atmosphere. The pyridine solution was added to the DMF solution and it was stirred over night at RT. With an external cooling trap all volatile components were removed under reduced pressure. The flask was flushed with argon and the transparent yellow oil was dissolved in a diluted HCl solution (0.1 M, 100 mL). If necessary the solution was made slightly acidic with conc. HCl to prevent oxidation of the thiol. It was extracted with chloroform (3 x 50 mL), dried over MgSO₄ and the organic solvent removed under reduced pressure. A white solid was obtained. Recrystallization in ethyl acetate gives white thin needles. Yield: 0.78 g, 3.1 mmol, 38 %. Abbreviation: FTz4Cys.



¹H NMR (400 MHz, CDCl₃, δ): 8.23 - 8.45 (1H, s, H^a), 6.43 - 7.09 (1H, 2x br, H^b), 4.59 - 5.02 (1H, 2x, m, H^c), 3.03 - 3.71 (4H, H^d, H^e), 2.48 - 2.69 (2H, q, H^f), 1.61 - 1.85 (6H, 2x s, H^g), 1.26 - 1.43 (1H, t, H^j) ppm.

¹³C NMR (75 MHz, CDCl₃, δ): 169.1 (C^l), 160.1 (C^A), 70.4 (C^H), 62.8 (C^C), 42.6 (C^E), 31.7 (C^G), 30.9 (C^G), 29.7 (C^D), 24.5 (C^F) ppm.

HSQC spectrum

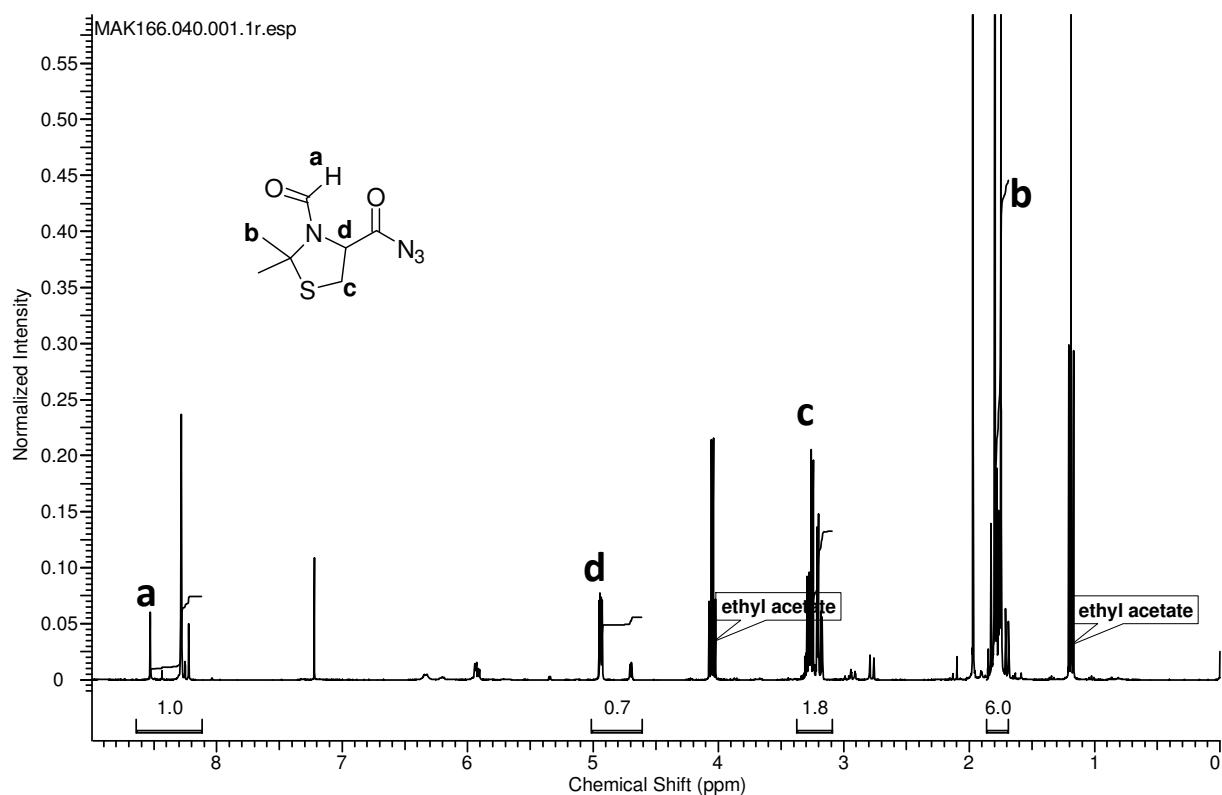


HRMS: m/z: 249.0694 [$\text{M}+\text{H}$] $^+$ (calcd. m/z: 249.0726)

5.2.21. Synthesis of 3-formyl-2,2-dimethylthiazolidine-4-carbonyl azide

Under argon atmosphere FTz4CA (500 mg, 2.64 mmol, 1.0 eq.) was dissolved in DMF (dry, 10 mL). Et_3N (0.4 mL, 2.9 mmol, 1.1 eq) was added. DPPA (0.62 mL, 2.9 mmol, 1.1 eq) was added dropwise. The clear colorless solution was stirred overnight and subsequently all volatile compounds removed under reduced pressure. Dissolving in DCM (100 mL) and washing with H_2O (3 x 100 mL) does not completely remove the aromatic impurities. The pure product was purified by column chromatography (10 cm silica; ethyl

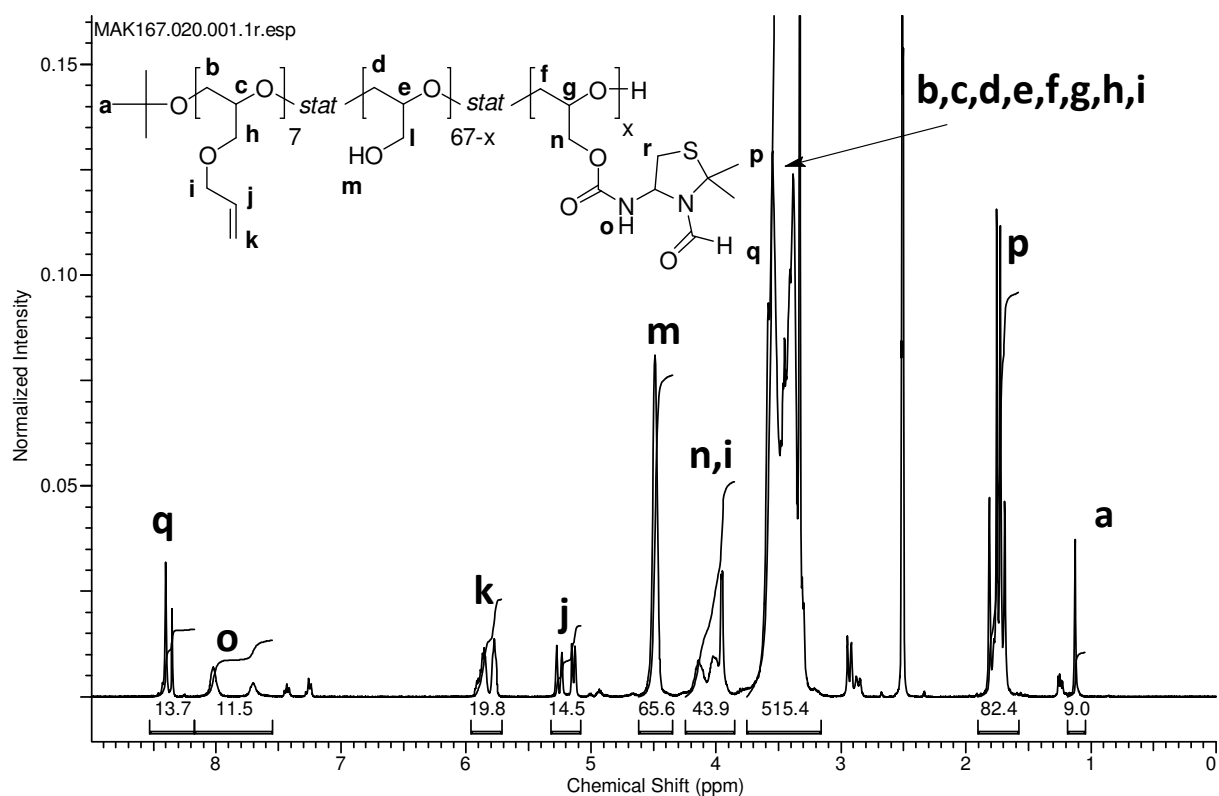
acetate:hexane = 1:2). UV-light (254 nm) was used to identify the spots on a TLC-plate. The aromatic compounds are obtained as first fraction ($R_f = 0.68$), whereas the acyl azide is obtained as second fraction ($R_f = 0.17$).



$^1\text{H NMR}$ (400 MHz, CDCl_3 , δ): 8.12 - 8.64 (1H, 2x s, H^{a}), 4.61 - 5.01 (1H, 2x m, H^{d}), 3.09 - 3.37 (2H, 2x m, H^{c}), 1.69 - 1.86 (6H, 2x s, H^{b}) ppm.

5.2.22. Polymer-analog functionalization with isocyanates

3-Formyl-2,2-dimethylthiazolidine-4-carbonyl azide (217 mg, 1.01 mmol, 14 eq wrt OH) was dissolved in DMF (4 mL) and heated to 90 °C for 1 h to induce Curtius rearrangement. Poly(glycidol-*stat*-allyl glycidyl ether) (0.400 g, $M_n = 5760 \text{ g mol}^{-1}$, 0.07 mmol) dissolved in DMF (6 mL) was added. DBTDL (1 drop) was added. It was stirred for 2d at RT. Followed by removal of all volatile components and subsequently dissolved in H_2O (25 mL). The turbid solution was centrifuged for 20 min at 2,000 rpm. The supernatant was dialyzed and lyophilized.



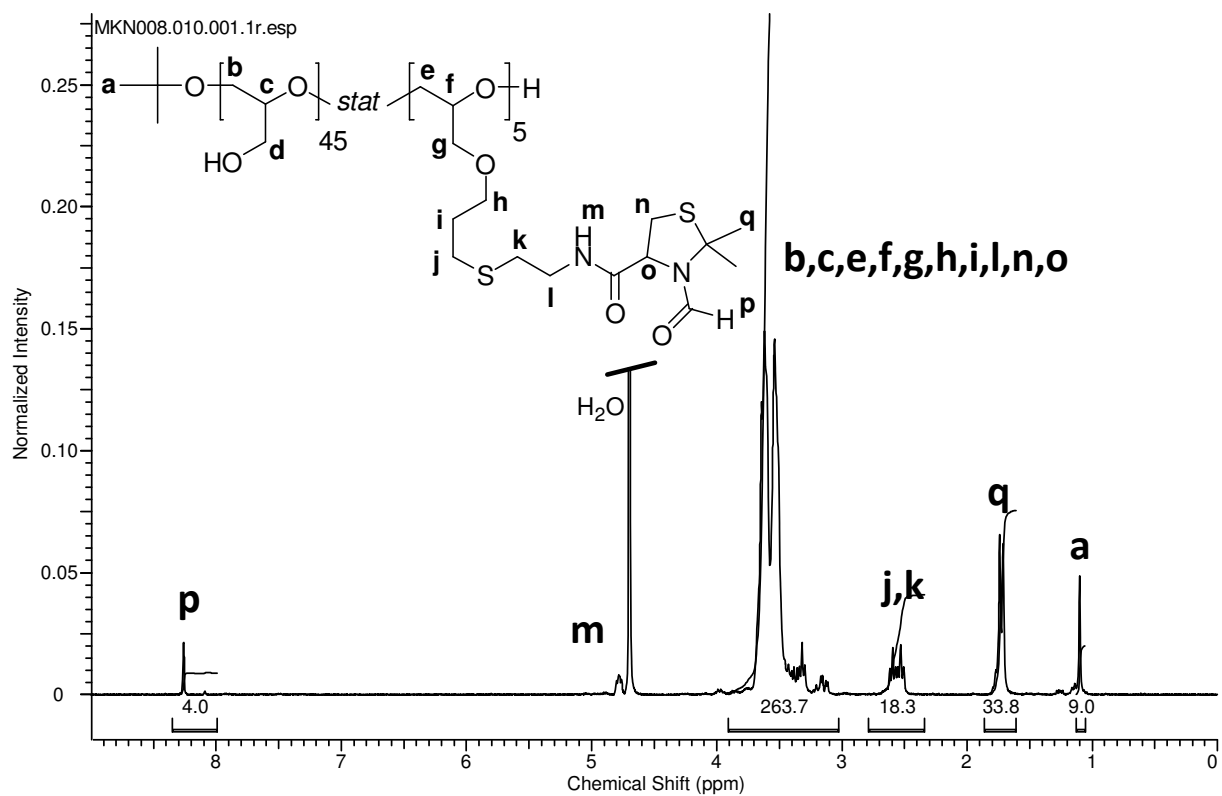
^1H NMR (400 MHz, DMSO-*d*₆, δ): 8.17 - 8.53 (14H, 2xs, H^q), 7.55 - 8.17 (12H, br, H^o), 5.71 - 5.96 (20H, m, H^k), 5.08 - 5.32 (14H, dd, H^j), 4.35 - 4.62 (66H, br, H^m), 3.85 - 4.24 (44H, H^{n,i}), 3.16 - 3.75 (515H, br, H^{b,c,d,e,f,g,h,i}), 1.58 - 1.90 (82H, H^p), 1.04 - 1.19 (9H, *reference*, H^a) ppm.

5.2.23. Polymer-analog functionalization with thiols with AIBN

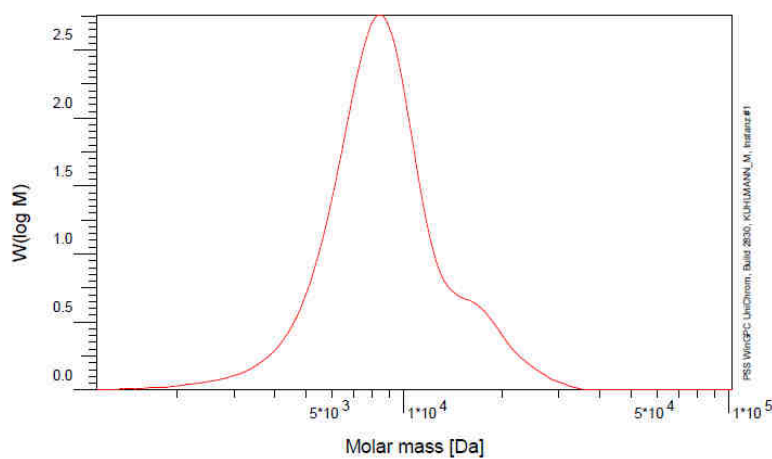
Mercaptothiazolidine (1.08 g, 4.3 mmol, 17 eq), poly(EEGE-*stat*-AGE) (0.500 g, $\text{DP}_{\text{allyl}} = 7$, $\text{DP}_{\text{EEGE}} = 67$, $n_{\text{allyl}} = 0.25$ mmol, 1.0 eq) and AIBN (35.6 mg, 0.84 eq) were dissolved in DMF (6 mL, $6.17 \cdot 10^{-3}$ M polymer-solution). 3 *freeze-pump-thaw* cycles were performed to degas the solution. It was heated to 75 °C for 22 h. All volatile components were removed under vacuum and the oil dissolved in THF (100 mL) and drop-by-drop HCl (conc, 1 mL) added. The deprotected functionalized poly(glycidol) precipitates during deprotection reaction. After decantation the oily residue (polymer) was dissolved in water and dialyzed. The experiments were repeated and the parameters shown in Table 23.

Table 23: Thiol-Ene Chemistry performed in DMF with poly(EEGE-stat-AGE) and mercaptothiazolidine using AIBN as radical source.

m_{polymer} [mg]	Allyl	Acetal	AIBN [mg]	AIBN [mmol]	Thiol [mg]	Thiol [mmol]	C_{polymer} [mol L ⁻¹]	T [°C]	T [h]	AIBN [eq]	AGE [eq]	Thiol [eq]	Conv. [%]
486	7	67	33.6	0.20	1,040	4.2	$6.00 \cdot 10^{-3}$	75	12	0.81	1.00	17	no CH ₃ signal
510	7	67	29.9	0.18	1,100	4.4	$6.30 \cdot 10^{-3}$	75	21	0.69	1.00	17	86
490	7	67	35.5	0.22	1,400	5.6	$6.05 \cdot 10^{-3}$	75	19	0.85	1.00	22	no allyl
320	7	67	40.0	0.24	0,770	3.1	$5.27 \cdot 10^{-3}$	85	22	1.47	1.00	19	97



¹H NMR (400 MHz, DMSO-*d*₆, δ): 7.99 - 8.35 (4H, H^p), 3.03 - 3.91 (264H, H^{b,c,e,f,g,h,i,l,n,o}), 2.34 - 2.79 (18H, H^{j,k}), 1.61 - 1.86 (34H, H^q), 1.05 - 1.13 (9H, H^a) ppm.



$$M_{\text{cal}} = 5151.85 \text{ g mol}^{-1}$$

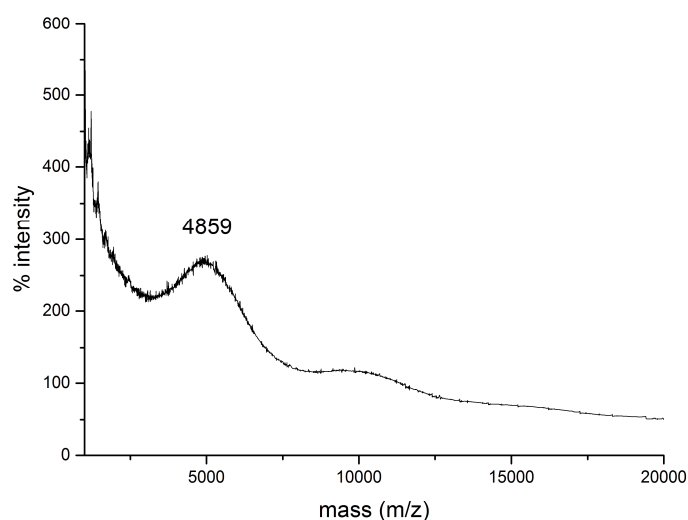
$$M_n = 7900 \text{ g mol}^{-1}$$

$$M_w = 9500 \text{ g mol}^{-1}$$

$$D = 1.21$$

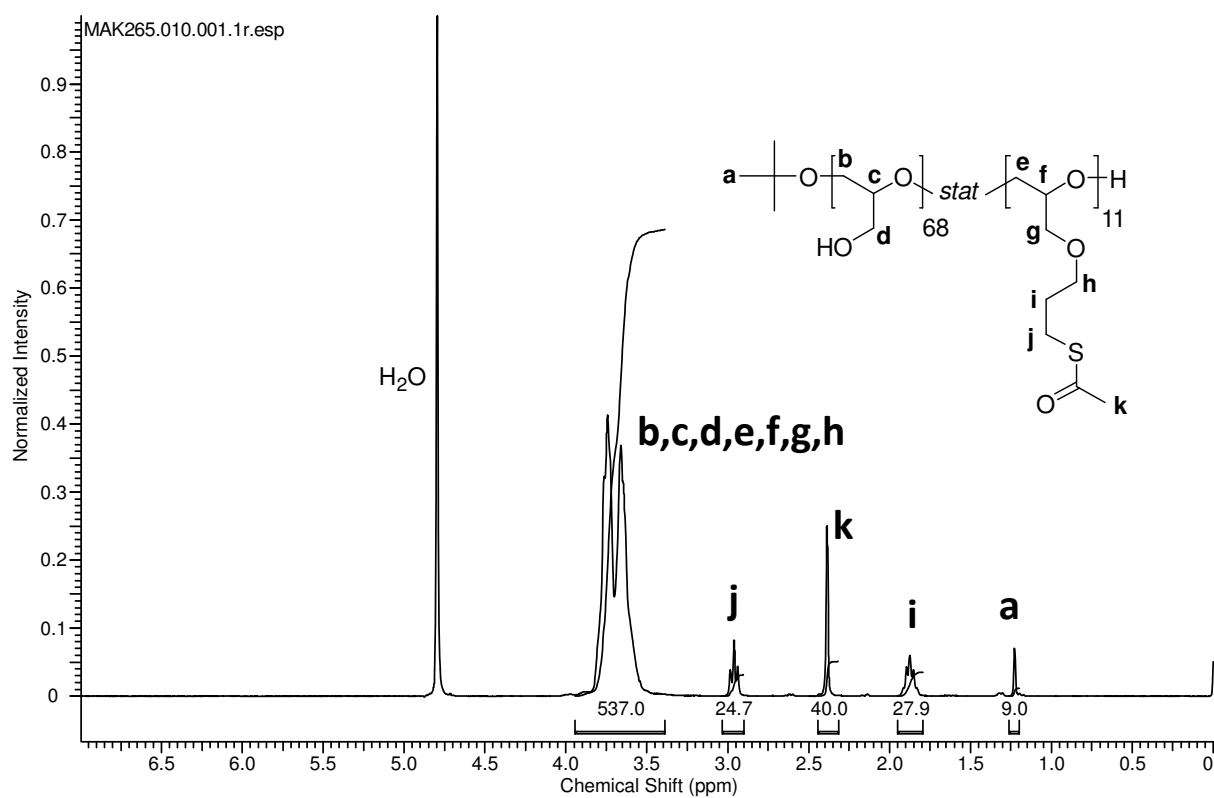
Table 24: Thiol-ene Chemistry performed with poly(EEGE-*stat*-AGE) or poly(glycidol-*stat*-allyl glycidyl ether) and mercaptothiazolidine using DMPA as photoinitiator and either a photoreactor (PR) or UV-LEDs (UV-LED).

Entry	Source	Solvens	Glycidol	Allyl:DP	Polymer [mg mL ⁻¹]	T [min]	DMPA [eq]	AGE [eq]	Thiol [eq]	Conversion [%]
1	PR	EtOH	OH	7:74	22.7	70	0.10	1.0	5.5	100
2	PR	EtOH	OH	7:74	8.8	10	0.66	1.0	5.2	100
3	PR	EtOH	OH	7:74	10.8	15	0.46	1.0	3.5	100
4	PR	EtOH	OH	7:49	18.4	15	0.49	1.0	3.5	100
5	PR	EtOH	OH	7:49	18.4	25	0.52	1.0	3.4	100
6	UV-LED	EtOH	OH	7:49	19.2	150	0.50	1.0	3.3	100
7	UV-LED	MeOH	Acetal	11:79	22.3	<10	0.90	1.0	6.2	100
8	UV-LED	MeOH	Acetal	11:79	50	60	0.59	1.0	2.3	100
9	UV-LED	MeOH	Acetal	11:79	27.6	120	0.52	1.0	1.9	100
10	UV-LED	MeOH:EtOH =1:2	Acetal	5:50	76.1	30	0.50	1.0	3.3	100
11	UV-LED	MeOH	Acetal	5:50	59.7	30	0.5	1.0	3.1	100



5.2.26. Polymer-analog functionalization with thioacetic acid via UV irradiation

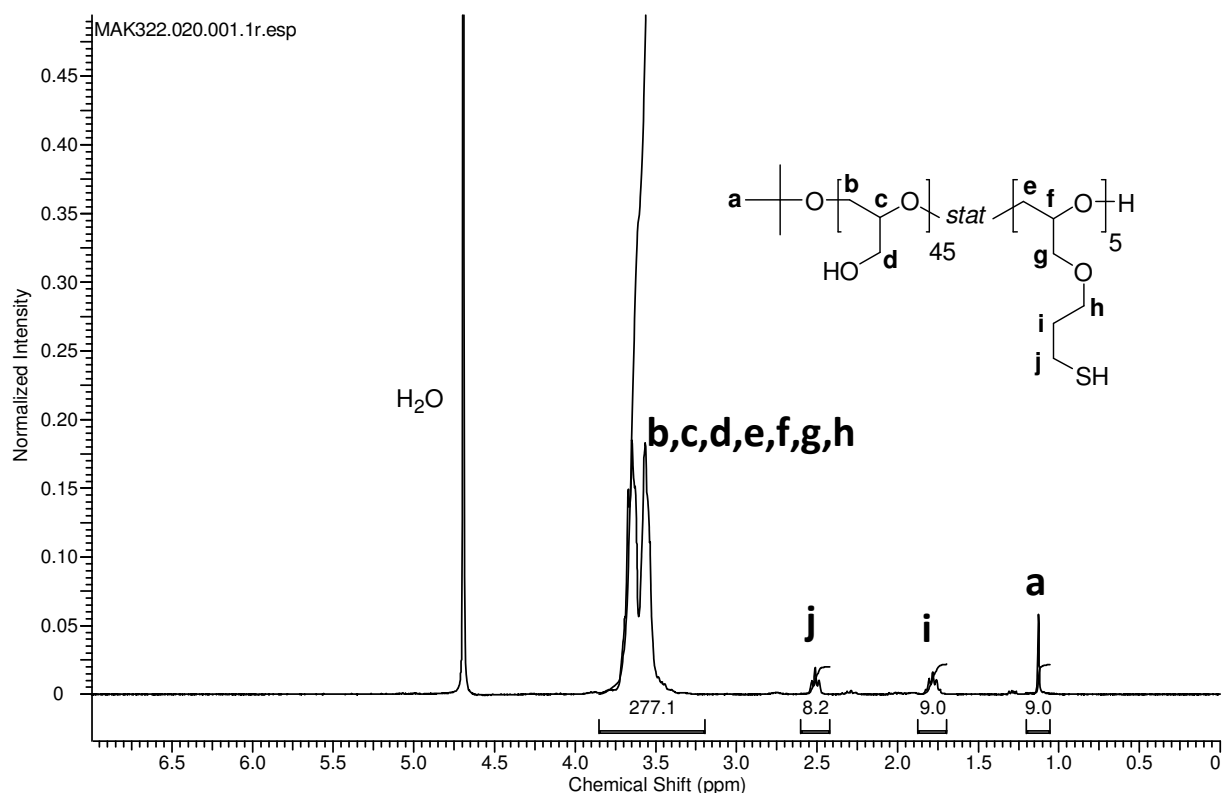
Under argon atmosphere poly(glycidol-*stat*-allyl glycidyl ether) ($DP_{\text{allyl}} = 11$, $DP_{\text{EEGE}} = 68$, 3 g, 2.97 mmol allyl) and DMPA (385 mg, 1.5 mmol, 0.5 eq wrt. allyl) were dissolved in EtOH (50 mL). Thioacetic acid was added (0.86 mL, 12 mmol, 4 eq. wrt allyl) and purged with argon for 30 min. It was irradiated with 4 LED-cubes (4x11 W, 2 h) placed around the flask. The solution was concentrated under reduced pressure (rotovap, 45 °C water bath) and the initial yellow clear solution became reddish upon concentration. Dissolving the red clear phase in THF (120 mL) was followed by addition of HCl (conc, 2 mL) drop-by-drop. Decantation yielded the white-orange THF-insoluble viscous oil that was soluble in H₂O. H₂O (20 mL) was added and stirred over night to completely dissolve the viscous oil that was subsequently dialyzed against H₂O.



¹H NMR (300 MHz, D₂O, δ): 3.39 - 3.94 (537H, H^{b,c,d,e,f,g,h}), 2.90 - 3.03 (25H, H^j), 2.32 - 2.44 (40H, H^k), 1.79 - 1.95 (28H, Hⁱ), 1.20 - 1.26 (9H, H^a) ppm.

5.2.27. Synthesis of ester-free thiol-functional poly(glycidol)

Poly(glycidol-*stat*-propyl-3-thioacetate glycidyl ether) ($DP_{\text{thioacetate}} = 5$, $DP_{\text{glycidol}} = 43$, 3 g, 3.6 mmol thioacetate) was dissolved in H_2O (100 mL). NaOH (1 M, 30 mL) was added. It was stirred at elevated T (2 h, 110 °C). A yellow, clear solution was obtained and concentrated (45 °C, 72 mbar; 55 °C, 50 mbar). Small gels were removed by filtration and HCl (1 M, 30 mL) added (compensation of NaOH). $NaHCO_3$ was added (saturated, 4 mL), until solution reacts neutral/basic. DTT was added until the complete gel was visibly dissolved. It was stirred under argon (overnight, RT). The solution was still a little bit turbid. Dialysis was performed under argon. For this a transport barrel (4 L volume) was filled with water and purged with argon for 30 min. The dialysis tube was placed in the degassed water and the lid closed. Water was changed three times over 2 days. A syringe was fixed to have a stream of argon from top to bottom. Under this argon flow the dialysis tube content was filtered, collected in three falcon tubes (50 mL) and lyophilized. Yield 2.4 g, 80 %.

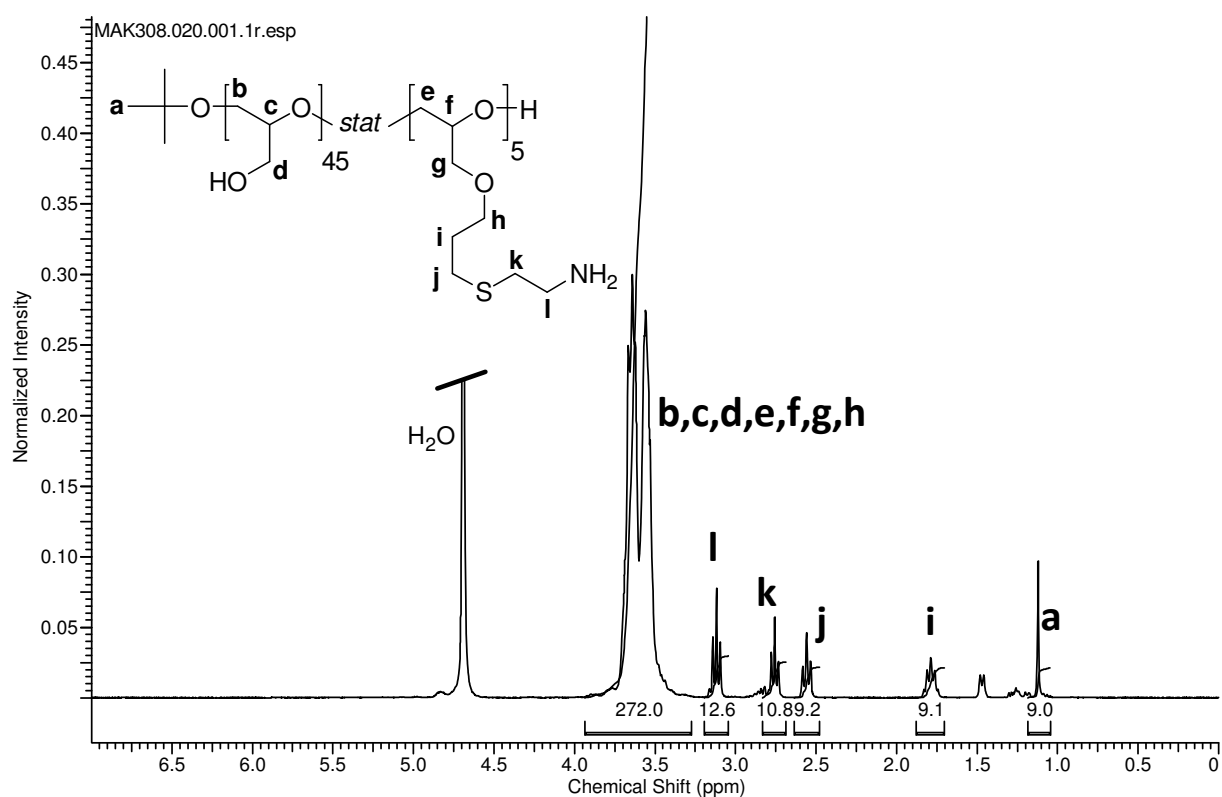


1H NMR (300 MHz, D_2O , δ): 3.39 - 3.97 (277H, br, $H^{b,c,d,e,f,g,h}$), 2.55 - 2.71 (8H, t, H^j), 1.81 - 1.99 (9H, q, H^i), 1.18 - 1.28 (9H, s, H^a) ppm.

Ellman assay: 5 thiols per polymer

5.2.28. Synthesis of amine-functional poly(glycidol)

Poly(ethoxy ethyl glycidyl ether-*stat*-allyl glycidyl ether) ($DP_{EEGE} = 45$, $DP_{allyl} = 5$, 2.283 g, 1.6 mmol allyl) was dissolved in ethanol (20 mL) and 10 min purged with argon. DMPA (208 mg, 0.81 mmol, 0.5 eq wrt allyl) and cysteamin*HCl (638 mg, 5.2 mmol, 3.5 eq) were added to the solution. A turbid solution was obtained that was sealed and 30 min irradiated with UV cubes (4x 11 W). The turbid solution was concentrated, dissolved in THF (200 mL) and HCl (conc, 10 drops) added. During 30 min stirring the precipitated polymer settle at the bottom of the beaker. Decantation of the THF was followed by dissolving the oily precipitate in H₂O (50 mL) to yield a yellow solution. It was dialyzed against H₂O and finally lyophilized.

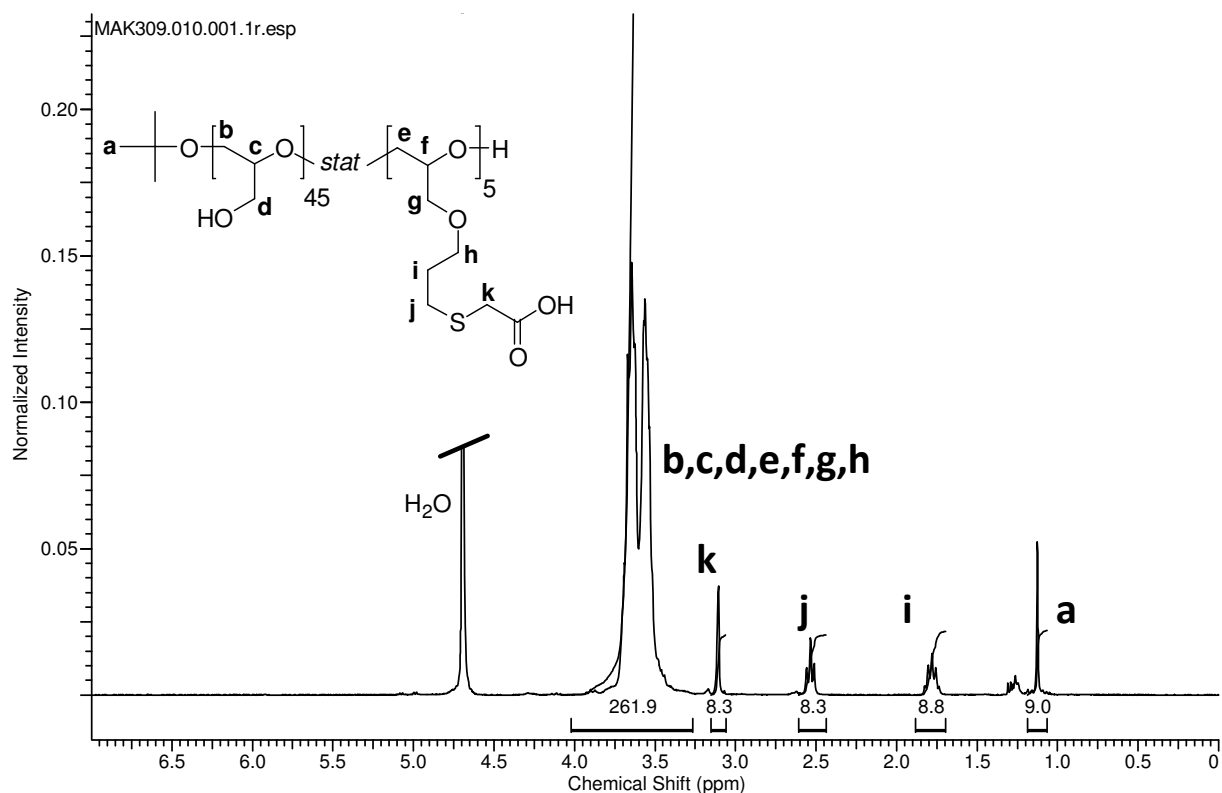


¹H NMR (300 MHz, D₂O, δ): 3.27 - 3.93 (272H, br, H^{b,c,d,e,f,g,h}), 3.04 - 3.19 (13H, quin, H^l), 2.69 - 2.83 (11H, t, H^k), 2.48 - 2.64 (9H, H^j), 1.70 - 1.88 (9H, quin, Hⁱ), 1.05 - 1.18 (9H, s, H^a) ppm.

5.2.29. Synthesis of carboxyl-functional poly(glycidol)

The polymer ($M_n = 7140$ g mol⁻¹, 2.283 g, 1.60 mmol allyl, 1 eq) was dissolved in ethanol (20 mL). It was purged with argon (10 min). Addition of DMPA (205 mg, 0.8 mmol, 0.5 eq) and thioglycolic acid (0.34 mL, $\delta = 1.505$ g mL⁻¹, 5.60 mmol, 3.5 eq wrt. allyl) and sealed with a septum. Irradiation with UV cubes (4x 11 W, 30 min). The solution was concentrated and THF (200 mL) added. HCl (conc. 10 drops) was added. The polymer precipitated. It was

stirred for additional 30 min and decanted. The precipitated polymer was dissolved in H₂O (50 mL) and NaHCO₃ (saturated) added until the solution reacted neutral/basic. Small gels were still visible. Dialysis was performed against H₂O including the small gel fraction. Dialysis water was changed every day for 3 d. The small gels were still visible. It was filtered and the aqueous solution lyophilized.



¹H NMR (300 MHz, D₂O, δ): 3.27 - 4.02 (262H, br, H^{b,c,d,e,f,g,h}), 3.06 - 3.15 (8H, s, H^k), 2.44 - 2.61 (8H, H^j), 1.69 - 1.88 (9H, quin, Hⁱ), 1.06 - 1.19 (9H, H^a) ppm.

5.2.30. Thiol-quantification (Ellman assay)

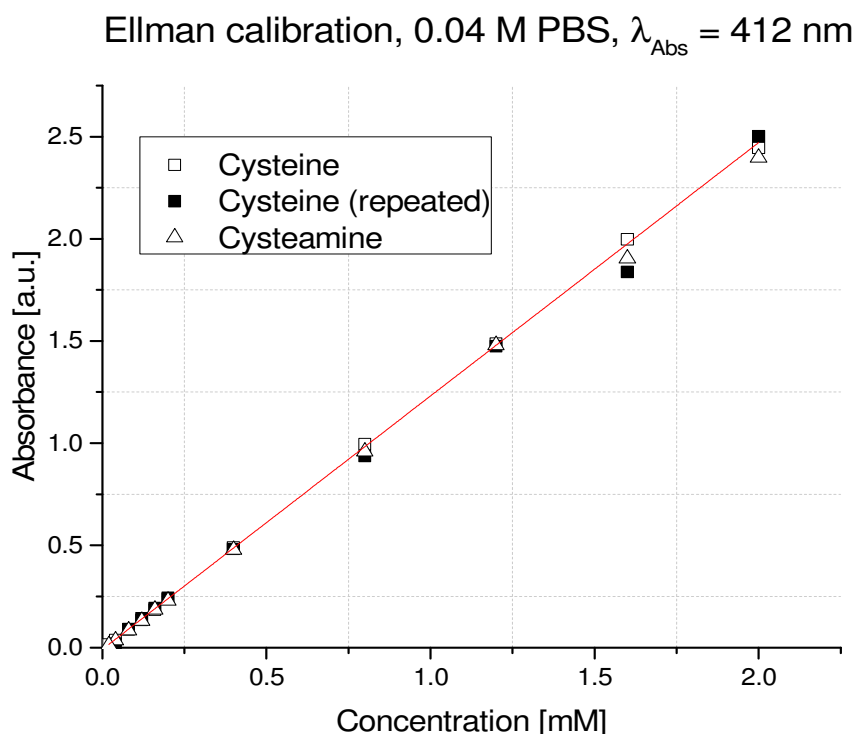
A solution of Ellman's reagent (5,5'-dithiobis(2-nitro-benzoic acid)) was prepared in 40 mM PBS (4x) yielding a final concentration of 0.01 M (4 mg mL⁻¹). For calibration with cysteine, cysteine·HCl·H₂O (35 mg) was dissolved in H₂O (100 mL), yielding a concentration of 2 mM cysteine. For calibration a concentration row of cysteine-solution with 2 mM, 1.6 mM, 1.2 mM, 0.8 mM, 0.4 mM, 0.2 mM, 0.08 mM were prepared using H₂O as solvent. The procedure is described for the polymer described in the synthesis of ester-free thiol-functional poly(glycidol) (5.2.27): The polymer (3.6 mg, M_{calc} = 4065 g mol⁻¹, theory: 4.4 μmol SH) was dissolved in H₂O (10 mL).

For the assay PBS buffer (1250 μL) was placed into 2 mL Eppendorf caps. The sample solution or calibration solutions (125 μL) were added. Ellman solution (25 μL) was added and it was mixed to obtain a homogeneous solution. It was incubated (5 min) and the absorbance measured at 412 nm. Plotting the measured absorbance against the initial concentration of the calibration stock solution gave a linear trend. The slope and intercept were determined using Origin 9.1G with a linear fit. Calibration was also possible using cysteamine.

By using the equation $y = mx + b$, with the intercept b and the slope m the concentration of the polymer solution can be calculated. An absorbance of 0.536 for the polymer example solution corresponds to a concentration of 0.4345 mM thiols in the initial solution. With 3.6 mg polymer and a theoretical SH-content of 4.4 μmol thiols/10 mL (0.44 mM, see above) the thiol-per-polymer is obtained by:

$$\frac{0.4345 \text{ mM}}{0.4400 \text{ mM}} \cdot 5 = 4.9.$$

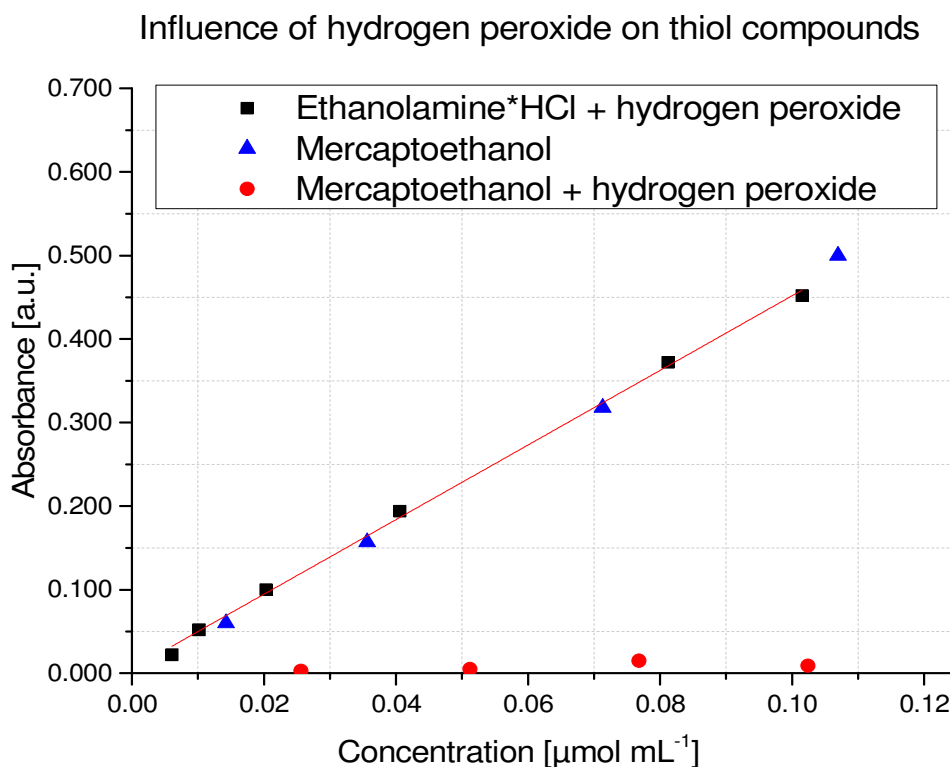
Hence with an assumed content of 5 thiol-units per polymer, Ellman gave a content of 4.9 thiol-units per polymer.



5.2.31. Cysteine-quantification (Oxidative TNBSA assay)

Sample solution (50 μL , 10 mg/mL of calibration compound and polymer) was diluted with $\text{H}_2\text{O}_2/0.1\text{ M NaHCO}_3$ ($c = 10\text{ mg/mL}$, 50 μL , 500 $\mu\text{g H}_2\text{O}_2$, 14.7 μmol , 3 eq. with respect to ethanolamine) solution and 4.950 mL of NaHCO_3 (0.1 M). The stock solution (99 $\mu\text{g/mL}$) was stored at 37 $^\circ\text{C}$ for 1 h before further dilution ensuring an equal oxidation prior to further dilutions. Samples (500 μL) were prepared with various concentrations (19.8 $\mu\text{g/mL}$ – 0.59 $\mu\text{g/mL}$). Due to the high molecular weight of the polymers two additional solutions with higher concentrations (99.0 $\mu\text{g/mL}$ and 49.5 $\mu\text{g/mL}$) were prepared. For blank solution, NaHCO_3 (0.1 M, 500 μL) without H_2O_2 was used. TNBSA solution (250 μL , 0.085 μmol TNBSA, 0.01 % in 0.1 M NaHCO_3) was added and it was stored at 37 $^\circ\text{C}$ for 2 h. The solutions turned yellow depending on the concentration. SDS solution (10 %, 250 μL) was added to each samples followed by the addition of HCl (1 M, 125 μL). The samples were closed, shaken and opened to remove the produced CO_2 . 1 mL of each solution was transferred to UV-Vis cuvettes and absorbance at 335 nm was measured. Calibration solutions with concentrations higher than 0.17 $\mu\text{mol/mL}$ ($c > 11.88\text{ }\mu\text{g/mL}$) were not used due to the restricting amount of TNBSA molecules in the sample.

The concentration of the polymers and the concentration of amines were calculated. The ratio between amine concentration and polymer concentration determined the amount of initial cysteines per polymer chain, as the thiols of the cysteines were oxidized prior to TNBSA assay.



5.2.32. Native Chemical Ligation[#]

Cysteine-functional polyglycidol was dissolved in filtered and degassed ligation buffer (6M GnHCl, 200 mM NaH₂PO₄, 200 mM 4-mercaptophenylacetic acid (MPAA) and 20 mM *tris*(2-carboxyethyl)phosphine (TCEP)). The pH was readjusted to 7.2 by the addition of NaOH or HCl and the mixture was added to the thioester peptide (0.5 mg, 179 nmol, sequence 390-410 of the tauprotein: Thz-EIVYKSPVVSVDTSRHLN with Thz: thiazolidine) to give a final concentration of 1.8 mM with respect to the peptide. The reactions were left for 2.5 h at RT before they were quenched by the addition of 1.5 ml H₂O containing 0.1% TFA and subsequently dialysed for 30 h (Spectra/Pore membrane dialysis, MWCO 3.5 kDa) against water.

The mixed ratios between peptide:polymer = 1:1, 3:1 and 5:1 equal cysteine:thioester = 5:1, 5:3 and 1:1 (Table 25).

Table 25: Ratios and used moles of peptide in comparison to the cysteine-functional polyglycidol

ratio peptide:polymer	ratio thioester:cysteine	peptide [nmol]	polymer [nmol]
1:1	1:5	179	179
3:1	3:5	179	60
5:1	1:1	179	36

After dialysis, the probes were analyzed by MALDI-TOF mass spectrometry.

5.2.33. Tricin SDS-PAGE

The chamber, consisting of two glass slides and two PTFE slides at both sides, was assembled and the lower gap sealed with a scotch tape. Agarose solution (10 mm height, 10 %) was heated and poured into the chamber as the bottom layer. It was waited for the agarose layer to cool and harden. The following solutions were prepared:

- **AB-6:** Acrylamide-solution (30 %, 100 mL) was mixed with bis(acryl amide) (1.82 g).
- **Gel buffer solution (3x):** 3.0 M tris, 1.0 M, HCl, 0.3 % SDS, pH = 8.45.
- **Cathode buffer (10x):** 1.0 M tris, 1.0 M tricine, 1.0 % SDS, pH = 8.25.
- **Anode buffer (10x):** 1.0 M tris, 0.225 M HCl, pH = 8.9.
- **Sample buffer:** 12 % SDS, 6 % mercaptoethanol, 30 % glycerol, 0.05 % coomassie blue, 150 mM tris/HCl (pH = 7.0).

First, the gel (16 %) was casted. For this AB-6, gel buffer (3x) and urea were mixed (quantity see Table 26). Upon a transparent and clear solution was obtained, first APS and subsequently TEMED were added. The beaker was gently shaken to reduce foam formation, but homogeneously distribute APS/TEMED. The solution was poured into the preassembled chamber ca 2 cm from the top edge of the slide (Figure 115). The 10 % gel was casted (1 cm), a small layer of H₂O added and hardened for 1 h. Pouring the sample gel was followed by the insertion of a PTFE comb to build the pockets for the samples. Removal of the scotch tape was performed and the plates assembled in the PAGE-apparatus. The upper vessel was filled with the cathode buffer (1x) and the lower batch with anode buffer (1x). The comb was carefully removed and the filled with the cathode buffer. Samples (10 µg per pocket) were each dissolved in sample buffer (15 µL), heated to 95 °C for 5 min. The marker (0.5 µL) was

dissolved in the sample buffer (14.5 μL) and heated to 95 $^{\circ}\text{C}$ for 5 min. The pockets filled with the samples. Empty pockets were filled with the sample buffer. A voltage of $U = 30\text{ V}$ was applied until the samples reached the interface sample-gel–10 % gel. Then $U = 90\text{ V}$ was applied. After the coomassie front reached 2 cm above the lower gel edge the gel was removed from the glass slides and incubated in a coomassie staining (methanol:acetic acid:coomassie = 20 %:7.5 %:0.1 %) overnight. Afterwards the gel was placed in a destaining solution (methanol:acetic acid = 20 %:7.5 %) and washed with the solution until a visible contrast between lines and gel-background was obtained.

Table 26: Solutions used for tricin-SDS-PAGE.

		16 % Gel/6 M Urea	10 % Gel	4 % Sample Gel
AB-6	ml	16.5	9.9	1.65
Gel Puffer (3x)	ml	10	10	3
Glycerol	g	-	3	-
Urea	g	10.8	-	-
Final volume	ml	30	30	12
APS (10 %)	μl	100	150	90
TEMED	μl	10	15	9

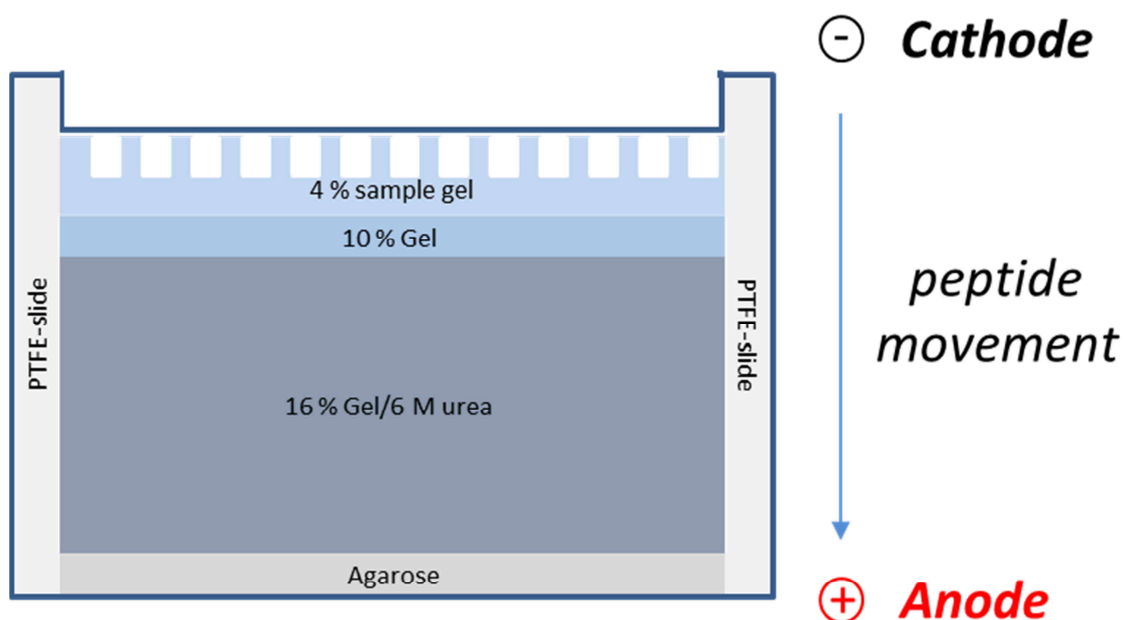


Figure 115: Assembled SDS-PAGE unit with different layers of gels.

6. Literature

-
- [1] N. Wiberg, Lehrbuch der Anorganischen Chemie, 2008.
- [2] J.M. Woof, D.R. Burton, Human antibody-Fc receptor interactions illuminated by crystal structures, *Nat. Rev. Immunol.*, 4 (2004) 89-99.
- [3] M. Valko, D. Leibfritz, J. Moncol, M.T.D. Cronin, M. Mazur, J. Telser, Free radicals and antioxidants in normal physiological functions and human disease, *Int. J. Biochem. Cell Biol.*, 39 (2007) 44-84.
- [4] G. Kim, S.J. Weiss, R.L. Levine, Methionine oxidation and reduction in proteins, *Biochimica Et Biophysica Acta-General Subjects*, 1840 (2014) 901-905.
- [5] X.Z. Shu, Y. Liu, Y. Luo, M.C. Roberts, G.D. Prestwich, Disulfide Cross-Linked Hyaluronan Hydrogels, *Biomacromolecules*, 3 (2002) 1304-1311.
- [6] X.Z. Shu, Y. Liu, F. Palumbo, G.D. Prestwich, Disulfide-crosslinked hyaluronan-gelatin hydrogel films: a covalent mimic of the extracellular matrix for in vitro cell growth, *Biomaterials*, 24 (2003) 3825-3834.
- [7] J. Groll, S. Singh, K. Albrecht, M. Moeller, Biocompatible and Degradable Nanogels via Oxidation Reactions of Synthetic Thiomers in Inverse Miniemulsion, *Journal of Polymer Science Part a-Polymer Chemistry*, 47 (2009) 5543-5549.
- [8] A. Rehor, J.A. Hubbell, N. Tirelli, Oxidation-Sensitive Polymeric Nanoparticles, *Langmuir*, 21 (2004) 411-417.
- [9] A. Bernkop-Schnurch, Thiomers: A new generation of mucoadhesive polymers, *Advanced Drug Delivery Reviews*, 57 (2005) 1569-1582.
- [10] A.M. Cantin, D.E. Woods, D. Cloutier, E.K. Dufour, R. Leduc, Polyethylene glycol conjugation at Cys(232) prolongs the half-life of alpha 1 proteinase inhibitor, *Am. J. Respir. Cell Mol. Biol.*, 27 (2002) 659-665.
- [11] T.E. Creighton, *Proteins - Structures and Molecular Properties*, 2nd ed., W. H. Freeman and Company, 1992.
- [12] A.L. Allred, E.G. Rochow, A scale of electronegativity based on electrostatic force, *J. Inorg. Nucl. Chem.*, 5 (1958) 264-268.
- [13] L. Brülisauer, M.A. Gauthier, J.-C. Leroux, Disulfide-containing parenteral delivery systems and their redox-biological fate, *Journal of Controlled Release*, 195 (2014) 147-154.
- [14] J.D. Smart, The basics and underlying mechanisms of mucoadhesion, *Advanced Drug Delivery Reviews*, 57 (2005) 1556-1568.

-
- [15] A. Ludwig, The use of mucoadhesive polymers in ocular drug delivery, *Advanced Drug Delivery Reviews*, 57 (2005) 1595-1639.
- [16] N.A. Peppas, J.J. Sahlin, Hydrogels as mucoadhesive and bioadhesive materials: A review, *Biomaterials*, 17 (1996) 1553-1561.
- [17] J.R. Gum, J.W. Hicks, N.W. Toribara, E.M. Rothe, R.E. Lagace, Y.S. Kim, The human MUC2 intestinal mucin has cysteine-rich subdomains located both upstream and downstream of its central repetitive region, *Journal of Biological Chemistry*, 267 (1992) 21375-21383.
- [18] J.T. Brosnan, M.E. Brosnan, R.F.P. Bertolo, J.A. Brunton, Methionine: A metabolically unique amino acid, *Livestock Science*, 112 (2007) 2-7.
- [19] T. Finkel, N.J. Holbrook, Oxidants, oxidative stress and the biology of ageing, *Nature*, 408 (2000) 239-247.
- [20] W. Droge, Free radicals in the physiological control of cell function, *Physiol. Rev.*, 82 (2002) 47-95.
- [21] S. Luo, R.L. Levine, Methionine in proteins defends against oxidative stress, *The FASEB Journal*, 23 (2009) 464-472.
- [22] F.Q. Schafer, G.R. Buettner, Redox environment of the cell as viewed through the redox state of the glutathione disulfide/glutathione couple, *Free Radical Biology and Medicine*, 30 (2001) 1191-1212.
- [23] P. Kuppusamy, H. Li, G. Ilangovan, A.J. Cardounel, J.L. Zweier, K. Yamada, M.C. Krishna, J.B. Mitchell, Noninvasive Imaging of Tumor Redox Status and Its Modification by Tissue Glutathione Levels, *Cancer Res.*, 62 (2002) 307-312.
- [24] C.-C. Song, F.-S. Du, Z.-C. Li, Oxidation-responsive polymers for biomedical applications, *Journal of Materials Chemistry B*, 2 (2014) 3413-3426.
- [25] E. Lallana, N. Tirelli, Oxidation-Responsive Polymers: Which Groups to Use, How to Make Them, What to Expect From Them (Biomedical Applications), *Macromolecular Chemistry and Physics*, 214 (2013) 143-158.
- [26] M. Haneklaus, L.A.J. O'Neill, R.C. Coll, Modulatory mechanisms controlling the NLRP3 inflammasome in inflammation: recent developments, *Curr. Opin. Immunol.*, 25 (2013) 40-45.
- [27] R. Zhou, A.S. Yazdi, P. Menu, J. Tschopp, A role for mitochondria in NLRP3 inflammasome activation, *Nature*, 469 (2011) 221-225.

-
- [28] G.M. Whitesides, J. Houk, M.A.K. Patterson, Activation parameters for thiolate-disulfide interchange reactions in aqueous solution, *The Journal of Organic Chemistry*, 48 (1983) 112-115.
- [29] P.A. Fernandes, M.J. Ramos, Theoretical Insights into the Mechanism for Thiol/Disulfide Exchange, *Chemistry – A European Journal*, 10 (2004) 257-266.
- [30] D.M. Rothwarf, H.A. Scheraga, Equilibrium and kinetic constants for the thiol-disulfide interchange reaction between glutathione and dithiothreitol, *Proceedings of the National Academy of Sciences*, 89 (1992) 7944-7948.
- [31] G.A. Bagiyan, I.K. Koroleva, N.V. Soroka, A.V. Ufimtsev, Oxidation of thiol compounds by molecular oxygen in aqueous solutions, *Russian Chemical Bulletin*, 52 (2003) 1135-1141.
- [32] T.J. Wallace, A. Schriesheim, The base-catalysed oxidation of aliphatic and aromatic thiols and disulphides to sulphonic acids, *Tetrahedron*, 21 (1965) 2271-2280.
- [33] S. Lenzen, The mechanisms of alloxan- and streptozotocin-induced diabetes, *Diabetologia*, 51 (2008) 216-226.
- [34] S. Singh, I. Zilkowski, A. Ewald, T. Maurell-Lopez, K. Albrecht, M. Moeller, J. Groll, Mild Oxidation of Thiofunctional Polymers to Cytocompatible and Stimuli-Sensitive Hydrogels and Nanogels, *Macromolecular Bioscience*, 13 (2013) 470-482.
- [35] J.W. Patterson, A. Lazarow, S. Levey, W.t.t.a.o.F.J. Lemm, REACTIONS OF ALLOXAN AND DIALURIC ACID WITH THE SULFHYDRYL GROUP, *Journal of Biological Chemistry*, 177 (1949) 197-204.
- [36] J.P. Barton, J.E. Packer, R.J. Sims, Kinetics of the reaction of hydrogen peroxide with cysteine and cysteamine, *Journal of the Chemical Society, Perkin Transactions 2*, 0 (1973) 1547-1549.
- [37] D. Luo, S.W. Smith, B.D. Anderson, Kinetics and mechanism of the reaction of cysteine and hydrogen peroxide in aqueous solution, *Journal of Pharmaceutical Sciences*, 94 (2005) 304-316.
- [38] M.B. Smith, *March's Advanced Organic Chemistry: Reactions, Mechanisms, and Structures*, 7th Edition ed., John Wiley and Sons, 2013.
- [39] J.R. Winther, C. Thorpe, Quantification of thiols and disulfides, *Biochimica Et Biophysica Acta-General Subjects*, 1840 (2014) 838-846.
- [40] G.L. Ellman, Tissue sulfhydryl groups, *Archives of Biochemistry and Biophysics*, 82 (1959) 70-77.

-
- [41] G.L. Ellman, A colorimetric method for determining low concentrations of mercaptans, *Archives of Biochemistry and Biophysics*, 74 (1958) 443-450.
- [42] R.E. Hansen, J.R. Winther, An introduction to methods for analyzing thiols and disulfides: Reactions, reagents, and practical considerations, *Analytical Biochemistry*, 394 (2009) 147-158.
- [43] A.D. Baldwin, K.L. Kiick, Tunable Degradation of Maleimide–Thiol Adducts in Reducing Environments, *Bioconjugate Chemistry*, 22 (2011) 1946-1953.
- [44] L.H.M. Vroomen, M.C.J. Berghmans, J.P. Groten, J.H. Koeman, P.J. van Bladeren, Reversible interaction of a reactive intermediate derived from furazolidone with glutathione and protein, *Toxicol. Appl. Pharmacol.*, 95 (1988) 53-60.
- [45] T. Toyooka, K. Imai, New fluorogenic reagent having halogenobenzofurazan structure for thiols: 4-(aminosulfonyl)-7-fluoro-2,1,3-benzoxadiazole, *Analytical Chemistry*, 56 (1984) 2461-2464.
- [46] T. Toyooka, K. Imai, Isolation and characterization of cysteine containing regions of proteins using 4-(aminosulfonyl)-7-fluoro-2,1,3-benzoxadiazole and high-performance liquid chromatography, *Analytical Chemistry*, 57 (1985) 1931-1937.
- [47] A. Barth, The infrared absorption of amino acid side chains, *Prog. Biophys. Mol. Biol.*, 74 (2000) 141-173.
- [48] F.T. Stepto Robert, Dispersity in polymer science (IUPAC Recommendations 2009), in: *Pure and Applied Chemistry*, 2009, pp. 351.
- [49] T. Eicher, S. Hauptmann, *The Chemistry of Heterocycles*, 2nd Edition ed., John Wiley & Sons, Inc., 2003.
- [50] M.J. Roberts, M.D. Bentley, J.M. Harris, Chemistry for peptide and protein PEGylation, in: *Advanced Drug Delivery Reviews*, 2002, pp. 459-476.
- [51] A.-L. Brocas, C. Mantzaridis, D. Tunc, S. Carlotti, Polyether synthesis: From activated or metal-free anionic ring-opening polymerization of epoxides to functionalization, *Progress in Polymer Science*, 38 (2013) 845-873.
- [52] A. Thomas, S.S. Müller, H. Frey, Beyond Poly(ethylene glycol): Linear Polyglycerol as a Multifunctional Polyether for Biomedical and Pharmaceutical Applications, *Biomacromolecules*, 15 (2014) 1935-1954.
- [53] S.R. Sandler, F.R. Berg, Room temperature polymerization of glycidol, *Journal of Polymer Science Part A-1: Polymer Chemistry*, 4 (1966) 1253-1259.

-
- [54] E.J. Vandenberg, Polymerization of glycidol and its derivatives: A new rearrangement polymerization, *Journal of Polymer Science: Polymer Chemistry Edition*, 23 (1985) 915-949.
- [55] H. Kautz, A. Sunder, H. Frey, Control of the molecular weight of hyperbranched polyglycerols, *Macromolecular Symposia*, 163 (2001) 67-74.
- [56] A. Sunder, R. Hanselmann, H. Frey, R. Mülhaupt, Controlled Synthesis of Hyperbranched Polyglycerols by Ring-Opening Multibranching Polymerization, *Macromolecules*, 32 (1999) 4240-4246.
- [57] T. Tsuruta, S. Inoue, H. Koenuma, Polymerization of epoxyorganosilanes, *Die Makromolekulare Chemie*, 112 (1968) 58-65.
- [58] A.O. Fitton, J. Hill, D.E. Jane, R. Millar, Synthesis of Simple Oxetanes Carrying Reactive 2-Substituents, *Synthesis*, 1987 (1987) 1140,1142.
- [59] D. Haamann, H. Keul, D. Klee, M. Möller, Star Shaped Polyglycidols End Capped with Vinyl sulfonate Groups and Conjugation Reaction with Dodecylamine, *Macromolecular Symposia*, 296 (2010) 1-4.
- [60] H. Keul, M. Möller, Synthesis and degradation of biomedical materials based on linear and star shaped polyglycidols, *Journal of Polymer Science Part A: Polymer Chemistry*, 47 (2009) 3209-3231.
- [61] M. Hans, H. Keul, M. Moeller, Chain transfer reactions limit the molecular weight of polyglycidol prepared via alkali metal based initiating systems, *Polymer*, 50 (2009) 1103-1108.
- [62] M. Erberich, H. Keul, M. Möller, Polyglycidols with Two Orthogonal Protective Groups: Preparation, Selective Deprotection, and Functionalization, *Macromolecules*, 40 (2007) 3070-3079.
- [63] M. Hans, P. Gasteier, H. Keul, M. Moeller, Ring-Opening Polymerization of ϵ -Caprolactone by Means of Mono- and Multifunctional Initiators: Comparison of Chemical and Enzymatic Catalysis, *Macromolecules*, 39 (2006) 3184-3193.
- [64] P. Dimitrov, S. Rangelov, A. Dworak, N. Haraguchi, A. Hirao, C.B. Tsvetanov, Triblock and Radial Star-Block Copolymers Comprised of Poly(ethoxyethyl glycidyl ether), Polyglycidol, Poly(propylene oxide) and Polystyrene Obtained by Anionic Polymerization Initiated by Cs Initiators, *Macromolecular Symposia*, 215 (2004) 127-140.

-
- [65] A. Dworak, G. Baran, B. Trzebicka, W. Wałach, Polyglycidol-block-poly(ethylene oxide)-block-polyglycidol: synthesis and swelling properties, *Reactive and Functional Polymers*, 42 (1999) 31-36.
- [66] D. Taton, A. Le Borgne, M. Sepulchre, N. Spassky, Synthesis of chiral and racemic functional polymers from glycidol and thioglycidol, *Macromolecular Chemistry and Physics*, 195 (1994) 139-148.
- [67] A. Dworak, I. Panchev, B. Trzebicka, W. Walach, Hydrophilic and amphiphilic copolymers of 2,3-epoxypropanol-1, *Macromolecular Symposia*, 153 (2000) 233-242.
- [68] B. Obermeier, H. Frey, Poly(ethylene glycol-co-allyl glycidyl ether)s: A PEG-Based Modular Synthetic Platform for Multiple Bioconjugation, *Bioconjugate Chemistry*, 22 (2011) 436-444.
- [69] B. Schulte, A. Walther, H. Keul, M. Möller, Polyglycidol-Based Prepolymers to Tune the Nanostructure of Microgels, *Macromolecules*, 47 (2014) 1633-1645.
- [70] D.M. Simons, J.J. Verbanc, THE POLYMERIZATION OF PROPYLENE OXIDE, *Journal of Polymer Science*, 44 (1960) 303-311.
- [71] R.K. Kainthan, J. Janzen, E. Levin, D.V. Devine, D.E. Brooks, Biocompatibility Testing of Branched and Linear Polyglycidol, *Biomacromolecules*, 7 (2006) 703-709.
- [72] W. Kwon, Y. Rho, K. Kamoshida, K.H. Kwon, Y.C. Jeong, J. Kim, H. Misaka, T.J. Shin, J. Kim, K.-W. Kim, K.S. Jin, T. Chang, H. Kim, T. Satoh, T. Kakuchi, M. Ree, Well-Defined Functional Linear Aliphatic Diblock Copolyethers: A Versatile Linear Aliphatic Polyether Platform for Selective Functionalizations and Various Nanostructures, *Advanced Functional Materials*, 22 (2012) 5194-5208.
- [73] P. Dimitrov, S. Rangelov, A. Dworak, C.B. Tsvetanov, Synthesis and Associating Properties of Poly(ethoxyethyl glycidyl ether)/Poly(propylene oxide) Triblock Copolymers, *Macromolecules*, 37 (2004) 1000-1008.
- [74] B. Obermeier, F. Wurm, H. Frey, Amino Functional Poly(ethylene glycol) Copolymers via Protected Amino Glycidol, *Macromolecules*, 43 (2010) 2244-2251.
- [75] V.S. Reuss, B. Obermeier, C. Dingels, H. Frey, N,N-Diallylglycidylamine: A Key Monomer for Amino-Functional Poly(ethylene glycol) Architectures, *Macromolecules*, 45 (2012) 4581-4589.
- [76] Z. Li, Y. Chau, Synthesis of Linear Polyether Polyol Derivatives As New Materials for Bioconjugation, *Bioconjugate Chemistry*, 20 (2009) 780-789.

-
- [77] A. Southan, E. Hoch, V. Schoenhaar, K. Borchers, C. Schuh, M. Mueller, M. Bach, G.E.M. Tovar, Side chain thiol-functionalized poly(ethylene glycol) by post-polymerization modification of hydroxyl groups: synthesis, crosslinking and inkjet printing, *Polymer Chemistry*, 5 (2014) 5350-5359.
- [78] M. Gervais, A.-L. Brocas, G. Cendejas, A. Deffieux, S. Carlotti, Synthesis of Linear High Molar Mass Glycidol-Based Polymers by Monomer-Activated Anionic Polymerization, *Macromolecules*, 43 (2010) 1778-1784.
- [79] J. Mao, Z. Gan, The Influence of Pendant Hydroxyl Groups on Enzymatic Degradation and Drug Delivery of Amphiphilic Poly glycidol-block-(epsilon-caprolactone) Copolymers, *Macromolecular Bioscience*, 9 (2009) 1080-1089.
- [80] Y. Koyama, M. Umehara, A. Mizuno, M. Itaba, T. Yasukouchi, K. Natsume, A. Suginaka, K. Watanabe, Synthesis of Novel Poly(ethylene glycol) Derivatives Having Pendant Amino Groups and Aggregating Behavior of Its Mixture with Fatty Acid in Water, *Bioconjugate Chemistry*, 7 (1996) 298-301.
- [81] K. Yoshikawa, Y. Yoshikawa, Y. Koyama, T. Kanbe, Highly Effective Compaction of Long Duplex DNA Induced by Polyethylene Glycol with Pendant Amino Groups, *Journal of the American Chemical Society*, 119 (1997) 6473-6477.
- [82] J. Meyer, H. Keul, M. Moeller, Poly(glycidyl amine) and Copolymers with Glycidol and Glycidyl Amine Repeating Units: Synthesis and Characterization, *Macromolecules*, 44 (2011) 4082-4091.
- [83] J. Groll, S. Singh, K. Albrecht, M. Moeller, Biocompatible and degradable nanogels via oxidation reactions of synthetic thiomers in inverse miniemulsion, *Journal of Polymer Science Part A: Polymer Chemistry*, 47 (2009) 5543-5549.
- [84] R.K. Kainthan, D.E. Brooks, Unimolecular Micelles based on Hydrophobically Derivatized Hyperbranched Polyglycerols: Biodistribution Studies, *Bioconjugate Chemistry*, 19 (2008) 2231-2238.
- [85] C.C.J. Culvenor, W. Davies, K.H. Pausacker, 232. Reactions of ethylene oxides. Part I. Preparation of ethylene sulphides and trithiocarbonates, *Journal of the Chemical Society (Resumed)*, (1946) 1050-1052.
- [86] H.R. Snyder, J.M. Stewart, J.B. Ziegler, The Synthesis of Amino Mercaptans from Olefin Sulfides¹, *Journal of the American Chemical Society*, 69 (1947) 2672-2674.
- [87] M. Sander, Thiiranes, *Chemical Reviews*, 66 (1966) 297-339.

-
- [88] M. Yokoyama, H. Ochi, A.M. Ueda, H. Tadokoro, INFRARED AND RAMAN-SPECTRA OF POLY(ETHYLENE SULFIDE) AND POLY(ETHYLENE-D4 SULFIDE), *Journal of Macromolecular Science-Physics*, B 7 (1973) 465-485.
- [89] J. Lal, Polymerization and copolymerization of 1-allyloxy-2,3-epithiopropene, *Journal of Polymer Science Part B: Polymer Letters*, 3 (1965) 969-971.
- [90] F. Lautenschlaeger, Alkylene Sulfide Polymerizations, *Journal of Macromolecular Science, Part A*, 6 (1972) 1089-1108.
- [91] E.J. Vandenberg, Mechanism aspects of the ring-opening polymerization of the episulfides compared to epoxides, *Journal of Polymer Science Part A-1: Polymer Chemistry*, 10 (1972) 329-354.
- [92] C. Bonnans-Plaisance, G. Levesque, Polymères thiocarboxyliques, 6. Réaction des dithiobenzoates d'ammonium quaternaire sur les chlorométhyloxirane et -thiirane; mise en évidence de la polymérisation anionique des thiiranes par les dithiocarboxylates d'ammonium quaternaire, *Die Makromolekulare Chemie*, 187 (1986) 2841-2851.
- [93] C. Bonnans-Plaisance, G. Levesque, Functional polythiiranes: 1. Comparative study of the anionic polymerization of mercaptomethylthiirane and hydroxymethylthiirane initiated by quaternary ammonium dithiobenzoate, *Polymer*, 32 (1991) 1318-1322.
- [94] C. Bonnans-Plaisance, G. Levesque, Homo- and copolymerization of unprotected 2-(hydroxymethyl)thiirane initiated by quaternary ammonium salts of dithiocarboxylic acids, *Macromolecules*, 22 (1989) 2020-2023.
- [95] C. Bonnans-Plaisance, S. Courric, G. Levesque, Functional polythiiranes, *Polymer Bulletin*, 28 (1992) 489-495.
- [96] C. Bonnans-Plaisance, P. Guerin, G. Levesque, Preparation and characterization of poly(thiirane) block copolymers with pendent hydroxy groups, *Polymer*, 36 (1995) 201-208.
- [97] A. Rehor, N. Tirelli, J.A. Hubbell, A New Living Emulsion Polymerization Mechanism: Episulfide Anionic Polymerization, *Macromolecules*, 35 (2002) 8688-8693.
- [98] Y. Watanabe, T. Aida, S. Inoue, Visible-light-mediated living and immortal polymerizations of epoxides initiated with zinc complexes of N-substituted porphyrins, *Macromolecules*, 23 (1990) 2612-2617.
- [99] T. Aida, K. Kawaguchi, S. Inoue, Zinc N-substituted porphyrins as novel initiators for the living and immortal polymerizations of episulfide, *Macromolecules*, 23 (1990) 3887-3892.

-
- [100] A. Kameyama, K. Shimotsuma, T. Nishikubo, Acyl group transfer polymerization of thiiranes with carboxylic acid derivatives, *Macromolecular Rapid Communications*, 15 (1994) 335-342.
- [101] E. Nicol, C. Bonnans-Plaisance, G. Levesque, A New Initiator System for the Living Thiiranes Ring-Opening Polymerization: A Way toward Star-Shaped Polythiiranes, *Macromolecules*, 32 (1999) 4485-4487.
- [102] A. Napoli, N. Tirelli, G. Kilcher, A. Hubbell, New Synthetic Methodologies for Amphiphilic Multiblock Copolymers of Ethylene Glycol and Propylene Sulfide, *Macromolecules*, 34 (2001) 8913-8917.
- [103] A. Suzuki, D. Nagai, B. Ochiai, T. Endo, Star-Shaped Polymer Synthesis by Anionic Polymerization of Propylene Sulfide Based on Trifunctional Initiator Derived from Trifunctional Five-Membered Cyclic Dithiocarbonate, *Macromolecules*, 37 (2004) 8823-8824.
- [104] C. Bonnans-Plaisance, P. Rétif, Functional polythiiranes 6: Hydrolysis of side chains ester and monothioacetal functions of comb-like polythiiranes, *Reactive and Functional Polymers*, 39 (1999) 9-18.
- [105] A. Napoli, N. Tirelli, E. Wehrli, J.A. Hubbell, Lyotropic Behavior in Water of Amphiphilic ABA Triblock Copolymers Based on Poly(propylene sulfide) and Poly(ethylene glycol), *Langmuir*, 18 (2002) 8324-8329.
- [106] M.J. Rosen, J.T. Kunjappu, Emulsification by Surfactants, in: *Surfactants and Interfacial Phenomena*, John Wiley & Sons, Inc., 2012, pp. 336-367.
- [107] K. Landfester, The generation of nanoparticles in miniemulsions, *Advanced Materials*, 13 (2001) 765-768.
- [108] J.K. Oh, C.B. Tang, H.F. Gao, N.V. Tsarevsky, K. Matyjaszewski, Inverse miniemulsion ATRP: A new method for synthesis and functionalization of well-defined water-soluble/cross-linked polymeric particles, *Journal of the American Chemical Society*, 128 (2006) 5578-5584.
- [109] D. Steinhilber, A.L. Sisson, D. Mangoldt, P. Welker, K. Licha, R. Haag, Synthesis, Reductive Cleavage, and Cellular Interaction Studies of Biodegradable, Polyglycerol Nanogels, *Advanced Functional Materials*, 20 (2010) 4133-4138.
- [110] S. Singh, I. Zilkowski, A. Ewald, T. Maurell-Lopez, K. Albrecht, M. Möller, J. Groll, Mild Oxidation of Thiofunctional Polymers to Cytocompatible and Stimuli-Sensitive Hydrogels and Nanogels, *Macromolecular Bioscience*, 13 (2013) 470-482.

-
- [111] S. Singh, F. Topuz, K. Hahn, K. Albrecht, J. Groll, Embedding of Active Proteins and Living Cells in Redox-Sensitive Hydrogels and Nanogels through Enzymatic Cross-Linking, *Angewandte Chemie International Edition*, 52 (2013) 3000-3003.
- [112] H. Lee, H. Mok, S. Lee, Y.-K. Oh, T.G. Park, Target-specific intracellular delivery of siRNA using degradable hyaluronic acid nanogels, *Journal of Controlled Release*, 119 (2007) 245-252.
- [113] J.P. Bearinger, S. Terrettaz, R. Michel, N. Tirelli, H. Vogel, M. Textor, J.A. Hubbell, Chemisorbed poly(propylene sulphide)-based copolymers resist biomolecular interactions, *Nature Materials*, 2 (2003) 259-264.
- [114] J.P. Bearinger, G. Stone, A.L. Hiddessen, L.C. Dugan, L. Wu, P. Hailey, J.W. Conway, T. Kuenzler, L. Feller, S. Cerritelli, J.A. Hubbell, Photocatalytic Lithography of Poly(propylene sulfide) Block Copolymers: Toward High-Throughput Nanolithography for Biomolecular Arraying Applications, *Langmuir*, 25 (2009) 1238-1244.
- [115] A. Napoli, M. Valentini, N. Tirelli, M. Muller, J.A. Hubbell, Oxidation-responsive polymeric vesicles, *Nat Mater*, 3 (2004) 183-189.
- [116] A.J. van der Vlies, C.P. O'Neil, U. Hasegawa, N. Hammond, J.A. Hubbell, Synthesis of Pyridyl Disulfide-Functionalized Nanoparticles for Conjugating Thiol-Containing Small Molecules, Peptides, and Proteins, *Bioconjugate Chemistry*, 21 (2010) 653-662.
- [117] A. Rehor, N.E. Botterhuis, J.A. Hubbell, N.A.J.M. Sommerdijk, N. Tirelli, Glucose sensitivity through oxidation responsiveness. An example of cascade-responsive nanosensors, *Journal of Materials Chemistry*, 15 (2005) 4006-4009.
- [118] C.E. Kast, A. Bernkop-Schnurch, Thiolated polymers - thiomers: development and in vitro evaluation of chitosan-thioglycolic acid conjugates, *Biomaterials*, 22 (2001) 2345-2352.
- [119] A. Bernkop-Schnurch, V. Schwarz, S. Steininger, Polymers with thiol groups: A new generation of mucoadhesive polymers?, *Pharmaceutical Research*, 16 (1999) 876-881.
- [120] V. Grabovac, D. Guggi, A. Bernkop-Schnurch, Comparison of the mucoadhesive properties of various polymers, *Advanced Drug Delivery Reviews*, 57 (2005) 1713-1723.
- [121] F.F. Davis, The origin of peganology, *Advanced Drug Delivery Reviews*, 54 (2002) 457-458.
- [122] A. Abuchowski, T. van Es, N.C. Palczuk, F.F. Davis, Alteration of immunological properties of bovine serum albumin by covalent attachment of polyethylene glycol, *Journal of Biological Chemistry*, 252 (1977) 3578-3581.

-
- [123] A. Abuchowski, J.R. McCoy, N.C. Palczuk, T. van Es, F.F. Davis, Effect of covalent attachment of polyethylene glycol on immunogenicity and circulating life of bovine liver catalase, *Journal of Biological Chemistry*, 252 (1977) 3582-3586.
- [124] S.N.S. Alconcel, A.S. Baas, H.D. Maynard, FDA-approved poly(ethylene glycol)-protein conjugate drugs, *Polymer Chemistry*, 2 (2011) 1442-1448.
- [125] M. Werle, A. Bernkop-Schnurch, Strategies to improve plasma half life time of peptide and protein drugs, *Amino Acids*, 30 (2006) 351-367.
- [126] H.S. Lu, C.L. Clogston, L.O. Narhi, L.A. Merewether, W.R. Pearl, T.C. Boone, Folding and oxidation of recombinant human granulocyte colony stimulating factor produced in *Escherichia coli*. Characterization of the disulfide-reduced intermediates and cysteine---serine analogs, *Journal of Biological Chemistry*, 267 (1992) 8770-8777.
- [127] F.M. Veronese, A. Mero, F. Caboi, M. Sergi, C. Marongiu, G. Pasut, Site-specific pegylation of G-CSF by reversible denaturation, *Bioconjugate Chemistry*, 18 (2007) 1824-1830.
- [128] Y. Chi, H. Zhang, W. Huang, J. Zhou, Y. Zhou, H. Qian, S. Ni, Microwave-assisted solid phase synthesis, PEGylation, and biological activity studies of glucagon-like peptide-1(7-36) amide, *Biorg. Med. Chem.*, 16 (2008) 7607-7614.
- [129] M.S. Rosendahl, D.H. Doherty, D.J. Smith, S.J. Carlson, E.A. Chlipala, G.N. Cox, A long-acting, highly potent interferon alpha-2 conjugate created using site-specific PEGylation, *Bioconjugate Chemistry*, 16 (2005) 200-207.
- [130] S. Brocchini, A. Godwin, S. Balan, J.-w. Choi, M. Zloh, S. Shaunak, Disulfide bridge based PEGylation of proteins, *Advanced Drug Delivery Reviews*, 60 (2008) 3-12.
- [131] P. Dawson, T. Muir, I. Clark-Lewis, S. Kent, Synthesis of proteins by native chemical ligation, *Science*, 266 (1994) 776-779.
- [132] D. Bang, B.L. Pentelute, S.B.H. Kent, Kinetically Controlled Ligation for the Convergent Chemical Synthesis of Proteins, *Angewandte Chemie*, 118 (2006) 4089-4092.
- [133] E.C.B. Johnson, S.B.H. Kent, Insights into the Mechanism and Catalysis of the Native Chemical Ligation Reaction, *Journal of the American Chemical Society*, 128 (2006) 6640-6646.
- [134] J.B. Blanco-Canosa, P.E. Dawson, An Efficient Fmoc-SPPS Approach for the Generation of Thioester Peptide Precursors for Use in Native Chemical Ligation, *Angewandte Chemie International Edition*, 47 (2008) 6851-6855.

-
- [135] N. Ollivier, J. Dheur, R. Mhidia, A. Blanpain, O. Melnyk, Bis(2-sulfanylethyl)amino Native Peptide Ligation, *Organic Letters*, 12 (2010) 5238-5241.
- [136] Y. Marsac, J. Cramer, D. Olschewski, K. Alexandrov, C.F.W. Becker, Site-specific attachment of polyethylene glycol-like oligomers to proteins and peptides, *Bioconjugate Chemistry*, 17 (2006) 1492-1498.
- [137] I.R. Ruttekolk, F. Duchardt, R. Fischer, K.-H. Wiesmuller, J. Rademann, R. Brock, HPMA as a Scaffold for the Modular Assembly of Functional Peptide Polymers by Native Chemical Ligation, *Bioconjugate Chemistry*, 19 (2008) 2081-2087.
- [138] I. van Baal, H. Malda, S.A. Synowsky, J.L.J. van Dongen, T.M. Hackeng, M. Merckx, E.W. Meijer, Multivalent Peptide and Protein Dendrimers Using Native Chemical Ligation, *Angewandte Chemie International Edition*, 44 (2005) 5052-5057.
- [139] B.-H. Hu, J. Su, P.B. Messersmith, Hydrogels Cross-Linked by Native Chemical Ligation, *Biomacromolecules*, 10 (2009) 2194-2200.
- [140] K.W.M. Boere, B.G. Soliman, D.T.S. Rijkers, W.E. Hennink, T. Vermonden, Thermoresponsive Injectable Hydrogels Cross-Linked by Native Chemical Ligation, *Macromolecules*, 47 (2014) 2430-2438.
- [141] P. Schmidt, L. Lochmann, B. Schneider, Structure and vibrational spectra of the sodium and potassium tert-butoxides, *J. Mol. Struct.*, 9 (1971) 403-411.
- [142] M.H. Chisholm, S.R. Drake, A.A. Naiini, W.E. Streib, Synthesis and X-ray crystal structures of the one-dimensional ribbon chains $[\text{MOBut}\cdot\text{ButOH}]_{\infty}$ and the cubane species $[\text{MOBut}]_4$ (M = K and Rb), *Polyhedron*, 10 (1991) 337-345.
- [143] W. Bauer, ^{133}Cs , ^1H two-dimensional heteronuclear Overhauser effect spectroscopy (HOESY): Structural analysis of organic caesium compounds by detection of short Cs,H contacts, *Magn. Reson. Chem.*, 29 (1991) 494-499.
- [144] A. Stolarzewicz, A new chain transfer reaction in the anionic polymerization of 2,3-epoxypropyl phenyl ether and other oxiranes, *Die Makromolekulare Chemie*, 187 (1986) 745-752.
- [145] C. Mariani, G. Modena, G.P. Pizzo, G. Scorrano, L. Kistenbrugger, The effect of crown ethers on the reactivity of alkoxides. Part 2. The reaction of potassium isopropoxide and 2,4-dinitrohalogenobenzenes in propan-2-ol-benzene, *Journal of the Chemical Society, Perkin Transactions 2*, (1979) 1187-1193.

-
- [146] B.A. Trofimov, B.V. Morozova, A.b.I. Mikhaleva, I.V. Tatarinova, M.V. Markova, J. Henkelmann, Synthesis of cross-linked polyethylene oxide-acetal macrocycles for solid superbase catalysts, *Journal of Applied Polymer Science*, 120 (2011) 3363-3369.
- [147] C.P. O'Neil, A.J. van der Vlies, D. Velluto, C. Wandrey, D. Demurtas, J. Dubochet, J.A. Hubbell, Extracellular matrix binding mixed micelles for drug delivery applications, *Journal of Controlled Release*, 137 (2009) 146-151.
- [148] T. Takido, K. Itabashi, An Efficient Synthesis of Unsymmetrical Sulfides Using Liquid-Liquid Phase-Transfer Catalysis, *Synthesis*, 1987 (1987) 817,819.
- [149] M. Keller, C. Sager, P. Dumy, M. Schutkowski, G.S. Fischer, M. Mutter, Enhancing the Proline Effect: Pseudo-Prolines for Tailoring Cis/Trans Isomerization, *Journal of the American Chemical Society*, 120 (1998) 2714-2720.
- [150] H. Jamet, M. Jourdan, P. Dumy, NMR and Theoretical Calculations: A Unified View of the Cis/Trans Isomerization of 2-Substituted Thiazolidines Containing Peptides, *The Journal of Physical Chemistry B*, 112 (2008) 9975-9981.
- [151] T. Shioiri, K. Ninomiya, S. Yamada, Diphenylphosphoryl azide. New convenient reagent for a modified Curtius reaction and for peptide synthesis, *Journal of the American Chemical Society*, 94 (1972) 6203-6205.
- [152] R.K. Smalley, T.E. Bingham, Thermolysis of acid azides in acetic anhydride, *Journal of the Chemical Society C: Organic*, (1969) 2481-2484.
- [153] F. Biedermann, E.A. Appel, J.s. del Barrio, T. Gruending, C. Barner-Kowollik, O.A. Scherman, Postpolymerization Modification of Hydroxyl-Functionalized Polymers with Isocyanates, *Macromolecules*, 44 (2011) 4828-4835.
- [154] G.T. Hermanson, Chapter 3 - Zero-Length Crosslinkers, in: G.T. Hermanson (Ed.) *Bioconjugate Techniques* (Second Edition), Academic Press, New York, 2008, pp. 213-233.
- [155] W. Hou, X. Zhang, F. Li, C.-F. Liu, Peptidyl N,N-Bis(2-mercaptoethyl)-amides as Thioester Precursors for Native Chemical Ligation[†], *Organic Letters*, 13 (2010) 386-389.
- [156] D. Macmillan, A.L. Adams, B. Premdjee, Shifting Native Chemical Ligation into Reverse through N S Acyl Transfer, *Israel Journal of Chemistry*, 51 (2011) 885-899.
- [157] J. Dheur, N. Ollivier, O. Melnyk, Synthesis of Thiazolidine Thioester Peptides and Acceleration of Native Chemical Ligation, *Organic Letters*, 13 (2011) 1560-1563.
- [158] N.G. Khusainova, O.A. Mostovaya, E.A. Berdnikov, R.A. Cherkasov, Reactions of buta-1,2-dienylphosphonate with thiols, *Russian Chemical Bulletin*, 52 (2003) 1033-1034.

-
- [159] M. Backes, L. Messenger, A. Mourran, H. Keul, M. Moeller, Synthesis and Thermal Properties of Well-Defined Amphiphilic Block Copolymers Based on Polyglycidol, *Macromolecules*, 43 (2010) 3238-3248.
- [160] R. Lomölder, F. Plogmann, P. Speier, Selectivity of isophorone diisocyanate in the urethane reaction influence of temperature, catalysis, and reaction partners, *Journal of Coatings Technology*, 69 (1997) 51-57.
- [161] C. Barner-Kowollik, F.E. Du Prez, P. Espeel, C.J. Hawker, T. Junkers, H. Schlaad, W. Van Camp, "Clicking" Polymers or Just Efficient Linking: What Is the Difference?, *Angewandte Chemie International Edition*, 50 (2011) 60-62.
- [162] N. ten Brummelhuis, C. Diehl, H. Schlaad, Thiol-Ene Modification of 1,2-Polybutadiene Using UV Light or Sunlight, *Macromolecules*, 41 (2008) 9946-9947.
- [163] P.G.M. Wuts, T.W. Greene, Protection for the Amino Group, in: *Greene's Protective Groups in Organic Synthesis*, John Wiley & Sons, Inc., 2006, pp. 696-926.
- [164] G. Pneumatikakis, Interactions of cysteinato-O-methylesterpalladium(II)- μ -dichloro-cysteinato-O-methylesterpalladium(II) with nucleosides and AMP, *Inorg. Chim. Acta*, 80 (1983) 89-94.
- [165] J. Meisenheimer, Ueber Reactionen aromatischer Nitrokörper, *Justus Liebigs Annalen der Chemie*, 323 (1902) 205-246.
- [166] H. Schagger, Tricine-SDS-PAGE, *Nat. Protocols*, 1 (2006) 16-22.
- [167] M.R. de Moreno, J.F. Smith, R.V. Smith, Mechanism studies of coomassie blue and silver staining of proteins, *Journal of Pharmaceutical Sciences*, 75 (1986) 907-911.

CURRICULUM VITAE

Personal Details

Full Name	Matthias Kuhlmann
Date of Birth	23.04.1983
Place of Birth	Essen, Germany
Nationality	German

Academic Career

Aug 2010 – now	Doctoral Studies University of Würzburg, Germany
Jan 2008 – Jun 2008	Research Internship (Organic Chemistry) University of Calgary, Canada Prof. Thomas Baumgartner Title: <i>“Starburst Dithieno[3,2-b:2',3'-d]phosphole Oligomers”</i>
Oct 2004 – Mar 2010	Diploma Studies (Chemistry) RWTH Aachen University, Germany Prof. Martin Möller Diploma-thesis title: <i>“Functional Polyglycidols for Targeted Delivery of Plasmids”</i>

Talks and Posters

Sep 2013	Deutsche Gesellschaft für Biomaterialien Tagung, Erlangen, Germany Poster: <i>„Cysteine-functional polyglycidols and their nanogel formation “</i>
Nov 2012	Deutsche Gesellschaft für Biomaterialien Tagung, Hamburg, Germany Poster: <i>„Dual setting calcium phosphate cements“</i>
Nov 2012	ChemSystM, Würzburg, Germany Poster: <i>“Cysteine functionalized Nanogels for Drug Delivery”</i>
Jun 2012	World Biomaterials Conference, Chengu, China Poster: <i>“ Redox-Sensitive Nanogels for Targeted Delivery of Proteins”</i> Poster: <i>“Dual setting calcium phosphate cements”</i>

May 2012	Würzburger Initiative Tissue Engineering, Würzburg, Germany Poster: <i>"Polyglycidol-based Nanogels for Targeted Protein-Delivery"</i>
Apr 2012	North-Bavarian Biomaterials Alliance, Würzburg, Germany Talk: <i>"Redox-sensitive nanogels for drug delivery"</i>
Nov 2010	Zing-Conference, Cancun, Mexiko Talk: <i>"Stimuli Responsive Nanogels based on Polyglycidols for Drug Delivery"</i>

ERKLÄRUNG

Hiermit erkläre ich an Eides statt, dass ich die vorliegende Dissertation selbstständig angefertigt und keine anderen als die von mir angegebenen Quellen und Hilfsmittel benutzt habe.

Ich erkläre außerdem, dass diese Dissertation weder in gleicher oder anderer Form bereits in einem anderen Prüfungsverfahren vorgelegen hat.

Würzburg, den

Matthias Kuhlmann